MYB67, a novel regulator of camalexin biosynthesis in *Arabidopsis thaliana*

Inaugural-Dissertation

zur
Erlangung des

Doktorgrades

der Mathematisch-Naturwissenschaftlichen

Fakultät der Universität zu Köln

vorgelegt von

Melina Ayaka Schwier

aus Sydney, Australien

Köln, March 2023

Die vorliegende Arbeit wurde an der Universität zu Köln im Institut für Pflanzenwissenschaften, in der Arbeitsgruppe von Prof. Dr. Stanislav Kopriva angefertigt.

Berichterstatter/in:	Prof. Dr. Stanislav Kopriva
	Prof. Dr. Alga Zuccaro
Prüfungsvorsitzender:	Prof. Dr. Kay Hofmann
Tag der mündlichen Pruüfung:	23. 05. 2023

In memory of

Ayako Matsuoka and Helmut Schwier

ABSTRACT

Camalexin, the primary phytoalexin of *Arabidopsis thaliana,* is an indole-derived secondary metabolite involved in defense mechanisms to counteract invading microorganisms. Camalexin can be synthesised in both shoots and roots and can also be exuded by the roots. Camalexin has emerged more recently as a key component allowing plants to gain biomass after colonisation of roots with plant growth promoting microbes. Although the signalling pathways leading to the production of camalexin have been largely explored, the regulatory networks that control the induction of its biosynthetic steps by pathogens and plant growth promoting microbes remain generally unknown, particularly in the roots.

MYB67, a member of the R2R3-MYB family, was found to be associated with the genes *CYP71A27* and *CYP71A28*, encoding cytochrome P-450 enzymes involved in camalexin biosynthesis in the roots. The aim of this work was to characterise MYB67's physiological function and explore its contribution to the transcriptional response in the roots upon inoculation with the pathogen *Burkholderia glumae* PG1 and the plant growth promoting rhizobacteria *Pseudomonas fluorescens* sp. CH267.

Spatial expression of *ProCYP71A27:GUS* after biotic elicitation was found to be influenced by MYB67. Loss of MYB67 led to increased resistance to *B. glumae* and a more efficient usage of the plant growth promoting effect stimulated by *P. fluorescens*. Furthermore, in response to both bacteria as well as the chitin oligosaccharide; chitohexaose, MYB67 seems to act as a negative regulator of camalexin biosynthesis at early stages. Even under mock conditions, *myb67* was found to have induction of camalexin associated genes. RNA-seq analyses revealed for the first time the transcriptional differences in WT roots between the pathogen and PGPB and provided substantial new knowledge of MYB67's contribution to the stress responses. Highlighting MYB67's definite role in plant innate immunity associated functions. Overall, MYB67 was also discovered to have a greater transcriptional regulatory impact in response to the PGPB than the pathogen.

The insights in this study support MYB67's involvement in the plant immune response, particularly the regulation of the camalexin signalling pathway to ensure its optimal homeostasis.

TABLE OF CONTENTS

LIST OF FIGURES

LIST OF TABLES

LIST OF ABBREVIATIONS

α	Alpha		et al.	*et alii/ae* (and others)
AA	Amino acid		ET	Ethylene
ABA	Abscisic acid		ETI	Effector triggered immunity
ABC	ATP-binding cassette		EtOH	Ethanol
AgNO$_3$	Silver nitrate		ETS	Effector triggered susceptibility
ANAC	*Arabidopsis* NAC protein		flg22	The 22 amino acids peptide
AT	*Arabidopsis thaliana*			derived from the bacterial
ATP	Adenosine 5'-triphosphate			flagellin
AZA	Azelaic acid		FC	Fold change
β	Beta		FPKM	Fragments per kb of exon model
bp	Base pair			per million
BRs	Brassinosteroids		FW	Fresh weight
BG	*Burkholderia glumae* PG1		g	gram
CB	Carbenicillin		gDNA	Genomic DNA
cDNA	Complementary DNA		GO	Gene ontology
CH	*Pseudomonas fluorescens* sp.		GOI	Gene of interest
	CH267		GSH	Glutathione
CHL	Chloramphenicol		GSH-IAN	Glutathione indole-3-acetonitrile
Col-0	*Arabidopsis* accession		GUS	□-glucuronidase
	Columbia-0		GWAS	Genome wide association study
CPM	Counts per million		h	Hour
CT	Cycle threshold		HCl	Hydrogen chloride
CYP	Cytochrome P450 enzyme		HTH	helix-turn-helix
Cys(IAN)	Cysteine indole-3-acetonitrile		hpi	Hours post inoculation
DAMPs	Damage-associated molecular		HPLC	High performance liquid
	patterns			chromatography
°C	Degree celsius		hpt	Hours post treatment
$_{dd}$H$_2$O	Double distilled water		HR	Hypersensitive response
	(Autoclaved MilliQ water)		IAA	Indole-3-acetic acid
DAP-seq	DNA affinity purification		IAN	Indole-3-acetonitrile
	sequencing		IAOx	Indole-3-acetaldoxime
DEGs	Differentially expressed genes		IR	Induced resistance
Δ	Delta		ISR	Induced systemic resistance
DMSO	Dimethyl sulfoxide		JA	Jasmonic acid
DNA	Deoxyribonucleic acid		kb	Kilobase
dNTP	Deoxynucleotide		Lab	Laboratory
dpi	Days post inoculation		LB	Lysogeny broth
e.g.	*exempli gratia* (for example)		LiCl	Lithium chloride
EDTA	Ethylenediaminetetraacetic acid		Log$_2$	Logarithm to the base 2

LORE	Lectin-like motifs	OD_{600}	Optical density at 600
LRR	Leucine rich repeat	PCR	Polymerase chain reaction
LysM	Lysine motifs	PIP	Pipecolic acid
M	Mock	PGP	Plant growth promoting
MAMPs	Microbe-associated molecular patterns	PGPB	Plant growth promoting rhizobacteria
MAPK	Mitogen-activated protein kinase	p	p-value
$\mu E*m^{-2}*s^{-1}$	Microeinsteins per second per square metre	PCA	Principal component analysis
		pH	Potential hydrogen
μg	Microgram	pmol	Picomole
μl	Microlitre	PRRs	Pathogen recognition receptors
μm	Micrometre	PTI	Pathogen triggered immunity
μM	Micromolar	q-value	Adjusted p-value
mL	Millilitre	R	Resistance
mm	Millimetre	RIN	RNA integrity number
mM	Millimolar	RLKs	receptor-like protein kinases
min	Minute	RLPs	receptor-like proteins
$MgCl_2$	Magnesium chloride	RNA	Ribonucleic acid
MTI	Microbe triggered immunity	RNA-seq	RNA sequencing
mRNA	Messenger RNA	ROS	Reactive oxygen species
MYB	Myeloblastosis, transcription factor family	rpm	Revolutions per minute
		RT	Reverse transcription
MS	Murashige and Skoog	SA	Salicylic acid
NAC	NAM (no apical meristem), ATAF1/2 (*Arabidopsis* transcription activation factor 1/2), CUC2 (Cup-shaped cotyledon 2) transcription factor superfamily	SAM	Shoot apical meristem
		SDS	Sodium dodecyl sulphate
		sec	Second
		SEM	Standard error of the mean
		qRT-PCR	Quantitative real time polymerase chain reaction
NASC	Nottingham *Arabidopsis* Stock Centre	T-DNA	Transfer DNA
		TF	Transcription factor
ng	nanogram	TPM	Transcripts per million
NHR	Non-host resistance	Trp	Tryptophan
NLR	Nucleotide-binding leucine rich repeat	UV	Ultraviolet
		V	Volts
OD	Optical density	WT	Wild type

1 │ INTRODUCTION

1.1 The plant immune system

In their natural environment, plants intimately interact with a plethora of living microorganisms that may be beneficial or harmful for their well-being (Bulgarelli et al., 2012). In order for their survival, plants have adapted sophisticated strategies to detect foreign properties to launch the appropriate responses against their potential threat (Jones and Dangl, 2006). In the last decade it was discovered that terrestrial plants are able to communicate with the rich, diverse, and highly complex ecosystem, including the microbiota communities within the soil, surrounding the roots and rhizosphere (Bulgarelli et al., 2012). The majority of plants are resistant to the pathogens they encounter, known as nonhost resistance (NHR), a possible result of co-evolution of plant-microbe interaction (Hückelhoven, 2005). Adapted pathogens are able to manipulate and suppress the plants' basal defense to overcome NHR for their own survival and to successfully complete the pathogen life cycle for basic compatibility (Lipka et al. 2008). Pathogens are considered successful not just after entering the host by either penetrating surface layers directly via mechanical pressure or enzymatic attack, through wounds or natural openings such as the stomata or lenticels, but only after proliferating within their host long enough to obtain nutrients, suppress plant defenses and continue their life cycle (Chisholm et al., 2006; Jones and Dangl, 2006).

Since plants lack an adaptive immune system, they have evolved a two-tiered innate immune system, on which they rely (Nürnberger and Kemmerling, 2006). The first layer is activation of pathogen- /microbe triggered immunity (PTI /MTI), which depends on the recognition of conserved pathogen- /microbe- associated molecular patterns (PAMPs /MAMPs) by extracellular transmembrane receptors or pattern recognition receptors (PRRs) (Zipfel et al., 2014; Jones and Dangl, 2006). In response to MTI, some microbes have acquired the ability to increase virulence by secreting effector molecules. These effectors are dispatched within the plant cell to manipulate the plant's behaviour to the microbe's benefit, suppressing MTI, to

overall bypass the defense response and achieve successful colonisation in the host, leading to effector triggered susceptibility (ETS) (Bardoel et al., 2011; Biegeard et al., 2015; Toruño et al., 2016). As a counterattack, plants evolved resistance (R) proteins that are generally members of the nucleotide-binding leucine rich repeat (NLR) family. These R proteins perceive microbe-specific effectors, thereby activating the second layer of plant defense, effector triggered immunity (ETI) (Jones and Dangl, 2006; Pieterse et al., 2009; Gao et al., 2013; Qi and Innes, 2013; Cui et al., 2015; De Coninck et al., 2015). Furthermore, some NLR receptors mimic plant immune components such as WRKY transcription factors (TFs) that are usually targets of the virulence effectors by presenting 'decoy' domains. The microbial effectors then bind to the decoy domains of NLR receptors instead of its intended target (Figure 1) (Le Roux et al., 2015; Sarris et al., 2015).
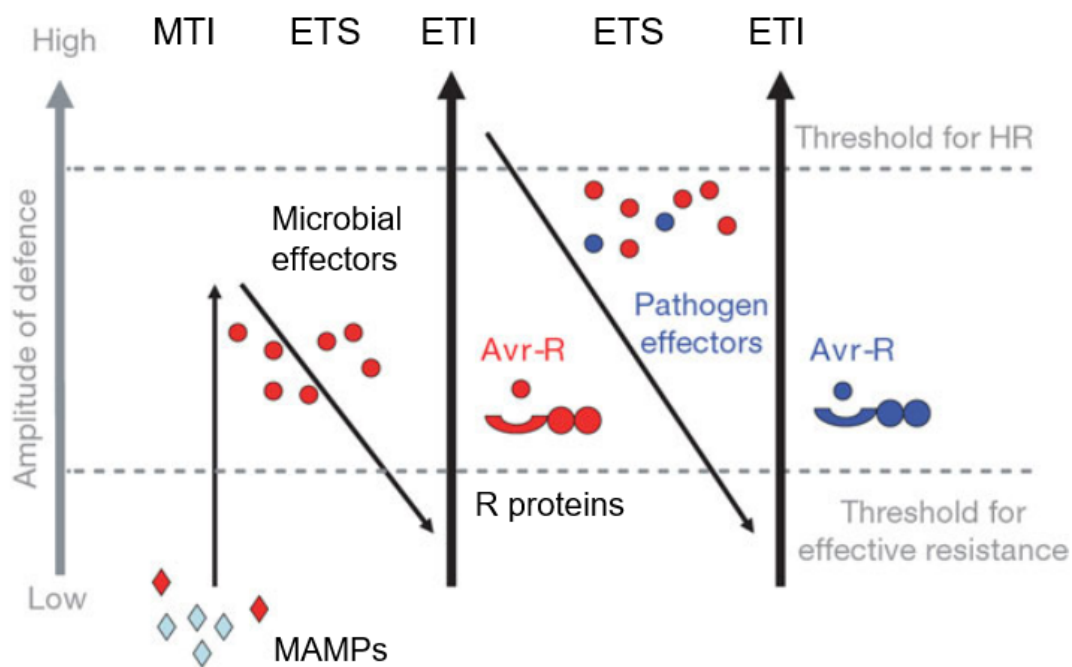
Figure 1: Scheme of MTI and ETI response. Modified from Jones and Dangl (2006).

MTI and ETI share many biochemical features and their induced immunity are complementary. ETI differs in the intensity of host responses, which is also effective against adapted pathogens, restricting the pathogen from spreading by triggering localised cell death, the hypersensitive response (HR) (Figure 1) (Dodds and Rathjen, 2010; Monaghan and Zipfel, 2012). After development of an HR, the induction of systemic acquired resistance (SAR) may

develop to deter unrelated virulent pathogens (Dodds and Rathjen, 2010; Monaghan and Zipfel, 2012). Plant growth promoting rhizobacteria (PGPB) that seek a symbiotic relationship with the plant deploy similar molecular strategies as pathogens in order to overcome the MAMP/PRR system (Hacquard et al., 2017; Mhlongo et al., 2018). Their chemical communication with the plant allows them to engage in a cooperative plant-microbe interaction that can lead to root colonisation (Hacquard et al., 2017; Mhlongo et al., 2018). This truly highlights the multifaceted management role of the plant in its innate immune system to differentiate between microbes to accurately eliminate pathogens and accommodate beneficial microbes.

1.2.1 MTI

MAMP-triggered MTI response is effective against the vast majority of potential pathogens. Plants can also sense endogenous elicitors, plant derived molecules from damage caused by pathogenic enzymes, these are referred to as damage associated molecular patterns (DAMPs), via cell surface localised PRRs (Eder and Cosio, 1994; Macho and Zipfel, 2014). Even though numerous highly conserved MAMPs that are essential for pathogens to invade plants have been identified, in comparison only several PRRs have been detected and intensively studied in *Arabidopsis thaliana* (Nürnberger and Kemmerling, 2006; Zipfel, 2008). Identified PRRs belong to one of two large protein families, either receptor-like protein kinases (RLKs) that consist of an extracellular ligand binding domain, a transmembrane domain and an intracellular serine/threonine protein kinase domain, while receptor-like proteins (RLPs) lack the kinase domain and usually form a complex with the adaptor protein SUPPRESSOR OF BIR1-1 (SOBIR1) (Zipfel, 2006; Miya et al., 2007; Wan et al., 2008; Macho and Zipfel, 2014). PRRs are further classified by their ectodomain structures consisting of a leucine rich repeat (LRR) domain (e.g., FLS2, EFR, PEPRs), lectin-like motifs (e.g., LORE) or lysine motifs (LysM) (e.g., LYK4/5; CERK1). These ectodomain structures bind to specific ligand classes including: proteins or peptides recognised by LRR-type PRRs (Chinchilla et al., 2006; Zipfel et al., 2006), carbohydrates such as chitin sensed by LysM-type PRRs (de Jonge et al., 2010; Marshall et al., 2011) and lipids perceived by lectin-containing PRRs (Ishikawa et al., 2013). For example, the most extensively investigated PRR in *A. thaliana* is the LRR-RLK FLAGELLIN SENSITIVE 2

(FLS2) that perceives a 22 amino acid peptide (flg22), a conserved region of bacterial flagellin (Felix et al., 1999; Gómez-Gómez and Boller, 2000). For successful ligand recognition, interaction with their LRR-RLK co-receptor BRASSINOSTEROID INSENSITIVE 1 (BRI1)-ASSOCIATED KINASE 1 (BAK1) is required (Heese et al., 2007; Petutschnig et al. 2014). In absence of flg22, the receptor-like cytoplasmic kinase (RLCK) *BOTRYTIS*-INDUCED KINASE 1 (BIK1) interacts with BAK1 and FLS2 (Lu et al., 2010). Upon binding of the flg22 epitope directly with FLS2, the BIK1-BAK1 complex dissociates and BAK1 forms a receptor complex with FLS2 and enters an active state (Chinchilla et al., 2007). BAK1 is required for multiple immune responses triggered by various MAMPs other than flagellin, including EF-tu, peptidoglycans, lipopolysaccharides, cold-shock protein and the oomycete elicitor INF1 in tobacco (*Nicotiana benthamiana*) and Arabidopsis (Chinchilla et al., 2007; Heese et al., 2007; Shan et al., 2008). Upon ligand recognition, RLKs or RLP-SOBIR1 receptors recruit co-receptors such as BAK1 or the chitin sensing LysM-RLK CHITIN ELICITOR RECEPTOR KINASE 1 (CERK1) allowing for transphosphorylation and subsequent activation of substrate proteins (Chinchilla et al., 2007; Miya et al., 2007; Sun et al., 2013; Cao et al., 2014; Petutschnig et al., 2014; Albert et al., 2015). This results in a range of physiological outputs including: generation of reactive oxygen species (ROS) via plasma membrane-borne NADPH oxidase, rapid influx of calcium ions, stomatal closure, callose deposition into the cell walls, activation of cascades of mitogen-activated protein kinases (MAPKs), production of defense hormones that subsequently induce expression of defense genes and accumulation of antimicrobial secondary metabolites (e.g. camalexin) (Jones and Dangl, 2006; Bittel et al., 2007; Dodds and Rathjen, 2010; Monaghan and Zipfel, 2012; Larroque et al., 2013).

These early responses are followed by massive transcriptional reprogramming and increased accumulation of phytohormones such as ethylene (ET), salicylic acid (SA) or jasmonate (JA) for both local and systemic responses that modulate further complex downstream signalling networks (Tsuda et al., 2008; Pieterse et al., 2012; Li et al., 2016a). However, the innate defense system is actually more complex as there are other phytohormones that interplay in the background including: abscisic acid (ABA), auxins, cytokinins, gibberellins and

brassinosteroids (BRs). Other signalling molecules such as strigolactones, azelaic acid (AZA) and pipecolic acid (PIP) have been reported to be associated with plant defense. All these costly mechanisms involved in innate immunity are hence tightly controlled and can promote cross-talk between pathways to fine tune and optimise their responses against the attacking microbe. Thus, these factors ensure the restriction of additional growth of non-adapted pathogens (Pieterse et al., 2012; Lozano-Durán and Zipfel, 2015; Berens et al., 2017; Yu et al., 2017).

Plant innate immune responses are also important for regulating interactions of plant commensal and symbiotic microbes (Villena et al., 2018; Rodriguez et al., 2019). Diverse genera of PGPB dominated by *Bacillus* and *Pseudomonas* spp. have been identified. They are able to grant plant health-promoting properties by modulating plant innate immunity, known as induced systemic resistance (ISR) (Bakker et al., 2007; Pieterse et al., 2014; Nguyen et al., 2022a). Without a competing pathogen, beneficial microbes do not usually tend to induce a large systemic defense response, but instead prepare plants for potential future pathogenic attacks, thus activating a primed resistance state for a faster and stronger defense against intruders (Conrath et al., 2006; Pieterse et al., 2014; Koprivova et al., 2019; Nguyen et al., 2022a). A typical induced resistance (IR) response is to induce the biosynthesis of secondary metabolites such as phytoalexins (Glawischnig et al., 2007).

1.2 Phytoalexins, including camalexin

The concept of phytoalexins was introduced by Müller and Borger in 1940, based on the finding that prior infection of potato (*Solanum tuberosum*) tuber tissue with an incompatible *Phytophthora infestans* induced resistance to following inoculation with a compatible *P. infestans*. This led to a hypothesis that substances (phytoalexins) were produced in response to the incompatible interaction, this in turn inhibited further growth of the subsequent pathogen and defended against later infection by additional compatible pathogens (Müller and Borger, 1940). Phytoalexins have since been described as low molecular weight, antimicrobial compounds elicited in plants in response to MAMPs or treatment with various abiotic elicitors

(Paxton, 1981; Glazebrook et al., 1997a/ 1997b; Thomma et al., 1999; Pangesti et al., 2016; Zhai et al., 2017). They are generally categorised into two primary groups: nitrogen-containing molecules (alkaloids) and nitrogen-deficient molecules (terpenoids and phenolics) (Patra et al., 2013).

In 1960, Cruickshank and Perrin first found the phytoalexin Pisatin in *Pisum sativum* to have antifungal activity after infection with *Sclerotinia fruticola*, which incited others to invest further research in the topic of phytoalexins and their biological functions. From this, emerged the further isolation and identification of additional phytoalexins with antifungal and antibacterial activity in various plant species of various families, including: camalexin and brassinin in Brassicaceae (Browne et al., 1991; Pedras et al., 2009), resveratrol and its transformation into viniferins in Vitaceae (Langcake and Pryce, 1976; Jeandet et al., 2002; Schnee et al., 2008), pisatin, medicarpin, gluciollins, arachidins, resveratrol in Fabaceae (Preisig et al., 1990, Blount et al., 1992, Burrow et al.,, 2001; Medina-Bolivar et al., 2007; Bamji and Corbitt, 2017; Sobolev, 2013), sakuranetin, momilactones, oryzalexins, zealexins, kauralexins in Poaceae (Dillon et al., 1997; Huffaker et al., 2011; Schmelz et al., 2011), and capsidiol and scopoletin in Solanaceae (Perrone et al., 2003; Araceli et al., 2007; Mialoundama et al., 2009; El Oirdi et al., 2010).

Unlike phytoanticipins, which are constitutively expressed within a plant with concentrations increasing upon stress, phytoalexins are synthesised and accumulated at the site of infection as a mechanism that plants employ to resist disease only after exposure to microbes or other effective stimuli (Darvill and Albershem, 1984; Van Etten et al., 1994, Tiku et al., 2018). It has been shown that phytoalexins are synthesised in high concentrations upon fungal (Sato, Kitazawa and Tomiyama, 1971; Bailey, 1974) as well as bacterial exposure (Lyon and Wood, 1975). Phytoalexin accumulation as a plant defense is not limited to exposure to pathogens, but also takes place after perception of specific MAMP elicitors and beneficial microbes (Gruau et al., 2015; Pangesti et al., 2016; Zhai et al., 2017). Since 1992, the main phytoalexin identified in the model plant Arabidopsis, was and still is, camalexin (Tsuji et al., 1992).

Camalexin (3-thiazol-2'-yl-indole) was isolated originally from the leaves of *Camelina sativa* in response to the fungal pathogen, *Alternaria brassicae* (Browne *et al.*, 1991). It was quickly considered as an integral hallmark of the plant's defensive machinery and became a topic of interest for the last 30 years (Ferrari et al., 2003; Nguyen et al., 2022b). This sulfur-containing tryptophan-derived secondary metabolite, is involved in response to biotic stress (Ausubel et al., 1995) as well as abiotic responses including heavy metals or UV-B light (Tsuji et al., 1993; Mert-Turk et al., 2003; Schuhegger et al., 2007). For its biosynthesis, activation of a particular set of genes is required (Glawischnig, 2007; Schuhegger et al., 2007; Jeandet 2018; Jeandet et al., 2013 and 2021; Mucha et al., 2019), which appears to be under the control of distinct signalling pathways responsive to major defense phytohormones such as salicylic acid (SA), jasmonic acid (JA) and ethylene (ET), depending on the challenging microorganism (Koornneef et al., 2008; López et al., 2008; Bigeard et al., 2015; Nguyen et al., 2022b).

1.2.1 Biosynthesis of camalexin

Camalexin is derived from its precursor, tryptophan, in a pathway that is initiated by two functionally redundant cytochrome P450 enzymes CYP79B2 and CYP79B3 to obtain the indole-3-acetaldoxime (IAOx) (Figure 2, Mikkelsen et al., 2000; Zhao et al., 2002; Glawischnig et al., 2004; Böttcher et al., 2009). IAOx can also be used for the biosynthesis of indole glucosinolates and the phytohormone indole-acetic acid (IAA) (Figure 2, Mikkelsen et al., 2000). In camalexin synthesis, the next step, dehydration of IAOx to indole-3-acetonitrile (IAN), is catalysed by CYP71A13 (Nafisi et al., 2007; Klein et al., 2013; Müller et al., 2015) and its close homolog, CYP71A12 (Millet et al., 2010; Saga et al., 2012). The *CYP71A12* and *CYP71A13* are located in tandem on chromosome II and have 89% similarity in their amino acid sequences (Pastorczyk et al., 2020). Observations of significantly reduced camalexin was seen in both *cyp71a12* and *cyp71a13,* and in the double mutant *cyp71a12 cyp71a13* after flg22, UV and silver nitrate (AgNO$_3$) treatments (Nafisi et al., 2007; Millet et al., 2010; Schlappi et al., 2010; Wang et al., 2012; Müller et al., 2015; Stringlis et al., 2018).

Next, the GLUTATHIONE-S-TRANSFERASE, GSTF6 is responsible for the conjugation of IAN to glutathione to synthesise GSH(IAN) (Figure 2, Su et al., 2011). The GSH(IAN) is then metabolised to Cys(IAN) by the γ-GLUTAMYL PEPTIDASES GGP1 and GGP3 (Figure 2, Geu-Flores et al., 2011; Møldrup et al., 2013). Involved in the GSH(IAN) metabolism additionally, are γ-GLUTAMYL TRANSPEPTIDASES GGT1 and GGT2 (Su et al., 2013), as well as GH3.5 (also known as WES1, Wang et al., 2012). The last two steps of the biosynthesis pathway from Cys(IAN) resulting first in dihydrocamalexic acid and then in camalexin are catalysed by CYP71B15 (also known as PHYTOALEXIN DEFICIENT 3, PAD3) (Figure 2, Zhou et al., 1999; Schuhegger et al., 2006; Böttcher et al., 2009). Mucha and colleagues (2019) propose that CYP71A12, CYP71A13, CYP71B15 and the less tightly associated CYP79B2 and ATR1 (ARABIDOPSIS P450 REDUCTASE 1) form a metabolic complex, in which GGP1 and GSTU4 can be recruited cooperatively and in a competing manner, respectively, to allow for camalexin biosynthesis (Mucha et al., 2019).
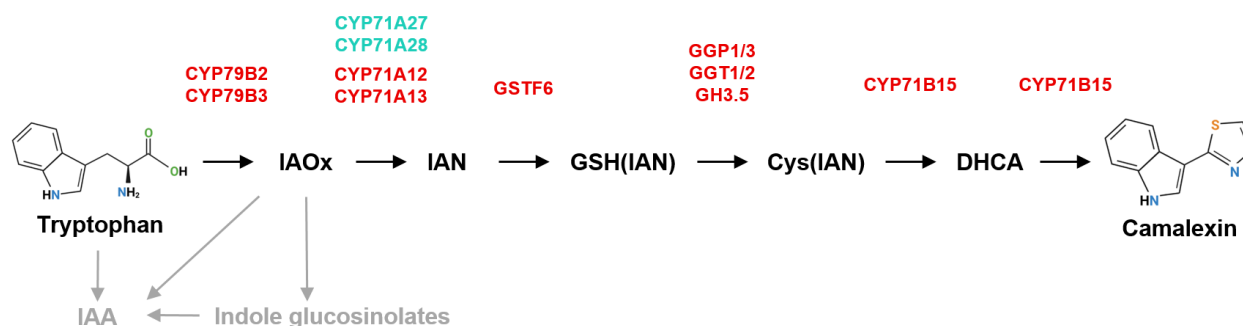
Figure 2: Camalexin biosynthesis pathway. Simplified schematic of camalexin biosynthesis which derived from tryptophan is catalysed by the well known enzymes (in red) and newly discovered (predominantly in roots) P450 enzymes CYP71A27 and CYP71A28, predicted to catalyse IAOx to IAN in turquoise. Alternative branching points from tryptophan and IAOx are depicted in grey, resulting in the biosynthesis of phytohormone IAA and indole glucosinolates. (Mikkelsen et al., 2000; Glawischnig et al., 2004; Wang et al., 2012; Koprivova et al., 2019; Nguyen et al., 2022)

Subsidiary phytoalexin deficient mutants (*pad1*, *pad2*, and *pad4*) that were discovered in a genetic screen for low accumulation of camalexin upon treatment with *Pseudomonas syringae*, were regarded to have indirect effects on the camalexin synthesis with *PAD1* and *PAD4* genes mediating upregulation of *PAD3* after pathogen infection (Glazebrook and Ausubel 1994; Glazebrook et al., 1996/ 1997a/ 1997b; Zhou et al., 1999). Contradictorily, *PAD1* and *PAD4* were observed not to be required for camalexin induction by fungal pathogens, as *PAD4* encodes a

protein with sequence similarity to lipases but *PAD1* remains yet to be identified (Ren et al., 2008). Even though *PAD2* encodes a γ-glutamylcysteine synthetase (GSH1) it was found alike with PAD3 to be required for mitogen protein kinase 3 and 6 (MAPK3/MAPK6)-induced camalexin after treatment with the steroid dexamethasone (DEX) (Ren et al., 2008). The mutant *pad3* is impaired in the last step of camalexin synthesis and therefore frequently used to validate camalexin function in *Arabidopsis*-microbe interactions (Glazebrook and Ausubel, 1994; Glazebrook et al., 1996; Thomma et al., 1999; Zhou et al., 1999). For instance, *pad3* is highly susceptible to necrotrophic pathogens including *Botrytis cinerea* (Ferrari et al., 2003 and 2007; Kliebenstein et al., 2005; van Baarlen et al., 2007), *Alternaria brassicicola* (Thomma et al.,1999; Nafisi et al., 2007) and *Plectosphaerella cucumerina* (Staal et al., 2006; Sanchez-Vallet et al., 2010). Camalexin was also reported to play a defensive role in response to hemibiotrophic pathogens such as *Colletotrichum* (Narusaka et al., 2004) and *Leptosphaeria maculans* (Bohman et al., 2004; Staal et al., 2006). Additionally, the *pad3* mutant demonstrated no differences in plant susceptibility to various strains of the hemibiotrophic *Pseudomonas syringae,* highlighting that accumulation of camalexin does not always correlate with pathogen resistance (Glazebrook et al., 1997a/ 1997b; Zhou et al., 1999, Bednarek, 2012). Although the accumulation of camalexin was not believed to be required for interactions with beneficial microbes, evidence has shown how rhizobial plant symbionts can modulate plant immune systems to launch an effective defense response in the means of priming against oncoming pathogenic threats (van de Mortel et al., 2012; Pangesti et al., 2016; Aziz et al., 2016; Verhagen et al., 2010; Koprivova et al., 2019; Koprivova et al., 2020). It was also suggested after examination of camalexin content in *Arabidopsis* plants induced by PGPB, *Pseudomonas fluorescens* sp. CH267, that plant innate immunity may not be the only role of camalexin but that the metabolite may also function in shaping the root associated soil microbiota (Koprivova et al., 2019; Jacoby et al., 2021). Beneficial bacteria *Pseudomonas simiae* WCS417r and *Pseudomonas fluorescens* SS101, for instance, induced accumulation of camalexin in roots and shoots, which subsequently induced ISR against phytopathogenic bacterium *P. syringae* pv. tomato (*Pst*) DC3000 (van de Mortel et al., 2012; Pangesti et al., 2016; Nguyen et al., 2022). Induction of camalexin biosynthetic genes by MAMPs such as bacteria-derived peptidoglycan (Gust et al., 2007), ET-inducing peptide

(Nep1)-like proteins (Qutob et al., 2006), and other mimicking stimuli including, chitosan (Povero et al., 2011), flg22, and cell wall-derived oligogalacturonides were observed (Qiu et al., 2008; Denoux et al., 2008; Millet et al., 2010).

However, the pathway may be more complex than originally thought, as two new genes that encode the isoforms of cytochrome P450 enzymes, *CYP71A27* and *CYP71A28* may also be involved. These two genes were originally identified in 2006 to be expressed in a root and stem specific way, but their function was not explored further (Schuler et al., 2006). They were recently found in a GWAS screen for variation in plant controlled microbiome function determined as microbial sulfatase activity in the rhizosphere (Koprivova et al., 2019). Characterization and detailed analysis of *CYP71A27* suggested its involvement in accumulation of camalexin in plant roots (Koprivova et al., 2019). The mutant *cyp71a27* (*cyp27*) showed a loss of plant growth promoting effect upon inoculation with the PGPB *P. fluorescens* sp. CH267. Additionally, the phenotypes of low sulfatase activity and low camalexin in soil grown roots, which was complemented by exogenous camalexin, was observed in *cyp27*, thus supporting the involvement of *CYP71A27* in the camalexin biosynthesis pathway (Koprivova et al., 2019). *CYP71A27* and *CYP71A28* have sequence similarity to the known camalexin biosynthetic genes *CYP71A12* and *CYP71A13*, moreover, *cyp71A27* showed comparable phenotypes to the mutants *cyp71A12* and *cyp71A13* (Koprivova et al., 2019). These findings along with PlantCyc database's predictions that *CYP71A27* and the related *CYP71A28* may be involved in the conversion of IAOx to IAN strongly attest to the suggestion that CYP71A27 and CYP71A28 are involved in the camalexin biosynthetic pathway, similarly to CYP71A12 and CYP71A13 (Koprivova et al., 2019).

1.2.2 Regulation of camalexin synthesis

Research on camalexin particularly accentuates the complexity of the regulatory mechanisms required for its biosynthesis, which may depend on the specific inducer or infecting pathogen. The biosynthesis of camalexin as a response to microorganisms and other external elicitors is reliant on the expression of various TFs that coordinate an elaborate network of

defense mechanisms involving multiple levels of signalling cascades, some of which are influenced by phytohormones such as SA, JA and ET (Nguyen et al., 2022b). For instance, studies where *Arabidopsis* JA signalling mutants were analysed in response to fungal necrotrophic plant pathogen *A. brassicicola,* suggested that camalexin synthesis was not JA-dependent (Thomma et al., 1999; Van Wees et al., 2003). Per contra, under inoculation with another necrotrophic fungus; *B. cinerea,* JA signalling was found involved in inducing camalexin accumulation (Rowe et al., 2010). JA signalling pathways were also associated with induction and priming of camalexin biosynthesis by the beneficial bacterium *P. simiae* against herbivores (Pangesti et al., 2016). Additional contrasting findings have been obtained, whereby camalexin production was SA-independent (Nawrath and Métraux, 1999; Roetschi et al., 2001) or SA-dependent (Heck et al., 2003; Denby et al., 2005). It was shown that ET signalling mutants had decreased production of camalexin when treated with the bacterial pathogen *P. syringae* or the fungal necrotroph, *A. brassicicola* (Thomma et al., 1999; Heck et al., 2003). Arabidopsis interaction with the mutualist fungus *Piriformospora indica* demonstrated how ABA can negatively regulate camalexin by repression of the genes *CYP71A12* and *WRKY33* (the master regulator of camalexin biosynthesis) (Peskan-Berghöfer et al., 2015). Camalexin synthesis was also suggested to be regulated by *Arabidopsis* miRNA (miR393), induced by flg22, by affecting the auxin signalling, which acts downstream of the ET signalling pathway (Figure 3) (Robert-Seilaniantz et al., 2008). Consistently, the AUXIN-RESPONSIVE FACTOR (*ARF9*) positively regulates camalexin production via activation of *CYP79B2, CYP71A13* and *PAD3* following *Pst* DC3000 infection (Figure 3) (Robert-Seilaniantz et al., 2011). It was found that suppression of auxin signalling resulted in the metabolic flow to be redirected from camalexin to glucosinolate production, for a more effective biotrophic resistance (Robert-Seilaniantz et al., 2008).

Recent works have illustrated regulation of camalexin biosynthesis through mitogen-activated protein kinase (MAPK) cascades. *B. cinerea* infection led to the activation of MAPK3/6 in an ET-independent manner, resulting in the up-regulation of *CYP79B2, CYP71A13* and *CYP71B15*, which in turn induce camalexin biosynthesis (Figure 3) (Ren et al., 2008; Xu et

al., 2008). Recently it was shown that after *B. cinerea* infection, the MAPK3/6 cooperatively functions with the CALCIUM-DEPENDENT PROTEIN KINASE 5 (CPK5) and CPK6 by differential phosphoregulation of WRKY33 activity to regulate camalexin biosynthesis (Zhou et al., 2020). In 2008, Qiu and colleagues showed that following *Pst* DC3000 inoculation, the WRKY33 had regulatory effects on the genes *PAD3* and *CYP71A13* through indirect interaction of another MAP kinase, *MAPK4* (Figure 3) (Qiu et al., 2008). The induction of *MPK4* and subsequent phosphorylation of *MAP KINASE SUBSTRATE 1, MKS1* results in the release of WRKY33 and in turn induces the camalexin biosynthetic genes (Qiu *et al*., 2008; Nguyen *et al*., 2022). Mao et al., (2011) further uncovered that the MAPK kinase (MKK) 4/MKK5-MPK3/6 cascade affected camalexin accumulation by transcriptional activation and phosphorylation of the WRKY33 after infection with *B. cinerea* (Figure 3). Two additional TFs WRKY18 and WRKY40 were also found to be involved in regulating the camalexin biosynthetic gene *CYP71A13* (Figure 3) (Pandey et al., 2010; Meng and Zhang, 2013). Even though these two transcription factors had been reported as negative regulators of MTI (Xu et al., 2006), it appears that they have a dual function, as they have additionally been observed as positive regulators of ETI, along with WRKY33 (Lozano-Durán et al., 2013; Schön et al., 2013; Schweizer et al., 2013). Since then, WRKY33 has been labelled as a condition-dependent master regulator of camalexin and glucosinolate, synthesis especially in response to ETI-eliciting bacterial pathogen *Pst* DC3000 *avrRpm1* and fungal necrotroph *B. cinerea* (Liu et al., 2015; Birkenbihl et al., 2017; Barco and Clay, 2019). Moreover, it was suggested that WRKY33 also initiates a feed-forward regulation of camalexin gene responses *via* the MYB51 (Barco and Clay, 2019; Barco and Clay, 2020). MYB34, MYB51 and MYB122 of the myeloblastosis (MYB) family of TFs have been previously revealed to also regulate camalexin biosynthesis (Frerigmann and Gigolashvili, 2014). In response to treatment with AgNO₃, flg22 and the necrotroph *Plectosphaerella cucumerina,* expression of *MYB51* and *MYB122* but not *MYB34* is up-regulated in *Arabidopsis*, which triggers biosynthesis of camalexin and its accumulation via *trans*-activation of the promoters *CYP79B2/CYP79B3* (Figure 3) (Frerigmann and Gigolashvili, 2014; Frerigmann et al., 2015; Frerigmann et al., 2016).

Another positive regulator of the camalexin biosynthesis pathway is ANAC042, a member of the NAC (NAM/ ATAF1/2 /CUC2) TF family (Saga et al., 2012). It was demonstrated that there were no changes in gene expression of *WRKY33* in the roots of *anac042* mutants, suggesting that ANAC042 functions independently of WRKY33 (Saga et al., 2012). Its regulation seems dependent on the introduced stress as well as the tissue and organ inoculated with the pathogen. Expression of *ANAC042* appears to be dependent on ET and not the JA signalling pathway upon flg22 treatment, which is consistent with flg22-dependent ROS production and ET-dependent expression of FLS2 (Mersmann et al., 2010; Saga et al., 2012; Boutrot et al., 2020). The mutant *anac042* was unable to properly express the biosynthetic responsive genes *CYP79B3, CYP71A12, CYP71A13* and *CYP71B15,* and therefore had reduced camalexin levels compared to the WT, resulting in high susceptibility to *A. brassicicola* infection (Figure 3) (Saga et al., 2012).

It was proposed by Wang and colleagues (2012), that the multifunctional acetyl amido synthetase, GH3.5 (Staswick et al., 2002 and 2005), previously reported to have a dual regulatory role in SA and auxin signalling upon pathogen infection, also played a role in the biosynthesis of camalexin on two levels: by conjugating ICA and cysteine in addition to directly regulating the camalexin biosynthetic genes *CYP79B2, CYP71A12, CYP71A13* and *CYP71B15* (Figure 3) (Zhang et al., 2007 and 2008; Wang et al., 2012). After *B. cinerea* infection, Zhou and colleagues (2022), demonstrated that the biosynthetic genes *CYP71A13* and *CYP71B15* are regulated by the transcriptional complex WRKY33 - ETHYLENE RESPONSE FACTOR 1 (ERF1), which is activated by the ET/JA and MPK3/MPK6 signalling pathways (Figure 3). Another recently discovered MPK3/MPK6-mediated TF regulating camalexin biosynthesis after *B. cinerea* infection was the ETHYLENE-RESPONSIVE ELEMENT BINDING PROTEIN (EBP, also known as ERF72) (Li et al., 2022). EBP was shown to bind to the promoter regions of *CYP71A13, CYP71B15* and *WRKY33* (Figure 3) (Li et al., 2022). ATP-binding cassette (ABC) transporters have also been mentioned to be associated with the regulation of camalexin secretion in the root, this was demonstrated in the mutants *Atabcc5* and *Atabcg37* that produced higher levels of camalexin in roots than wildtype (Badri et al., 2012). The secretion of camalexin was defective in the pleiotropic drug resistance transporters PEN3 and PDR12 double mutant

pen3 pdr12, which also demonstrated severe hypersensitivity to exogenous camalexin application and high susceptibility to *B. cinerea*, suggesting the association of these transporters with camalexin (He et al., 2019). The accumulated knowledge over the decades presents no straightforward and comprehensive answer to how camalexin synthesis, accumulation, and exudation is regulated. The challenge is thus, to further analyse the camalexin biosynthesis pathway and attempt to fill in the gaps, with a greater focus on plant roots. Since new P450 CYPs have been identified (CYP71A27 and CYP71A28) to play a role in producing camalexin, specifically in the roots, the crucial question in how these are regulated and by which TFs they are regulated by will be examined further.
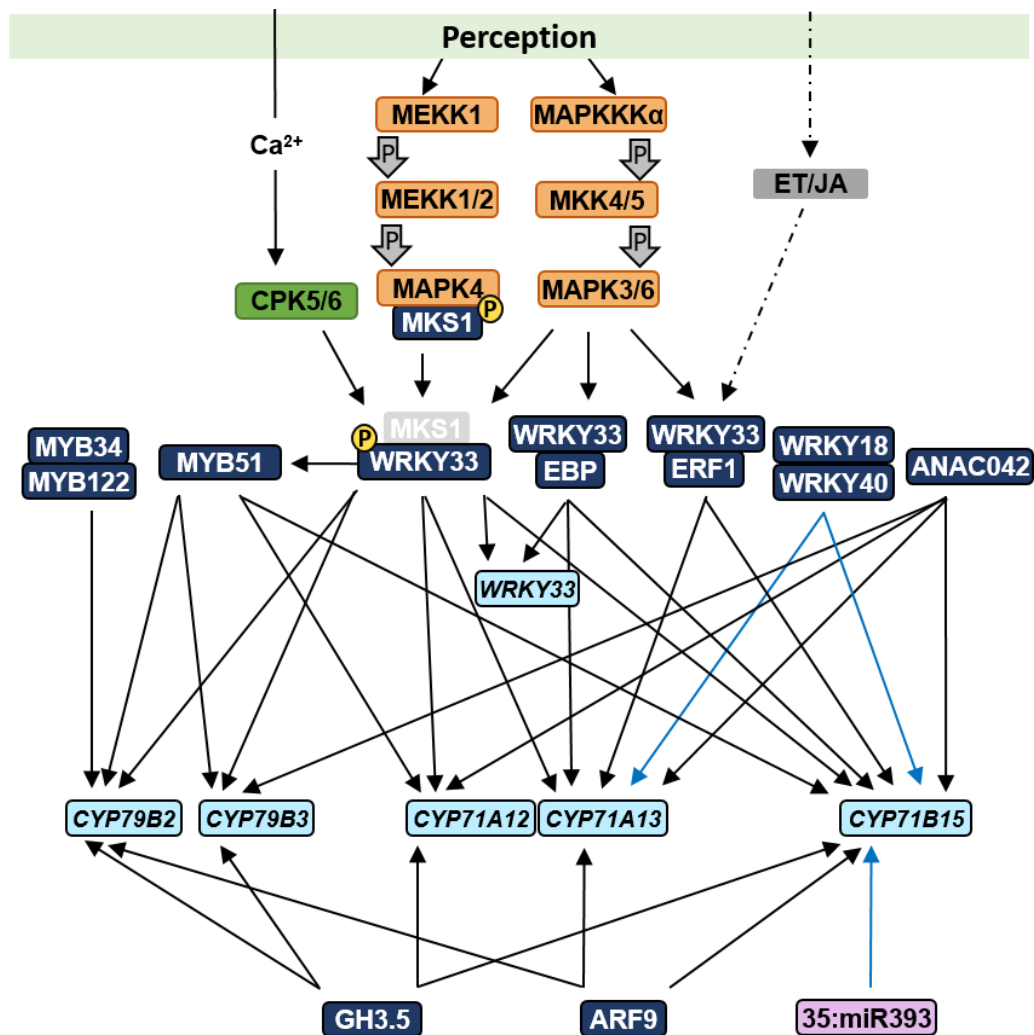
Figure 3: Regulatory network controlling camalexin biosynthetic genes. Simple schematic of a summary of TFs (dark blue), miRNA (light purple), mitogen-activated protein kinases (orange), calcium-dependent protein kinase (in green), hormone signalling pathway ET/JA (grey). Black dashed lines indicate multiple steps that occur in between. Associated with interacting (black arrows) and suppressing (blue arrows) gene transcripts (light blue) GH3.5 (also known as WES1) and EBP (also known as ERF72) (Li et al., 2022; Nguyen et al., 2022b; Zhou et al., 2022).

1.3 Transcription factors relevant for the study

1.3.1 MYB

MYB TFs represent one of the largest protein families in plants (Riechmann and Ratcliffe, 2000). The first plant *MYB* gene (*COLORED1; ZmMYBC1*) was isolated from *Zea mays* in 1987 (Paz-Ares et al., 1987). MYB TFs have a conserved N-terminal DNA binding region known as the MYB domain, which is composed of three imperfect repeats, of highly conserved 52 amino acid residues each, that participate in binding DNA and a variable C-terminal responsible for regulatory activity (Lipsick, 1996; Stracke et al., 2001). The second and third repeats can form a helix-turn-helix (HTH) structure with three regularly spaced tryptophans creating a hydrophobic core that recognizes specific DNA sequences (Ogata et al., 1996). Plant MYB proteins have been classified into four major groups based on the number and position of repeats: 4R-MYB, R1R2R3-MYB, R2R3-MYB and R1-MYB (Rosinski and Atchley, 1998; Jin and Martin, 1999; Stracke et al., 2001; Dubos et al., 2010).

The largest MYB group in plants is the R2R3-MYB subfamily (Rosinski and Atchley, 1998), participating in diverse roles such as control of primary and secondary metabolism, cell fate and identity, plant development and responses to biotic and abiotic stresses (Yanhui et al., 2006; Dubos et al., 2010). Within the R2R3-MYBs, the MYBs have been further divided into subgroups and within the subgroups, paralogs have been identified to control the same metabolic pathway in different cell types (Stracke et al., 2007). For instance, genes in the S6 subfamily are associated with anthocyanin biosynthesis and secondary cell wall formation, S22 subfamily MYBs respond to droughts and pathogen invasion, etc (Stracke et al., 2001; Feller et al., 2011). In general, most MYBs have been identified in the shoots with studies on roots being slightly neglected until recently (Chen et al., 2022).

The R2R3-MYBs MYB34, MYB51 and MYB122 in the subfamily S12 regulate the biosynthesis of indolic glucosinolates and, in addition, seem to positively regulate camalexin

biosynthesis (Stracke et al., 2001; Gigolashvili et al., 2004; Frerigmann and Gigolashvili, 2014; Frerigmann et al., 2015; Frerigmann et al., 2016). Very few plant TFs have been identified to have a dual function in regulation; to act as both transcriptional activators and repressors, depending on the DNA binding sequences or interaction with co-factors. Some that have been identified are WRKY33 in camalexin and ABA biosynthesis, WRKY53 in leaf senescence and in terms of MYBs, MYB51 has also been reported to have dual functionality by activating *CYP79B2* and *CYP79B3* expression to increase flux of IAOx to ICN (indole-3-carbonylnitrile) and repressing *CYP82C2* expression to decrease flux of ICN to 4OH-ICN (4-hydroxy-ICN) (Barco and Clay, 2020).

1.3.1.1 The R2R3-MYB; MYB67

The putative transcription factor MYB67 (*AT3G12720*) previously named ATY53 is another member of the R2R3-MYB family, its predicted structure by AlphaFold can be seen in Figure 4. MYB67 is classified into subfamily S13 and has 11 paralogs, including MYB61, MYB83 and MYB103, which have been reported to be associated with secondary cell wall biosynthesis (Öhmanet al., 2013; Geng et al., 2020). According to BioGrid, experimental data from yeast-two hybrid assays have shown six interactors with MYB67, these were: RVE1, EIL2, ERF107 (Trigg *et al.*, 2017), AT3G28715 (Braun et al., 2011), CYCA2;3 and AT5G57860 (Braun et al., 2011; Altmann et al., 2020), other predicted protein-protein interactions from eFP Browser can be seen in Supplemental Figure S1E.
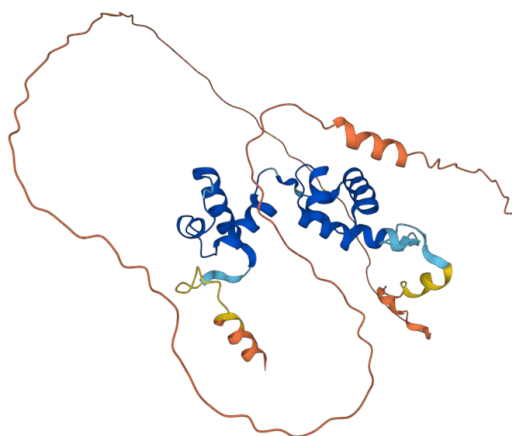
Figure 4: Predicted three-dimensional structure of MYB67 by AlphaFold. The model confidence is according to a per-residue confidence score (pLDDT, 0 - 100), by colour: ■ very high (p-LDDT > 90), ■ confident (90 > p-LDDT > 70), ■ low (70 > p-LDDT > 50) and ■ very low (p-LDDT < 50).

Tissue specific expression patterns from databases such as Cell Type Specific Arabidopsis eFP Browser (Waese et al., 2017) revealed the expression of *MYB67* to be predominantly in the seeds and roots (Supplemental Figure S2). The expression pattern of *MYB67* inferred from ePlant Visualization Tool illustrated its involvement in plant triggered immunity. Up-regulated expression of *MYB67* can be seen 10 hours post infection (hpi) with the plant pathogenic nematode; *Heterodera schachtii,* also known as the beet cyst eelworm (Figure 5A). *MYB67 in silico* expression was also apparent under treatment with both virulent and avirulent strains of the well known gram-negative bacterial pathogen, *Pseudomonas syringae* (Figure 5, C & E). From all elicitors tested by the Nuernberger laboratory, *MYB67* was expressed the highest upon treatment with flg22 (Figure 5D). Even upon inoculation with the well documented fungus-like microorganism, known to cause potato blight; the oomycete, *Phytophthora infestans,* the transcript was shown to be elevated (Figure 5B).
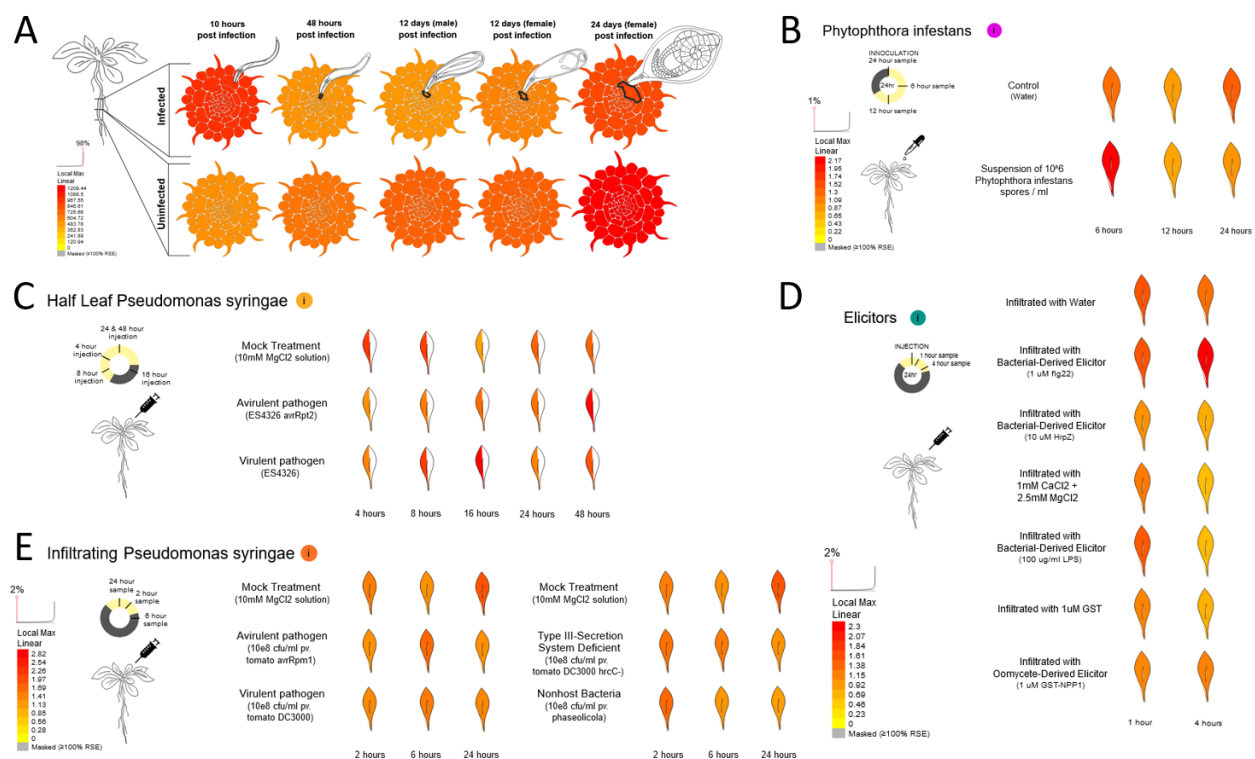
Figure 5: *In silico* expression pattern of *MYB67* upon biotic stresses. Biotic Stress eFP at bar.utoronto.ca/eplant by Waese et al., 2017. Average of data values are shown. *A. thaliana* plant material was used. **A:** *H. schachtii* eFP from RNA-seq data. **B:** Results generated by the Scheel Lab. 5 week old Col-0, for treatment plants were grown at 20°C day/18°C night, 8/16 hour (h) light/dark conditions. For treatment 10 ul-drops were placed per leaf. Measurements were in triplicates. **C:** Results generated by the Dong Lab. 4 week old Col-0, plants were grown under 16/8 h light/dark conditions. Half of a plant leaf was injected with *P. syringae*, while the other half was collected on a time course for analysis. Measurements were recorded in duplicates. **D:** Results generated by the

Nuernberger Lab. 5 week old Col-0, plants were grown under 8/16 h light/dark conditions. Samples were infiltrated with elicitors in triplicates. **E:** Results provided by the Nuernberger Lab. 5 week old Col-0, plants were grown under 8/16 h light/dark conditions and transferred to 16/8 light/dark conditions for the treatment with *P. syringae*. **B-E:** RNA was isolated and hybridised to the ATH1 GeneChip, normalised by GCOS normalisation, TGT 100. This study is part of the AtGenExpress project. **B, D & E:** funded by the DFG. **C:** funded by the NSF.

Usage of the *in silico* database co-expression analysis implicated association of *MYB67* with *CYP71A28,* which has been recently identified to be a part of camalexin biosynthesis network (*CYP71A27* was not present on ATH1 chip) (Figure 6). To examine whether MYB67 binds to the camalexin biosynthesis and regulatory genes, the online tool Plant Regulomics was utilised, a data-driven interface that integrates multi-omics data, including transcriptomic and epigenomic data sets to retrieve upstream regulators of selected genes (Ran et al., 2020). Within 1000 bp upstream of the gene of interest (GOI), MYB67 is predicted to bind to the promoter regions of the camalexin biosynthetic genes *CYP79B2, CYP79B3, CYP71A27,* and *CYP71A28* (Supplemental Table S1). Additionally, MYB67 was also found to bind to the promoter regions of *MYB51* and *WRKY18*, both of which encode transcription factors that are known to regulate the biosynthesis of camalexin (Supplemental Table S1). Preliminary data showed that *myb67* showed lower sulfatase activity similar to that of *cyp71a27* (*cyp27*) and *cyp71a28* (*cyp28*), lower transcript levels of *CYP71A27* and *CYP71A28*, in addition to mis-regulation of glucosinolate and camalexin biosynthesis gene expression in comparison to WT Col-0.

Figure 6: Network of genes co-expressed with *CYP71A28*. The network of genes co-expressed with *CYP71A28* was retrieved from the ATTED-II database. Genes encoding transcription factors are identifiable by hexagons, *MYB67* has been highlighted with a blue border.

The *in silico* analyses and co-expression data are indications of MYB67's involvement in the PTI response. This in combination with the predictions from Plant Regulomics for upstream regulators of camalexin specific genes, MYB67 is a good candidate to conduct further analysis in uncovering whether it specifically plays a role in regulating camalexin biosynthesis. Thus, the interest to uncover novel parts of the transcriptional regulatory network of MYB67, to in turn possibly identify new components of the camalexin biosynthetic pathway, specifically in roots.

1.3.2 NAC

The *NAC* gene superfamily is another large group of TFs widespread in plants but not found thus far in other eukaryotes (Riechmann et al., 2000). NAC transcription factors have also been found to have transcriptional control in various processes including development of shoot apical meristem (SAM) (Aida et al., 1997), embryo development (Duval et al., 2002), formation of lateral roots (Xie et al., 2000), leaf senescence (Guo and Gan, 2006), formation of secondary cell wall (Mitsuda et al., 2000), plant hormone control as well as abiotic and biotic responses (Ren et al., 2000; Nakashima et al., 2007; Wang et al., 2009; Wu et al., 2009; Takasaki et al., 2010; Xue et al. 2011; Ji et al., 2014; Mao et al., 2014). The NAC proteins possess a conserved N-terminal NAC domain comprising five subdomains (A-E) of about 150 amino acids and a variable C-terminal transcription regulatory region (Ooka et al., 2003; Jensen et al., 2010; Puranik et al., 2012). Ernst and colleagues, in 2004 provided the first structural template for the N-terminal NAC domain in Arabidopsis, illustrating that the NAC domain consists of a twisted antiparallel β-sheet sandwiched between two helices, that can bind both DNA and other proteins. *ATAF1* was one of the first reported NAC genes involved in both biotic and abiotic stress, its expression was induced by wounding, drought, ABA and pathogen attack (Lu et al., 2007; Jensen et al., 2008; Wu et al., 2009). Many more NAC TFs have been identified to positively or negatively regulate plant immunity in response to biotrophic, hemi-biotrophic and necrotrophic pathogens, explained in great detail in Yuan et al., (2019), including ANAC042, the transcriptional regulator of camalexin.

1.3.2.1 The NAC TF ANAC038

ANAC038 (*AT2G24430*) is another unexplored TF encoding gene depicted in Figure 6 to be co-expressed with *MYB67* and *CYP71A28*. Due to its co-expression with *MYB67*, in addition to evidence from Plant Regulomics predicting ANAC038's binding to *MYB67*, *CYP71A27* and *CYP71B15*, *anac038* was also selected for downstream analysis.

1.4 *Burkholderia glumae* and *Pseudomonas fluorescens*

First described in 1956 in Japan, the seed and soil borne phytopathogenic *B. glumae* is the causal agent for bacterial panicle blight in its host, rice (Goto and Ohata, 1956; Nandakumar et al., 2009; Mizobuchi et al., 2018). *B. glumae* PG1 (also known as BGR1; formerly *Pseudomonas glumae*) has a broad host range and is a gram-negative, aerobic, rod-shaped bacteria, able to grow at 11-40 ℃ but its optimal temperature for growth ranges between 30-35 ℃ (Kurita et al., 1967; Nandakumar et al., 2009; Ham et al., 2011). Crop fields severely infested with *B. glumae* have been reported to result in 75% loss in yield due to reduction in grain weight, sterility of florets, inhibition of seed germination as well as year-to-year transmission of the pathogen due to its seed-borne nature (Trung et al., 1993). Its pathogenicity and virulence factors consist of lipase activity (Ham et al., 2011), release of phytotoxin toxoflavin (Jeong et al., 2003; Kim et al., 2004; Ham et al., 2011), and its flagella driven motility (Kim et al., 2007; Ham et al., 2011). The *B. glumae* PG1 strain used in co-cultivation studies with *A. thaliana* resulted in reduction of plant growth and the mutant *cyp27* was found to be even more susceptible to the root pathogen (Ham et al., 2011; Koprivova et al., 2019).

On the other hand, *Pseudomonas* spp. strains have been utilised in studies on understanding PGPB and their interactions with host plants. Not only are they consistently enriched in the rhizosphere across diverse plant taxa, but strains in this genus have also been found to modulate diverse and beneficially agronomically significant traits (Mendes et al., 2011; Bulgarelli et al., 2012). This includes traits such as plant growth, herbivore resistance, direct

competition with pathogens through release of antimicrobial compounds as well as modulating plant systemic defenses (Pieterse et al., 1996; Van Oosten et al., 2008; Couillerot et al., 2009; Vacheron et al., 2013). *Pseudomonas fluorescens* (found in soil and water) are also gram-negative, rod shaped bacteria that possess multiple flagella and grow optimally between 25-30 ℃ (David *et al.*, 2018). One of the most well known beneficial *Pseudomonas* strains is WCS417 (formerly *P. fluorescens,* now *P. simiae*) (Pieterse et al., 2021). Haney and colleagues (2016a) have demonstrated via full length 16S rRNA sequence, that the *P. fluorescens* sp. WCS417 is ~ 97 % identical to *P. fluorescens* sp. CH267, which was isolated from roots of wild *Arabidopsis* plants (Haney et al., 2016a). Arabidopsis plants inoculated with *P. fluorescens* sp. CH267 and WCS417 were shown to have enhanced resistance against the cabbage looper herbivore (*Trichoplusia ni*), but the enhanced resistance in CH267 came at the cost of defense and resulted in susceptibility against a bacterial pathogen (Haney et al., 2016b). It was suggested that camalexin is required for beneficial plant root-microbe interactions since *P. fluorescens* sp. CH267 was illustrated to only promote growth in wild-type (WT) plants but not in nine *Arabisopsis* accessions with variation in the amino acid sequence of *CYP71A27* (Koprivova et al., 2019).

1.5 Aims

Accumulation and exudation of specialised metabolites are integral for plant-microbe interactions and their tradeoff between plant development and defense. So far, only a few transcription factors have been identified to regulate the biosynthesis of camalexin after exposure to both pathogenic and plant growth promoting microbes. The *in silico* and *in vivo* performed preliminary research substantiates MYB67's potential role as a mediator of camalexin biosynthesis. Therefore, my thesis aims are:

1. **To characterise MYB67's function** by determining whether the loss of *MYB67* in *A. thaliana* affects the induction of camalexin synthesis by the pathogenic strain *B. glumae* PG1 and the PGPB *P. fluorescens* sp. CH267. MYB67 and related TF mutants were analysed by measuring camalexin content via HPLC and expression of camalexin biosynthetic genes by qRT-PCR. Additionally, histochemical (GUS) staining assisted in further characterisation of *MYB67* and its influence on *CYP71A27* spatial expression upon biotic and MAMP elicitor treatments.

2. **To compare the transcriptional responses of the roots to inoculation with a pathogenic and PGP bacteria and to determine the contribution of MYB67 to the responses.** Verification of the RNA-seq was achieved by qRT-PCR and mutants of MYB67's target genes were also tested with *B. glumae* and *P. fluorescens* to assess their influence on camalexin biosynthesis.

In summary, this PhD thesis provides new insights into the transcriptional changes upon biotic perturbation with *B. glumae* and *P. fluorescens* and the regulatory network of MYB67 as well as its role as a negative regulator of camalexin biosynthetic genes.

2 │ RESULTS

The *in silico* analyses and co-expression data are indications of MYB67 involvement in the PTI response and with the addition of predictions from Plant Regulomics for upstream regulators, MYB67 is a good candidate to conduct further analysis in uncovering whether it specifically plays a role in regulating camalexin biosynthesis. Thus, the interest to uncover novel parts of the transcriptional regulatory network of MYB67, to in turn possibly identify new components of the camalexin biosynthetic pathway.

2.1 Spatial expression pattern of *ProCYP71A27:GUS* alters upon the loss of *MYB67*

Koprivova and colleagues (2019) found significant differences of the *CYP71A27* expression pattern between mock and *P. fluorescens sp.* CH267 treated roots already after 24 h inoculation. To analyse the expression patterns of *MYB67* and to test if the loss of MYB67 affects the *CYP71A27* expression pattern, Col-0 and *myb67* transgenic plants were transformed with the *GUS* gene driven by the promoter of *MYB67* or *CYP71A27,* respectively. Two independent lines were used for expression analysis of *MYB67*.

To visualise potential changes in the expression of the genes, these lines were treated for 24 h with either *B. glumae* PG1 or *P. fluorescens sp.* CH267; the pathogenic and PGP bacteria, respectively (used in our group as biotic stress inducers of camalexin synthesis). As shown in Figure 7, under mock conditions both *ProCYP71A27* and *ProMYB67* were expressed in the stele of the root up until the transition zone. Supplemental Figure S3 also showed that *ProCYP71A27* was additionally expressed in the hypocotyl and throughout the maturation and elongation zone of the root. *ProMYB67* was not expressed in the hypocotyl but strongly visible in the region of the shoot apical meristem (SAM), throughout the root maturation and elongation zone, as well as defined spots at the base of newly forming lateral roots (Supplemental Figure S3). There were no changes upon treatments of the expression patterns of *GUS* under control of the promoters in

other tissues (Supplemental Figure S3). Even under the mock condition there was a stronger blue stain in *ProCYP71A27:GUS myb67* in comparison to *ProCYP71A27:GUS,* suggesting that MYB67 influences the expression of *CYP71A27* (Figure 7 and Supplemental Figure S4). Upon inoculation with *B. glumae* PG1, the *ProCYP71A27* expression pattern in the *myb67* mutant compared to mock appears to have more intense blue and is slightly closer to the root tip. In comparison to the transgenic line expressing *ProCYP71A27:GUS* in the WT the expression of *ProCYP71A27:GUS myb67* appears significantly closer to the root tip; this difference is not clearly seen under mock conditions. Indicating that *MYB67* affects the expression pattern of *CYP71A27* under *B. glumae* stress.

When exposed to *P. fluorescens sp.* CH267, the expression of *MYB67* was no longer present in the stele but in 'patches'. The expression pattern of *ProCYP71A27:GUS* in *myb67* in comparison to the WT upon *P. fluorescens* was stronger than in mock (Figure 7 and Supplemental Figure S4). The results suggest that both bacteria influence the spatial expression of *CYP71A27* upon the loss of *MYB67*. Furthermore, interestingly the expression pattern of *ProMYB67:GUS,* appears to be transient upon treatment with flg22, with stronger expression at 2 hours post treatment (hpt) (Supplemental Figure S4). At this time-point, the expression pattern of *ProCYP71A27:GUS* was quite weak; however, the expression pattern of *ProCYP71A27:GUS* is significantly enhanced in the *myb67* mutant (Supplemental Figure S4B). The expression of *ProCYP71A27:GUS* also appears to be stronger and closer to the root tip in the time points 30 min and 1 hpt with flg22 (Supplemental Figure S4). Suggesting again, that MYB67 influences expression of *CYP71A27*.
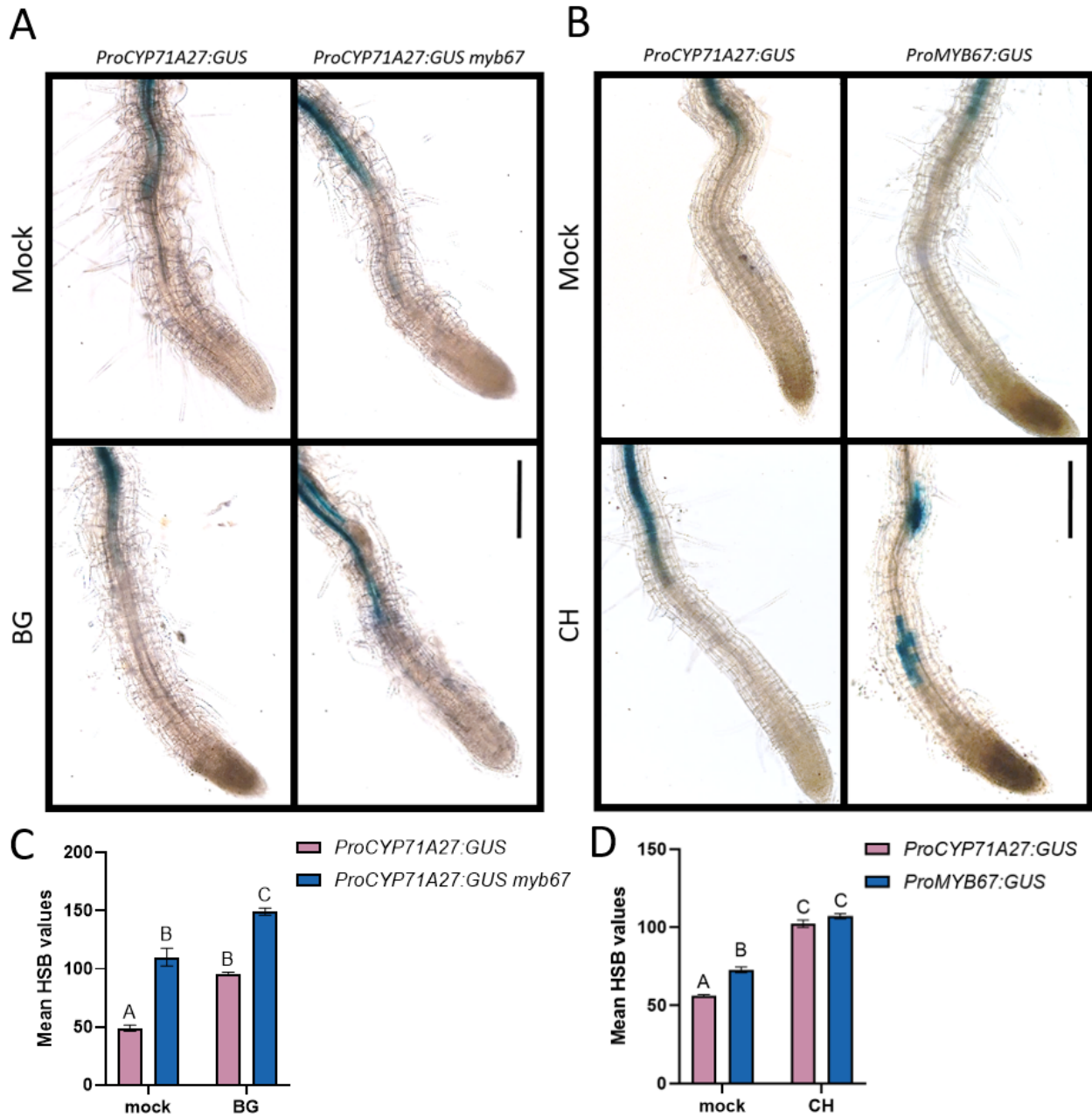
Figure 7: Expression patterns of *ProCYP27:GUS, ProMYB67:GUS* and *ProCYP27:GUS myb67* in response to biotic stresses. Five-day-old seedlings were transferred to ½ Murashige and Skoog (MS) liquid media, then the six-day-old seedlings were treated with 10 mM $MgCl_2$ (mock), (**A**) *B. glumae* PG1 (BG; OD_{600} = 0.04) or (**B**) *P. fluorescens sp.* CH267 (CH; OD_{600} = 0.04) for 24 h and collected for GUS staining. **A&B** are two separate experimental sets. Scale bar, 100 µm, at least 10 independent roots were stained and analysed. **C&D:** Quantification of GUS activity of A & B, respectively, as seen in Béziat et al., (2016). Student's *t*-test p-value <0.05.

2.2 Temporal and spatial camalexin synthesis and exudation in *myb67* upon pathogenic and PGPB induction

For the last three decades, camalexin synthesis, accumulation and exudation have been studied with eliciting agents such as $AgNO_3$ (Schuhegger et al., 2006), synthetic flagellin (Millet et al., 2010) as well as exposure to various microorganisms. Some of these microorganisms that have been reported to induce camalexin synthesis in *Arabidopsis* roots were the root fungal pathogen *Verticillium longisporum* (Iven et al., 2012), the root infecting oomycete *Pythium sylavticum* (Bednarek et al., 2005), the bacterial pathogen *Pst* DC3000 (Bednarek, 2012) as well as the PGPB *P. fluorescens sp.* CH267 (Koprivova et al., 2019).

To evaluate whether the synthesis of camalexin and its exudation triggered by the pathogenic rhizobacteria *B. glumae* PG1 (Gao et al., 2015) and the PGPB, *P. fluorescens sp.* CH267 (Haney et al., 2016a; Koprivova et al., 2019), is affected in *myb67*, the seedlings were grown hydroponically and inoculated via liquid media. Figure 8A illustrates the temporal accumulation of camalexin in the shoot tissue induced by both bacteria, with *B. glumae* elicited plants accumulating more camalexin than *P. fluorescens* inoculated seedlings after the time point 48 hpi. The mutant *myb67* under treatment with the pathogen accumulated ca. 2300 pmol camalexin g^{-1} fresh weight (FW) at 72 hpi, whereas the WT Col-0 reached 1500 pmol g^{-1} FW, thus the *myb67* accumulated 36.5% more camalexin than the WT (Figure 8A). At 96 hpi, *myb67* had 34.6 % more camalexin than the WT. Even inoculation with the PGPB *P. fluorescens* resulted with *myb67* accumulating 33.5 % more camalexin than the WT at 72 hpi (Figure 8A). Unlike treatment with the pathogen, treatment with *P. fluorescens* at 96 hpi was not distinguishable between the genotypes, however, at 120 hpi, *myb67* produced 62.6 % more camalexin than the WT (Figure 8A).

The relative expression of camalexin synthesis genes was analysed to determine whether loss of MYB67 affects their regulation. RNA was extracted from root samples harvested at 72 hpi as at this time point, significant differences between the mutant and WT under treatment

with both bacteria were depicted. Transcript levels of *CYP71A12, CYP71A27* and *CYP71B15* were higher in *myb67* compared to the control under both bacterial treatments (Figure 8B). *CYP71A13* transcript levels were down-regulated in *myb67* compared to WT when treated with *P. fluorescens* but elevated with *B. glumae;* interestingly the opposite was true for transcript levels of *CYP71A28* (Figure 8B). Under mock conditions, *myb67* displayed a lower expression of the five camalexin biosynthesis genes than the WT (Figure 8B). Notably, previous data showed that under mock, *myb67* accumulated significantly higher amounts of camalexin in comparison to the WT Col-0 (Supplemental Figure S5).
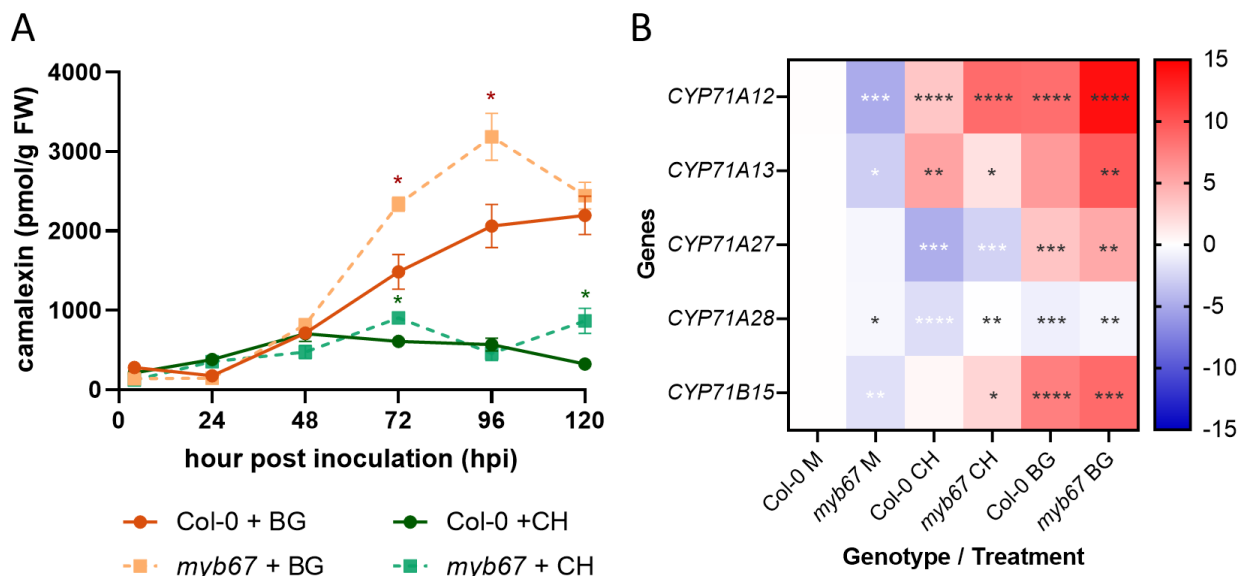
Figure 8: Camalexin accumulation and expression of camalexin synthesis genes in Col-0 and *myb67* upon *B. glumae* PG1 and *P. fluorescens sp.* CH267 inoculation. Col-0 (WT) and *myb67* plants were grown on a nylon net in hydroculture for 7 days and were inoculated with 10 mM $MgCl_2$ (M; mock), *B. glumae* PG1 (BG; OD_{600} = 0.0005) or *P. fluorescens sp.* CH267 (CH; OD_{600} = 0.0001) and harvested at different time points. **A**: time course of camalexin accumulation measured by HPLC in shoots. **B**: Gene expression of camalexin synthesis genes of root samples at 72 hpi. Relative gene expression ($2^{-\Delta\Delta Ct}$) displayed in $\log_2$ Fold change (FC) was determined by qRT-PCR. The housekeeping gene *TIP41* served as a reference and values were compared against Col-0 mock. Data represented as means ± SEM from 4 biological replicates, each corresponding to at least 30 seedlings. Asterisks indicate significant differences against the control (*$p<0.05$, **$p<0.01$, ***$p<0.001$ and ****$p<0.0001$, Student's *t*-test).

Camalexin synthesis and exudation in response to *B. glumae* PG1 has recently been discovered to be coordinated between roots and shoots (Koprivova et al., 2023). Furthermore, camalexin synthesis was shown to be correlated in all three compartments: shoots, roots and exudates. To assess whether loss of MYB67 affects the accumulation of camalexin upon

bacterial treatment, shoots, roots and exudates of hydroponically grown seedlings of *myb67* and the WT Col-0 were analysed (Figure 9). Camalexin synthesis was elicited in all three compartments by both bacteria in WT Col-0 and the mutant *myb67* (Figure 9 A & B). The accumulation of camalexin induced by the bacteria differed between genotypes, but was distributed similarly amongst compartments. In Col-0 samples, 55.5 %, 37.8 % and 6.7 % of the total camalexin produced after treatment with the pathogenic strain were found present in shoots, roots and exudates, respectively. A similar distribution was observed after treatment with the PGPB with 59.7 % in shoots, 34.7 % in roots and 5.6 % in exudates. Comparably, the mutant *myb67* had a accumulated camalexin distribution of 54.6 % (shoots), 38.5 % (roots) and 6.91 % (exudates) when treated with the pathogen, and 59.7 % (shoots), 35.4 % (roots) and 4.94 % (exudates) when co-cultivated with the PGPB. In comparison to WT Col-0, *myb67* inoculated with *B. glumae* accumulated 58 %, 61.2 % and 62.3% more camalexin in shoots, roots and exudates, respectively. *myb67* inoculated with the PGPB increased camalexin accumulation by 71.5 %, 73.3 %, and 59.7% in shoots, roots, and exudates, respectively, compared to WT Col-0.
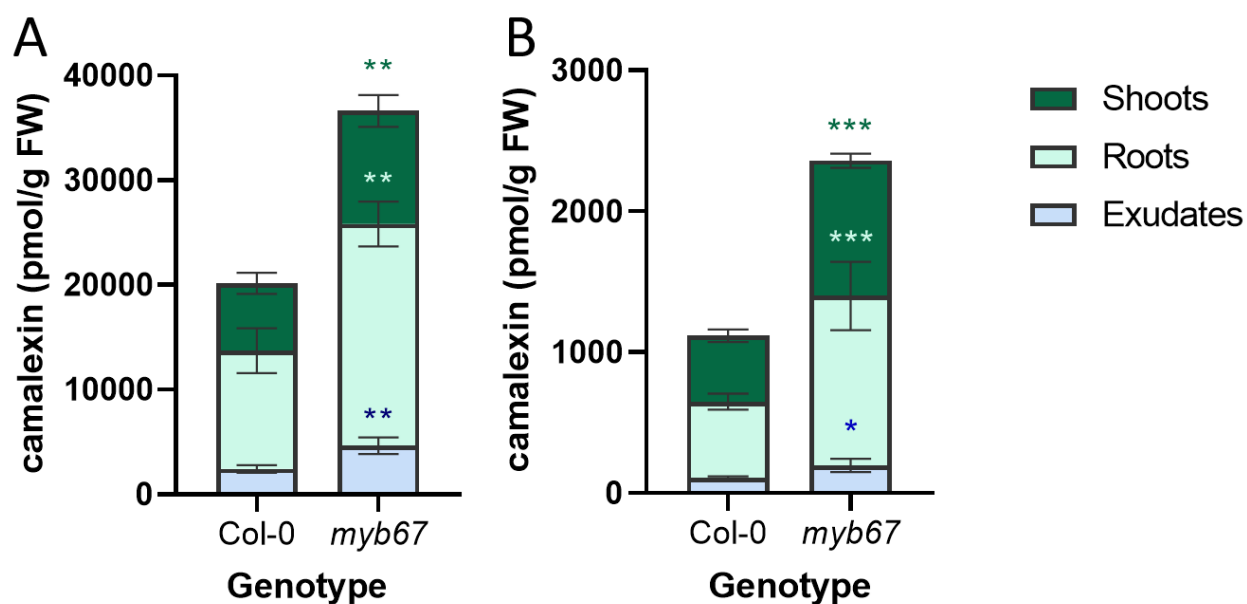
Figure 9: Spatial distribution of camalexin induced by *B. glumae* PG1 and *P. fluorescens sp.* CH267 in WT and *myb67*. Col-0 (WT) and *myb67* plants were grown on a nylon net in hydroculture for 7 days and were inoculated in the solution with 10 mM $MgCl_2$ (mock), (**A**) *B. glumae* PG1 (BG; OD_{600} = 0.0005) or (**B**) *P. fluorescens sp.* CH267 (CH; OD_{600} = 0.0001), harvested 3 dpi. Data represented as means ± SEM from 4 biological replicates, each corresponding to at least 30 seedlings. Asterisks indicate significant differences against the WT (*$p<0.05$, **$p<0.01$ and ***$p<0.001$, Student's *t*-test). A calibration curve of external standards were utilised to determine the camalexin amount in the samples.

2.3 The mutant *myb67* has increased resistance to *B. glumae* PG1 and utilises the growth promoting effect caused by *P. fluorescens sp.* CH267 more effectively than wild type

Despite the limitations that accompany the traditional co-cultivation methods on agar plates, one advantage is the ability to quantify changes in the fresh weight (FW) of single seedlings in response to various treatments. To evaluate whether the loss of *MYB67* affects plant growth, the mutant and wildtype were cultivated on ½ MS media containing sucrose before being transferred to Hoagland media supplemented with pathogenic or PGP bacteria for 14 days. To determine the difference in growth between the mock and each treatment, the total FW of each seedling was measured. Camalexin was extracted and measured by HPLC from both shoot and root tissue, providing insight into the accumulation of the phytoalexin in each tissue when co-cultivated with the bacteria on agar plates. In 2019, Koprivova and colleagues illustrated *B. glumae*'s effect of inhibiting growth in Col-0. This response was clearly apparent in WT Col-0 seedlings when accompanied by the pathogenic strain *B. glumae,* resulting in 65.6 % smaller seedlings; this impaired growth was visible as seedlings not only had smaller shoots, but shorter and slightly brownish roots (Figure 10A). After *B. glumae* inoculation, the mutant seedlings resembled the WT but were 59% smaller compared to *myb67* mock (Figure 10A). Camalexin levels in *myb67* shoots upon pathogenic stress were 68.7 % higher than in WT Col-0 (Figure 10B). In contrast, *myb67* roots had 40.2 % less camalexin than the WT (Figure 10C). In comparison to the pathogenic strain the PGPB inoculated seedlings overall accumulated less camalexin in the root tissue (Figure 10C). The total FW of the *B. glumae* treated seedlings being higher in the mutant compared to the WT suggests that *myb67* has increased resistance to *B. glumae*'s growth inhibition in comparison to the WT.
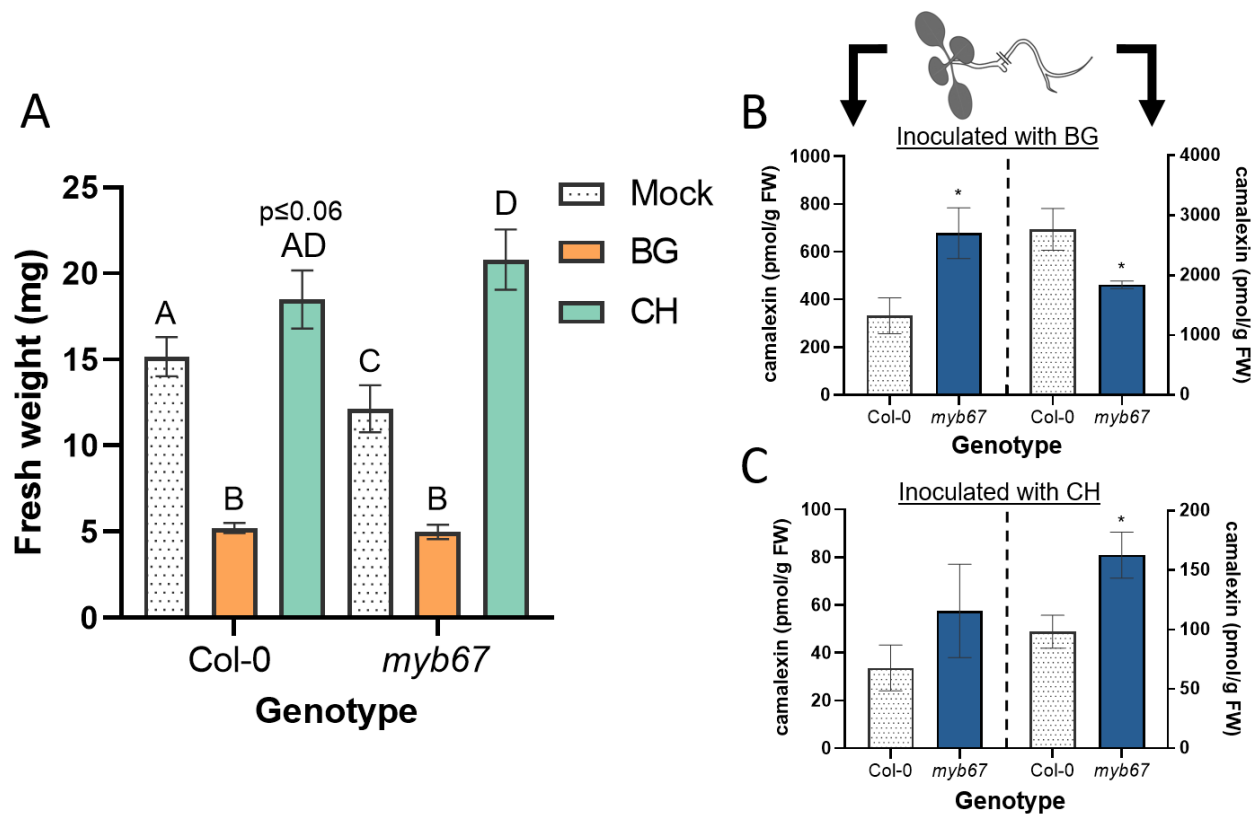
Figure 10: Traditional co-cultivation of Col-0 and *myb67* with *B. glumae* PG1 and *P. fluorescens sp.* CH267. Six-day-old Col-0 (WT) and *myb67* seedlings were transferred to Hoagland media supplemented with 10 mM MgCl$_2$ (mock), *B. glumae* PG1 (BG; OD$_{600}$ = 0.05) or *P. fluorescens sp.* CH267 (CH; OD$_{600}$ = 0.01) and harvested 14 days post inoculation (dpi). **A:** Fresh weight was measured from a total of ~ 40 seedlings from four independent plates. p-value <0.05. **B&C:** Camalexin content was measured from shoot (left) and root (right) (indicated by seedling schematic) tissue samples by high-performance liquid chromatography (HPLC). **B:** Samples treated with *B. glumae* PG1. **C:** Samples treated with *P. fluorescens sp.* CH267. (asterisk indicates p<0.05, Student's *t*-test). The *Arabidopsis* seedling was drawn using BioRender.com.

Koprivova et al. (2019) recently discovered that camalexin may play a significant role for plants to benefit from PGPB. The growth promoting effect elicited by *P. fluorescens* which was expected in WT Col-0 was not reproducible to a statistically significant level (Figure 10A) (Koprivova et al., 2019). However, the mutant *myb67* displayed a growth promotion with the average fresh weight of *myb67* seedlings treated with *P. fluorescens* being 52.9 % greater than the average FW of *myb67* mock treated seedlings (Figure 10A). Also camalexin accumulated to higher levels in shoots and roots of *myb67* compared to WT (Figure 10 B&C). These results suggest that the loss of MYB67 allows the plant to utilise the growth promotion effect of *P. fluorescens* more effectively.

2.4 High accumulation of camalexin in shoots of *myb67* is triggered by treatment with *B. glumae* and *P. fluorescens* but not flg22

To examine whether the effects of the 22 amino acid fragment of bacterial flagellin (flg22) induces camalexin similarly to the pathogenic and PGP bacterial strains in the genotypes Col-0 and *myb67*. Each bacteria and flg22 were implemented in the hydroponic solution and plant samples were harvested 3 days post inoculation (3 dpi). Preliminarily performed hydroponic assays illustrated a strong correlation of camalexin content in shoots and roots as shown in Figure 9, thus only shoot tissue was utilised to measure camalexin by HPLC. As shown in Figure 11, the shoot tissue of *myb67* accumulated 71.9 % more camalexin than WT Col-0 when treated with the pathogenic bacteria (Figure 11A) and 78.7 % more camalexin upon treatment with PGPB (Figure 11B). There were no differences in the mutant *cyp27* when compared with the WT Col-0. Treatment with the synthetic flg22, illustrated significantly lower camalexin accumulated in both mutants than in the WT, Col-0; *myb67* accumulated 67.5 % less than the WT Col-0 (Figure 11C). The mutant *cyp27* also accumulated 79.8 % less camalexin upon treatment with flagellin. At 3 days post inoculation, it was also evident that the flg22 treatment accumulated the least amount of camalexin in the shoots compared to the other bacterial treatments (Figure 11C).
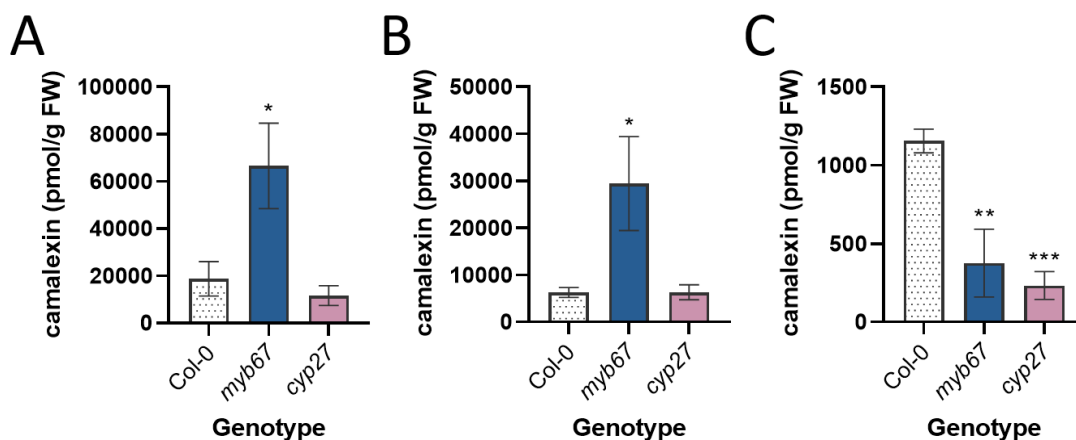
Figure 11: Camalexin induced in the shoots by *B. glumae* PG1, *P. fluorescens sp.* CH267 and flg22 of hydroponically grown WT and mutants. Col-0 (WT), *myb67* and *cyp27* plants were grown on a nylon net in hydroculture for 7 days and were inoculated in the solution with 10 mM $MgCl_2$ (mock), (**A**) *B. glumae* PG1 (BG; OD_{600} = 0.0005), (**B**) *P. fluorescens sp.* CH267 (CH; OD_{600} = 0.0001) or (**C**) 1 µM flg22, harvested 3 dpi. Data represented as means ± SEM from 4 biological replicates, each corresponding to at least 30 seedlings. Asterisks indicate significant differences against the WT (*$p<0.05$, **$p<0.01$ and ***$p<0.001$, Student's *t*-test).

2.5 Early defense response inducers, flg22 and chitin influence camalexin synthesis and PTI gene expression stronger in *myb67* than in Col-0

Since flagellin is known to induce early defense responses, the time point 3 dpi may be too late to detect the peak of camalexin synthesised in response to flg22. Millet et al., (2010) previously demonstrated that camalexin accumulates transiently and rapidly in response to flg22. PTI elicitors such as chitin however, are not well known to induce camalexin, although there have been reports of chitin-induced *CYP71A15* expression and increased induction when chitin treatment is preceded by flg22, highlighting the impact of priming (Giovannoni et al., 2021). Short oligomers (hexamer and heptamer) were shown to be the most effective elicitors of chitinase activity (Roby et al., 1987). As a result, it has become common to use the deacetylated chitosan hexamer, chitohexaose (derived from chitin) as an elicitor to trigger plant innate immunity (Okawa et al., 2003; Ishikawa et al., 2014; Shi et al., 2019; Li et al., 2020). Therefore, how the loss of MYB67 will affect the biosynthesis of camalexin upon application of early plant defense response inducers flg22 and chitin were investigated in a time course manner. Hydroponically grown seedlings were treated with flg22 and chitin in the solution, and the shoots were used to measure the camalexin content. The accumulation of camalexin upon treatment with flg22 was below a detection limit for all time points other than the time point 2 hpt (data not shown). Nevertheless, from the GUS staining of *ProMYB67:GUS* it was seen that flagellin triggered a rapid response and *MYB67* was highly expressed close to the root tip after 2 h incubation with flg22 (Supplemental Figure S4). The loss of this transient expression of *MYB67* may have resulted in the peak in camalexin accumulated at 2 hpt.

Chitosan, a 90 % deacetylated chitin, was reported to induce camalexin after 27 h (Barco, Kim & Clay, 2019). Hence, it was expected to detect camalexin after inoculation with chitin. Camalexin accumulation after chitin treatment was low, similar to treatment with flg22. Nevertheless, chitin-induced camalexin levels were consequently higher in *myb67* shoots

between 4 h and 48 h and decreased to lower levels than WT Col-0 at 72 h (Figure 12A). There were no significant differences at 2 h when inoculated with chitin (Figure 12A).

To elucidate whether transcriptional responses of genes involved in plant immunity were triggered also in the roots, I analysed the expression of *CYP71A12,* a key enzyme responsible for camalexin biosynthesis thus a camalexin marker (Figure 12B; Millet et al., 2010). *myb67* showed higher expression of *CYP71A12* in the control (time point 0) than WT, as expected given the high levels of accumulated camalexin seen in the mock condition (Supplemental Figure S5). At 2 hpt, flg22-induced transcript levels of *CYP71A12* were considerably higher in *myb67* than WT, whereas chitin-treated *myb67* and WT showed no difference in transcript levels. The expression of transcription factor *WRKY33,* a major regulator of SA signalling, ET-JA crosstalk, redox homeostasis and camalexin biosynthesis, was also assessed for early indications of PTI response (Birkenbihl et al., 2012). Similarly, *WRKY33* expression was unchanged at 2 hpt in WT and *myb67* treated with chitin, but induced upon treatment with flg22 (Figure 12C). Interestingly, at 4 hpt, *WRKY33* expression in *myb67* treated with chitin was significantly lower than WT as it was reduced to untreated WT like levels (0 hpt), in contrast *myb67* treated with flg22 had significantly higher *WRKY33* gene expression in comparison to the WT (Figure 12C). In addition, *ANAC042,* which encodes a transcription factor that regulates camalexin production (Saga et al., 2012), was also analysed. Its transcript level in the mutant after both treatments was higher than that of the WT at 2 hpt, however the expression was the same in both genotypes at 4 and 8 hpt. However, at 8 hpt the expression of *ANAC042* differs significantly between treatments (Figure 12D).
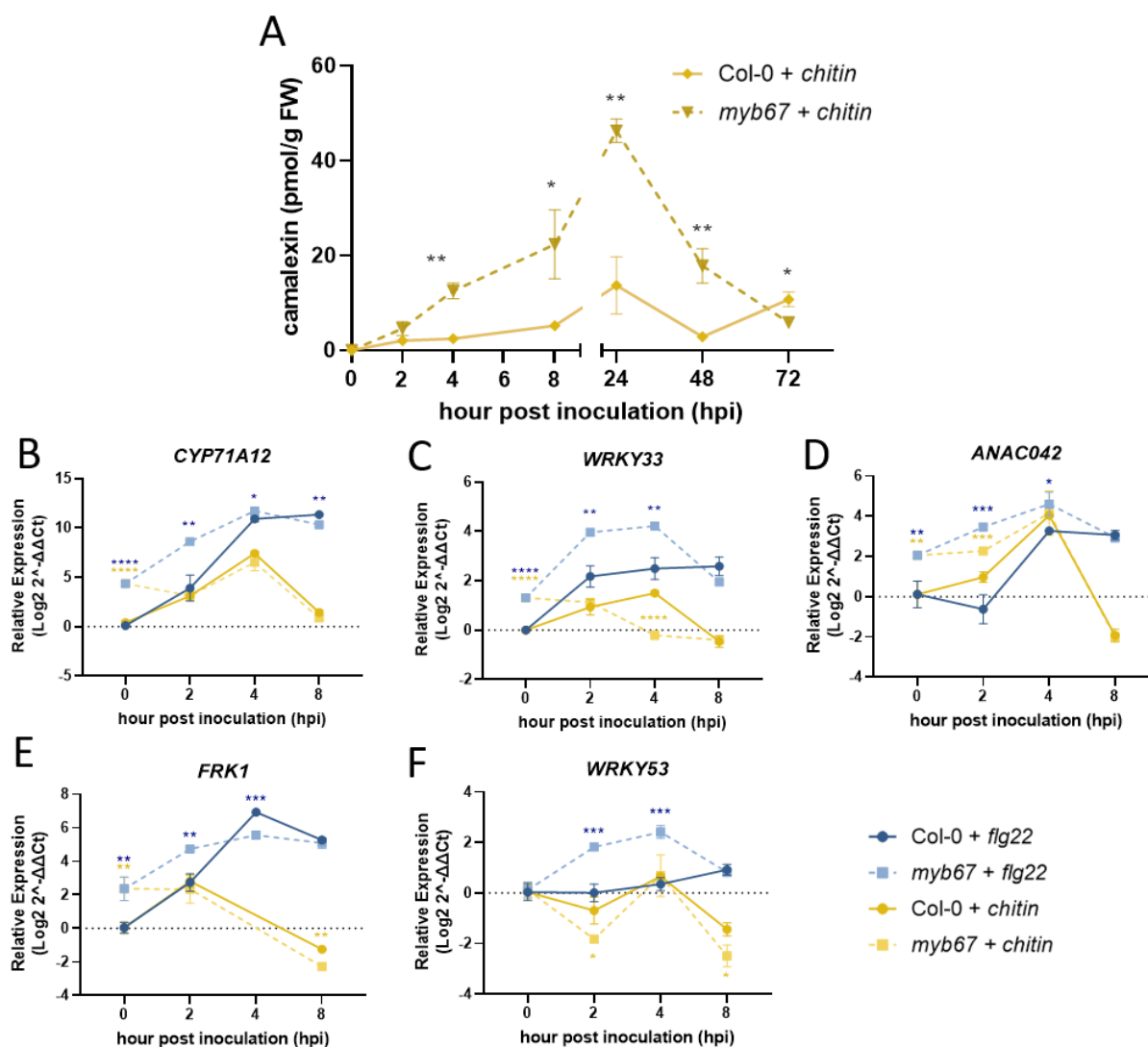
Figure 12: Temporal analysis of camalexin accumulation in the shoots and expression of genes involved in immunity in roots of Col-0 and *myb67* upon flg22 and chitin treatment. Col-0 (WT) and *myb67* plants were grown on a nylon net in hydroculture for 7 days and was treated in the solution with 10 mM MgCl₂ (M; mock), 1 µM flg22 or 1 µM chitohexaose (for the chitin treatment) and harvested in a time course manner. **A:** The time course of camalexin accumulation measured by HPLC was from shoots. Asterisks indicate significant differences against the control (*p<0.05, **p<0.01, Student's *t*-test). **B-F:** Gene expression analysis of root samples at 2 hpi. Relative gene expression ($2^{-\Delta\Delta Ct}$) displayed in log₂ was determined by qRT-PCR. The housekeeping gene *TIP41* served as a reference and values were compared against Col-0 mock. Data represented as means ± SEM from 4 biological replicates, each corresponding to at least 30 seedlings. Different letters represent significant differences of at least p<0.05 (Student's *t*-test).

To examine the transcriptional response to flagellin, the flagellin responsive kinase *FRK1* transcript levels were measured. As expected, *FRK1* was up-regulated by flg22, not only in WT but also in *myb67* at 2 hpt, but unaffected by the chitin treatment in both genotypes until 8 hpt (Figure 12E). The mutant upon flg22 treatment, however, failed to express *FRK1* to the level of

WT at 4 hpt (data for chitin at 4 hpt is unavailable) (Figure 12E). Even though WRKY53 is mainly known for its general role in senescence regulation (Zentgraf & Doll 2019), *WRKY53* expression has been shown to be induced by hydrogen peroxide (Miao *et al.,* 2004; Xie *et al.,* 2014) and SA (Miao et al., 2007; Zentgraf & Doll, 2019) but negatively regulated by JA (Miao et al., 2007, Zentgraf & Doll 2019). Treatment with flg22 and chitin did not affect transcript levels of *WRKY53* in WT Col-0 at 2 and 4 hpi, but it was up-regulated upon flg22 treatment and down-regulated upon chitin treatment at 8 hpt. Opposingly, the expression of *WRKY53* in *myb67* was positively induced by flg22 at 2 and 4 hpt, in contrast, treatment with chitin resulted in fluctuating expression of *WRKY53* with down regulation of the transcript at 2 and 8 hpt (Figure 12F).

Overall, the loss of *MYB67* affected the synthesis of camalexin after treatment with the two elicitors. Only at 2 hpt upon chitin treatment, *myb67* showed no significant differences of accumulated camalexin in comparison to the WT. This was also reflected in the gene expression data with no changes in transcript levels of *CYP71A12* and *WRKY33* with the exception of *ANAC042* between the mutant and WT at 2 hpt. *WRKY33* transcript levels at 4 hpt upon chitin treatment is lower but the accumulation of camalexin in *myb67* is higher than WT, which could suggest that the higher camalexin levels are WRKY33 independent. On the other hand, upon treatment with flg22, the loss of *MYB67* resulted in a higher expression than WT of all genes at 2 hpt. Treatment with chitin in *myb67* affected the genes *WRKY33*, *WRKY53* and *ANAC042*, specifically. Synthetic bacterial and fungal fragments thus induced a transient response to synthesise camalexin in *myb67*. MYB67 appears to modulate camalexin biosynthesis in the early time points by indirect suppression and not through direct binding with *CYP71A12, WRKY33* and *ANAC042* (Supplemental Table S1).

2.6 The NAC & MYB mutants show a similar pattern of camalexin accumulation to that of *myb67*

The MYB family is one of the most abundant transcription factor families in plants, representing about 9% of total TFs in *Arabidopsis* (Reichmann et al., 2000; Peng et al., 2016). MYB proteins have been reported to be structurally and functionally more variable compared to animal homologues (Rosinski & Atchley 1996). In plants, MYB proteins have diverse roles spanning from plant development, growth and regulation of metabolism (Stracke, Werber & Weisshaar 2001; Dubos et al., 2010) to essential roles in abiotic stress tolerance (Li, Ng & Fan 2015), phytohormone signal transduction, and disease resistance (Yanhui et al., 2006; Ambawat et al., 2013). MYBs are also known to have diverse regulatory functions, in roots, this includes managing cell division and differentiation, response to biotic and abiotic stresses, and mediating phytohormone signals (Wang, Niu & Zheng 2021; Chen et al., 2022).

MYB genes from the same subfamily tend to regulate similar biological processes in roots (Chen et al., 2022). Therefore, it was decided to explore additional MYBs in close relation to MYB67 to compare and determine whether they function similarly (Figure 13). The closest MYB related to MYB67 is MYB26, however, it was not included due to its sterility (Yang *et al.*, 2007). Based on T-DNA availability, MYB61, MYB83 and MYB103 were selected for further analysis. MYB61 has been reported to play a role in lignification and photomorphogenesis (Newman et al., 2004; Dubos et al., 2005), deposition of seed coat mucilage (Penfield et al., 2001; Liang et al., 2005), and regulation of stomata function (Romano et al., 2012). *MYB83* has been shown to redundantly regulate the secondary wall biosynthesis in fibers and vessels (McCarthy et al., 2009). *MYB103,* a target of SND1 (secondary wall associated NAC domain protein 1), is responsible for the control of biosynthesis of secondary cell wall, including hemicellulose, cellulose and syringyl lignin (Zhong et al., 2008; Öhmanet al., 2013). Thus, the mutants *myb61, myb83* and *myb103* were obtained from NASC and tested if their response to the pathogen and PGPB would result in similar changes in camalexin synthesis as in *myb67*. Furthermore, included in the analysis was the mutant *anac038*, predicted to have a role in control

of suberin synthesis (Calvo-Polanco et al., 2021) selected due to its co-expression with *MYB67* (as seen in Atted-II, Figure 6).
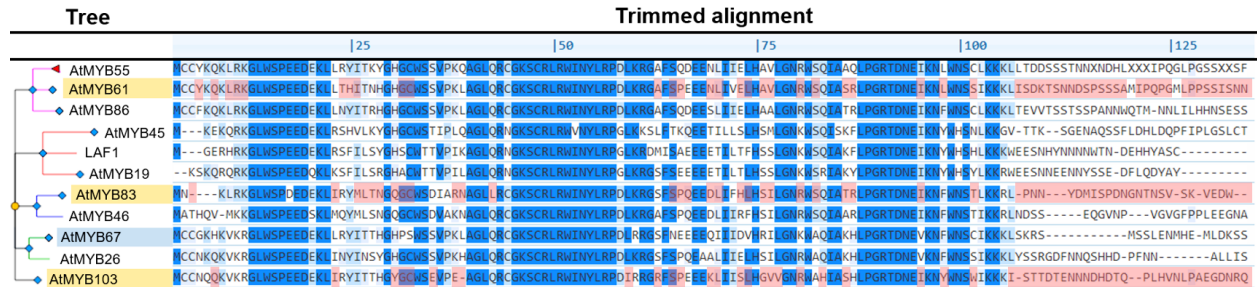
Figure 13: Phylogenetic analysis of MYB67 in the MYB gene family of Arabidopsis. The reduced tree was acquired from PANTHER along with the trimmed alignment of the proteins, to determine MYBs of structural similarity to MYB67 (highlighted in blue). Selected MYBs for further analysis are highlighted in yellow (MYB61, MYB83 and MYB103) highlighted in pink are the locations where they are explicitly different to MYB67 in addition to the dark and light blue for the overlapping amino acids.

Inoculation with *B. glumae* resulted in all mutants to accumulate significantly more camalexin in roots than the WT Col-0 (Figure 14A). Similarly, the amount of camalexin in the exudates was similar across all mutants with exception of *myb61*, with higher amounts than in Col-0. However, in the shoots, only *myb67, nac038, myb61* and *myb83* accumulated at least 50 % more camalexin than the WT Col-0, *myb103* was the only mutant that had significantly lower camalexin accumulated in the shoots.

Upon inoculation with the PGPB, in both shoots and roots, *nac038, myb61, myb83* and *myb103* have a similar response to *myb67* with more camalexin synthesised and accumulated than the WT Col-0 (Figure 14B). Due to variations in the root samples, *myb67* and *myb103* however, are not statistically significant. The exudates show higher amounts of camalexin secreted from the roots of *myb67, myb61* and *myb83,* than WT Col-0, but WT-like levels in *nac038* and *myb103*.
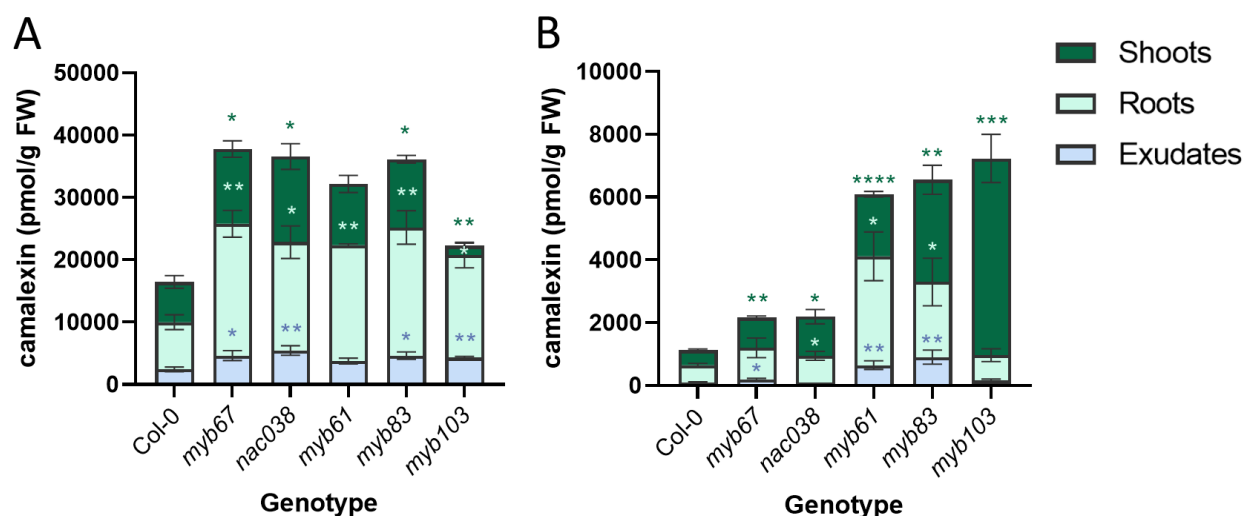
Figure 14: Spatial distribution of camalexin induced by *B. glumae* PG1 and *P. fluorescens sp.* CH267 in WT and mutants. Col-0 (WT) and *Arabidopsis* mutant plants were grown on a nylon net in hydroculture for 7 days and was inoculated in the solution with 10 mM MgCl$_2$ (mock), (**A**) *B. glumae* PG1 (BG; OD$_{600}$ = 0.0005) or (**B**) *P. fluorescens sp.* CH267 (CH; OD$_{600}$ = 0.0001), harvested 3 dpi. Data represented as means ± SEM from 4 biological replicates, each corresponding to at least 30 seedlings. Asterisks indicate significant differences against the WT (*p<0.05, **p<0.01 and ***p<0.001, Student's *t*-test).

The alterations in accumulated camalexin in the other mutants were similar to that of *myb67*, therefore, we also determined the expression of camalexin synthesis genes (Figure 15). As expected, *CYP71A12* transcript levels were elevated in all genotypes as a response to biotic stress (Figure 15A). *myb67* and *nac038* had the highest expression of *CYP71A12* under pathogenic stress, in contrast *myb61* and *myb83* showed less than the WT Col-0; whereas in *myb103* the expression was unchanged (Figure 15A). *P. fluorescens*-induced *CYP71A12* expression, although also elevated, was lower than upon treatment with the pathogen and expression did not differ between the WT Col-0 and *myb67, anac038* and *myb103* (Figure 15A). *CYP71A12* transcript levels induced by the PGPB in *myb61* and *myb83* were significantly lower than in WT Col-0. The transcript levels of *CYP71A13* were the same between the pathogenic and PGP bacteria treated roots of WT (Figure 15B). This was not true for the mutants, with *CYP71A13* transcript levels being up-regulated more upon treatment with the pathogen *B. glumae* than the PGPB *P. fluorescens* (Figure 15B). Interestingly, the mock root samples of the *myb* mutants had a lower expression of *CYP71A13* whereas *anac038* had higher expression when compared to the mock of WT Col-0 (Figure 15B). *myb67* and *anac038* upon pathogenic treatment had comparable levels of *CYP71A13* to that of the WT, whereas *myb61, myb83* and

myb103 were significantly higher. Interestingly, *myb67* failed to induce *CYP71A13* expression upon treatment with PGPB and was similarly expressed to that of WT mock condition. In contrast, *anac038* had significantly higher expression of *CYP71A13* under PGPB inoculation. *CYP71A27* and *CYP71A28* had significantly lower expression than their parallel pair *CYP71A12* and *CYP71A13* (Figure 15). All mutants had lower expression of *CYP71A27* in the mock treatment than the WT (Figure 15C). The treatment with the PGPB resulted in a lower expression of *CYP71A27* than the WT mock but this was unvarying in all genotypes (Figure 15C). The pathogen on the other hand elicited higher expression of *CYP71A27* but only *myb67* and *anac038* had expression levels higher than the WT (Figure 15C). Upon comparison to WT Col-0 mock, *CYP71A28* transcript levels were either down-regulated or unaffected in all genotypes under both bacteria treatments (Figure 15D). Corresponding to *CYP71A12,* expression of *CYP71B15* was also induced in response to the pathogenic bacteria *B. glumae* in all genotypes. Unlike *CYP71A12,* however, treatment with the PGPB did not result in high expression of *CYP71B15* (Figure 15E). *myb67* and *myb103* had a similar pattern, with the PGPB-elicited expression of *CYP71B15* reaching WT mock levels whereas the mock treatment of both mutants already showed a down regulation of the gene in comparison to WT Col-0 mock (Figure 15E). According to the gene expression of the camalexin genes, *nac038* reflects most similarly to *myb67,* whereas *myb61, myb83* and *myb103* under pathogen stress have opposite responses to that of *myb67*. In both treatments, *myb61* and *myb83* are alike in their response across all camalexin biosynthetic genes, suggesting they function similarly. The loss of *myb103* appears to be insignificant when in contact with PGPB, but is comparable to *myb61* and *myb83* when under pathogenic stress.
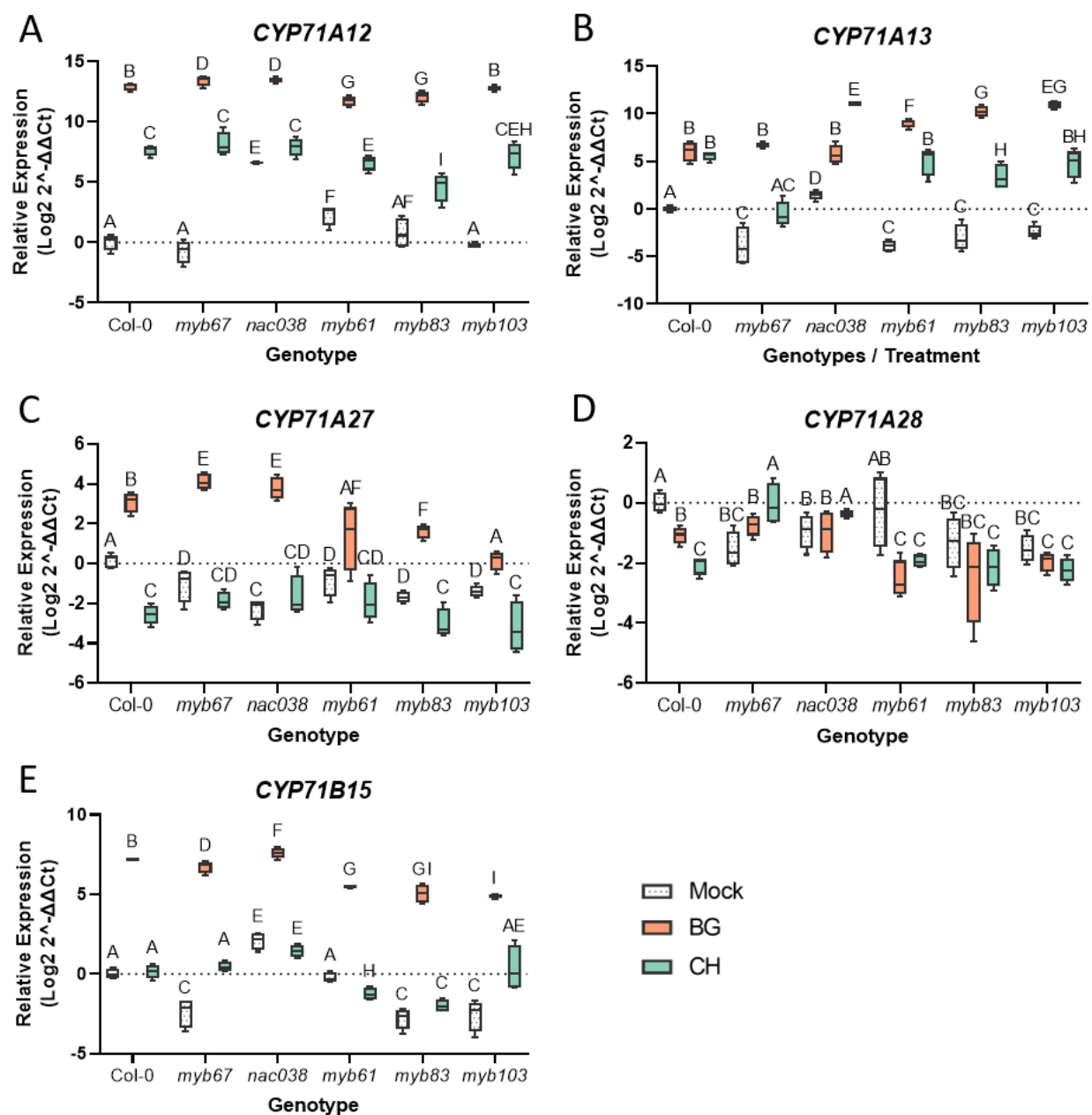
Figure 15: Relative expression of camalexin biosynthesis genes induced by *B. glumae* PG1 and *P. fluorescens sp.* CH267 in the roots of WT and mutants. Col-0 (WT) and T-DNA lines *myb67, nac038, myb61, myb83, myb103* lines were grown on a nylon net in hydroculture for 7 days and were inoculated in the solution with 10 mM MgCl₂ (mock), *B. glumae* PG1 (BG; OD₆₀₀ = 0.0005) or *P. fluorescens sp.* CH267 (CH; OD₆₀₀ = 0.0001), root samples were harvested 3 dpi. Relative gene expression ($2^{-\Delta\Delta Ct}$) displayed in log_2 was determined by qRT-PCR in roots. The housekeeping gene *TIP41* served as a reference and values were compared against Col-0 mock. Data represented as means ± SEM from 4 biological replicates, each corresponding to at least 30 seedlings. The data presented represents at least two independent experimental replicates. Different letters represent significant differences of at least $p < 0.05$ (Student's *t*-test).

2.7 Transcriptional responses in the roots to *B. glumae* and *P. fluorescens* inoculation and the significance of MYB67 in the transcriptional network

The previous chapters showed that loss of MYB67 alters camalexin biosynthesis upon treatments with pathogen and PGP bacteria. In order to analyse the full transcriptional network of MYB67, the mutant and WT were subjected to RNA-seq analysis. RNA was isolated from roots of hydroponically grown WT Col-0 and *myb67* co-cultivated with *B. glumae* PG1 and *P. fluorescens sp.* CH267 (Figure 16A). RNA purity and quality controls showed the integrity number (RIN) of at least 7, with OD260/280 of 1.8-2.1 and OD260/230 > 1.5 for all samples. The obtained read lengths were 150 bp; each file containing the sequenced reads were provided with FastQC quality reports but a second FastQC quality control was conducted after a trimming process to remove the adapters with the tool *trimmomatic* (Bolger et al., 2014). Mapping of the RNA-seq reads to the *Arabidopsis* genome for reference (obtained from TAIR) resulted in high overall alignment efficiencies of over 95 % (Supplemental Table S3).

From the normalised gene expression values, the distribution of the transformed data was checked and a principal component analysis (PCA) was performed to further check the quality and variation of the data (Figure 16 B&C). PC1 represents the largest variation of 62 % and is correlated with mock and *B. glumae* treatment (p=6.48 x 10^{-15}), whereas PC2 is correlated with mock and *P. fluorescens* treatment (p=9.61 x 10^{-13}) (Figure 16 C). Variation between genotypes is represented in PC4 (p=3.13 x 10^{-3}) (Supplemental Figure S6D).
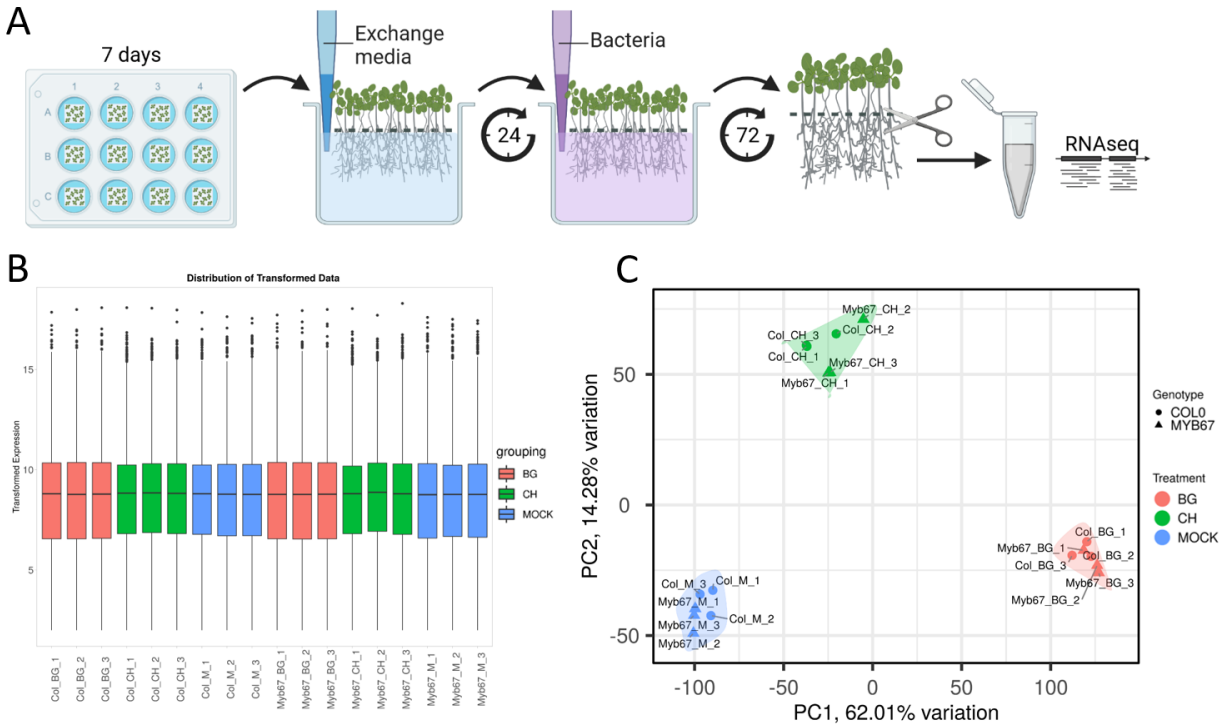
Figure 16: Investigation of transcriptional reprogramming of Col-0 and *myb67* upon *B. glumae* and *P. fluorescens* treatment. A: Schematic representation of the experimental design. Created with BioRender. **B:** Boxplot of the distribution of transformed data across all replicates. Treatments are represented by colour; mock (blue), BG (*B. glumae*- red) and CH (*P. fluorescens*-green). **C:** PCA illustrated in a bi-plot of normalised expression values (log$_2$-transformed counts to transcripts per million (TPM)), depicting PCA1 and PCA2. Genotypes are indicated by circles (Col-0) and triangles (*myb67*), and the treatments mock, BG and CH are indicated by different colours; blue, red and green respectively.

2.7.1 Differentially expressed genes resulting from the transcriptome response to *B. glumae* and *P. fluorescens* in WT and *myb67* roots

Differentially expressed genes (DEGs) for each genotype and treatment were determined using limma-voom with a q-value of <0.05 and a log$_2$ fold change (FC) < -1 and > 1. The MA plots (Supplemental Figure S7) shows a general overview of the DEGs and Figure 17 depicts it in greater detail.

B. glumae triggered a massive transcriptional reprogramming, significantly altering the expression of 6,081 and 6,860 genes in Col-0 and *myb67* respectively (Figure 17A). Although the number of DEGs were less in the treatment with *P. fluorescens* than with *B. glumae*, the number of DEGs varied more dramatically between genotypes, with 26.4 % more DEGs in *myb67* than the WT Col-0 (Figure 17A). This suggests that the pathogen induces significantly

more transcriptomic regulation in plants of both genotypes, whereas the PGPB may not induce transcriptomic change as intensely. The heatmap visualisation of the 6,860 DEGs reveals that the majority of genes that are up-regulated in the PGPB treated WT Col-0 and *myb67* are expressed similarly in mock treated samples, whereas in contrast, they are down-regulated in pathogen-treated samples (Figure 18A). Likewise, those down-regulated in the PGPB treatment, appeared to be generally up-regulated in the pathogen-treated samples (Figure 18A). Only a small fraction of genes were observed to be regulated similarly in response to both bacteria (Figure 18A). Furthermore, a much smaller portion can be observed, where the two bacteria evoke a different response in terms of gene regulation (enlarged in Figure 18A).
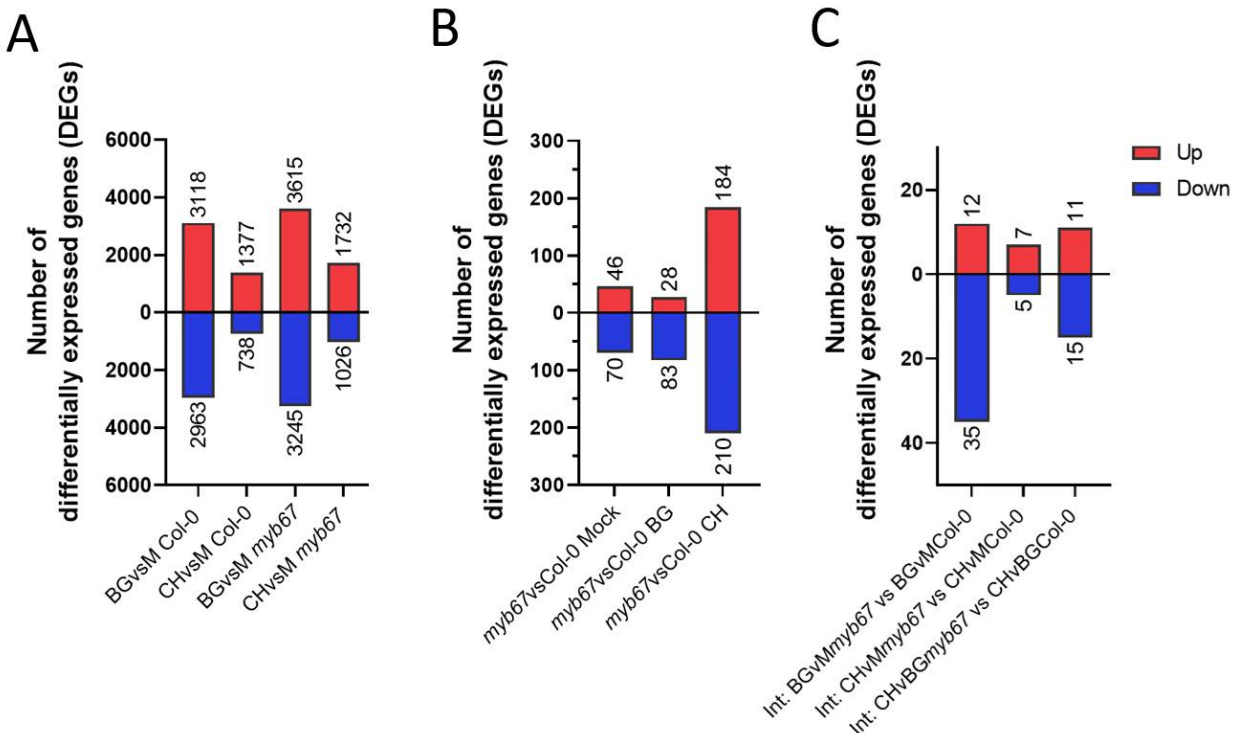
Figure 17: The resulting DEGs from the transcriptome response to *B. glumae* (BG) and *P. fluorescens* (CH) in WT and *myb67* in roots. DEGs were determined with limma-voom (iDEP1.0) and were filtered with the following criteria: q-value <0.05 and $1 < \log_2 FC < -1$. up-regulated genes in red, down-regulated genes in blue. **A:** The comparisons between treatments in Col-0 and *myb67* **B:** The comparisons between genotype in each treatment **C:** The list of DEGs upon comparison between interactions (interaction terms capture the differential response to treatment among two genotypes).

For the second aim of comparing the transcriptional response of the roots to inoculation with a pathogen and PGPB and determining the contribution of MYB67 to the responses, *myb67* roots were analysed and visualised in Figure 17B & 18B. When comparing DEGs between the

two genotypes, under mock conditions, 116 DEGs represent the basal change in gene expression caused by the deletion of *MYB67* (Figure 17B). The largest transcriptional reprogramming between genotypes was observed following PGPB inoculation, with 394 DEGs when *MYB67* is knocked out (Figure 17B). During pathogenic stress, 111 DEGs were found in *myb67*vsCol-0, which was slightly less than the basal transcriptomic change seen under mock treatment (Figure 17B). MYB67 regulation of genes appears to be mostly treatment dependent, with only some clusters indicating variation between the genotypes (Figure 18B). The enlarged sections of the heatmap highlight more clearly some of the mis-regulation of genes due to the loss of *MYB67* (Figure 18B).
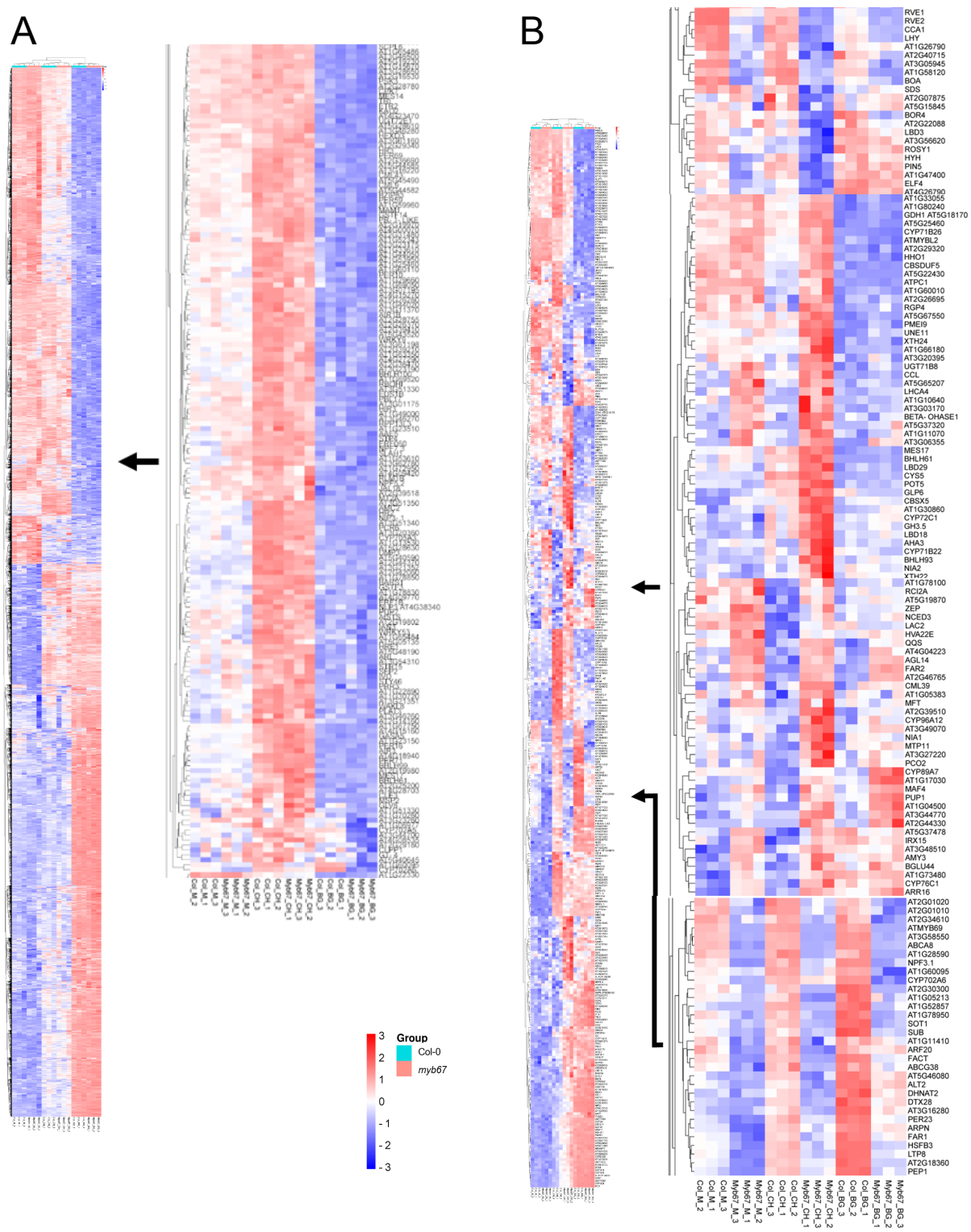
Figure 18: Heatmap of DEGs from the transcriptome response to *B. glumae* (BG) and *P. fluorescens* (CH) in WT and *myb67* in roots. DEGs were determined with limma-voom (iDEP1.0) and were filtered with the following criteria: q-value <0.05 and 1 < log₂ FC < -1. Dataset illustrating z-score of processed data. Complete cluster method with the distance method: euclidean was used. Genes are listed on the right (not italicised), sample names are listed the same for **A-C** as seen in **C**. The 'group' refers to the genotype. **A:** DEGs from treatment vs mock, (Gene names are not included for legibility) **B:** DEGs from mutant vs WT.
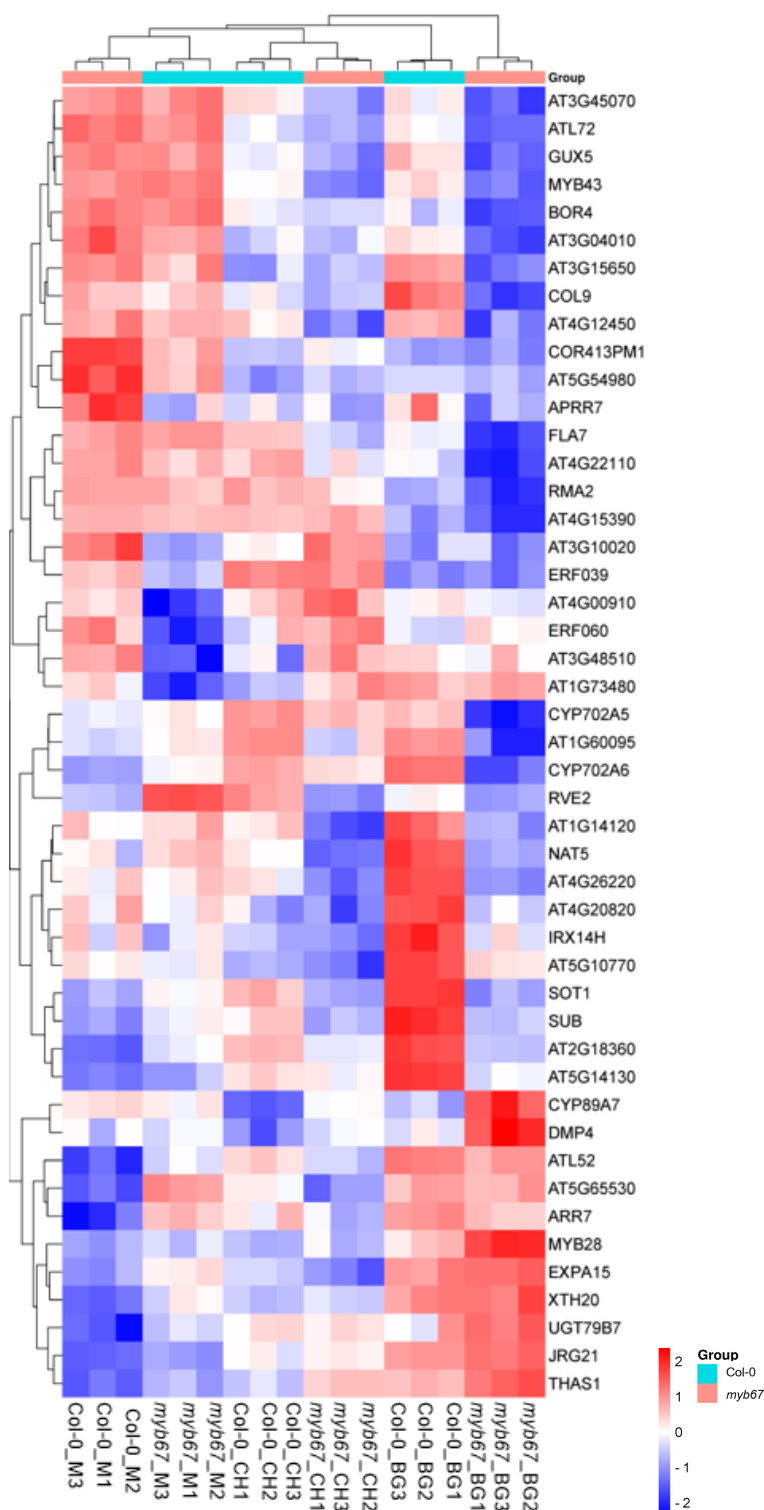
Figure 19: Heatmap of DEGs of the interaction terms from the transcriptome response to *B. glumae* (BG) and *P. fluorescens* (CH) in WT and *myb67* in roots. DEGs were determined with limma-voom (iDEP1.0) and were filtered with the following criteria: q-value <0.05 and 1 < log$_2$ FC < -1. Dataset illustrating z-score of processed data. Complete cluster method with the distance method: euclidean was used. Genes are listed on the right (not italicised), sample names are listed at the bottom. The 'group' refers to the genotype.

The analysis of the interaction terms, which are the differential response to treatment among the two genotypes, revealed that only a few DEGs were influenced. Most DEGs (47 genes) that were affected were in the interaction between the pathogenic response among *myb67* and WT (Figure 17C), whereas the PGPB response among the two genotypes resulted in 12 DEGs (Figure 17C). The differential response between the treatments among the genotypes, showed that there were 26 DEGs (Figure 17C). This can be visualised in the heatmap of the 47 DEGs including: *MYB28* encoding the positive regulator of aliphatic methionine-derived glucosinolates, thalianol (*THAS1*) and titrepene associated genes (*CYP702A5* and *CYP702A6*) and the *JA-REGULATED GENE 21* (*JRG21*) (Figure 19). High transcription of *MYB28* in *myb67* samples inoculated with the pathogen suggest that there could also be an increase of aliphatic glucosinolates (Gigolashvili et al., 2008).

The TF encoding genes *ANAC038, MYB61, MYB83* and *MYB103* (that were explored earlier in the thesis) were observed to be transcriptionally regulated mostly in response to the treatment (Figure 20). *MYB83* appears to be more strongly differentially expressed between the genotypes in comparison to the others (Figure 20). Suggesting that its activation may rely more on MYB67. This correlates to the Plant Regulomics prediction that MYB67 binds only to the promoter region of *MYB83* (Supplemental Table S1).
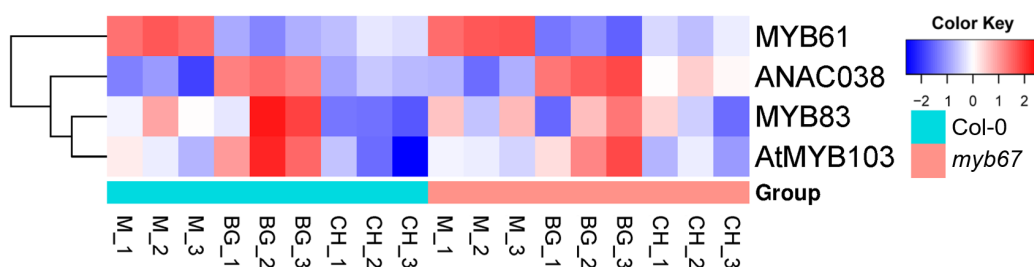
Figure 20: Heatmap of the additional TFs explored in this thesis in response to *B. glumae* (BG) and *P. fluorescens* (CH) in WT and *myb67* in roots. Dataset illustrating z-score of processed data. Complete cluster method with the distance method: euclidean was used. Genes are listed on the right (not italicised), sample names are listed at the bottom. The 'group' refers to the genotype.

To have an overview of the regulation of the camalexin associated genes in *myb67*, the processed data was visualised in a heatmap (Figure 21). Overall, the treatment with the

pathogenic bacteria results in a similar expression of camalexin associated genes between the WT and *myb67* (Figure 21). Interestingly, more camalexin associated genes are down-regulated in response to the pathogen than the PGPB, this might be the pathogen's attempt to bypass the plant's immune system. This also suggests that the camalexin related genes that are induced by the pathogen are responsible for the high induction of camalexin accumulated in the pathogen treated samples. In general, more camalexin related genes appear to be induced by PGPB than the pathogenic bacteria, however as the accumulation of the metabolite is less than the pathogen, there must be another signalling mechanism occurring recognising that it is a beneficial bacteria. This highlights the treatment-dependent regulation of these genes.
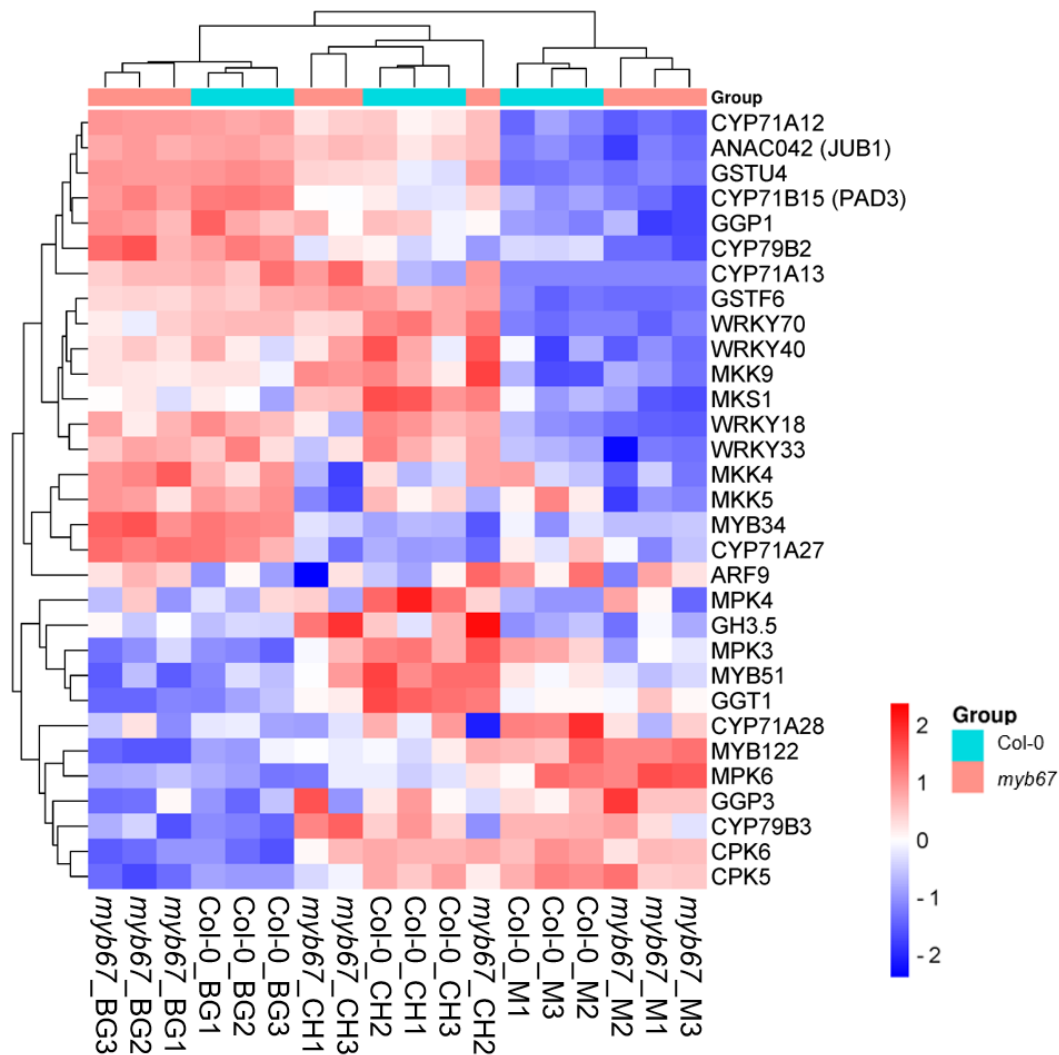
Figure 21: Heatmap of camalexin associated genes from the processed data of transcriptome response to *B. glumae* (BG) and *P. fluorescens* (CH) in WT and *myb67* in roots. Dataset illustrating z-score of processed data. Complete cluster method with the distance method: euclidean was used. Genes are listed on the right (not italicised), sample names are listed at the bottom. The 'group' refers to the genotype.

The biosynthetic genes *CYP71A12* and *CYP71A13* are induced similarly in comparison to the mock treatment, however upon inoculation with the PGPB *CYP71A13* is higher in expression in *myb67* than in the WT (Figure 21). On the other hand, *CYP71A27* and *CYP71A28* are distinctly regulated, firstly *CYP71A27* is expressed differently according to the bacterial treatment and *CYP71A28* is down-regulated upon the pathogen and in *myb67* upon inoculation with the PGPB. The camalexin associated genes *MPK4* and *GH3.5* are the only genes that are induced in PGPB but not in the pathogenic treatment. *MKK5* is down-regulated in *myb67* in both the PGPB and mock. Furthermore, *MPK3* and *MYB51* are also expressed alike. The heatmap illustrates how the genes associated to camalexin are expressed but in order to determine if these DEGs are overlapping in treatment and or genotype they were further analysed and drawn into venn diagrams.

2.7.1.1 Comparison of DEGs in WT roots between the pathogenic and PGP rhizobacteria responses

For the first time, this thesis presents transcriptional responses in Col-0 roots in response to inoculation with the pathogen, *B. glumae* and the PGPB, *P. fluorescens*. Figure 17A illustrates the up- and down- regulated genes in each bacterial treatment in the WT Col-0. To determine how many of these DEGs are shared between the bacterial treatments, the list of DEGs were visualised in a venn diagram. In the WT, a total of 1,538 DEGs were common between the pathogen and PGPB treatment (Figure 22A). Figure 22B, shows specifically how the DEGs are regulated. Of the 1,538 shared DEGs, 814 genes were up-regulated and 574 genes were down-regulated in response to both bacteria. In general there were more DEGs in the treatment analyses in *myb67* with 622 more DEGs common between treatments in comparison to the WT (Supplemental Figure S8). From the remaining shared DEGs in the WT, 133 genes were found up-regulated in response to the PGPB but down-regulated in response to the pathogen (Figure 22B). In contrast, 17 genes were up-regulated in response to the pathogen but down-regulated in response to the PGPB (Figure 22B). Furthermore, there were 1,857 more genes up-regulated exclusively in the response to the pathogen that were not present in the PGPB and 2,109 additional genes exclusively down-regulated in response to the pathogen but not the PGPB.

Supplemental Figure S9 reflects further insight into the transcriptional changes between treatments against the mock when comparing WT and the mutant (as well as the following GO analyses in Supplemental Figure S9a-d).
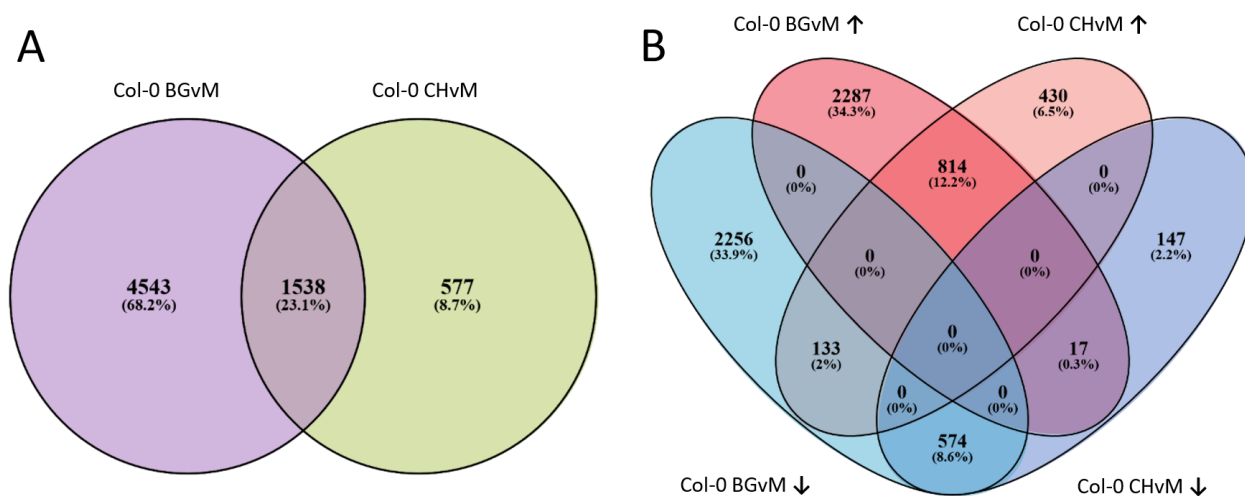
Figure 22: The shared DEGs from the transcriptome responses between treatments in WT roots. Venn diagrams of up- and down-regulated genes are indicated by up-facing and down-facing arrows **A:** The total shared DEGs between treatments against mock in Col-0. *B. glumae* (BG- in purple) and *P. fluorescens* (CH- in green). **B:** The shared up- (shades of red) /down- (shades of blue) regulated genes between treatments against mock. Venn diagrams were made in Venny 2.1.

2.7.1.2 Transcriptional alterations caused by the loss of MYB67 in response to inoculation with the pathogen and PGP bacteria

To examine the effects of the loss of *MYB67* and grasp greater understanding of MYB67's transcriptional network, the DEGs in the mutant were compared with the WT in each treatment as seen in Figure 17B. From the total of 513 DEGs found across all the treatments, 58 DEGs were found only in mock condition, 59 DEGs were found only upon treatment with the pathogen and 313 DEGs were found only upon inoculation with PGPB (Figure 23A). From the 83 shared DEGs, 55 DEGs were common between the bacterial treatments, 30 which were exclusively shared between the pathogen and PGPB and 25 genes that had altered expression in *myb67* in all treatments (Figure 23A). Excluding the 25 shared DEGs amongst all three treatments, 26 DEGs were also identified as common between the PGPB and mock whereas only 2 DEGs were shared between the pathogen and mock (Figure 23A).
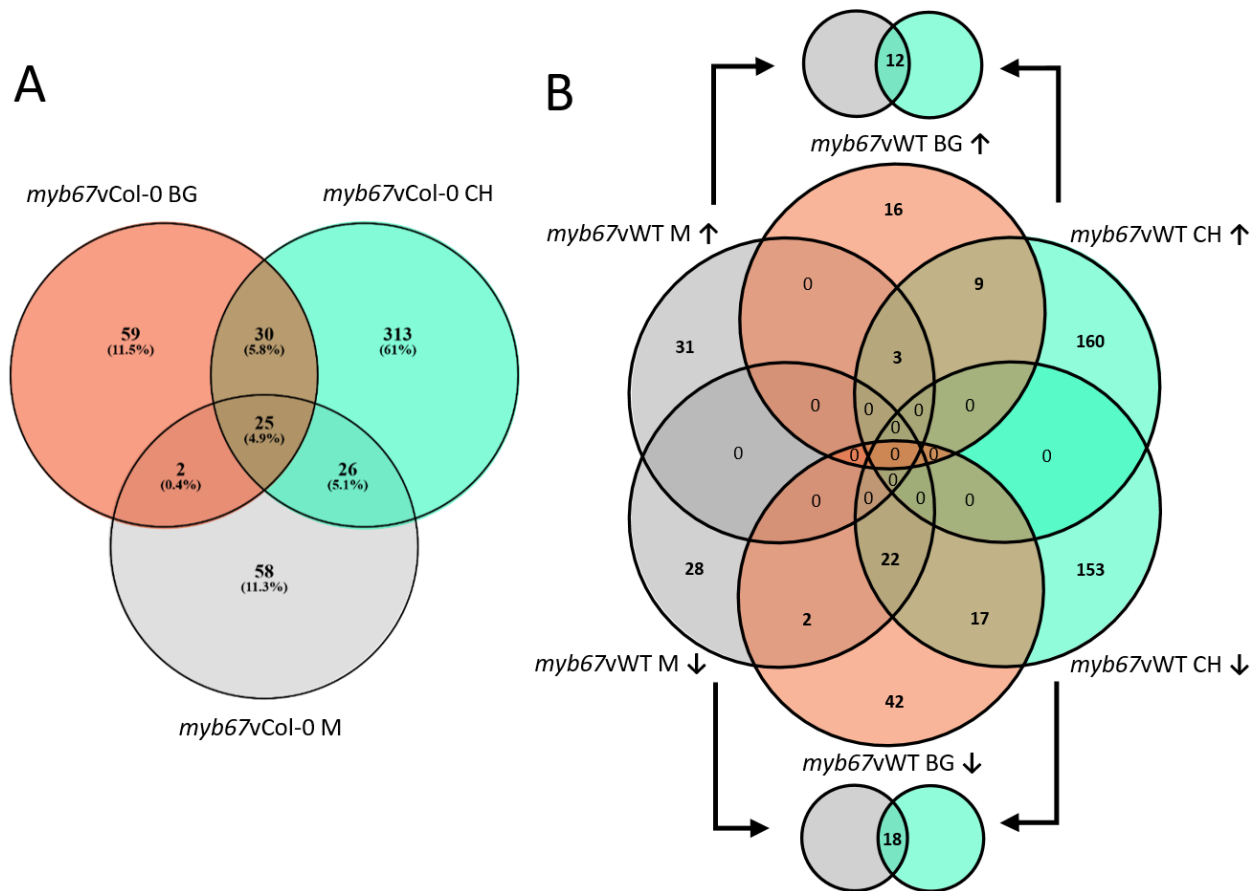
Figure 23: The shared DEGs between genotypes in mock (M), *B. glumae* (BG) and *P. fluorescens* (CH). Venn diagrams of **A:** Total shared DEGs between genotypes in each treatment. **B:** shared up/down-regulated genes of *myb67* compared against WT Col-0 in each treatment. up/down-facing arrows indicate up/down-regulated genes respectively. BG in red, CH in green and M in grey. Venn diagrams were made in Venny 2.1 and powerpoint.

Upon further examination of whether the shared DEGs are similarly expressed, no up- and down-regulated genes were identified as overlapping among all treatments (Figure 23B). Amongst all three treatments, 3 genes were up-regulated and 22 genes were down-regulated in *myb67* (Figure 23 A&B). Within the 22 severely down-regulated genes, the uncharacterised MYB protein *MYB69*, which was previously shown to be co-expressed with *MYB67* was also listed (Figure 6 & 23B). DEGs shared exclusively between mock and PGPB, in *myb67* were composed of 12 up-regulated and 18 down-regulated genes (Figure 23B). Mock and the pathogen inoculated *myb67* samples exclusively shared 2 genes, which were both down-regulated (Figure 23B). Furthermore, exclusively between the pathogenic and PGPB conditions, *myb67* had 9 and 17 genes that were up- and down-regulated, respectively (Figure 18B). Solely within the mock treatment, *myb67* was responsible for up-regulating 31 genes and

down-regulating 28 genes. From the 28 up-regulated genes in *B. glumae*, 16 were not overlapping with any other condition, whereas from the 83 down-regulated genes, 50.6% of genes (42 genes) were found to not be shared with any other condition (Figure 23B). Of the 172 up-regulated genes in *myb67* treated with CH, 160 genes (93%) did not overlap with any other. From the total of 192 down-regulated genes in *myb67* treated with CH, 153 genes (79.7%) were not shared (Figure 23B). From this analysis, DEGs encoding other TFs were identified with MapMan. The *P. fluorescens*-treated *myb67* induced the most TFs while the least differentially expressed TFs were in response to *B. glumae* (Supplemental Figure S10, Thimm et al., 2004). This highlights MYB67's significant transcriptional regulatory contribution in response to the PGPB.
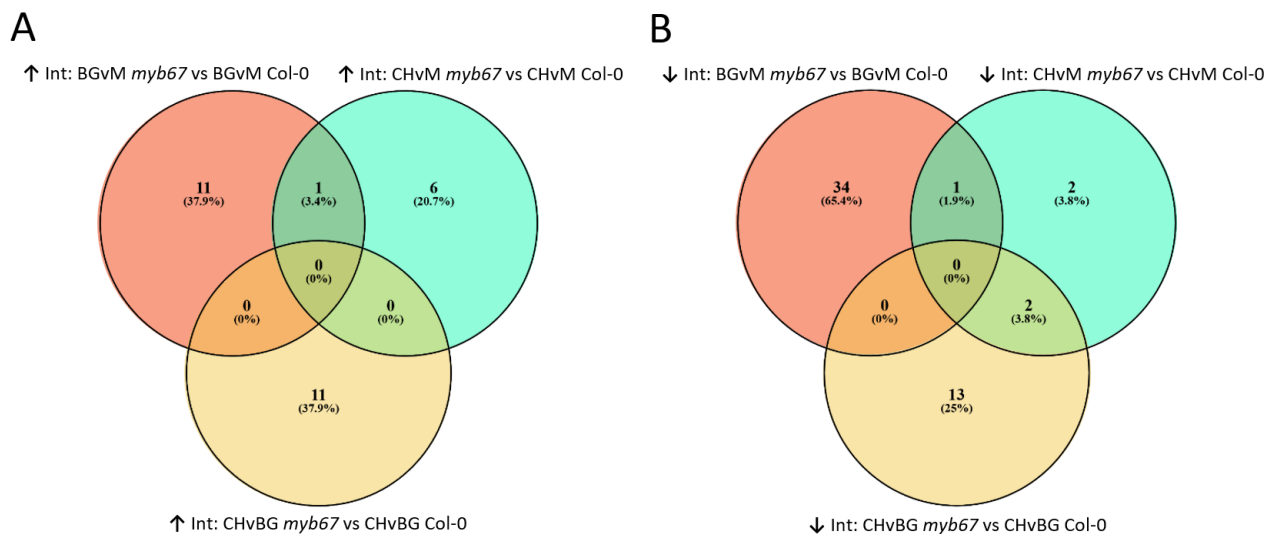
Figure 24: The shared DEGs between the interaction terms. Venn diagrams of **A:** Up-regulated genes shared between interactions (int) which reflect the differential response to treatment among two genotypes **B:** shared down-regulated genes of interaction terms. Up/down-facing arrows indicate up/down-regulated genes respectively. BGvM in red, CHvM in green and BGvCH in yellow. Venn diagrams were made in Venny 2.1 and powerpoint.

For further investigation into the differential response to treatment among the genotypes, the DEGs determined from the interaction terms were assigned into venn diagrams (Figure 24). From the 12 up-regulated genes that responded to *B. glumae* when compared against mock between the WT and mutant, only 1 was found to be shared (Figure 24A). This 1 of 7 genes was also up-regulated in response to *P. fluorescens* (Figure 24A). When examining the response of the pathogen against the PGPB between the genotypes, 11 genes were found up-regulated, none of which were found to be common. Amongst the down-regulated genes, 1 of 35 genes in

response to the pathogen compared to mock between the genotypes, was revealed to be shared with the group in response to the PGPB compared to mock between the genotypes (Figure 24B). The latter interaction term also showed to have 2 down-regulated genes that did not overlap at all and 2 additional down-regulated genes that were common with the response of pathogens compared against the PGPB between the genotypes (Figure 24B). In addition to the 2 shared genes, the interaction term CHvBG *myb67* vs CHvBG Col-0 had 13 genes that were also found to be down-regulated (Figure 24B).

2.7.2 Gene ontology analyses on the DEGs

To investigate the possible functions of the shared DEGs, the overlapping genes were subjected to GO analysis with METASCAPE and filtered for p-value of < 0.001 (Zhou et al., 2019).

Transformed data of all samples were subjected to *k*-means analysis to obtain clustering from a total of 6,860 genes across all treatments and genotypes to then determine the general GO enrichment within each cluster. Transformed counts were determined with EdgeR in iDEP 1.0, where the elbow method was applied in order to determine the *k*-value and a max z-score of 3 was used (Figure 25). Cluster 1 as the largest cluster, revealed to be enriched in immune responses such as: 'response to chemical', 'response to wounding', 'response to toxic substance', 'phenylpropanoid biosynthetic and metabolic processes' and 'secondary metabolic process' (Figure 25). It was within cluster 1 where the camalexin associated genes *CYP71A27, WRKY18, WRKY33* were expressed as well as the TFs *ANAC038* and *MYB103* that were also examined (Supplemental Figure S11). 'Response to chemical' was also highly enriched in cluster 2 along with hypoxia and stress related terms (Figure 25). Cluster 2 also housed the camalexin biosynthetic genes *CYP71A12, CYP71A13, CYP71B15, GSTF6* and the camalexin associated genes *GSTU4* and *ANAC042* (Supplemental Figure S11). The second largest cluster, cluster 3 had photosynthesis related terms of GO enrichment, where the genes *MYB122, MYB34,* and the TF encoding gene *MYB61* (explored in this thesis) were also found (Figure 25, Supplemental Figure S11). Cluster 4 was enriched predominantly in immune responses (Figure 25). Observed to be categorised into cluster 4 were the camalexin associated genes *GGT1/2, GH3.5, MYB51,*

MKK9, WRKY40 and *WRKY70* as well as the gene coexpressed with *MYB67*; *MYB69* (Supplemental Figure S11). Finally, cluster 5 which did not house any camalexin related genes, was mostly enriched in 'external encapsulating structure organisation', 'cell wall organisation' as well as other developmental processes (Figure 25).

Figure 25: The GO enrichment tree from the *k*-Means clustering of DEGs. GO enrichment of biological processes according to each cluster from k-means clustering. iDEP1.0 was used and the transformed data was obtained by EdgeR: log2 (counts per million (CPM) + Pseudo count c of 4) with min CPM as 0.5. max z-score of 3.

2.7.2.1 Biological processes enriched from DEGs in response to the treatment

Examination of the overlapping 814 up-regulated genes between the pathogen and PGPB in WT roots, showed that GO terms enriched were associated mostly with plant immunity (Figure 26B). Whereas genes similarly down-regulated in response to the two bacteria are involved in plant homeostasis, transport and development (Figure 26A). In response to the

pathogen, the GO term from down-regulated genes, with the smallest p-value was 'root morphogenesis' (Figure 27A). This is the process in which anatomical structures of the roots are produced and organised, the down-regulation of this process correlates with the phenotype of shortened, brownish roots seen in *Arabidopsis* upon inoculation with *B. glumae*. Additional indications of processes related to plant growth and development that are down-regulated in response to the pathogen include: 'cellular response to nitric oxide', 'cytokinin-activated signalling pathway', photosynthesis related processes, etc. (Figure 27A).
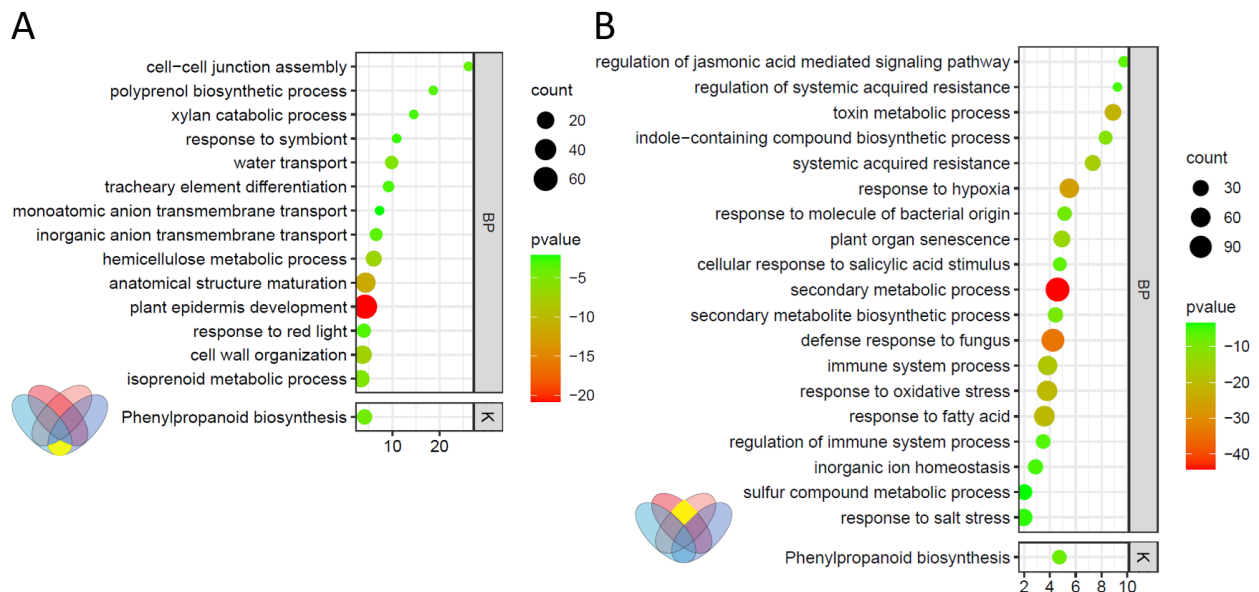
Figure 26: Summary of the top GO clusters from similarly regulated genes between *B. glumae* and *P. fluorescens* in WT roots. From the top GO terms (max 20) include enriched KEGG (shortened to K) pathways. The x-axis is the enrichment. The simplified venn diagram schematic illustrates the genes used to determine the GO enrichment (in yellow). **A:** down-regulated. **B:** up-regulated. p-value was filtered for < 0.0001.

The plant appears to have many stress related biological processes up-regulated in response to the pathogen. Such as: heat/salt/decreased oxygen levels/starvation/oxidative stress, 'secondary metabolite processes' which links well with 'phenylpropanoid metabolic processes' and 'flavonoid metabolic process' the secondary metabolite for ROS quenching and induction of HR (Mierziak et al., 2014) (Figure 27B).

Overall, GO terms enriched from up-regulated genes in response to the PGPB are different to the pathogen, yet are still related to defense eg. 'defense response to fungus', 'respiratory burst involved in defense response', 'systemic acquired resistance' (Figure 27D).

Unlike in response to the pathogen, an external microbe is clearly sensed and not only JA but SA and ET related processes are also enriched (Figure 27D). Additionally, 'inorganic ion homeostasis', 'response to zinc ion' and 'import into cell' may suggest that growth and developmental processes are not stunted upon exposure to *P. fluorescens*. In the general overview of GO terms enriched from significantly down-regulated genes in response to the PGPB, there were considerably less processes in comparison to the pathogen and were observed to be more involved in cell wall biogenesis and organisation (Figure 27C).
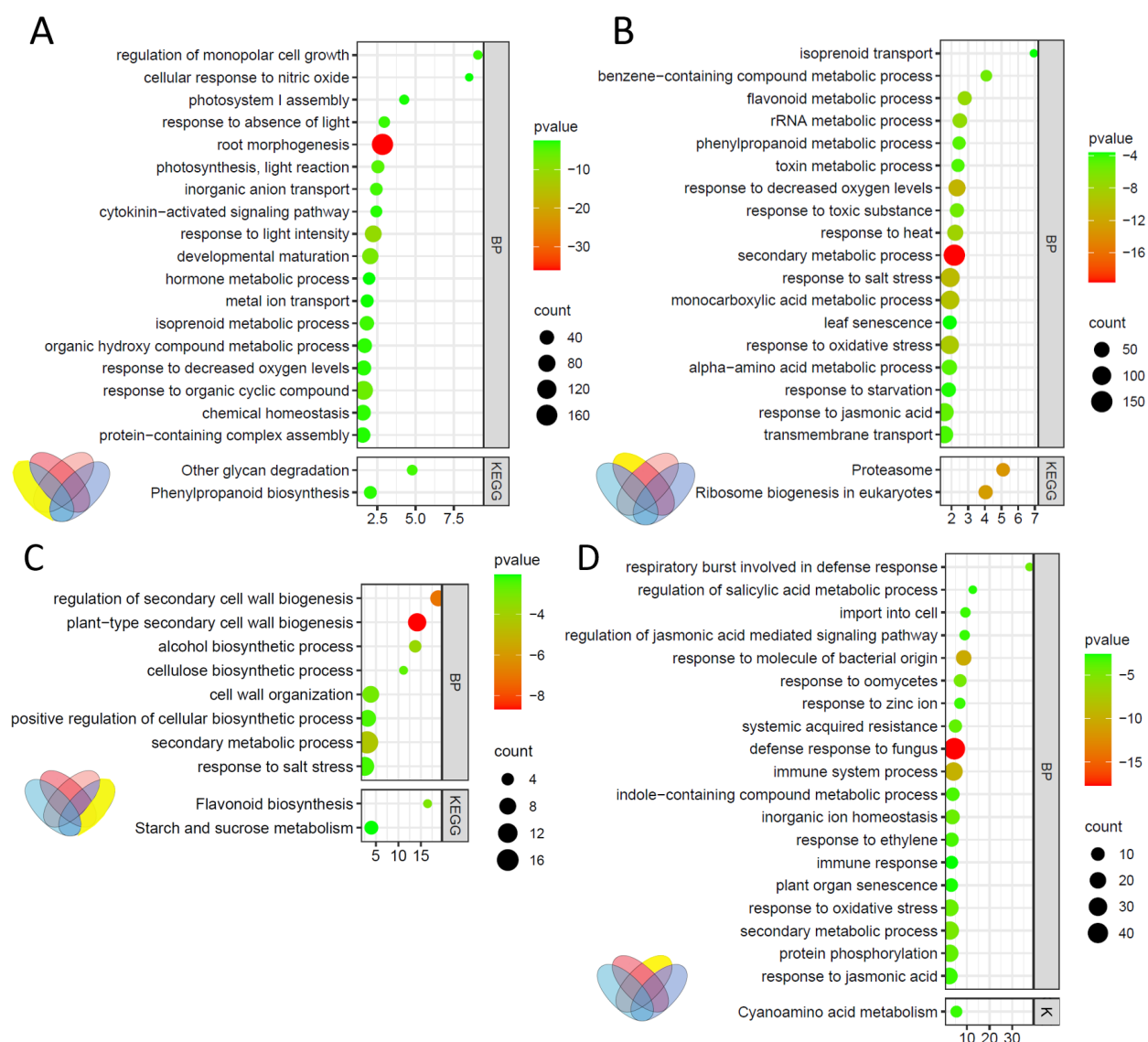
Figure 27: Summary of top GO clusters of up- and down- regulated genes in *B. glumae* and *P. fluorescens* in WT roots. From the top GO terms (max 20) include enriched KEGG pathways. The x-axis is the enrichment. The simplified venn diagram schematic illustrates the genes used to determine the GO enrichment (in yellow). **A&B:** in response to *B. glumae*. **C&D:** in response to *P. fluorescens*. **A&C:** down-regulated. **B&D:** up-regulated. p-value was filtered for < 0.0001.

Furthermore, genes that are regulated oppositely in response to the two bacteria are seen in Figure 28. GO terms from down-regulated and up-regulated genes in response to the pathogen and PGPB, respectively, were 'response to organic cyclic compound', 'root morphogenesis' coherent with the different phenotypes of the roots, and 'response to oxidative stress' including the differential expression of *WRKY53,* known to further activate the camalexin associated gene *WRKY18* downstream and the KEGG pathway 'phenylpropanoid biosynthesis' (Figure 28A). From the 17 genes up-regulated and down-regulated in response to the pathogen and PGPB, respectively, the GO terms 'secondary metabolic process', 'positive regulation of cellular biosynthetic process' including *MYB46*, and the KEGG pathway 'flavonoid biosynthesis' were enriched. MYB46, known to modulate disease susceptibility to *B. cinerea* in *Arabidopsis* may also be significant in the effects of pathogenic and PGP bacteria in *Arabidopsis* (Ramirez et al., 2011) (Figure 28B).
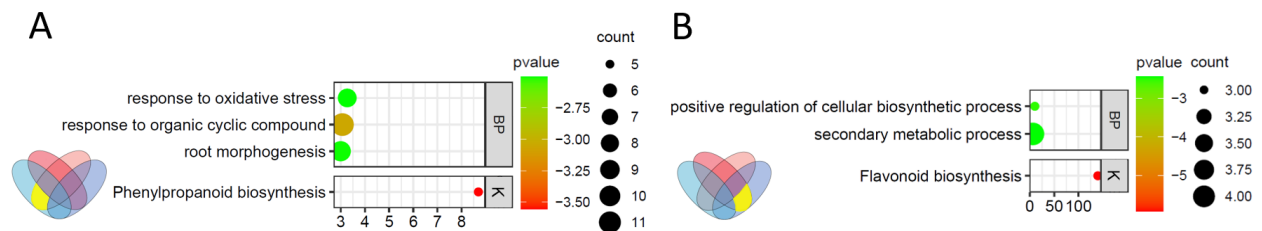
Figure 28: Summary of top GO clusters of opposite regulated genes in *B. glumae* and *P. fluorescens* in WT roots. From the top GO terms (max 20) include enriched KEGG (shortened to K) pathways. The x-axis is the enrichment. The simplified venn diagram schematic illustrates the genes used to determine the GO enrichment (in yellow). **A:** down-regulated in *B. glumae* and up-regulated in *P. fluorescens*. **B:** up-regulated in *B. glumae* and down-regulated in *P. fluorescens*. p-value was filtered for < 0.0001.

Indications of slight variations in regulation can already be observed in the GO analyses of the DEGs in response to the pathogen and the PGPB in comparison to the mock treatment in the mutant, *myb67* (Supplemental Figure S12 and S12a). Overall, the insights into the transcriptomic changes in response to both bacteria in the WT, illustrates that the pathogen and the PGPB manoeuvre through the plant's immunity differently.

2.7.2.2 Biological processes enriched from the DEGs due to the loss of *MYB67*

To uncover the consequences of *MYB67* loss of function, the transcriptional network analysis subjected to GO enrichment revealed biological processes that were severely affected in the mutant. The observations made in this section assisted in answering the second aim. The GO term enrichment from the DEGs between the genotypes showed that under basal conditions (mock) exclusively, MYB67 is responsible for repressing biological processes such as: 'circadian rhythm', 'negative regulation of DNA templated transcription', 'external encapsulating structure organisation', 'response to light intensity and to red or far red light', and 'response to cold' as well as inducing 'post embryonic development' (Figure 29 A&B). When observing GO terms from the 42 down-regulated genes exclusively under treatment with the pathogen that do not overlap with any others, suggest that MYB67 is also responsible for regulating 'secondary metabolite biosynthesis processes' and as shown with the KEGG pathway; 'flavonoid biosynthesis' (Figure 29C). The 16 genes that were solely up-regulated upon pathogen exposure did not result in any enriched GO terms. Furthermore, from the 160 exclusively up-regulated genes upon treatment with the PGPB resulted in an enrichment of defense associated GO terms, such as: 'camalexin biosynthetic process', 'toxin metabolic process', 'callus formation' and 'response to jasmonic acid' (Figure 29D). The genes associated with the 'camalexin biosynthetic process' included *GSTU4*, *CYP71A13*, and *GH3.5*, suggesting that MYB67 is involved in repressing these genes under PGPB stress. On the other hand, from the treatment with the PGPB, 153 genes that were down-regulated in comparison to WT, showed enrichment of other stress responsive processes and development (Figure 29E). Revealing that MYB67 is also involved in transcriptional reprogramming of immune system responsive genes such as *WRKY54*, *WRKY53*, *WRKY59*, *CBP60G*.

Between all treatments (mock, BG and CH), the down-regulated genes that were found differentially expressed in *myb67* in comparison to WT had a GO enrichment of 'secondary metabolic processes' that consisted of four genes, two of which are unknown and the others were identified as *FAR1* and *FACT* (Supplemental Figure S13A). The enriched biological processes

from the 18 down-regulated genes present only between the mock and PGPB were similar to those only seen in the mock ('circadian rhythm', 'regulation of post-embryonic development') (Supplemental Figure S13B). Within these GO terms were the genes *CCA1*, *RVE1*, *BOA* and *LHY*, which are likely influenced by MYB67. The 17 down-regulated genes that were exclusively common between the pathogenic and PGP bacteria inoculated samples resulted in the GO terms 'small molecule biosynthetic processes' (including: *MYB43, DHNAT2*) and 'secondary metabolic processes'(Supplemental Figure S13C). The other overlaps did not produce any GO terms and consisted mostly of unknown genes.
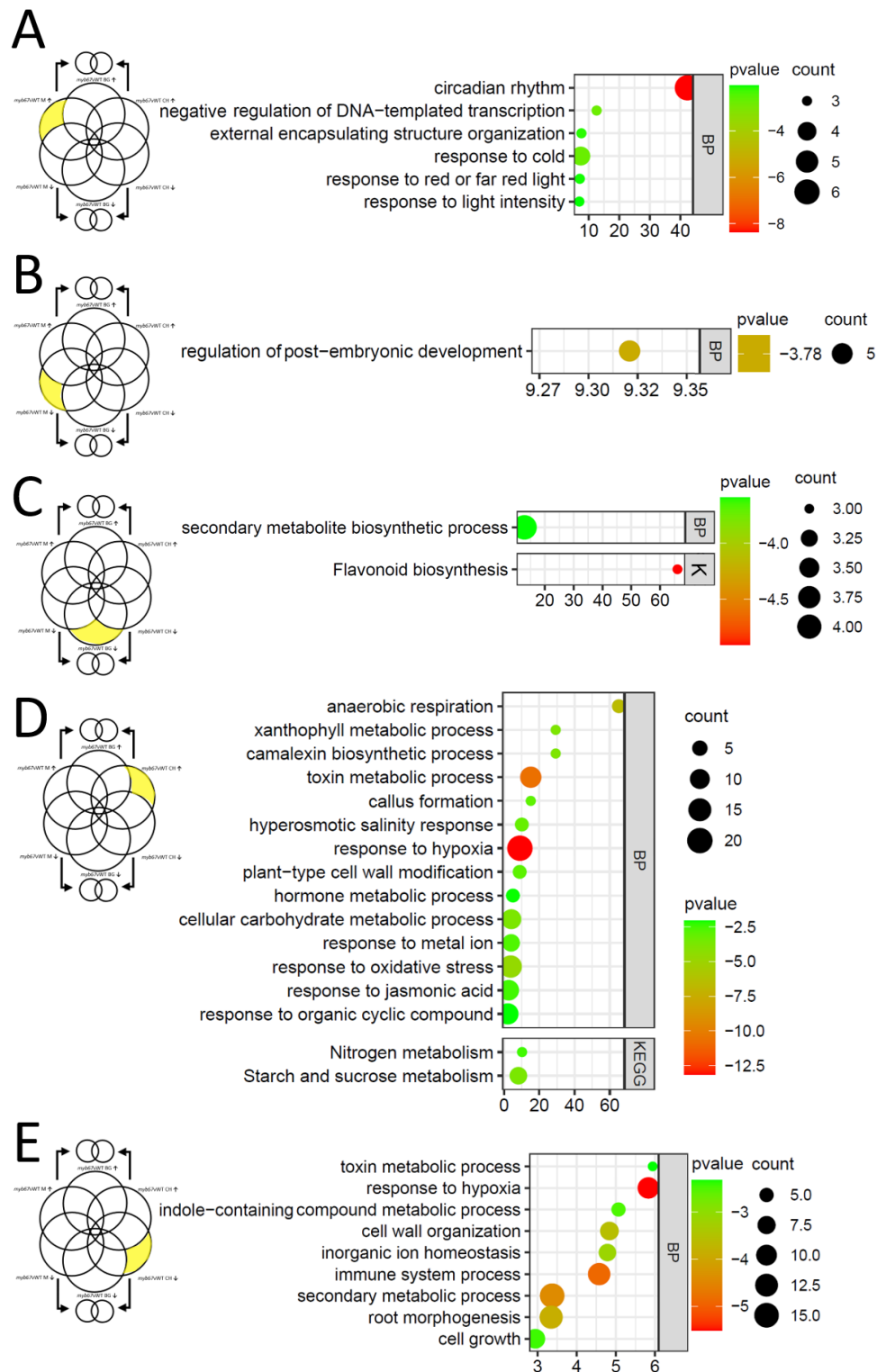
Figure 29: Summary of the top GO clusters of *myb67*vWT DEGs in the individual treatments, exclusively. From the top GO terms (max 20) include enriched KEGG (shortened to K) pathways. The x-axis depicts the enrichment. The simplified venn diagram schematic illustrates the shared genes used to determine the GO enrichment. Shared genes **A-D:** up-regulated. **B, C & E:** down-regulated. **A&B:** exclusively in mock treated *myb67*vWT. **C:** exclusively in BG treated *myb67*vWT. **D & E:** exclusively in CH treated *myb67*vWT. p-value was filtered for < 0.0001.

Due to the fact that there were only a few DEGs from the interaction terms, GO enrichment analysis was not possible for all the shared sets of genes as well as for the interaction of the pathogenic treated *myb67* and WT comparison. The only GO terms derived from the up-regulated genes between the pathogen treated genotypes were, 'response to hypoxia' and 'secondary metabolic process' (Supplemental Figure S14A). Similarly, when the mutant and WT PGPB interactions were compared to the pathogenic bacteria the GO term 'secondary metabolic process' was enriched, as was 'cellular response to abiotic stimulus' (Supplemental Figure 14B).

Overall, the GO analyses revealed that MYB67 is involved in biological processes associated with plant innate immunity in response to both bacterial treatments, particularly between the genotypes. MYB67 appears to be tightly associated with the circadian rhythm under mock conditions, possibly to modulate the balance between development and plant defense preparations. The involvement of MYB67 in plant stress responses is also supported further by its differential expression in other published transcriptional comparisons (Supplemental Figure S15).

2.8. Analysis of MYB67 target genes

In parallel, publicly available DAP-seq data, uploaded from Joseph R Ecker Lab, La Jolla, California (GSE60141) were also subjected to quality control with FastQC and then mapped against the reference genome using BowTie2 (O'Malley et al., 2016). Furthermore, MACS2 and MACS2 callpeak tools were used to find the binding peaks and call peaks from alignment; producing a list of target genes of MYB67. This list consisted of a total of 13,671 target genes that were then joined with the RNA-seq DEGs obtained previously. Resulting in a total of 10,317 unfiltered target genes that were differentially expressed amongst all comparisons. The list was then re-filtered for a q-value of < 0.05 in the set comparing genotypes treated with PGPB (as it contained the most DEGs) (Figure 30B), as well as all the comparisons between treatments in *myb67* and WT (Figure 30C). The remaining 248 and

1,100 direct target genes of MYB67 were then subjected to GO enrichment to determine the biological processes the MYB67 target genes are involved in.
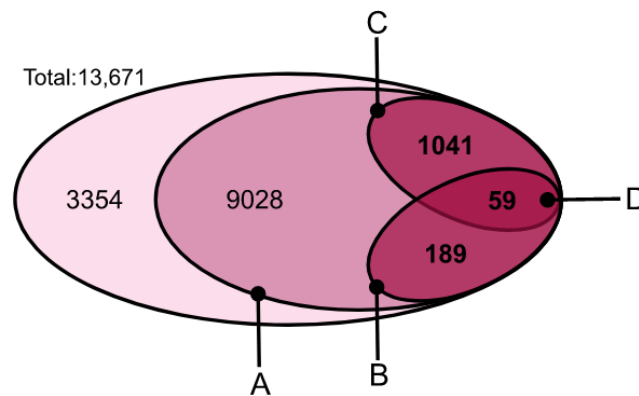
Figure 30: Target genes of MYB67. From the total list of target genes obtained from the DAP-seq **A:** unfiltered DEGs across all comparisons that are direct targets of MYB67. **B:** 248 DEGs are direct targets of MYB67 in *myb67*vsWT (across all treatment comparisons). **C:** 1100 target genes differentially expressed in all treatments comparisons (in both WT and *myb67*). **D:** overlapping genes between the comparisons. **B-D:** filtered by q-value of < 0.05.

Analysis of enriched GO terms of MYB67 target genes, which were selected by comparison to the DEGs obtained from the RNA-seq analysis, revealed that the most significant biological process was the 'secondary metabolic process', a broad group consisting of genes that overlap into the other processes listed in the graph above (Figure 31). Many target genes of MYB67 appear to be involved in plant immunity, as processes such as 'defense response to fungus', 'response to jasmonic acid', 'phenylpropanoid biosynthesis', 'cutin, suberine and wax biosynthesis', as well as 'toxic metabolic process' and 'lignan metabolic process' were enriched (Figure 31). Under the 'toxic metabolic process', the biological process 'camalexin biosynthetic process' is listed, the MYB67 target genes within this GO term were *WRKY33*, *NAC042*, *GGP1* and *AT5G41750*. The protein encoded by the gene *ERF1* (present in 'response to jasmonic acid') depends on forming transcriptional complexes with WRKY33 and binds directly to the promoters of *CYP71A13* and *CYP71B15* to activate their expression (Zhou et al., 2022). Additionally, the JA responsive gene *EBP* (also known as *ERF72*) was also a target gene of MYB67. Other target genes of MYB67 present that are JA responsive were *EPS1*, *ERF2*, *ChiC*, *ST2A*, *JAZ1/6/10*, *TT4*, *LOX1*, *5PTASE11*, *FBS1*, *MMP*.
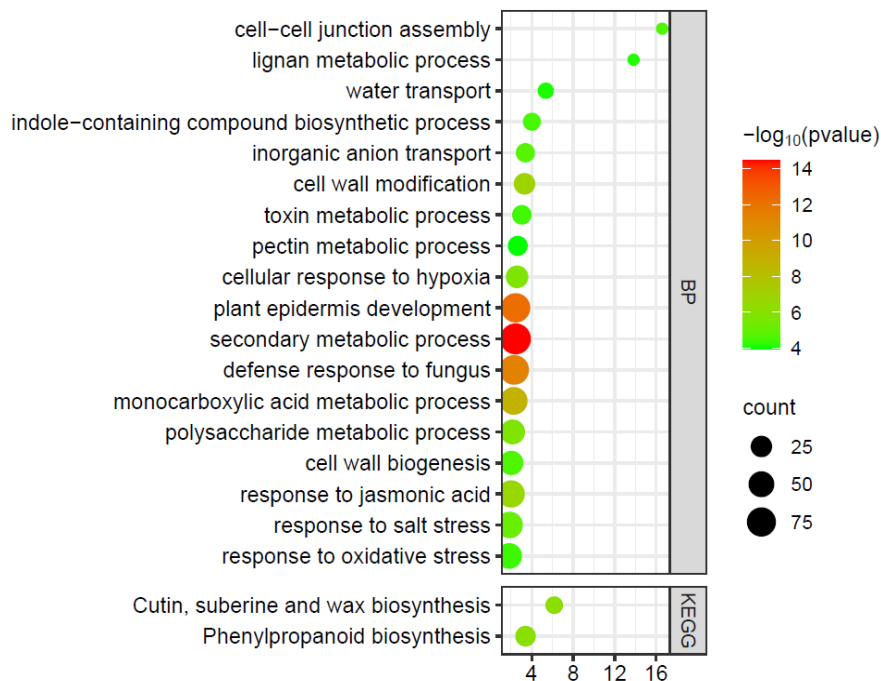
Figure 31: GO enrichment of the 1100 DEGs upon treatment comparison that are direct target genes of MYB67. GO enrichment of target genes selected that overlap with DEGs q-value of < 0.05 and a log$_2$FC of < -1 and > 1 in each set (BGvM in Col-0, CHvM in Col-0, BGvM in *myb67*, CHvM in *myb67*) log$_{10}$(p-value) of -2 is represented by 0.01.

The GO term 'defense response to fungus', consisted of SA responsive genes that overlap in other GO terms including: *WRKY18/54/62*, *RGL2*, *DOX1*, *PFA-DSP3*, *YLS2*, *EP1*, *Rap2.6L*, *ANAC087*, *RLK1*, *CBP60G*, *EP1*, *NPR4* and *FBS1*. Additional target genes of MYB67 categorised into 'defense response to fungus' include also *RBOHD*, *SDF2*, *PLA2A*, *ATERDJ3B*, *MYB30/45*, *CYP71B7*, *FMO/1*, *CYP83B1*, *BZS1*, *BES1*, *LGT9*, *PR4*, *PUB24*, *LTPG1/2*, *MES9*, *NAC6* as well as many others. Another innate immune response enriched within the target genes of MYB67 is the 'phenylpropanoid biosynthetic process', categorised into the 'secondary metabolic process' GO term (Figure 31). Phenylpropanoid biosynthetic and metabolic associated genes included: *CAD4/9*, *PRR1/2*, *DIR5*, *POM1*, *LAC11*, *MYB63*, *TT4*, *UGT73C7*, *PER4,* as well as *GPAT5*, *FAR1/5* and *CYP86A1/B1;* the latter are some of the genes also involved in suberin biosynthesis within 'cutin, suberine and wax biosynthesis' of the KEGG pathway (Figure 31). Moreover, the genes *CASP1*, *CASP2*, *CASP3* and *CASP5,* which are involved in the formation of the casparian strip present in the GO term 'cell-cell junction assembly', may affect the transport of certain proteins important for plant defense (Figure 31).
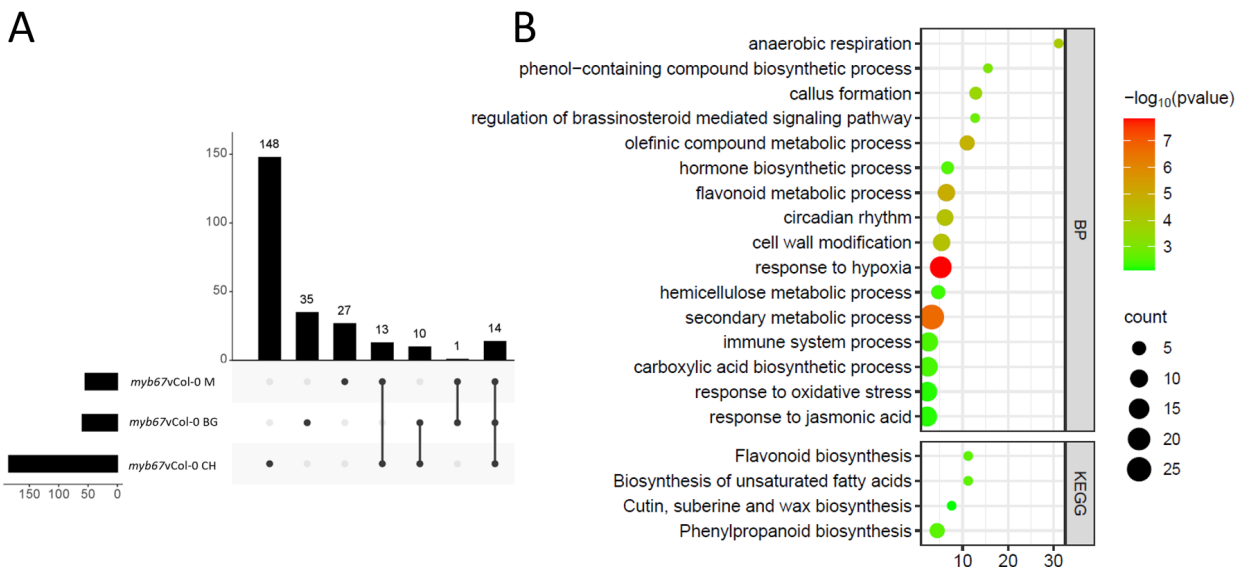
Figure 32: 248 direct target genes of MYB67 differentially expressed between genotypes. A: UpsetPlot of shared target genes that overlap with treatments. **B:** GO enrichment of all target genes seen in **A**, q-value of < 0.05 determined separately from each set (*myb67*vCol-0 in M, BG, CH) $\log_{10}$(p-value) of -2 is represented by 0.01.

In order to gain insight in MYB67's transcriptional network it was crucial to evaluate the differences between genotypes in each treatment, therefore, the target genes acquired were compared against the DEGs obtained in the *myb67*vsCol-0 analyses (Figure 32A). Direct target genes of MYB67 that are differentially expressed in *myb67* in comparison to WT appear to be significantly involved in 'response to hypoxia' which include the annotated genes *CBP60G, PROPEP3, ADH1, SUS1, PLA2A, TCH4, CYP707A3* etc. These genes were only found to be differentially expressed in *myb67* among the PGPB treatment. Within the 'secondary metabolic process' the annotated genes identified (*CYP82C4, KCS2, MYBL2*; three genes present only in the PGPB treatment, as well as *FAR1* and *FACT*) are involved in phenylpropanoid pathway. Another defense response MYB67 appears to be involved in is 'callus formation' including the annotated genes: *JMJD5*, only present in the PGPB treatment were *LBD16, LBD18, LBD29* and *EXPA17*. The latter is also involved in 'cell wall modification' along with *CASP4, UGE1, EXP15, RHS12, EXPA17, TBL3, EXP1, EXPA10* and *TCH4* (the last six genes which are exclusively differentially expressed in PGPB treatment). Target genes that are exclusively in the treatment with the pathogen had genes also present in 'secondary metabolic process' (*4CL5, CCR1, MYB85*), 'flavonoid biosynthesis' (*SSL2, TT7, TT4*), and 'response to jasmonic acid (*TT4* along with *LBD20*).

From the 14 common DEGs between *myb67* and WT in all three treatments *HSFB3, FAR1, RVE2, SUB, CYP702A6, MYB69*, and *ABCA8* are the annotated direct target genes identified (Figure 32A). Shared exclusively between BG and CH in *myb67*vsCol-0, the 10 overlapping genes included the annotated genes *MYB43*, *PUP1* and *DUF567*. There was only 1 target gene shared exclusively between BG and M (Figure 32A). The target genes that were common between CH and M in *myb67*vsCol-0 comprise of the annotated genes *RVE1, VSP1, TAF1* and *CCL* (Figure 32A). The annotated target genes shared between the treatments were enriched in the GO terms 'secondary metabolic process', 'circadian rhythm', 'response to jasmonic acid' and the KEGG pathway 'cutin, suberine and wax biosynthesis'.

A selection of annotated genes were visualised for comparison in a heatmap in Figure 33A; DEGs present in *myb67*vsCol-0 across all treatments that were explicitly not in the DAP-seq were also included in further analysis (Figure 33B). From the two sets, not all genes were used in the continued work due to acquirability and availability of T-DNA lines.
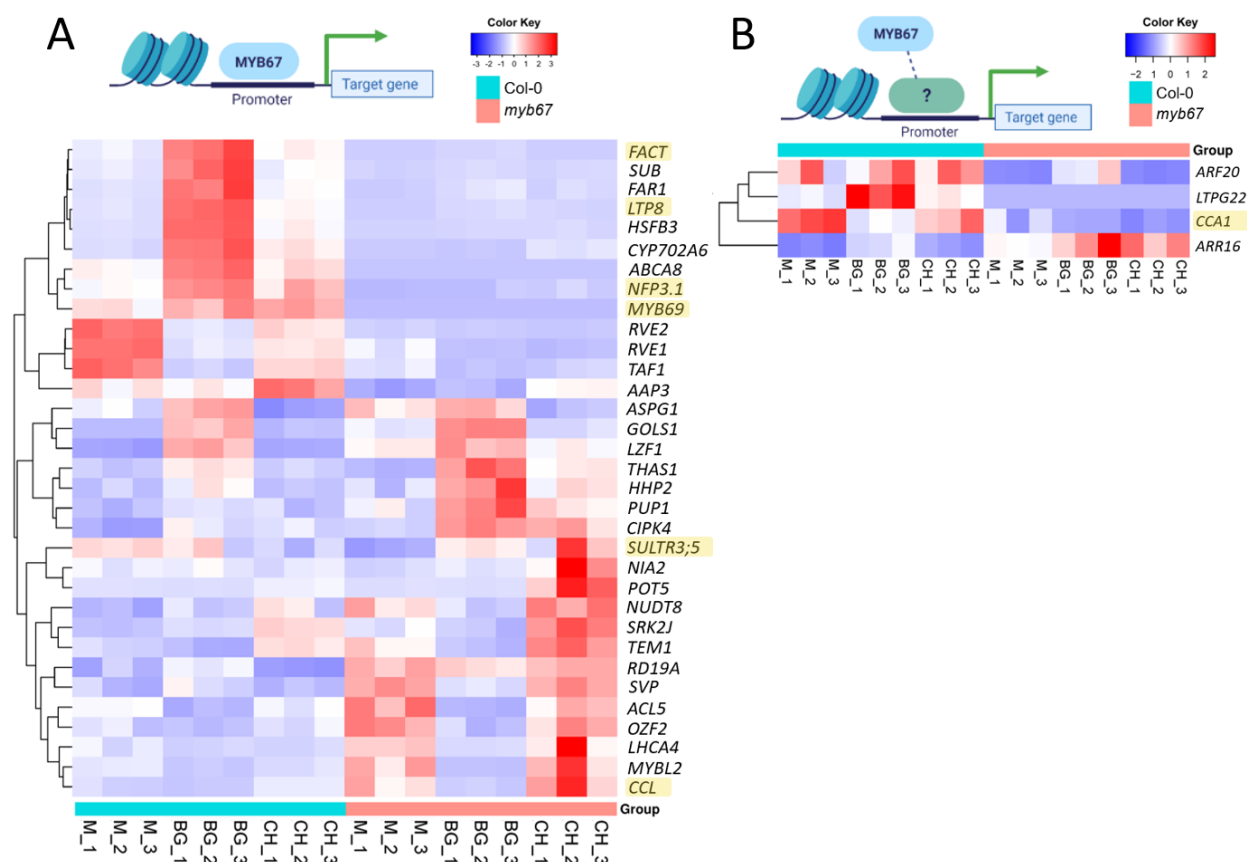
Figure 33: DEGs upon genotype comparison overlapping with DAP-seq. A: UpsetPlot of shared target genes that overlap with DEGs present in genotype comparison. **A:** Heatmap of selected annotated target genes from DAP-seq dataset illustrating z-score of TPM values of *myb67*vsCol-0 DEGs. **B:** TPM values of DEGs that are not target genes of MYB67 were selected for comparison, as depicted in schematic (thus possible indirect targets as illustrated). Heatmaps were created with SRplot using pheatmap package, colour key is based on z-score.

Camalexin specific genes that were identified via DAP-seq were not significant in all RNA-seq comparisons, however, the genes that had a q-value < 0.05 were specified with coloured dots, this can be observed in Figure 34. After analysis of both the DAP-seq and RNA-seq, a selection of genes was used to perform qRT-PCRs to verify the expression patterns of the RNA-seq; several can be seen under Supplemental Figure S16.
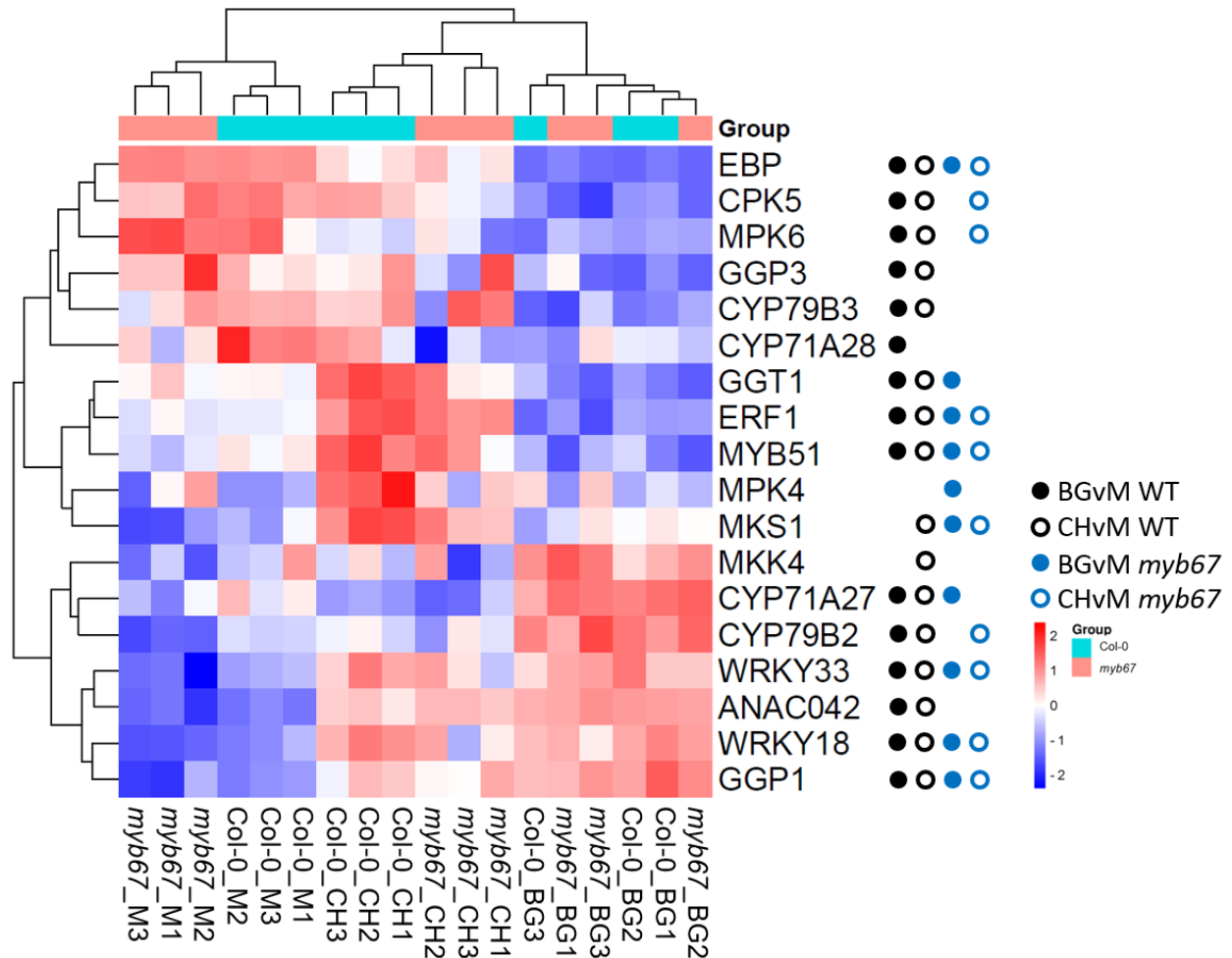
Figure 34: Heatmap of camalexin associated target genes of MYB67. TPM values are illustrated in z-score. Complete cluster method with the distance method: euclidean was used. Genes are listed on the right (not italicised), sample names are listed at the bottom. The 'group' refers to the genotype. The circles next to the genes are indicative of q-value < 0.05 in the RNA-seq analysis of BGvM WT (solid black), CHvM WT (black and white), BGvM *myb67* (solid blue), and CHvM *myb67* (blue and white).

2.8.1 Candidate target genes of MYB67 reflect similar function in regulating biosynthesis of camalexin

The potential target genes of *MYB67* that were also found to be differentially expressed upon inoculation with the pathogenic bacteria, *B. glumae* and the PGPB, *P. fluorescens* were selected and homozygous mutants of these genes were obtained. The indirect target gene (*CCA1*) and the direct target genes of MYB67 (*CCL, NPF3.1, POT5, SULTR3.5, FACT, LTP8* and *MYB69*) are described below. The *CIRCADIAN CLOCK ASSOCIATED 1* (*CCA1*) an indirect target of MYB67 is a master circadian oscillator in a transcriptional feedback loop with the *LATE*

ELONGATED HYPOCOTYL (*LHY*) and the *TIMING OF CAB EXPRESSION 1* (*TOC1* also known as *APRR1*) (Wang and Tobin, 1998; Lidder et al., 2005). Likewise, the *CCR-LIKE* (*CCL*) is involved in circadian processes as well as the messenger RNA decay pathway (Lidder et al., 2005). The NITRATE TRANSPORTER1/PEPTIDE TRANSPORTER FAMILY (NPF) member *NPF3.1* gene expression was induced by nitrogen limiting solution in *A. thaliana* and can transport nitrate and nitrile (Pike et al., 2014). Under low nitrate conditions NPF3.1 was shown to be involved in transporting gibberellins (GAs) (David et al., 2016). The gene *POT5* known also as *HAK5* has been identified as a potassium transporter, required for plant growth and potassium acquisition from low potassium solutions in the presence of salinity (Nieves-Cordones et al., 2010; Rubio at al., 2000) and shown to be regulated by the transcription factor MYB77 (Feng et al., 2021). The SULFATE TRANSPORTER 3;5 (SULTR3.5) was discovered to reinforce SULTR2;1's essential function of root-to-shoot transport of sulfate within the sulfate transport system (Kataoka et al., 2004). *SULTR3.5* with its subfamily members were found to promote stress-induced synthesis of cysteine, triggering the biosynthesis of the phytohormone ABA which could then regulate stomatal closure by dynamic transport of sulphate into the chloroplasts (Chen et al., 2019). The acyltransferase FATTY ALCOHOL: CAFFEOYL-CoA CAFFEOYL TRANSFERASE (FACT) is responsible for catalysing the essential step of alkyl caffeate synthesis, the transfer of caffeoyl group from the caffeoyl-CoA thioester to a fatty alcohol acceptor (Kosma et al., 2012). It was also found to play a role in incorporating caffeate into seed coat suberin (Kosma et al., 2012). LTP8 is a putative PR (pathogenesis- related) protein which belongs to the lipid transfer protein family and has been shown to have involvement in antimicrobial activity (Jülke and Müller, 2015). The SND1 regulated transcription factor MYB69 was found to have developmental associations in secondary wall thickening of cells (Zhong et al., 2008), but is otherwise unexplored.

The *Arabidopsis* T-DNA mutant lines *ccl*, *fact*, *ltp8*, *myb69*, *cca1*, *npf3.1*, *pot5* and *sultr3.5* were tested to see whether their camalexin response in shoots induced by root-inoculated *B. glumae* and *P. fluorescens* and if this response corresponded to the phenotype shown in *myb67*. Under pathogenic stress, *ccl*, *myb69*, *cca1*, *npf3.1*, and *pot5* accumulated more camalexin

than WT, similar to the mutant *myb67* (Figure 35 A&C). The mutants *fact* and *sultr3.5* had WT-like levels of camalexin, whereas *ltp8* accumulated 50% less camalexin than the WT (Figure 35 A&C). Camalexin accumulation induced by the PGPB revealed that, with the exception of *myb69,* all mutants had high camalexin accumulated in the shoots, which corresponded to the response produced by *myb67* (Figure 35 B&D). This suggests that the mutants are more sensitive to treatment with the PGPB.
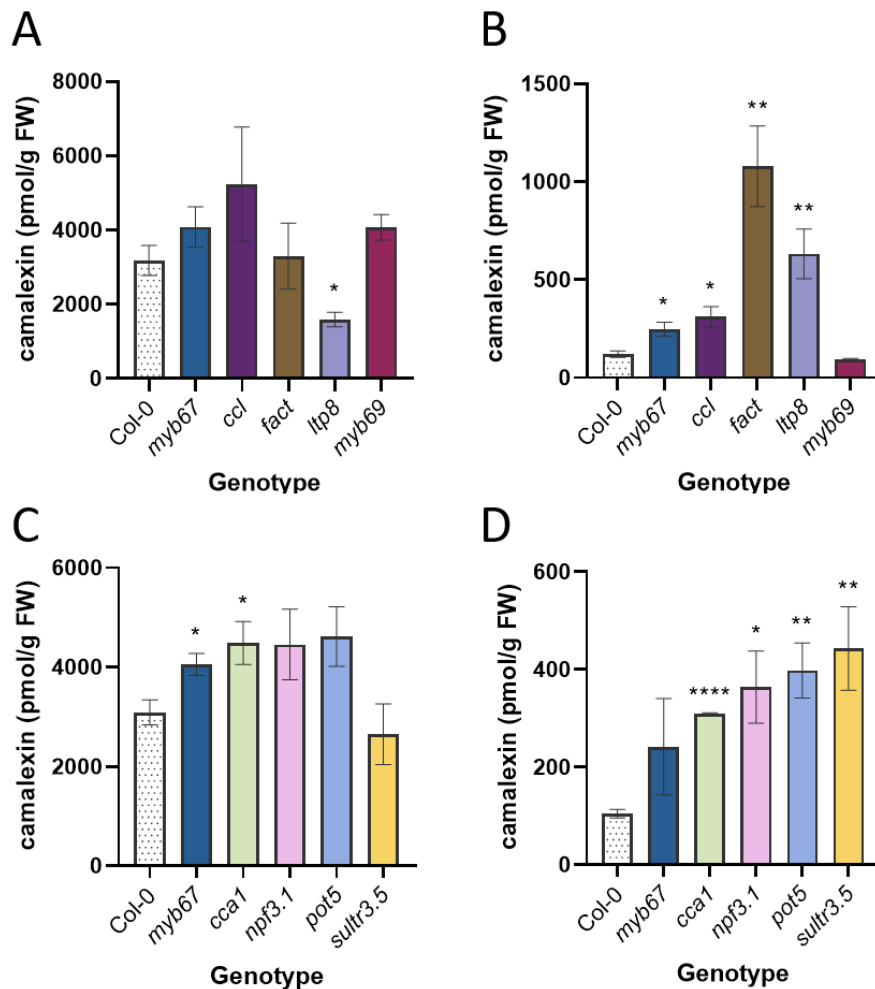
Figure 35: Camalexin accumulated in shoots upon inoculation with *B. glumae* PG1 and *P. fluorescens sp.* CH267 in Col-0 and mutants. Col-0 (WT) and T-DNA lines *myb67, ccl, fact, ltp8, myb69, cca1, npf3.1, pot5 and sultr3.5* were grown on a nylon net in hydroculture for 7 days and was inoculated in the solution with 10 mM $MgCl_2$ (mock), (**A & C**) *B. glumae* PG1 (BG; OD_{600} = 0.0005) or (**B & D**) *P. fluorescens sp.* CH267 (CH; OD_{600} = 0.0001), samples were harvested 3 dpi. Values were compared against Col-0 mock. Data represented as means ± SEM from 4 biological replicates, each corresponding to at least 30 seedlings. Asterisks indicate significant differences against the control (*$p<0.05$, **$p<0.01$, ***$p<0.001$ and ****$p<0.0001$, Student's *t*-test).

3 | DISCUSSION

Production of secondary metabolites is a critical characteristic of plant adaptation mediated by plant-microbe interactions. External threats can be mitigated by the phytoalexin camalexin, which is synthesised at the site of attack after environmental stresses (Bednarek, 2012). Key enzymes and genes involved in the pathway to synthesis camalexin, as well as transcription factors further upstream that influence its biosynthesis have been largely identified in shoots (Ren et al., 2008; Nguyen et al., 2022). However, the decades of research on camalexin have shed some light but yielded no clear and comprehensive answer to how camalexin synthesis, accumulation, and exudation are regulated in the roots.

The identification of CYP71A27 in a GWAS, based on sulfatase activity also showed a link between camalexin accumulation and exudation in shaping the root microbiome, making it the most recent addition to the small number of known metabolites capable of influencing microbiota in the rhizosphere (Koprivova et al., 2019; Koprivova et al., 2020). Camalexin was also shown to be important in establishing growth-promoting effects from the beneficial bacteria *P. fluorescens* sp. CH267 by *cyp27*'s (*cyp71a27*) loss of the effect (Koprivova et al., 2019). The inability to amplify the entire coding region of *CYP71A27*'s adjacent gene, *CYP71A28,* prevented clear conclusions about this gene from being drawn (Koprivova et al., 2019). Although *CYP71A27* was not found to be responsible for camalexin exudation, it was clearly indicated that it was involved in the metabolite's biosynthesis, particularly in root tissue. The regulation of camalexin in roots is not well understood, and the modulation of the "new" P450 CYPs *CYP71A27* and *CYP71A28* in particular has not been investigated.

Studying the roots in comparison with stems, leaves, flowers or fruits has been sparse because they are 'the half hidden' part and are therefore difficult to extract from the soil (Lux and Rost, 2012). There has been much debate on the limitations and large variation when applying the traditional co-cultivation methods, such as the inability to have separation of shoots and roots upon treatment. To overcome these problems, a change in our methodology was made

to the newly adapted hydroponic system. Unlike traditional co-cultivation methods on agar plates where both shoots and roots are in contact with the media supplemented with the bacteria, the hydroponic method allows for easy and clear separation of roots and shoots due to the use of a sterile nylon membrane, that aims to concentrate the site of infection to the roots. It can also be argued that it mimics nature slightly more, where plants are mainly faced with their rhizobial microbes through the soil and thus the roots. The hydroculture also enables measurement of the amount of camalexin exuded from the roots, a key prerequisite of camalexin's role in shaping the microbiome (Millet et al., 2010; Koprivova et al., 2019).

MYB67 was predicted to be associated with regulating camalexin biosynthesis. Similar to the genes *CYP71A27* and *CYP71A28, MYB67* is preferentially expressed in the root, but transcripts are also present in the leaves. *MYB67* was also suggested to be co-expressed with *CYP71A28*. The *myb67* mutant was previously shown to have lower transcript levels of *CYP71A27* and *CYP71A28* in contrast to the WT Col-0, as well as similar sulfatase activity to that of the mutants *cyp27* and *cyp28*. Furthermore, mis-regulation of key glucosinolate and camalexin genes were similar to that of *cyp27* and *cyp28* (data not shown, communication with Dr. Koprivova). These results in addition to the Plant Regulomic predictions of MYB67 interacting with the promoter regions of *CYP79B2, CYP79B3, CYP71A27, CYP71A28, MYB51* and *WRKY18,* further corroborated the involvement of MYB67 in regulating camalexin biosynthesis (Supplemental Table S1). As a result, *MYB67* emerged as a promising candidate for further investigation and characterisation of its relationship with *CYP71A27, CYP71A28* and camalexin.

Several prominent observations resulted from the physiological characterisation of MYB67's function and analysis of MYB67's entire transcriptional profile following exposure to the pathogenic and plant growth promoting bacteria. Firstly, MYB67 affects the spatial expression of the *CYP71A27* gene encoding a camalexin biosynthesis enzyme in the roots. Second, the absence of MYB67 permits the plant to take advantage of the PGP effect more efficiently than the WT and elicits greater resistance to the pathogen. Third, MYB67 negatively

regulates the production of camalexin in response to both bacteria and the elicitors, flg22 and chitohexaose. *MYB67* is only transiently expressed in response to flagellin, and camalexin biosynthesis suppression by MYB67 is equally temporary. Fourth, although the expression of camalexin associated genes is regulated in a treatment-dependent manner, MYB67 appears to be capable of regulating various camalexin signalling pathways to ensure its optimal homeostasis. Furthermore, MYB67 may be involved in modulating plant innate immune processes as *myb67* does not require an external inducer to trigger camalexin associated gene expression. Moreover, camalexin biosynthesis is not the primary signalling pathway for which MYB67 is responsible, as it appears to be engaged in circadian and photosynthetic regulation, suberin and cell wall associated processes, and other plant innate immune responses such as phenylpropanoid and terpenoid biosynthesis. Lastly, the target genes identified via DAPseq and the MYB67 related mutants as well as *anac038* were discovered to have comparable functions to MYB67.

3.1 MYB67 influences the expression of *CYP71A27*

Koprivova and colleagues (2019) revealed changes in *ProCYP71A27* controlled GUS expression of 7 day old seedlings following 24 h of treatment with *P. fluorescens* CH267, demonstrating a substantial difference between mock and *P. fluorescens* sp. CH267-treated plants. They also showed that flg22 caused a shift in spatial expression of *CYP71A27* closer to the root tips; however, cocultivation with PGPB *P. simiae* WCS417 resulted in an overall decrease in *CYP71A27* expression levels (Koprivova et al., 2019). *CYP71A27* expression after treatment with *B. glumae* in the WT and *myb67* mutant was investigated for the first time in this thesis. Additionally, the *MYB67* promoter controlling the GUS reporter gene was also analysed in order to characterise the *MYB67* expression pattern in young *Arabidopsis* seedlings. Expression of *MYB67* in six day old seedlings was strongly active in the roots, root-hypocotyl junction regions and near the shoot apical meristems (SAM) (Supplemental Figure S3). This was comparable to that of *ANAC042* demonstrated by Saga and colleagues, (2012). Which may suggest similar activity. Overall under mock conditions, the expression of *ProMYB67:GUS* was observed further away from the root tip than *ProCYP71A27:GUS*. However, *ProMYB67:GUS* in a time-sensitive manner, only after flg22 treatment, was no longer restricted and visualised to be

highly expressed closer to the root tip at 2 hpt (Supplemental Figure S4). These results support the prediction that *MYB67* is involved in regulating metabolic activity invoked in specific tissues in response to microbes, but in a time-dependent manner. The histochemical assays also revealed that MYB67 has an effect on the expression pattern of *CYP71A27*. The expression of *ProCYP71A27:GUS* in the *myb67* after incubation with flg22 was time dependent; it dramatically changed, already after 30 min, reduced slightly after 1 h and was no longer present 72 hpt (Supplemental Figure S4). After flg22 treatment, rapid and transient expression of *MYB67,* closer to the root tip does not further affect the intensity of *ProCYP71A27:GUS* expression at 2 hpt. Under mock conditions and in response to the *B. glumae* or flg22 the GUS expression is stronger in *ProCYP71A27:GUS* in the *myb67* in comparison to the WT (Figure 7, Supplemental Figure S4). Further quantification of this assay by measuring the GUS activity will further verify MYB67's role in suppressing *CYP71A27* expression and controlling its spatial expression in the roots. CYP71A27 however lacks the heme-binding site, thus it is not an active enzyme. Regardless of it being non-functional, it has a distinct role in camalexin biosynthesis, its role however needs to be explored further to determine the consequences of *CYP71A27* suppression by MYB67 (communication with Prof. Dr. Kopriva; Koprivova et al., 2019). Nevertheless, MYB67 appears to influence the spatial expression pattern of *ProCYP71A27:GUS*. Expression of *MYB67* in the root even under mock conditions may be vital as it is a sensitive organ exposed to numerous microbes and MYB67's regulatory role in the roots may be required in maintaining homeostasis in preparation of inducing plant immunity.

3.2 *myb67* is able to benefit more from the PGP effect induced by *P. fluorescens* and has increased resistance to growth inhibition by *B. glumae*

Crop diseases and excess use of artificial pesticides remains a serious challenge for sustainable agriculture (Jiao et al., 2021). Our struggle to improve crop productivity has been greatly focused on the application of pesticides that are not readily broken down and remain in

the soil as toxic residues that have been shown to affect human health (Gilden et al., 2010). The use of PGPB is an environmentally friendly alternative of controlling plant disease and increasing crop yield. PGPB that both suppress plant disease and directly stimulate plant growth have thus become a focus of research for their implementation in our future food production for overall consistent and sustainable biocontrol (Jiao et al., 2021). Additionally, understanding how plants can deter harmful microbes whilst benefiting from growth promoting microorganisms will only aid research for commercial application in the agricultural field.

Co-cultivation with *P. fluorescens* sp. CH267 increased the fresh weight of Col-0 but not of the mutant *cyp27;* the PGP effect was restored in the mutant when camalexin was introduced with the bacteria, while it led to the loss of PGP effect in the WT (Koprivova et al., 2019). The *cyp27* mutant that produced less camalexin than WT was considerably more susceptible to the growth inhibition by *B. glumae* (Koprivova et al., 2019). As *myb67* was demonstrated to accumulate high amounts of camalexin in the hydroponic co-cultivation method it was of interest to explore how the pathogenic and PBP bacteria influence the *myb67* growth and camalexin in the traditional co-cultivational context. After 2 weeks of incubation with *B. glumae* and *P. fluorescens*, *myb67* showed increased resistance to *B. glumae*'s growth inhibition and was able to utilise *P. fluorescens'* growth promoting ability more effectively than Col-0 (Figure 10A).

After 2 weeks of incubation, camalexin levels in the PGPB treated *myb67* roots were higher than in WT (Figure 10C). Overall, the amount of camalexin in the PGPB treated seedlings, however, was still less than the pathogenic treated seedlings. The generally lower accumulation in PGPB treated plants in comparison to the pathogen treated ones was expected due to the multi-leveled strategies beneficial microbes employ to suppress host immunity and establish a mutualistic relationship (Yu et al., 2019). The higher camalexin in the mutant than the WT implies that the accumulation does not have a negative effect on the growth promoting effect. In general, the levels of camalexin after 2 weeks, could suggest that the plant has maintained lower levels of synthesis as a form of priming to prevent future pathogenic attacks and/or allowing it to switch to plant growth and development in its vulnerable state. This is

further supported by the fact that PGP *Pseudomonas* strains have been known to modulate plant immunity by ISR and inducing biosynthesis of secondary metabolites is a typical IR response (Bakker et al., 2007; Chassot et al., 2008; Pieterse et al., 2014). Camalexin has thus been reported to be elevated in primed plants and restored PGP effects in mutants that have lost it (Koprivova et al., 2019; Nguyen et al., 2022). If so, *myb67* with higher accumulated camalexin than WT may have had stronger priming and thus greater resistance to future pathogenic attack; nevertheless, this would need to be tested with a secondary pathogenic inoculation. It would also be interesting to examine if *myb67* is still able to utilise the growth promotion from *P. fluorescens* after feeding of purified camalexin or if like WT it loses its ability (Koprivova et al., 2019).

Overall, *B. glumae* appears to have evaded the plant innate immunity and successfully suppressed plant development in both WT and *myb67* (Figure 10A). *B. glumae* PG1 has been reported to successfully colonise WT plants well (Li Chen, unpublished Dissertation, 2023). While camalexin levels in *myb67* roots are lower than WT after 2 weeks of co-cultivation with *B. glumae*, the mutant exhibits improved resistance towards the pathogen's growth inhibition (Figure 10 A&B). It would be interesting to see if the increased resistance observed can be improved by a previous priming of camalexin accumulation induced by *P. fluorescens*, a similar concept shown by Nguyen and colleagues (2019a). It can be argued that the significantly higher camalexin accumulation in *myb67* compared to WT at early stages of response (3 dpi as seen in the hydroponics, Figure 9A) may have been sufficient to induce camalexin biosynthesis to enhance resistance and limit *B. glumae* proliferation. There are several issues with this theory: first and foremost, growth on plates is a completely different system than hydroponics and since measurements were not recorded at the 3 dpi, we cannot confidently state that *myb67* provoked a similar response in the hydroponic system. Second, bacterial colonisation in *myb67* has not been assessed in this set, therefore the pathogen's ability to proliferate within the mutant is unknown. Lastly, without further research within this system, it is difficult to theorise whether MYB67 has induced other PTI responses such as ROS or enhanced callose deposition. For example, the gene encoding a positive regulator of aliphatic glucosinolates, *MYB28,* was significantly elevated in

B. glumae treated *myb67,* which could add to the resistance against the pathogen (Figure 19). Furthermore, the seedlings in this system are grown on plates for 2 weeks, allowing the pathogen to have direct contact with the entire plant, it is probable that the camalexin produced in the shoots had a greater effect on pathogen resistance. This is consistent with the higher camalexin levels found in *myb67* shoots (Figure 10B).

3.3 MYB67, a negative regulator of camalexin?

Extensive research on R2R3-MYBs has demonstrated that MYB TFs are implicated in the regulation of primary and secondary metabolism, such as flavonoid, lignin, and phenylpropanoid biosynthesis, as well as the control of glucosinolate biosynthesis and a variety of abiotic stress responses including drought, salt/nutrient stress, gravity, and light (Chen et al., 2022). MYB34, MYB51, and MYB122 have been shown to regulate the biosynthesis of both glucosinolates and camalexin after pathogen exposure or treatment with elicitors (Frerigmann and Gigolashvili, 2014). It was discovered that these MYBs were involved in the induction of camalexin after $AgNO_3$ and flg22 treatment using double and triple mutants, (Frerigmann et al., 2015 and 2016). In contrast to the MYBs being identified as positive regulators, the triple mutant *myb34/myb51/myb122* demonstrated higher levels of camalexin after infection with the necrotrophic fungus *P. cucumerina,* insinuating that *MYB34, MYB51,* and *MYB122* negatively regulated camalexin in response to this pathogen (Frerigmann et al., 2016). Compared to the WT, *myb67* accumulated higher amounts of camalexin, which was observed at 3 dpi on multiple occasions in response to the pathogen and PGP bacteria (Figures 8A, 9, 11, 14, and 36). These findings thus suggest that MYB67, a member of the R2R3-MYB family, similarly to MYB34, MYB51 and MYB122, negatively regulates camalexin synthesis in response to both the pathogenic bacteria *B. glumae* and the PGPB, *P. fluorescens.*

Chitin is a major component of fungal cell walls that also serves as a MAMP, eliciting various defence reactions (Gust et al., 2007; Miya et al., 2007; Denoux et al., 2008). Chitosan, the deacetylated derivative of chitin, has been used since 1980 as a means to induce phytoalexin

synthesis in pea pods (Hadwiger and Beckman, 1980). Chitosan can also stimulate lignification, callose formation as well as activate ROS production in various plant species (Povero et al., 2011). *CYP79B2*, *CYP79B3*, *CYP71A13*, and *CYP71B15* have been shown to be induced after treatment with chitosan (Povero et al., 2011). Camalexin was shown to be induced after 27 h of treatment with chitosan by Barco, Kim and Clay, (2019), so it was expected that camalexin would be induced in the WT after treatment with chitohexaose (as our chitin treatment) (Figure 12A). Between 4 hpt and 48 hpt, the mutant *myb67* produced more camalexin after being treated with chitin than the WT, indicating again that MYB67 can act as a negative regulator of camalexin biosynthesis upon chitin treatment at early stages (Figure 12A). Camalexin is elicited in response to various microorganisms but its regulation varies upon each treatment (Nguyen et al., 2022b). It is significant to highlight that MYB67 may be involved in regulating camalexin biosynthesis in response to both bacteria and fungi. Camalexin has been reported to be effective primarily against necrotrophic fungal pathogens such as *B. cinerea* and *A. brassicicola* (Thomma et al., 1999; Ferrari et al., 2003). Since only a component of the fungal cell wall (chitohexaose) was utilised, it would be informative to test additional live fungal strains on *myb67* to determine if they elicit a comparable response.

The dynamics of synthesising camalexin in the hydroponic system varied between the pathogen and PGP bacteria treatment. In the WT, initial camalexin synthesis triggered by *B. glumae* appeared to be slower but resulted in a significantly stronger response than the PGPB, *P. fluorescens*, which elicited a more rapid but transient response (Figure 8A). Camalexin levels in *B. glumae* and *P. fluorescens* were comparable to those found in Koprivova and colleagues (2023). At 24 hpi, the camalexin accumulated in the mutant *myb67* was comparable to the WT, but at later time points, *B. glumae* induced a stronger response in *myb67* than in the WT (Figure 8A). This indicates that MYB67 may be required to negatively regulate camalexin biosynthesis after inoculation with *B. glumae*. Notwithstanding, accumulation of camalexin in response to *B. glumae* after 2 weeks in traditional co-cultivation assay illustrated lower levels in *myb67* than WT roots (Figure 10B). If MYB67 is a repressor of camalexin, how is this explained? One hypothesis is that MYB67 has a dual regulatory function to repress and activate in a

time-dependent manner. Secondly, MYB67's activity could be repressed through an unknown mechanism. Thirdly, since *myb67* portrayed increased resistance, other defense mechanisms such as deployment of R proteins could be the cause of the increased resistance in the mutant. Additionally, the lower levels of camalexin may correlate to the amount of bacteria present and therefore this would have to be assessed to verify whether MYB67 is also necessary to activate camalexin biosynthesis at later stages or if the bacterial proliferation is affected and thus the amount of camalexin. Similarly, at 3 dpi, *myb67* had accumulated less camalexin than the WT after treatment with chitin (Figure 12A) and flg22 (Figure 11C). Especially since Plant Regulomics predicts MYB67's binding to the genes *CYP79B2, CYP79B3, CYP71A27,* and *CYP71A28* as well as regulators of camalexin biosynthesis (*MYB51, WRKY18*). This could suggest that MYB67 may have a dual regulatory role in acting as a repressor and activator via multiple avenues for camalexin biosynthesis that is not only treatment dependent but time-dependent also. MYB67 may thus be required for this fine-tuning of camalexin production to WT-like levels.

3.3.1 *nac038* and MYB67 homolog mutants are functionally similar to *myb67*

After exposure to the pathogenic bacteria strain *B. glumae* PG1, similarly to *myb67,* the mutants: *nac038, myb61, myb83* and *myb103* accumulated significantly higher amounts of camalexin in the roots (Figure 14A). The amount of accumulated camalexin in the mutants *myb61* and *myb103* did not correlate well between the shoots and roots (Figure 14). In the shoots the two latter mutants had less accumulated camalexin in comparison to the WT, suggesting that they do not play a role in activating the biosynthesis of camalexin in the shoots or for are impaired in rapid transport of camalexin from roots to shoots (Figure 14A). It would be interesting to assess the mutants *myb61* and *myb103* if they play a role in the coordination of camalexin between shoots and roots (Koprivova et al., 2023). With focus on the roots, the qRT-PCR results indicate that after *B. glumae* inoculation, MYB61 is responsible for activating *CYP71A12, CYP71A13, CYP71A27, CYP71A28,* and *CYP71A15* expression (Figure 15). On the other hand, MYB83 plays a role in inducing the transcripts of *CYP71A12, CYP71A13, CYP71A27,* and *CYP71A15* (Figure 15). Since MYB103 was not predicted to bind to any of the

camalexin associated genes, it may activate the genes *CYP71A13, CYP71A27, CYP71A28* and *CYP71B15* indirectly (Figure 15, Supplemental Table S1). Interestingly, all three MYBs appear to be required to suppress the gene expression of *CYP71A13* upon treatment with *B. glumae* (Figure 15). In response to the PGPB, only *myb61* and *myb83* had significant differences in expression of *CYP71A12* and *CYP71A15* (Figure 15). Additionally, after treatment with the PGPB, MYB83 appeared to be responsible for inducing the gene expression of *CYP71A13* (Figure 15). Plant Regulomics did not predict the binding of MYB61 and MYB83 to *CYP71A12, CYP71A13,* and *CYP71A15,* insinuating that the regulation of these genes are through an indirect mechanism whereas *CYP71A27* and *CYP71A28* are directly regulated (Supplemental Table S1).

MYB61, MYB83 and MYB103 have been reported to be associated with secondary cell wall biosynthesis, which in itself is also crucial for plant immunity and resistance against microbes (Newman et al., 2004; Dubos et al., 2005; Zhong et al., 2008; McCarthy et al., 2009; Öhman et al., 2013; Geng et al., 2020; Swaminathan et al., 2022). On the other hand, the *myb* mutants (with compromised cell walls) may be more susceptible to bacteria, allowing them to proliferate more within the plant, which in turn elicits stronger defense responses. It would be informative to evaluate the titre of bacteria within the plant before making final conclusions. Since the cell wall is the first physical barrier that microbes have to break through, making the cell wall a dynamic and highly controlled structure, any alterations in the cell wall integrity triggers disease responses. Changes in cellulose and lignin biosynthesis have been shown to underpin the synthesis of other phenolic compounds including phytoalexins (Malinovsky et al., 2014). Thus, whether changes in the secondary cell wall caused by genetic mutations influence camalexin biosynthesis indirectly or directly is uncertain, but they clearly play a role in its biosynthesis. It is possible that MYB61 and MYB83 are involved in influencing other camalexin associated genes directly, which were also predicted by Plant Regulomics (Supplemental Table S1). MYB61 is hypothesised to interact likewise with MYB67 to: *CYP79B2, CYP79B3, CYP71A27, CYP71A28,* and *MYB51* (Supplemental Table S1). MYB83 on the other hand was predicted to bind to the promoter regions of: *CYP79B3, CYP71A27, CYP71A28, GGP1, ANAC042, MYB51, MYB122* as well as itself *MYB83* (Supplemental Table S1). Additionally,

both MYB61 and MYB83 were shown to potentially bind to *MYB67* also. This would result in a feedback loop between MYB67 and MYB83 as they both are predicted to interplay with each others' gene expression (Supplemental Table S1).

anac038 was most similar to *myb67* after inoculation with both the pathogen and the PGPB in its influence on the camalexin biosynthesis genes *CYP71A12, CYP71A27* and *CYP71A28,* as well as its accumulation and exudation of camalexin (Figure 15). Only for *CYP71B15* was the expression higher in *anac038* than both WT and *myb67,* in addition to higher transcript levels of *CYP71A13* in *nac038* in comparison to both WT and *myb67* after exposure with the PGPB (Figure 15E). The biggest differences between *anac038* and *myb67* were seen under mock conditions in the expression of *CYP71A13* and *CYP71B15* (Figure 15 B&E). Plant Regulomics predicted that ANAC038 binds to the promoter regions of *MYB67, CYP71A27* and *CYP71B15* in addition to *MYB61, MYB83* and *MYB103* (Supplemental Table S1). It is possible that ANAC038 represses camalexin on a transcriptional level by directly suppressing *CYP71A27* and *CYP71B15,* and indirectly suppressing *CYP71A12* and *CYP71A28*. Speculations that ANAC038 is involved in regulating the MYBs: *MYB61/83/103*, including *MYB67* for camalexin biosynthesis and other biological processes could be made, but would have to be investigated, at least in their expression of *anac038*. It would be valuable to further explore if double mutants would severely affect the camalexin biosynthetic gene expression in addition to its accumulation. Analysis of single cell transcriptomic data revealed that ANAC038 and MYB67 function similarly in association with suberin lamellae (Cao et al., 2022). Thus, it is possible that they have other similar functions as shown currently to negatively regulate the biosynthesis of camalexin.

3.4 MYB67's regulation of specific camalexin biosynthetic genes is treatment dependent

The understanding of how camalexin is regulated in the roots is quite limited. Further investigation on the physiological aspect of MYB67 and how it regulates the biosynthesis of

camalexin was initially examined with qRT-PCRs. In response to chitin, MYB67 generally appears to negatively regulate camalexin biosynthesis, this is regulated independently of *CYP71A12, WRKY33* and *ANAC042* (Figure 12 B-D). Furthermore, the transcript levels of *WRKY33* in *myb67* were even lower than in WT roots at 4 hpi, suggesting that MYB67 may have a dual regulatory function and is required also to activate *WRKY33* for WT-like levels or MYB67's ability is repressed (Figure 12 C). This timely dependent regulation could already be indications of MYB67's connections to the clock genes, which will be discussed later in greater detail. Due to the fact that only a few camalexin associated genes were assessed it is not possible to conclude how MYB67 negatively regulates camalexin in response to chitohexaose. Further analysis is thus necessary to attempt to determine its regulation. Millet and colleagues (2010), reported that flg22 strongly induces *CYP71A12*, which was comparable to the obtained results. Since flg22 treated *myb67* had higher transcript levels of *CYP71A12*, it is likely that the high camalexin accumulated at 2 hpi is due to a lack of repression of *CYP71A12* by MYB67 (Figure 12B). The induced expression of *CYP71A12* could be due to high expression of *WRKY33* as WRKY33 is known to positively regulate its target *CYP71A12*. It has been established that expression of *WRKY33* and *ANAC042* is induced by flg22 (Qiu et al., 2008; Saga et al., 2012). MYB67 also regulates camalexin through *WRKY33* and *ANAC042*, as high expression of these genes was observed in *myb67* at 2 and 4 hpi (Figure 12). This suggests that MYB67 might be responsible for maintaining flg22-induced camalexin biosynthesis through multiple signalling pathways. Even at control conditions, the expression of *CYP71A12, WRKY33, ANAC042* and *FRK1* were significantly higher in the mutant than the WT (Figure 12). Suggesting that MYB67 plays a role in regulating defense associated genes in untreated plants possibly in preparations for an external threat. This is further supported by the higher readout of camalexin in *myb67* compared to WT in mock (Supplemental Figure S5).

B. glumae inoculated WT roots were found to have increased expression of *CYP71A12, CYP71A13, CYP71A27* and *CYP71B15* (Figure 8 & 21). The mutant, *myb67* had even higher transcript levels of *CYP71A12* and *CYP71A27*, which could explain its higher levels of camalexin than the WT. MYB67 after treatment with *B. glumae* in the hydroponic system

represses the expression of *CYP71A12* and *CYP71A27* in the roots (Figure 8 & 21). It is likely that the regulation of *CYP71A12* is achieved indirectly as Plant Regulomics did not predict MYB67 to be binding to the promoter region of *CYP71A12* and it was not identified as a target from the DAP-seq (Supplemental Table S1). Regulation of *CYP71A12* could be done through WRKY33 or ANAC042; whose expression might be modulated by MYB67, according to the DAP-seq (Figure 36). *GGP1* is another example that was not predicted to be a target but was shown to be a direct target of MYB67 and was differentially expressed between the genotypes after treatment with the pathogen (Supplemental Table S1 and Figure 34). *WRKY18*, *MYB51*, *GGT1* and *CYP71A27* on the other hand, were predicted to be MYB67's target genes, this coincides with the DAP-seq and they were also found to be statistically significant in the *myb67* in the BGvM comparison (Figure 34, Figure 36 and Supplemental Table S1). The RNA-seq revealed the additional camalexin associated genes that were mis-regulated, but were not identified to have a q-value < 0.05.

CYP71A12 has been reported to be induced after exposure to commensal bacteria but its induction appears largely dependent on the beneficial bacteria encountered (Nguyen *et al.,* 2022a). *CYP71A12* was induced by *P. fluorescens* but no differences were seen between the WT and mutant (Figure 15). Interestingly, in the mock, *myb67* had lower levels of *CYP71A13, CYP71A27, CYP71A28,* and *CYP71B15* than the WT (Figure 15). In response to *P. fluorescens* *CYP71A13, CYP71A28* and *CYP71B15* expression was increased in *myb67* in comparison to *myb67* mock, and only for *CYP71A28* were the transcript levels even greater than PGPB treated WT samples. This induced expression may have been sufficient in causing the higher accumulation of camalexin than WT. The MYB67 regulation of camalexin after exposure to the PGPB is most likely more complex. *P. fluorescens* highly induced accumulation of camalexin in the mutant may not be due to a direct regulatory effect of MYB67 on the camalexin genes, instead, MYB67 may indirectly suppress expression of *GH3.5, MKK9, CYP79B3, GSTF6* and *CYP71A13*, since they were seen to be elevated in *myb67* (Figure 21). For instance, the JA responsive gene *EBP* (also known as *ERF72*) was also found to be a target gene of MYB67 (Figure 34 and Figure 36). EBP was identified recently to influence camalexin biosynthesis by directly targeting *CYP71B15* and *CYP71A13* as well as indirectly targeting *WRKY33* (Li et al.,

2022). Similar to *EBP*, *ERF1* was identified as a target of MYB67 and acts downstream of EIN2 (Figure 36, Zhou et al., 2022). EIN2 also signals the TF EIL2 that leads to ethylene responses, which MYB67 is predicted to interact with on a protein level (Figure 36, Supplemental Figure S1; Binder, 2020). EIL2 is not known to influence camalexin biosynthesis but MYB67 may indirectly regulate its biosynthesis through ERF1 as it was recently reported as an essential positive regulator of camalexin (Zhou et al., 2022).
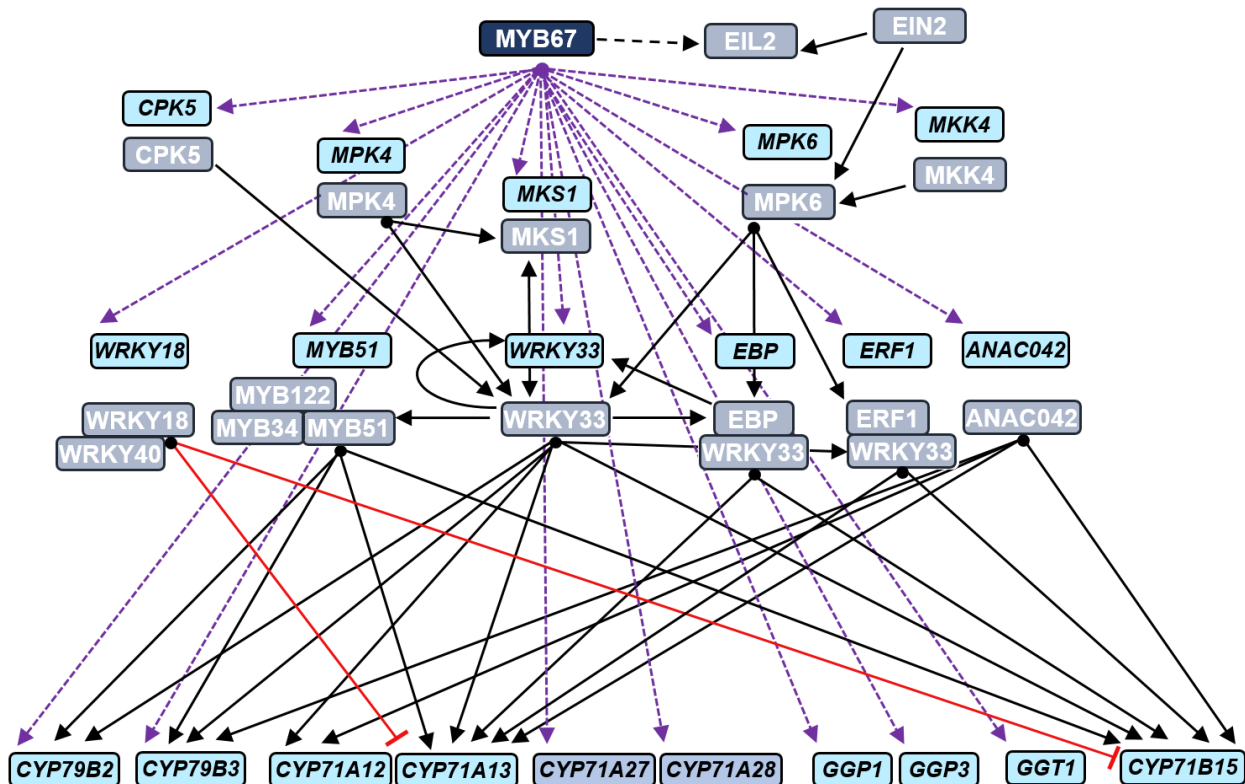
Figure 36: Summary schematic of MYB67's transcriptional network to regulate camalexin biosynthetic genes. The protein of interest (MYB67, dark blue), gene transcripts (light blue), 'new' CYP transcripts (shaded blue), Proteins (grey with white font). The purple dashed lines indicate MYB67's direct binding, red lines (suppression), black lines (interaction /activation), black dashed lines (predicted protein interaction) (DAP-seq; Li et al., 2022; Nguyen et al., 2022b; Zhou et al., 2022).

As mentioned previously, under flg22 treatment *WRKY33* and *NAC042* expression were strongly affected, despite Plant Regulomics's prediction that MYB67 does not bind to these promoter regions, it was shown with the DAP-seq that they are indeed direct targets (Figure 12, Figure 36 and Supplemental Table 1). *GGP1* was also not identified as a direct target through Plant Regulomics but the DAP-seq indicated that it was (Figure 36). The RNA-seq adds to the DAP-seq data as *WRKY33* and *GGP1* were all significantly differentially expressed between

genotypes (Figure 34). However, it is also plausible that MYB67 is required to activate the expression of negative regulators of camalexin, for overall repression of the metabolite after exposure with the PGPB. Two candidates for that may be the camalexin negative regulators *WRKY18* and *WRKY40*, which were shown to be down-regulated in *myb67* (Pandey et al., 2010). Other camalexin associated genes that were also found significantly down-regulated in *myb67* after treatment with the PGPB, and are also target genes of MYB67 include: *CPK5, MAPK6, MYB51, MKS1, CYP79B2, WRKY33* and *GGP1* (Figure 34 and Figure 36). The down-regulation of these genes does not explain the high accumulation of camalexin that was found in the mutant in comparison to the WT but still suggests that MYB67 could have a dual function in activating these genes for WT-like biosynthesis of camalexin. Or that there are other TFs that act more dominantly in its regulation. *MYB67* expression is triggered in WT after inoculation with both bacteria, it is thus possible that there is a feed-back loop occurring where transcription of *MYB67* is activated by camalexin itself. Camalexin feeding experiments may elucidate this hypothesis. Since camalexin is the readout we used of MYB67's affect in plant immunity, it could potentially be involved in multiple stages from recognition of an elicitor, to camalexin synthesis and exudation; it would be thus interesting in the future to determine where it makes the greatest impact. In order to clarify further, MYB67's regulatory role, double mutants can be utilised to narrow the pathways the protein is involved in to modulate camalexin biosynthesis in response to PGPB.

3.4.1 Regulation by protein-protein interactions

Another possible mechanism of regulation is the formation of other homo- and hetero-multimeric complexes that may be formed with MYB67 in order to regulate the biosynthesis of camalexin. Similar to that of the MYB34-MYB51-MYB122 complex, MYB30-MYB55-MYB110 complex and the MYB11-MYB12-MYB111 complex for regulating secondary metabolites: glucosinolates, hydroxycinnamic acid amides (HCAAs) and flavonoids, respectively (Meraj *et al.,* 2020). The MYB-like TF, REVEILLE1 (RVE1) is known for being involved in the circadian clock and auxin pathways (Rawat *et al.,* 2009). It has also been shown to stabilise a DELLA protein RGA-like2 (RGL2) to depress seed germination and enhance seed

dormancy (Yang *et al.,* 2020a). RVE1 was also shown to interact with MYB67 on a protein level and affect its transcription (Supplemental Figure S1 D&E and Supplemental Table S1). MYB67 has a MYB-like binding domain, which RVE1 could potentially interact with (Supplemental Figure S1D). Additionally, RVE1 was predicted to interact with a number of camalexin associated genes including: *CYP79B2, CYP79B3, CYP71A12, GGP1, CYP71B15, ANAC042, MKS1, MAB51, MYB122, WRKY18* and *WRKY40* as well as a possible camalexin responsive gene, *ANAC038* (Supplemental Table S1)*.* Furthermore, *RVE1* was significantly down-regulated after both bacterial treatments in *myb67* compared to WT (Figure 19B). The DAPseq also revealed *RVE1* as a target of MYB67. It is thus a possibility that protein-protein interaction occurs between RVE1 and MYB67 and potentially even a complex feedback loop. Since RVE1 also interacts with proteins containing WD repeats such as TPL (TOPLESS PROTEIN) and TPR2 (TOPLESS RELATED PROTEIN 2) (Li *et al.,* 2016b; Yang *et al.,* 2020b), both of which are known JA signalling repressors, it may be worth investigating if all these proteins interact together to form a complex and interact or co-interact with MYB67 to assist in its regulatory roles. Furthermore, MYB67 is thought to interact with ETHYLENE INSENSITIVE 3-LIKE 2 (EIL2) which may indirectly regulate the biosynthesis of camalexin through the ET signalling pathway (Figure 36, Supplemental Figure S1 D&E). Thus, it would be informative to pinpoint which hormonal signalling pathway MYB67 is primarily involved in. This can simply be done by using various hormone related mutants as well as adding external hormones to *myb67* and observing if there are any differences in the production of camalexin.

3.5 MYB67's regulatory role in other biological processes

The previous chapters have established that MYB67 plays a transcriptional regulatory role in the biosynthesis of camalexin, which was reflected in the mis-regulation of numerous camalexin associated genes. The target gene mutants that accumulated camalexin following PGPB inoculation were similar to *myb67,* indicating that they function in similar biological processes; however these target genes are also associated to various pathways (Figure 35D). This only emphasises MYB67's multidisciplinary role in numerous processes. Additionally, the GO

analyses support the fact that MYB67 may be involved in other biological processes. For instance, under mock conditions and shared with down-regulated genes in PGPB, MYB67 appears to be significantly involved in 'circadian rhythm' (Supplemental Figure S13B). Although *CCA1* and *LHY* are not direct targets of MYB67, they were shown to be significantly down-regulated in *myb67* across all treatments, as have the target genes *APRR1 (TOC1)* and *RVE1* (Figure 18B, Figure 33). The morning expressed CCA1 and LHY suppress the evening genes including *TOC1*, *ELF3* and *ELF4*, which in turn are required for *CCA1* and *LHY* transcription (Farré, 2012). This is simply the tip of the iceberg when it comes to the intricate positive and negative feedback loops required for proper circadian clock function. The circadian clock is interlinked with environmental cues such as temperature and light that influence the release of growth factors such as PHYTOCHROME-INTERACTING FACTORS (PIFs) (Paik et al., 2017; Creux and Harmer, 2019). TOC1 has been found to bind directly to PIF4 to inhibit their ability to activate transcription (Nusinow et al., 2011; Creux and Harmer, 2019). Transcription of PIF4 however, is repressed by the evening complex ELF3-ELF4 and positively regulated by CCA1 (Nozue et al., 2007; Nusinow et al., 2011; Creux and Harmer, 2019). *PIF4* was also identified as MYB67 target by DAP-seq and was found to be highly up-regulated in *myb67* after PGPB inoculation. Due to the down-regulation of the other clock genes they are unable to prevent PIF4 from functioning, and as a growth factor, it may have aided *myb67* in utilising the growth promotion effect from *P. fluorescens* (Paik et al., 2017). Because *RVE1* was also considerably down-regulated in *myb67,* it is unlikely that growth is promoted through the clock output RVE1, which can promote expression of the auxin biosynthetic enzyme, *YUC8,* for growth independently from PIF4 (Rawat et al., 2009). Plant Regulomics anticipates that LHY binds to the promoter region of *MYB67* (data not shown), thus there may be an undiscovered feedback loop in which MYB67 is involved in repressing *PIF4*, activating transcription of *ELF4* in response to PGPB inoculation and activating the clock output *RVE1* (Yang et al., 2021a). The fact that *myb67* resulted in low transcription of the clock related genes in comparison to the WT, strongly suggests that MYB67 somehow is involved in the coordination of the biological rhythmicity and its subsequent metabolic and physiological functions. Also associated with the circadian clock and light reactions are the mechanisms between sugar and starch. Suggested by

the GO enrichment, MYB67 is involved in sucrose/starch breakdown and carbon consumption: therefore, it may be beneficial in the future to measure these components in *myb67* and to determine the light reactions of photosynthesis in *myb67* (using a pulse amplitude fluorometer)*,* that may affect PIF4, for instance. There was also evidence that *MYB67* is significantly affected upon ABA treatment as well as under iron deficiency and phosphate starvation (Supplemental Figure S15). It thus implies that MYB67 plays a role in the plant's ability to acquire nutrients necessary for chlorophyll production and thus photosynthesis, as well as helping the plant absorb other nutrients to improve overall growth and development.

Moreover, MYB67 may play a role in monitoring the crosstalk between growth and defense at the level of the cell wall, the plant's first defensive barrier. Target genes of MYB67 are involved in cell wall modifications, callose formation, cell wall biogenesis, lignan metabolic process, hemicellulose metabolic process and the KEGG pathway cutin, suberin and wax biosynthesis. ANAC038 and MYB67 have been previously shown to be specifically involved in controlling the forming of suberin lamellae in the endodermis of roots and MYB67's homologs in secondary cell wall biosynthesis (Newman et al., 2004; Dubos et al., 2005; Zhong et al., 2008; McCarthy et al., 2009; Öhman et al., 2013; Cao et al., 2022). This further suggests MYB67's potential role in these pathways as well. *MYB67* was observed to be highly expressed upon callus inducing media (Supplemental Figure S15; Fan et al., 2012; Xu et al., 2012). *EXPA1* and *EXPA10* were under both GO terms 'cell wall modifications' and 'callus formation'. *EXP10* (a target gene of MYB67), was up-regulated in *myb67* in comparison to WT after PGPB inoculation. Overexpression of *EXP10* has been shown to result in larger leaves and has been reported to work specifically in controlling leaf size (Cho et al., 2000). Expansins are generally thought to be associated with growth control. *EXPA1* was another shoot and root expressed EXPA gene up-regulated in the mutant after PGPB inoculation. Not only is *EXPA1* a target gene of MYB67 but also a target gene for the cytokinin-responsive ARR1 and its homologues ARR10 and ARR12 (Samalova et al., 2020). Upon auxin-induced lateral root initiation, *EXPA1* is involved in pericycle cell wall remodelling for expansion and correct positioning of the first anticlinal divisions (Ramakrishna et al., 2019). In contrast to cell loosening activity by *EXPA10*,

overexpression of *EXP1* was found to increase cell wall rigidity in root cells and consequently root growth arrest; this corresponds with the roots being somewhat smaller in *P. fluorescens* treated seedlings compared to mock (Samalova et al., 2020). MYB67 is likely responsible for repressing these cell wall modifying genes upon exposure with microbes to adjust for the plant's defense.

Other ET-responsive abiotic stress pathways such as salt and hypoxia stress are also significantly enriched in *myb67* after inoculation with *P. fluorescens* (Figure 29 D&E). ET modulates salinity via NA^+/ K^+ homeostasis, this is maintained through intricate signalling between ET, H_2O_2, cytosolic calcium and extracellular ATP (Shekhawat et al., 2023). In plants, insufficient oxygen availability or hypoxia, usually arise from heavy rains and subsequent flooding (Lang et al., 2020). ET alone cannot trigger the core hypoxia genes and it is unclear how the plant precisely survives in low O_2 (Shekhawat et al., 2023). MYB67's target gene *ADH1,* up-regulated in *myb67* after PGPB treatment, is responsible for further activating hypoxia marker genes under both anoxic and normoxic conditions (Papdi et al., 2015). What is also known is that at low levels of O_2 ET-induced expression of genes related to nitrogen, carbon glycolysis and anaerobic respiration increases (Shekhawat et al., 2023). This is supported in the GO enrichment of 'anaerobic respiration', and 'nitrogen metabolism' from up-regulated genes in *myb67* after contact with the PGPB (Figure 29D). The mis-misregulation of genes associated with hypoxia and hyperosmotic salinity responses due to the loss of *MYB67* and presence of PGPB, highlights the additional stress the plant is under. *MYB67* was shown to be highly expressed under salt and osmotic stresses (Supplemental Figure S15, Ran et al., 2019). This further demonstrates the importance of MYB67 and suggests its role in maintaining homeostasis for possibly a smoother transition between plant growth and defense. Endophytic microbes are known to adjust ET concentrations in plants (Shekhawat et al., 2023). Some research has shown that some beneficial microbes degrade ET precursor, ACC, and suppress ET-induced host defense systems to promote growth of the microbes. In contrast, other examples show that ET can have a detrimental effect on certain beneficial microbes (Shekhawat et al., 2023). Therefore,

the mis-regulation of ET-related genes in *myb67* may be attributable to *myb67*'s susceptibility to *P. fluorescens*.

To validate the DAP-seq, constructs containing the promoter region of the target genes with the GUS reporter as well as the MYB67 driven by the cauliflower mosaic virus (CaMV) 35S promoter were created (plasmids not shown in this thesis). This can be used to evaluate the TF's interactions to the promoter regions of the selected target genes. It would be beneficial to conduct this experiment to further support the results. Otherwise, a CHIPseq could contribute to the analysis performed in this thesis.

3.6 Conclusions and outlook

Our research provided answers to several critical questions regarding MYB67's transcriptional network, function, and connection to camalexin biosynthesis upon biotic stress. This was achieved via physiological approaches, RNA-seq and DAP-seq analyses which assisted in determining target genes of MYB67 that were differentially expressed in response to a pathogen and beneficial bacteria.

The histochemical analyses showed that the expression pattern and intensity of *ProCYP71A27:GUS* was elevated in the mutant *myb67* especially after treatment with *B. glumae*, highlighting the suppressive regulatory effect MYB67 has on the spatial expression pattern of *ProCYP71A27:GUS* in roots in response to the pathogen.

The loss of MYB67 had a significant impact on the accumulation and exudation of camalexin after inoculation with the pathogen *B. glumae* and the beneficial bacteria *P. fluorescens*. The high response of accumulated camalexin and induction of camalexin associated genes in the mutant was similar in response to both bacteria, illustrating MYB67's role as a negative regulator of camalexin biosynthesis. The *myb67* was shown to have enhanced resistance to the pathogen and also increased susceptibility to the PGPB, thereby benefiting from growth

promotion more efficiently than WT Col-0. This insight could be the beginning of understanding the plant's ability to differentiate between pathogenic and beneficial bacteria, which could then be applied in commercially relevant crop plants and improving agricultural yield without using harmful pesticides.

To better understand MYB67's role in regulating camalexin biosynthesis, double and/or triple mutants with camalexin associated genes should be produced to determine how proper camalexin accumulation and exudation is ensured. Many research papers focus on either studying the response to bacteria or MAMP elicitors; bacteria mimic the interactions with plants in nature better than MAMP elicitors. In this thesis, we explored the effects in response to both bacterial treatments as well as flg22 and chitohexaose, and established MYB67 to act as a negative regulator in all treatments, however more transiently in response to elicitors. Nevertheless, further investigation of how loss of MYB67 influences camalexin accumulation in response to additional beneficial and pathogenic bacterial strains as well as fungal strains will provide greater insight to whether MYB67's role in plant immunity is restricted to specific microorganisms.

The analyses of camalexin content and gene expression of camalexin biosynthesis genes in the MYB67 homolog mutants and *anac038* showed that they were functionally similar to *myb67* (Figure 14 & 15). Comparably, MYB67 target genes demonstrated that the mutants of the indirect target (*cca1*) and direct targets (*ccl*, *fact*, *ltp8*, *npf3.1*, *pot5* and *sultr3.5*) responded similarly to *myb67* in accumulating camalexin, after pathogenic and PGP bacterial stress, highlighting that they function in similar pathways whereas *myb69* did not.

The RNA-seq analysis of the WT and mutant roots, illustrated the similarities and differences in eliciting plant innate immunity in response to a pathogen and plant growth promoting bacteria and demonstrated the significance of MYB67's role in the responses. The comprehensive transcriptional network of MYB67 across all treatments highlighted its fine-tuning regulatory role in the biosynthesis of camalexin, by both directly and indirectly targeting camalexin associated genes in a treatment-dependent manner. Furthermore, MYB67

demonstrated function on multiple levels of plant innate immunity as well as perhaps growth and development.

Future work can branch out in numerous directions. There have been indications that MYB67 may be involved in regulating the tradeoff between plant defense and development. Some evidence shows that MYB67 modulates the circadian rhythm genes and responses to light (both crucial for plant development), especially under mock conditions as well as secondary cell wall associated genes for root growth and development (Figure 29A, 32B). Upon external threat, MYB67 is involved processes associated with defence, for instance, at the first level of contact with microbes, influencing genes associated with the physical barrier (the cell wall), especially callus formation in response to PGPB inoculation as well as influencing nitrogen, starch, and sucrose metabolism (Figure 29 D&E). Therefore determining if the TF serves to maintain a balance between plant defense and development could be achieved by additional gene expression analyses. Since MYB67 has been established to play a role in defense the question on how much effect it has on plant development is still unanswered, for example whether it affects nutritional uptake with or without bacteria present. Thus, testing *myb67* with exogenous growth stimulants and other biotic stresses could be examined.

As MYB67 is clearly involved in plant innate immunity, its involvement with the hormonal signalling pathways is inevitable, which was further supported in Figure 32B. *myb67* should thus be examined in response to SA, JA, ABA and especially ET treatments to narrow down the primary signalling pathway that MYB67 functions in. This could also give further insight into the ET-induced salt and hypoxia stress related genes. As already mentioned, 'circadian rhythm' was also enriched and direct target genes indicated associations with the circadian clock, therefore, double mutants of *myb67* and clock genes under modulations of light could also give indications of alterations in plant growth and development at distinct stages. GO analyses also identified MYB67 to be involved in oxidative stress (Figure 32). To clarify MYB67's role in other early defense mechanisms, investigations into ROS production and callose deposition in *myb67* compared to the WT should be conducted. MYB67's involvement in suberin and association with secondary cell wall biosynthesis was further supported in the

RNA-seq and GO enrichment of the target genes determined from the DAP-seq. Therefore, to gain insight into MYB67's potential role in cell wall associated processes, histochemical staining can be used to obtain quantitative results to further understand the secondary cell wall formation and structure in *myb67*. For example methods including: phloroglucinol-HCl or mäule staining (for lignification), congo red and calcofluor white staining (for polysaccharides) or Toluidine blue O to differentially stain polysaccharides and lignin could be used (Mitra and Loqué, 2014). The KEGG pathways for starch, sucrose and nitrogen metabolism were also enriched in response to inoculation with the PGPB in *myb67*, this indicates that there is a connection to plant nutrition and development (Figure30 D). Furthermore, *MYB67* expression was found to be influenced by iron and phosphate deficiencies, according to Plant Regulomics (Supplemental Figure S15). Since certain rhizobacteria such as *P. fluorescens*, can fix nitrogen from the environment and release iron and phosphate into the soil, it may be interesting to investigate whether *P. fluorescens* sp. CH267 can assist *myb67* in obtaining these nutrients for growth.

Overall MYB67 was identified as a negative regulator of camalexin in response to the pathogen, *B. glumae* and PGP bacteria, *P. fluorescens*. The mutant *myb67* was more resistant to the growth inhibition inflicted by the pathogen and in parallel illustrated greater susceptibility to the PGP effect from the beneficial bacteria than the WT. Although the regulatory network of MYB67 in modulating camalexin production as well as the tradeoff between plant immunity and development in the response to both bacterial strains will still need to be unravelled, this thesis already provides valuable insights into the mechanisms of its transcriptional regulation and the effects of pathogenic and PGP bacterial infection on gene expression. The following years will only further substantiate the characterisation of MYB67.

4 │ MATERIALS AND METHODS

4.1 Materials

4.1.1 Plant Materials

Arabidopsis thaliana accession Columbia (Col-0, CS number: CS76778) was used as the wild type (WT) and the background for the *A. thaliana* mutants utilised in this study.

Table 1: *A. thaliana* mutants used in this study

Mutant	Gene locus	Mutation	Line
abca8	AT3G47790	T-DNA	SAIL_546_A02
anac038	AT2G24430	T-DNA	SAIL_784_G11
cyp27	AT4G20240	T-DNA	SALK_053817C
fact	AT5G63560	T-DNA	SALK_034447C
ltp8	AT2G18370	T-DNA	GK-448E07
npf3.1	AT1G68570	T-DNA	SALK_130095C
myb61	AT1G09540	T-DNA	SM_3.30853
myb67	AT3G12720	T-DNA	SM_3_39883
myb69	AT4G33450	T-DNA	SM_3.32482
myb83	AT3G08500	T-DNA	SALK_093099C
myb103	AT1G63910	T-DNA	SAIL_337_C03
pot5	AT4G13420	T-DNA	SALK_074868C
rve2	AT5G37260	T-DNA	SALK_051842C
sultr3.5	AT3G12720	T-DNA	SAIL_768_D11C1

4.1.2 Bacterial Strains

Pseudomonas fluorescens sp. CH267 and *Burkholderia glumae* PG1 (Table 2) were used as the plant growth promoting rhizobacteria (PGPB) and pathogenic rhizobacteria respectively, for hydroponic assays as well as traditional co-cultivation assays within this study.

Table 2: Bacterial species and growth conditions

Species	Strain	Genome ID	Antibiotic	Temperature	Source	Reference
Burkholderia glumae	PG1	595500.3	25 µg/mL Chloramphenicol (CHL)	30°C	Prof. Dr. K.E. Jäger, Heinrich Heine University of Düsseldorf	Gao et al., (2015)
Pseudomonas fluorescens	CH267	294.334	50 µg/mL Carbenicillin (CB)	28°C	Prof. Dr. J. R. Dinneny, Stanford University	Haney et al., (2016a)

4.1.3 Chemicals, Kits, Media & Solutions

Chemicals and enzymes used in this work were obtained from Agilent Technologies (Santa Clara, United States of America), Carl-Roth (Karlsruhe, Germany), Invitrogen (Karlsruhe, Germany), Merck (Darmstadt, Germany), New England Biolabs (Ipswich, United States of America), Promega (Madison, United States of America), Sigma-Aldrich (Munich, Germany) and QIAGEN (Hilden, Germany).

Table 3: Kits used in this study

Kit	Purpose	Company
DNAse Treatment	DNAse Treatment	Thermo Scientific
QuantiTect® Reverse Transcription Kit	cDNA synthesis	Qiagen
GoScript™ Reverse Transcription Mix	cDNA synthesis	Promega
Go*Taq*® qRT-PCR Master Mix	qRT-PCR	Promega

4.1.4 Oligonucleotides

Table 4: Oligonucleotides used in this study

Locus	Name	Sequence (5'- 3')	Name	Sequence (5'- 3')
		PCR		
AT3G47790	ABCA8_LP	CAGATGCTAAAAAGGCGACTG	ABCA8_RP	CACCAATCACCTCTTGCTTTC
AT2G24430	ANAOC38 F-RT	GAACAAGGAGATCATCAGCAGC	ANAOC38 R-RT	GATGGCCAGTATCCATCCAAG
AT2G46830	CCA1_LP	CGTCCTTCCTTCAATCTTTCC	CCA1_RP	CTCAGTCCACCTTCACGTTG
AT3G26740	CCL_LP	AAACATGGTTTCAGGTGCAAG	CCL_RP	GATTACTTCGCATGCTTCAGC
AT5G63560	FACT_LP	CAAAAGCATGGAATTTGTGTG	FACT_RP	GAGGACCTCGAAGACATCTCC
AT5G22500	FAR1_LP	CAAGGTTTGCAGCCTAGTCAC	FAR1_RP	AGTGACTGCGTTTTATGGTGC
AT2G18370	LTP8_LP	AATGTCTAGCGATCATTTCCG	LTP8_RP	TCAACATCAAGAAACGCTGTG
AT1G09540	MYB61_F-RT	GGAGACATTCTTGCTGTTACAAAC	MYB61_R-RT	GGACTGACCAAAAGAGACGG
AT1G63910	MYB103_F-RT	GGTCATCACTCATGCTGCAAC	MYB103_R-RT	CGAAGAAGGGAAAGAAGAAGATAAG
AT3G12720	myb67 LP	CAGGCTTCCATTGAAGACAC	myb67 RP	GGTCAGATGTTGATGGAATGG
AT4G33450	MYB69_LP	CTTTCGATACCTCCATAGCCC	MYB69_RP	CAGGTTGGTCGTGATCAAATC
AT1G68570	NPF3.1_LP	TTCGAAGATATGATGAACCGG	NPF3.1_RP	TGGTTCTAACATGTTAGGTCATCC
AT4G13420	POT5_LP	CATAGCTTTTTGTCACTTTGATTC	POT5_RP	TTGTTGAGTTTACTTTGGCCG
AT5G19600	SULTR3.5_LP	CAGCAAAGCTTCTTCCAATTG	SULTR3.5_RP	ATTTTACGCACAAAACCGATG
		qRT-PCR		
AT2G43000	ANAC042-F	ACCAAAAACCGATTGGATGAT	ANAC042-R	CTGCAAAGTGTCCATACCTCTG
AT2G30750	CYP71A12-F	TGTGGTGTTTGGTCCCTATG	CYP71A12-R	CTCCAGCTTCTTGATCATTTCAT
AT2G30770	CYP71A13-F	GATGTTGTGTTTGCTCCCTATG	CYP71A13-R	TTGTTGGTGAGCAGATTGAGA
AT4G20240	CYP71A27-F	CCCTACGGAGAAGATTGGAA	CYP71A27-R	CCAGCTTCTCTGTCATTACTTTGA
AT4G20235	CYP71A28-F	TTCTCCTCCTACGGCGAATA	CYP71A28-R	GAGGAGGATGGACAGTGCATAAA
AT3G26830	CYP71B15-F	CACCACTGATCATCTCAAAGGA	CYP71B15-R	CGGTCATTCCCCATAGTGTT
AT2G19190	FRK1_F	GCCAACGGAGACATTAGAG	FRK1_R	CCATAACGACCTGACTCATC

AT3G12720	MYB67_F1_22	GAAGCTCCGATGTTGCCTAG	MYB67_R1_22	CATCATCATCCACTCCCACTAC
AT4G34270	TIP41_F	GAACTGGCTGACAATGGAGTG	TIP41_R	ATCAACTCTCAGCCAAAATCG
AT3G47790	qABCA_F	CCAAGTACCGGGCTAGATCC	qABCA_R	TGTGGTGAGTATTATCGCCCC
AT4G15396	qCYP702A6_F	GGTATGCCGAAGAGCTTAGCG	qCYP702A6_R	CTCCTTCCTTCAGGTGTGTGC
AT2G18370	qLTP8_F	ACGGAGTTAAGAGTTTAGCGG	qLTP8_R	AGAAGCATCAACGGGCAAG
AT3G58550	qLTPG22_F	ATGCCAACCGTGCAATGAGCC	qLTPG22_R	GAGGCTGGTGAATCTGGAAGC
AT4G33450	qMYB69_F	GCTTAAAGCTCATCGGATCC	qMYB69_R	GAGAAGTTTTCCCGTTTGCG
AT1G68570	qNPF3.1_F	ACAATCATCTTCTACGACCGC	qNPF3.1_R	CGCTTTACTTCGACGAATCC
AT2G38470	WRKY33_F	TTCGTATGGCTGCTTCTTTTC	WRKY33_R	TGAGGTTTAGGATGGTTGTGG
AT4G23810	WRKY53_F	CACCAGAGTCAAACCAGCCATTAC	WRKY53_R	CTTTACCATCATCAAGCCCATCGG

Table 5: Media and Solutions used in this study

Name	Components
½ Murashige and Skoog (MS)	2.45 g/L Murashige and Skoog medium 1% (w/v) Sucrose pH 5.8 For plates, includes 0.5% agarose
Luria-Bertani (LB)	1% (w/v) Trypton 1% (w/v) NaCl 0.5% (w/v) Yeast extract For plates, includes 1.5% agarose
YEB Liquid Media	0.5% (w/v) Trypton 0.5% (w/v) Beef extract 0.1% (w/v) Yeast extract 0.5% (w/v) Sucrose 0.2% (v/v) of 1 M $MgSO_4$ pH 7.0 with NaOH For plates, includes 1.6% agarose
DNA Isolation Buffer	0.2 M pH 8.0 Tris 0.025 M EDTA 0.25 M NaCl 0.5% SDS
Histochemical Staining Solution	10% Triton X 100 0.5 M Na PO_4 (pH 7.2) 100 mM K FerroCyanid 100 mM K FerriCyanid 100 mM X-Gluc
RNA Extraction Buffer	80 mM Tris pH 9.0 150 mM LiCl 50 mM EDTA 5% LiCl
gDNA extraction Buffer (Magic Buffer for Genotyping)	50 mM Tris/HCl pH 7.2 300 mM NaCl 10% Sucrose

4.2 Methods

4.2.1 Plant Growth Conditions

Prior to use, *Arabidopsis* seeds were sterilised for 3 h with chlorine gas by adding 2.5 mL of 37% HCl to 125 mL sodium hypochlorite in a desiccator under the hood. For sowing the seeds in their respective systems (agar plates or hydroponic system), sterile 0.1% agarose was used. For stratification seeds were placed in the dark for 3 days at 4°C. Then the plates were transferred into growth chambers (Percival Scientific / Panasonic) for incubation at 22°C in long day conditions (16h light/ 8 h darkness, 150 $\mu E*m^{-2}*s^{-1}$). Those in hydroponic systems were subjected to an additional etiolation period of 3 days (remained covered in foil) in the growth chambers before uncovering for further incubation periods.

4.2.1.1 Plant growth on ½ MS Agar plates

Sterilised seeds were sown on ½ MS agar plates containing 0.5% sucrose. Then stratified and placed vertically into the growth chambers as mentioned in section 4.2.1, for genotyping, square plates were grown horizontally. Most experiments on square plates were incubated for 5 days after stratification unless specified otherwise.

4.2.1.2 Plant growth in hydroponic system

Within each well of the 12 well plate, nylon membranes (Franz Eckert, PP-105/16, size: 14x14 mm) were positioned on 1 mL of ½ MS liquid media containing 0.5% sucrose using sterilised tweezers. Using 0.1% agarose, ca. 30 sterilised seeds were transferred onto each nylon membrane. The 12 well plates were wrapped in aluminium foil for stratification (3 days) and etiolation (3 days) as described above before removing the foil for an additional incubation period of 7 days in the growth chamber. The liquid media was then replaced with ½ MS media without sucrose under sterile conditions and incubated for additional 24 h, before being subjected to treatment with bacteria (see 4.2.2.1 for preparation of bacterial suspension) or flg22 (section 4.2.3). The treated plates were then incubated for an additional 3 days under the same conditions.

Afterwards, the shoots and root samples were collected, fresh weight was measured and the samples were immediately frozen in liquid nitrogen. Each well was collected as a biological replicate, resulting in at least four biological replicates per genotype and treatment.

4.2.1.3 Genotyping *Arabidopsis* mutants

To obtain homozygotes, T-DNA mutant lines were sterilised and sown on square plates as described in section 4.2.1.1. Under sterile conditions a small leaf from a seedling was homogenised in a 1.5 mL tube containing 3 glass beads and 600 µl of gDNA extraction buffer (Magic Buffer, Table 5). The gDNA was used in PCR reactions for genotyping with respective primer pairs. Homozygotes were selected by visualisation of PCR reactions via gel electrophoresis (1% agarose gel, run at 130 V for 30 min, Benchtop 1 kb ladder (Promega)), seedlings were transferred into soil and grown in the greenhouse to produce seeds for further use.

Table 6: PCR Reaction for genotyping

Compound	Volume (µl)
10x PCR Buffer	4
25 mM MgCl2	2
10 mM dNTP Mix	0.4
10 µM Forward Primer	2
10 µM Reverse Primer	2
Go*Taq* Flexi Polymerase (5U/µl)	0.1
$_{dd}H_2O$	8.5
gDNA template	1
Total volume 1x reaction:	20

Table 7: PCR program for genotyping

PCR step	Temperature (°C)	Time
Initial denaturation	95	3 min
Denaturation	95	45 sec
Annealing	52	45 sec
Elongation	72	1 min 30 sec
Final elongation	72	3 min
End	12	∞

4.2.2 Bacterial Growth Conditions

For preparation of bacterial inoculum *P. fluorescens* and *B. glumae* were grown from their cryo-stocks on LB media with respective antibiotics (Table 2).

4.2.2.1 Bacterial infection assay

To obtain the bacterial suspension for inoculation of hydroponic 12-well plates, overnight bacterial cultures were centrifuged for 5 min at 3200 rpm. To wash the bacteria the pellets were resuspended in 1 mL filter sterilised 10 mM $MgCl_2$ and centrifuged at the same conditions, this was repeated twice. The final pellet was then resuspended in 4 mL of 10 mM $MgCl_2$ in a 15 mL falcon, the OD_{600} of 1 mL of the bacterial suspension was measured and by series of dilutions a final OD_{600} of 0.0001 (*P. fluorescens*) and OD_{600} of 0.0005 (*B. glumae*) was obtained. For the hydroponic assays, 7 µl of the diluted bacterial suspensions was inoculated into each well; 10 mM $MgCl_2$ was used as the mock control. The plates were then transferred back into the growth chamber for a 3 day incubation period and then harvested. For traditional co-cultivation assays, a final OD_{600} of 0.01 (*P. fluorescens*) and OD_{600} of 0.05 (*B. glumae*) was used.

4.2.3 flg22 and chitohexaose infection assay

Plants were grown hydroponically as described in 4.2.1. 1 µM flg22 or chitohexaose was added to each well and the plants were harvested in a time course, after 2, 4, 8, 24, 48, and 72 h (unless specified otherwise).

4.2.4 β-glucuronidase (GUS) Histochemical Staining

For the GUS reporter assay, seedlings were grown on 1⁄2 MS plates with 0.5% sucrose as previously described and after 5 days transferred into 12-well plates containing 1 mL of 1⁄2 MS liquid media containing 0.5% sucrose and placed into the growth chamber. The following day, the bacteria was washed as described in 4.2.2.1 and inoculated in the wells, the plates were then incubated overnight in the growth chambers. The media was then replaced with GUS-staining solution (composition: see Table 5) and incubated at 37°C overnight. The next day, plants were

washed at room temperature with 10% EtOH for 30 min, 30% EtOH for 1 h and 50% EtOH for 1 h. Samples were stored in 70% EtOH at 4°C or in 50% glycerol for long term storage. Photos were taken using a Leica DMRB microscope with or a Leica MZ 16 F stereo microscope with 10x, 20x and 40x magnifications.

4.2.5 Metabolite Analysis via HPLC

4.2.5.1 Camalexin extraction and isolation from plant material

Frozen plant material harvested from 12-well plates were used for extracting camalexin. To samples containing shoot tissue, 200 µl of dimethylsulfoxide (DMSO) was added, whereas for root tissue, only 100 µl of DMSO was used and all samples were homogenised. Samples were left shaking at room temperature for 20 min at 1000 rpm and then centrifuged at room temperature for 20 min at 15000 rpm. The supernatant was transferred into new tubes and centrifuged again under the same conditions. About 80% of the supernatant was then transferred into high-performance liquid chromatography (HPLC) vials and stored at -20℃ before injection in the HPLC.

4.2.5.2 Camalexin extraction and isolation from exudates

Per well of the 12-well plate, 1 mL of the liquid exudates was harvested and stored at -80℃. For purification of exudates, the samples were defrosted at room temperature and centrifuged at 10℃ for 20 min at 15000 rpm. DSS-18 columns (Supelco, Sigma-Alrich) were washed with 1 mL of 100% acetonitrile and with 1 mL of ½ MS medium without sucrose. The supernatants were pipetted onto the columns and washed with 1 mL of 5% acetonitrile. Once the flow through was discarded 1 mL screw caps were placed under the columns to collect the extracts by 500 µl of 90% acetonitrile, 0.1% formic acid. The solvents were dried in a speed vacuum overnight. The following day, 50 µl DMSO was added into each tube, vortexed and shaken at 22℃ at 1000 rpm for 30 min. Subsequently, tubes were centrifuged at room temperature at 15000 rpm for 20 min and ~45 µl of the supernatant transferred into HPLC vials for analysis.

4.2.5.3 Quantification of Camalexin

For measurement of camalexin, the Thermo Scientific Dione UltiMate 3000 HPLC system was used with a Waters Spherisorb ODS-2, 250 mm x 4.6 mm, 5 μm column. The fluorescence detection (FLD) was set to a sensitivity of 3 with an excitation at 318 nm and emission at 368 nm. For measurement, 20 μl of extracts were injected and camalexin was resolved using a gradient of acetonitrile in 0.01% formic acid (Table 16) and a flow rate of 1 mL per minute. For the quantification of camalexin, external standards (20, 40, 80, 160, 320 nmol/μl) were used and the approximate retention time of camalexin was at 27-31.5 min.

Table 8: HPLC solvent gradient for camalexin measurement

Time (min)	Solvent A (%)	Solvent B (%)
0	97	3
5	97	3
10	90	10
18	40	60
20	20	80
40	0	100
50	0	100
52.5	100	0
56	100	0
58	97	3
60	97	3

4.2.6 Gene Expression Analysis via qRT-PCR

For cDNA synthesis, DNAseI treatment (Thermo Fisher Scientific) paired with Promega GoScript™ Reverse Transcription Kit (Promega) was supplemented for QuantiTect® Reverse Transcription Kit due to product availability.

4.2.6.1 Total RNA extraction and isolation

Total RNA was extracted and isolated as described in Koprivova et al., 2019, by phenol-chloroform-isoamyl alcohol mix (PCI-mix) and LiCl precipitation. Frozen samples were homogenised directly from liquid nitrogen with RNA extraction buffer (for roots 600 μl, shoots

500 µl). After vortexing 500 µl of the PCI-mix (25:24:1; v/v) was added. The samples were then vortexed and left rotating on a rotor at 200 rpm during sample preparation and for an additional 5 min after the last sample. Subsequently, the samples were centrifuged at room temperature for 25 min at 15000 rpm. The upper phase was transferred into new tubes containing 500 µl of PCI-mix, vortexed, and centrifuged at room temperature for 20 min at 15000 rpm. This step was repeated before finally transferring the supernatants into new tubes containing 150 µl of 8M LiCl, mixed and placed at -20°C overnight to precipitate the RNA. The following day, the samples were centrifuged at 4℃ for at least 30 min at 15000 rpm. The supernatant was discarded and 300 µl of $_{dd}H_2O$ was added to the pellet. The samples were gently vortexed and incubated at 65℃ shaking at 500 rpm for 10 min. Afterwards, 100 µl of 8 M LiCl was added, vortexed briefly and placed at -20℃ overnight for second RNA precipitation. The next day, the samples were pelleted by centrifugation at 4℃ for at least 30 min at 15000 rpm. The pellets were washed with 400 µl of 70% EtOH and centrifuged at the same conditions for 10 min. The supernatant was then discarded and the pellet air dried for 5 min at room temperature. Once the pellet was dry, 15 µl (for roots) or 20 µl (for shoots) of RNase free H_2O was added and the samples were incubated at 65℃ shaking at 450 rpm for 20 min to dissolve the pellets. RNA concentration and purity was determined with a NanoDrop (2000c Spectrophotometer, Thermo Scientific) and stored at -20℃.

4.2.6.2 Complementary DNA (cDNA) Synthesis

DNase treatment and first-strand cDNA synthesis was carried out as with the QuantiTect® Reverse Transcription Kit. Adjusted from the manufacturer's instructions for a total volume of 6 µl reaction, and 800 ng of RNA was used. The reaction components are listed in table 9 and the instructions according to the manufacturer were followed. Samples were stored at -20℃.

Table 9: DNase treatment reaction

Components	Volume (µl)
Reverse transcriptase buffer	2
Primer mix	0.5
Reverse transcriptase	0.5
RNA and $_{dd}H_2O$ for 800 ng of RNA	3
Total volume 1x reaction:	6

4.2.6.3 Quantification of gene expression via qRT-PCR

For qRT-PCR, Go*Taq*® Master Mix (Promega) was utilised and in combination with the primers and cDNA, pipetted in technical replicates, the samples were measured using a CFX96 Touch Real-Time PCR Detection System (BioRad, Munich, Germany). Transcript levels were quantified with CFX Manager Software and normalised to the housekeeping/ reference gene *TAP42 INTERACTING PROTEIN OF 41 KDA (TIP41)* using the $2^{-\Delta\Delta CT}$ method.

Table 10: qRT-PCR Reaction

Compound	Volume (µl)
10 µM Forward Primer	2
10 µM Reverse Primer	2
Go*Taq* qRT-PCR Master Mix	5
cDNA template	1
Total volume 1x reaction:	10

Table 11: qRT-PCR Program

PCR step	Temperature (℃)	Time
Initial denaturation	95	3 min
Denaturation	95	15 sec
Annealing	59	30 sec
Elongation	72	30 sec
Final elongation	55	1 min
End	12	∞

4.2.7 RNA-seq

4.2.7.1 RNA Isolation for RNA-seq

Total RNA was extracted and isolated from hydroponically grown root samples with PureLink Plant RNA reagent (Thermo Fisher Scientific) as described in the manufacturer's instructions. RNA integrity number (RIN^e) of samples were pre-determined with a bioanalyzer (Agilent 2100 Bioanalyzer) before sending the RNA-Seq samples to Novogene (Cambridge, UK) until then, the samples were stored at -80℃.

4.2.7.2 RNA-seq performed by Novogene

Novogene purified mRNA from total RNA using poly-T oligo-attached magnetic beads. cDNA was synthesised using random hexamer primers, followed by second strand cDNA synthesis. Library construction also entailed end repair, A-tailing, adapter ligation, size selection, amplification and purification before verification with Qubit, qRT-PCR and detection of size distribution with a bioanalyzer. Which was then sequenced with paired-end 150 bp reads using Illumina NovaSeq 6000.

4.2.7.3 RNA-seq: Processing and Bioinformatic analysis of data

Raw data was received as Illumina FastQ (fq.gz) files, containing the sequencing reads of each sample along with the associated FastQC quality reports. The adapters were removed for all files by processing with *Trimmomatic* (trimming tool, Supplemental Table S4). The trimmed files were subjected to a second quality control with FastQC, resulting in alignment process ability of 96-98 %. The sequencing reads were then mapped to the reference genome (TAIR10) using HiSAT2 with default parameters. The resulting reads were then counted with HTseq with default parameters and normalised to FPKM and TPM values. By utilising limma-voom, differential gene expression could be identified, further online visualisation tools such as iDEP9.5, SRplots and Venny 2.1.0 were used.

4.2.8 DAP-seq Analysis

4.2.8.1 DAP-seq: Processing and Bioinformatic analysis of data

Publically available data released in 2019 from Joseph R Ecker's Lab at the HHMI-Salk-Institute (SRA: SRX1412448, GSE60141) was subjected to quality control with FastQC and then reads were mapped against the reference genome using the processing tool BowTie2 under default parameters. To find peaks of binding, the reads were processed with default parameters using MACS2 and then applied to MACS2 callpeak tool to identify the peaks. This analysis resulted in a list of gene IDs of MYB67's target genes.

4.2.9 Data Processing and Statistical Analysis

For statistical analyses, bases were met on mixed linear model functions where log-transformations were done if necessary to meet assumptions of the mixed linear model. In regards to two-tailed Student's t-tests performed, standard errors were calculated with variance from the model fittings and Benjamin-Hochburg method was applied to p-values for pairwise comparisons of means. Softwares, packages and online tools used are listed in Table 12.

Table 12: Software, packages and online tools used in this study

Software/ Online tools/ packages	Use	Reference
AlphaFold	3D structure predictions	Jumper et al., (2021); Varadi et al., (2022)
ApE	A plasmid editor for primer design	Davis and Jorgensen (2022)
Atted-II	Co-expression analysis	Obayashi et al., (2018)
BioRender	Illustrations	BioRender.com
ePlant eFP Browser	In silico expression analyses	Waese et al., (2017)
Galaxy Europe	Analysis platform	Afgan et al., (2018)
Trimmomatic 0.38	Trimming adapters	Bolger et al., (2014)
FastQC 0.11.9	Quality control	Andrews, (n.d.)
HISAT2 2.1.0	Mapping RNA-seq reads	Kim et al., (2015)
Htseq 0.9.1	Count RNA-seq reads	Anders et al., (2014)
Limma-voom 3.50.1	Analysing DEGs	Liu et al., (2015)
BowTie2 2.5.0	Mapping DAP-seq reads	Langmead et al., (2009)
MACS 2. 2.7.1	Identifying peaks	Zhang et al., (2008)
GraphPad Prism	Statistics tool to build graphs	Motulsky, (n.d.)
iDEP 1.0	Integrated differential expression and pathway analysis	Ge et al., (2018)
ImageJ	Processing microscopic images	Schneider et al., (2012)
MapMan	Gene expression tool	Thimm et al., (2004)
Metascape	GO analysis	Zhou et al., (2019)
Panther	MYB67 phylogenetic analysis	Tang et al., (2019); Thomas et al., (2022)
Plant Regulomics	Data-driven interface	Ran et al., (2020)
SALK T-DNA express	Gene mapping tool/ T-DNA primers	Alonso et al., (2003)
SRplot		SRplot (2021)
UpSetR package	Upset plot visualisation	Conway et al., (2017)
pheatmap package 1.0.8	Heatmap visualisation	Kolde (2019)
bubble plot	GO enrichment	SRplot (2021)
Venny 2.1.0	Creating Venn diagrams	Oliveros (2007-2015)

5 │ REFERENCES

Aida, M., Ishida, T., Fukaki, H., Fujisawa, H., & Tasaka, M. (**1997**). Genes Involved in Organ Separation in Arabidopsis: An Analysis of the Cup-Shaped Cotyledon Mutant. *The Plant Cell*, *9*(June), 841–857.

Afgan, E., Baker, D., Batut, B., van den Beek, M., Bouvier, D., Cech, M., … Blankenberg, D. (**2018**). The Galaxy platform for accessible, reproducible and collaborative biomedical analyses: 2018 update. *Nucleic acids research*, *46*(W1), W537–W544. https://doi.org/10.1093/nar/gky379

Albert, N. W., Lewis, D. H., Zhang, H., Schwinn, K. E., Jameson, P. E., & Davies, K. M. (**2011**). Members of an R2R3-MYB transcription factor family in Petunia are developmentally and environmentally regulated to control complex floral and vegetative pigmentation patterning. *Plant Journal*, *65*(5), 771–784. https://doi.org/10.1111/j.1365-313X.2010.04465.x

Albert, I., Böhm, H., Albert, M., Feiler, C. E., Imkampe, J., Wallmeroth, N., … Nürnberger, T. (**2015**). An RLP23-SOBIR1-BAK1 complex mediates NLP-triggered immunity. *Nature Plants*, *1*(October), 1–9. https://doi.org/10.1038/nplants.2015.140

Alonso, J. M., Stepanova, A. N., Leisse, T. J., Kim, C. J., Chen, H., Shinn, P., … Ecker, J. R. (**2003**). Genome-wide insertional mutagenesis of Arabidopsis thaliana. *Science (New York, N.Y.)*, *301*(5633), 653–657. https://doi.org/10.1126/science.1086391

Altmann, M., Altmann, S., Rodriguez, P. A., Weller, B., Elorduy Vergara, L., Palme, J., … Falter-Braun, P. (**2020**). Extensive signal integration by the phytohormone protein network. *Nature*, *583*(7815), 271–276. https://doi.org/10.1038/s41586-020-2460-0

Ambawat, S., Sharma, P., Yadav, N. R., & Yadav, R. C. (**2013**). MYB transcription factor genes as regulators for plant responses: An overview. *Physiology and Molecular Biology of Plants*, *19*(3), 307–321. https://doi.org/10.1007/s12298-013-0179-1

Anders, S., Pyl, P. T., & Huber, W. (**2014**). HTSeq–a Python framework to work with high-throughput sequencing data. *Bioinformatics*, *31*(2), 166–169. https://doi.org/10.1093/bioinformatics/btu638

Andrews, S. (n.d.). *FastQC A Quality Control tool for High Throughput Sequence Data*. http://www.bioinformatics.babraham.ac.uk/projects/fastqc/

Araceli, A. C., Elda, C. M., Edmundo, L. G., & Ernesto, G. P. (**2007**). Capsidiol production in pepper fruits (Capsicum annuum L.) induced by arachidonic acid is dependent of an oxidative burst. *Physiological and Molecular Plant Pathology*, *70*(1–3), 69–76. https://doi.org/10.1016/j.pmpp.2007.07.002

Ausubel, F. M., Katagiri, F., Mindrinos, M., & Glazebrook, J. (**1995**). Use of Arabidopsis thaliana defense-related mutants to dissect the plant response to pathogens. *Proceedings of the National Academy of Sciences of the United States of America*, *92*(10), 4189–4196. https://doi.org/10.1073/pnas.92.10.4189

Aziz, A., Verhagen, B., Magnin-Robert, M., Couderchet, M., Clément, C., Jeandet, P., & Trotel-Aziz, P. (**2016**). Effectiveness of beneficial bacteria to promote systemic resistance of grapevine to gray mold as related to phytoalexin production in vineyards. *Plant and Soil*, *405*(1–2), 141–153. https://doi.org/10.1007/s11104-015-2783-z

Badri, D. V., Chaparro, J. M., Manter, D. K., Martinoia, E., & Vivanco, J. M. (**2012**). Influence of ATP-Binding Cassette Transporters in Root Exudation of Phytoalexins, Signals, and in Disease Resistance. *Frontiers in Plant Science*, *3*(July). https://doi.org/10.3389/fpls.2012.00149

Bailey, J. A. (**1974**). The relationship between symptom expression and phytoalexin concentration in hypocotyls of Phaseolus vulgaris infected with Colletotrichum lindemuthianum. *Physiol. Plant Pathol.* 4:477-88.

Bakker, P. A. H. M., Pieterse, C. M. J., & Van Loon, L. C. (**2007**). Induced systemic resistance by fluorescent Pseudomonas spp. *Phytopathology*, *97*(2), 239–243. https://doi.org/10.1094/PHYTO-97-2-0239

Bamji, S. F., & Corbitt, C. (**2017**). Glyceollins: Soybean phytoalexins that exhibit a wide range of health-promoting effects. *Journal of Functional Foods*, *34*, 98–105. https://doi.org/10.1016/j.jff.2017.04.020

Barco, B., Kim, Y., & Clay, N. K. (**2019**). Expansion of a core regulon by transposable elements promotes Arabidopsis chemical diversity and pathogen defense. *Nature Communications*, *10*(1), 1–12. https://doi.org/10.1038/s41467-019-11406-3

Barco, B., & Clay, N. K. (**2020**). Hierarchical and Dynamic Regulation of Defense-Responsive Specialized Metabolism by WRKY and MYB Transcription Factors. *Frontiers in Plant Science*, *10*(January), 1–21. https://doi.org/10.3389/fpls.2019.01775

Bardoel, B. W., van der Ent, S., Pel, M. J., Tommassen, J., Pieterse, C. M., van Kessel, K. P., & van Strijp, J. A. (**2011**). Pseudomonas evades immune recognition of flagellin in both mammals and plants. *PLoS pathogens*, *7*(8), e1002206. https://doi.org/10.1371/journal.ppat.1002206

Bednarek, P., Schneider, B., Svatoš, A., Oldham, N. J., & Hahlbrock, K. (**2005**). Structural complexity, differential response to infection, and tissue specificity of indolic and phenylpropanoid secondary metabolism in Arabidopsis roots. *Plant Physiology*, *138*(2), 1058–1070. https://doi.org/10.1104/pp.104.057794

Bednarek, P. (**2012**). Chemical warfare or modulators of defence responses - the function of secondary metabolites in plant immunity. *Current Opinion in Plant Biology*, *15*(4), 407–414. https://doi.org/10.1016/j.pbi.2012.03.002

Berens, M. L., Berry, H. M., Mine, A., Argueso, C. T., & Tsuda, K. (**2017**). Evolution of Hormone Signaling Networks in Plant Defense. *Annual Review of Phytopathology*, *55*, 401–425. https://doi.org/10.1146/annurev-phyto-080516-035544

Béziat, C., Kleine-Vehn, J., Feraru, E. (**2017**). Histochemical Staining of β-Glucuronidase and Its Spatial Quantification. In: Kleine-Vehn, J., Sauer, M. (eds) Plant Hormones. Methods in Molecular Biology, vol 1497. Humana Press, New York, NY. https://doi.org/10.1007/978-1-4939-6469-7_8

Bigeard, J., Colcombet, J., & Hirt, H. (**2015**). Signaling mechanisms in pattern-triggered immunity (PTI). *Molecular Plant*, *8*(4), 521–539. https://doi.org/10.1016/j.molp.2014.12.022

Binder B. M. (**2020**). Ethylene signaling in plants. *The Journal of biological chemistry*, *295*(22), 7710–7725. https://doi.org/10.1074/jbc.REV120.010854

Binns, D., Dimmer, E., Huntley, R., Barrell, D., O'Donovan, C., & Apweiler, R. (**2009**). QuickGO: a web-based tool for Gene Ontology searching. Bioinformatics (Oxford, England), 25(22), 3045–3046. https://doi.org/10.1093/bioinformatics/btp536

Birkenbihl, R. P., Diezel, C., & Somssich, I. E. (**2012**). Arabidopsis WRKY33 is a key transcriptional regulator of hormonal and metabolic responses toward Botrytis cinerea infection. *Plant Physiology*, *159*(1), 266–285. https://doi.org/10.1104/pp.111.192641

Birkenbihl, R. P., Kracher, B., & Somssich, I. E. (**2017**). Induced genome-wide binding of three arabidopsis WRKY transcription factors during early MAMP-triggered immunity. *Plant Cell*, *29*(1), 20–38. https://doi.org/10.1105/tpc.16.00681

Bittel, P., & Robatzek, S. (**2007**). Microbe-associated molecular patterns (MAMPs) probe plant immunity. *Current Opinion in Plant Biology*, *10*(4), 335–341. https://doi.org/10.1016/j.pbi.2007.04.021

Blount, J. W., Dixon, R. A., & Paiva, N. L. (**1992**). Stress responses in alfalfa (Medicago sativa L.) XVI. Antifungal activity of medicarpin and its biosynthetic precursors; implications for the genetic manipulation of stress metabolites. *Physiological and Molecular Plant Pathology*, *41*(5), 333–349. https://doi.org/10.1016/0885-5765(92)90020-V

Bohman, S., Staal, J., Thomma, B. P. H. J., Wang, M., & Dixelius, C. (**2004**). Characterisation of an Arabidopsis-Leptosphaeria maculans pathosystem: Resistance partially requires camalexin biosynthesis and is independent of salicylic acid, ethylene and jasmonic acid signalling. *Plant Journal*, *37*(1), 9–20. https://doi.org/10.1046/j.1365-313X.2003.01927.x

Bolger, A. M., Lohse, M., & Usadel, B. (**2014**). Trimmomatic: A flexible trimmer for Illumina sequence data. *Bioinformatics*, *30*(15), 2114–2120. https://doi.org/10.1093/bioinformatics/btu170

Böttcher, C., Westphal, L., Schmotz, C., Prade, E., Scheel, D., & Glawischnig, E. (**2009**). The multifunctional enzyme CYP71b15 (Phytoalexin deficient3) converts cysteine-lndole-3-acetonitrile to camalexin in the lndole-3-acetonitrile metabolic network of arabidopsis thaliana. *Plant Cell*, *21*(6), 1830–1845. https://doi.org/10.1105/tpc.109.066670

Boutrot, F., Segonzac, C., Chang, K. N., Qiao, H., Ecker, J. R., Zipfel, C., & Rathjen, J. P. (**2010**). Direct transcriptional control of the Arabidopsis immune receptor FLS2 by the ethylene-dependent transcription factors EIN3 and EIL1. *Proceedings of the National Academy of Sciences of the United States of America*, *107*(32), 14502–14507. https://doi.org/10.1073/pnas.1003347107

Bulgarelli, D., Rott, M., Schlaeppi, K., Ver Loren van Themaat, E., Ahmadinejad, N., Assenza, F., … Schulze-Lefert, P. (**2012**). Revealing structure and assembly cues for Arabidopsis root-inhabiting bacterial microbiota. *Nature*, *488*(7409), 91–95. https://doi.org/10.1038/nature11336

Burow, M. E., Boue, S. M., Collins-Burow, B. M., Melnik, L. I., Duong, B. N., Carter-Wientjes, C. H., … Mclachlan, J. A. (**2001**). Phytochemical glyceollins, isolated from soy, mediate antihormonal effects through estrogen receptor α and β. *Journal of Clinical Endocrinology and Metabolism*, *86*(4), 1750–1758. https://doi.org/10.1210/jc.86.4.1750

Calvo-Polanco, M., Ribeyre, Z., Dauzat, M., Reyt, G., Hidalgo-Shrestha, C., Diehl, P., … Boursiac, Y. (**2021**). Physiological roles of Casparian strips and suberin in the transport of water and solutes. *New Phytologist*, *232*(6), 2295–2307. https://doi.org/10.1111/nph.17765

Cao, Y., Liang, Y., Tanaka, K., Nguyen, C. T., Jedrzejczak, R. P., Joachimiak, A., & Stacey, G. (**2014**). The kinase LYK5 is a major chitin receptor in Arabidopsis and forms a chitin-induced complex with related kinase CERK1. *ELife*, *3*, 1–19. https://doi.org/10.7554/eLife.03766

Cao, S., He, C., Zhao, X., Yu, R., Li, Y., Fang, W., … Chen, D. (**2022**). Comprehensive integration of single-cell transcriptomic data illuminates the regulatory network architecture of plant cell fate specification. *BioRxiv*. https://doi.org/10.1101/2022.10.24.513543

Castro-Mondragon, J. A., Jaeger, S., Thieffry, D., Thomas-Chollier, M., & Van Helden, J. (**2017**). RSAT matrix-clustering: Dynamic exploration and redundancy reduction of transcription factor binding motif collections. *Nucleic Acids Research*, *45*(13), 1–13. https://doi.org/10.1093/nar/gkx314

Chassot, C., Buchala, A., Schoonbeek, H. J., Métraux, J. P., & Lamotte, O. (**2008**). Wounding of Arabidopsis leaves causes a powerful but transient protection against Botrytis infection. *Plant Journal*, *55*(4), 555–567. https://doi.org/10.1111/j.1365-313X.2008.03540.x

Chen, Z., Zhao, P. X., Miao, Z. Q., Qi, G. F., Wang, Z., Yuan, Y., … Xiang, C. Bin. (**2019**). SULTR3s function in chloroplast sulfate uptake and affect ABA biosynthesis and the stress response. *Plant Physiology*, *180*(1), 593–604. https://doi.org/10.1104/pp.18.01439

Chen, Z., Wu, Z., Dong, W., Liu, S., Tian, L., Li, J., & Du, H. (**2022**). MYB Transcription Factors Becoming Mainstream in Plant Roots. *International Journal of Molecular Sciences*, *23*(16). https://doi.org/10.3390/ijms23169262

Chinchilla, D., Bauer, Z., Regenass, M., Boller, T., & Felix, G. (**2006**). The Arabidopsis receptor kinase FLS2 binds flg22 and determines the specificity of flagellin perception. *Plant Cell*, *18*(2), 465–476. https://doi.org/10.1105/tpc.105.036574

Cho, H. T., & Cosgrove, D. J. (**2000**). Altered expression of expansin modulates leaf growth and pedicel abscission in Arabidopsis thaliana. *Proceedings of the National Academy of Sciences of the United States of America*, *97*(17), 9783–9788. https://doi.org/10.1073/pnas.160276997

Conrath, U., Beckers, G. J. M., Flors, V., García-Agustín, P., Jakab, G., Mauch, F., … Mauch-Mani, B. (**2006**). Priming: Getting ready for battle. *Molecular Plant-Microbe Interactions*, *19*(10), 1062–1071. https://doi.org/10.1094/MPMI-19-1062

Conway, J.R., Lex, A. and Gehlenborg, N. (**2017**). UpSetR: An R package for the visualization of intersecting sets and their properties. Bioinformatics, 33, 2938–2940.

Couillerot, O., Prigent-Combaret, C., Caballero-Mellado, J., & Moënne-Loccoz, Y. (**2009**). Pseudomonas fluorescens and closely-related fluorescent pseudomonads as biocontrol agents of soil-borne phytopathogens. *Letters in Applied Microbiology*, *48*(5), 505–512. https://doi.org/10.1111/j.1472-765X.2009.02566.x

Creux, N., & Harmer, S. (**2019**). Circadian rhythms in plants. *Cold Spring Harbor Perspectives in Biology*, *11*(9), 1–18. https://doi.org/10.1101/cshperspect.a034611

Cruickshank, I. A. M., & Perrin, D. R. (**1960**). *August 27, 1960 NATURE 799*. *880*(4739), 799–800.

Cui, H., Tsuda, K., & Parker, J. E. (**2015**). Effector-triggered immunity: from pathogen perception to robust defense. *Annual review of plant biology*, *66*, 487–511. https://doi.org/10.1146/annurev-arplant-050213-040012

Darvill, A. G., & Albersheim, P. (**1984**). Phytoalexins and their Elicitors-A Defense Against Microbial Infection in Plants. *Annual Review of Plant Physiology*, *35*(1), 243–275. https://doi.org/10.1146/annurev.pp.35.060184.001331

David, L. C., Berquin, P., Kanno, Y., Seo, M., Daniel-Vedele, F., & Ferrario-Méry, S. (**2016**). N availability modulates the role of NPF3.1, a gibberellin transporter, in GA-mediated phenotypes in Arabidopsis. *Planta*, *244*(6), 1315–1328. https://doi.org/10.1007/s00425-016-2588-1

David, B. V., Chandrasehar, G., & Selvam, P. N. (**2018**). Pseudomonas fluorescens: A Plant-Growth-Promoting Rhizobacterium (PGPR) With Potential Role in Biocontrol of Pests of Crops. In *New and Future Developments in Microbial Biotechnology and Bioengineering: Crop Improvement through Microbial Biotechnology*. https://doi.org/10.1016/B978-0-444-63987-5.00010-4

Davis, M. W., & Jorgensen, E. M. (**2022**). ApE, A Plasmid Editor: A Freely Available DNA Manipulation and Visualization Program. *Frontiers in bioinformatics*, *2*, 818619. https://doi.org/10.3389/fbinf.2022.818619

de Bruijn, W. J. C., Gruppen, H., & Vincken, J. P. (**2018**). Structure and biosynthesis of benzoxazinoids: Plant defence metabolites with potential as antimicrobial scaffolds. *Phytochemistry*, *155*, 233-243. https://doi.org/10.1016/j.phytochem.2018.07.005

De Coninck, B., Timmermans, P., Vos, C., Cammue, B. P., & Kazan, K. (**2015**). What lies beneath: belowground defense strategies in plants. *Trends in plant science*, *20*(2), 91–101. https://doi.org/10.1016/j.tplants.2014.09.007

de Jonge, R., van Esse, H. P., Kombrink, A., Shinya, T., Desaki, Y., Bours, R., van der Krol, S., Shibuya, N., Joosten, M. H., & Thomma, B. P. (**2010**). Conserved fungal LysM effector Ecp6 prevents chitin-triggered immunity in plants. *Science (New York, N.Y.)*, *329*(5994), 953–955. https://doi.org/10.1126/science.1190859

Denby, K. J., Jason, L. J. M., Murray, S. L., & Last, R. L. (**2005**). ups1, an Arabidopsis thaliana camalexin accumulation mutant defective in multiple defence signalling pathways. *Plant Journal*, *41*(5), 673–684. https://doi.org/10.1111/j.1365-313X.2005.02327.x

Denoux, C., Galletti, R., Mammarella, N., Gopalan, S., Werck, D., De Lorenzo, G., Ferrari, S., Ausubel, F. M., & Dewdney, J. (**2008**). Activation of defense response pathways by OGs and Flg22 elicitors in Arabidopsis seedlings. *Molecular plant*, *1*(3), 423–445. https://doi.org/10.1093/mp/ssn019

Dillon, V. M., Overton, J., Grayer, R. J., & Harborne, J. B. (**1997**). Differences in phytoalexin response among rice cultivars of different resistance to blast. *Phytochemistry*, *44*(4), 599–603. https://doi.org/10.1016/S0031-9422(96)00619-X

Dodds, P. N., & Rathjen, J. P. (**2010**). Plant immunity: Towards an integrated view of plantĝ€" pathogen interactions. *Nature Reviews Genetics*, *11*(8), 539–548. https://doi.org/10.1038/nrg2812

Dubos, C., Willment, J., Muggins, D., Grant, G. H., & Campbell, M. M. (**2005**). Kanamycin reveals the role played by glutamate receptors in shaping plant resource allocation. *Plant Journal*, *43*(3), 348–355. https://doi.org/10.1111/j.1365-313X.2005.02458.x

Dubos, C., Stracke, R., Grotewold, E., Weisshaar, B., Martin, C., & Lepiniec, L. (**2010**). MYB transcription factors in Arabidopsis. *Trends in Plant Science*, *15*(10), 573–581. https://doi.org/10.1016/j.tplants.2010.06.005

Duval, M., Hsieh, T. F., Kim, S. Y., & Thomas, T. L. (**2002**). Molecular characterization of AtNAM: A member of the Arabidopsis NAC domain superfamily. *Plant Molecular Biology*, *50*(2), 237–248. https://doi.org/10.1023/A:1016028530943

Eder, J., and Cosio, E. G. (**1994**). Elicitors of plant defense responses. Int. Rev. Cytol. 148, 1–36. doi: 10.1016/S0074-7696(08)62404-3

El Oirdi, M., Trapani, A., & Bouarab, K. (**2010**). The nature of tobacco resistance against Botrytis cinerea depends on the infection structures of the pathogen. *Environmental Microbiology*, *12*(1), 239–253. https://doi.org/10.1111/j.1462-2920.2009.02063.x

Ernst, H. A., Olsen, A. N., Skriver, K., Larsen, S., & Lo Leggio, L. (**2004**). Structure of the conserved domain of ANAC, a member of the NAC family of transcription factors. *EMBO Reports*, *5*(3), 297–303. https://doi.org/10.1038/sj.embor.7400093

Fan, M., Xu, C., Xu, K., & Hu, Y. (**2012**). LATERAL ORGAN BOUNDARIES DOMAIN transcription factors direct callus formation in Arabidopsis regeneration. *Cell research*, *22*(7), 1169–1180. https://doi.org/10.1038/cr.2012.63

Farré, E. M. (**2012**). The regulation of plant growth by the circadian clock. *Plant Biology*, *14*(3), 401–410. https://doi.org/10.1111/j.1438-8677.2011.00548.x

Felix, G., Duran, J. D., Volko, S., & Boller, T. (**1999**). Plants have a sensitive perception system for the most conserved domain of bacterial flagellin. *Plant Journal*, *18*(3), 265–276. https://doi.org/10.1046/j.1365-313X.1999.00265.x

Feller, A., MacHemer, K., Braun, E. L., & Grotewold, E. (**2011**). Evolutionary and comparative analysis of MYB and bHLH plant transcription factors. *Plant Journal*, *66*(1), 94–116. https://doi.org/10.1111/j.1365-313X.2010.04459.x

Feng, J., Liu, T., Qin, B., Zhang, Y., & Liu, X. S. (**2012**). Identifying ChIP-seq enrichment using MACS. *Nature Protocols*, *7*(9), 1728–1740. https://doi.org/10.1038/nprot.2012.101

Ferrari, S., Plotnikova, J. M., De Lorenzo, G., & Ausubel, F. M. (**2003**). Arabidopsis local resistance to Botrytis cinerea involves salicylic acid and camalexin and requires EDS4 and PAD2, but not SID2, EDS5 or PAD4. *Plant Journal*, *35*(2), 193–205. https://doi.org/10.1046/j.1365-313X.2003.01794.x

Ferrari, S., Galletti, R., Denoux, C., De Lorenzo, G., Ausubel, F. M., & Dewdney, J. (**2007**). Resistance to Botrytis cinerea induced in arabidopsis by elicitors is independent of salicylic acid, ethylene, or jasmonate signaling but requires PHYTOALEXIN DEFICIENT3. *Plant Physiology*, *144*(1), 367–379. https://doi.org/10.1104/pp.107.095596

Frerigmann, H., & Gigolashvili, T. (**2014**). MYB34, MYB51, and MYB122 distinctly regulate indolic glucosinolate biosynthesis in arabidopsis Thaliana. *Molecular Plant*. https://doi.org/10.1093/mp/ssu004

Frerigmann, H., Glawischnig, E., & Gigolashvili, T. (**2015**). The role of MYB34, MYB51 and MYB122 in the regulation of camalexin biosynthesis in Arabidopsis thaliana. *Frontiers in Plant Science*, *6*(AUG). https://doi.org/10.3389/fpls.2015.00654

Frerigmann, H., Piślewska-Bednarek, M., Sánchez-Vallet, A., Molina, A., Glawischnig, E., Gigolashvili, T., & Bednarek, P. (**2016**). Regulation of Pathogen-Triggered Tryptophan Metabolism in Arabidopsis thaliana by MYB Transcription Factors and Indole Glucosinolate Conversion Products. *Molecular Plant*, *9*(5), 682–695. https://doi.org/10.1016/j.molp.2016.01.006

Gao, R., Krysciak, D., Petersen, K., Utpatel, C., Knapp, A., Schmeisser, C., … Streit, W. R. (**2015**). Genome-wide RNA sequencing analysis of quorum sensing-controlled regulons in the plant-associated Burkholderia glumae PG1 strain. *Applied and Environmental Microbiology*, *81*(23), 7993–8007. https://doi.org/10.1128/AEM.01043-15

Ge, S.X., Son, E.W. & Yao, R. (**2018**). iDEP: an integrated web application for differential expression and pathway analysis of RNA-Seq data. *BMC Bioinformatics* 19, 534. https://doi.org/10.1186/s12859-018-2486-6

Geng, H., Wang, M., Gong, J., Xu, Y., & Ma, S. (**2021**). An Arabidopsis expression predictor enables inference of transcriptional regulators for gene modules. *Plant Journal*, *107*(2), 597–612. https://doi.org/10.1111/tpj.15315

Geu-Flores, F., Moldrup, M. E., Böttcher, C., Olsen, C. E., Scheel, D., & Halkier, B. A. (**2011**). Cytosolic γ-glutamyl peptidases process glutathione conjugates in the biosynthesis of glucosinolates and camalexin in arabidopsis. *Plant Cell*, *23*(6), 2456–2469. https://doi.org/10.1105/tpc.111.083998

Gigolashvili, T., Berger, B., Mock, H. P., Müller, C., Weisshaar, B., & Flügge, U. I. (**2007**). The transcription factor HIG1/MYB51 regulates indolic glucosinolate biosynthesis in Arabidopsis thaliana. *Plant Journal*, *50*(5), 886–901. https://doi.org/10.1111/j.1365-313X.2007.03099.x

Gigolashvili, T., Engqvist, M., Yatusevich, R., Müller, C., & Flügge, U. I. (**2008**). HAG2/MYB76 and HAG3/MYB29 exert a specific and coordinated control on the regulation of aliphatic glucosinolate biosynthesis in Arabidopsis thaliana. *New Phytologist*, *177*(3), 627–642. https://doi.org/10.1111/j.1469-8137.2007.02295.x

Gilden, R. C., Huffling, K., & Sattler, B. (**2010**). Pesticides and health risks. *JOGNN - Journal of Obstetric, Gynecologic, and Neonatal Nursing*, *39*(1), 103–110. https://doi.org/10.1111/j.1552-6909.2009.01092.x

Giovannoni, M., Lironi, D., Marti, L., Paparella, C., Vecchi, V., Gust, A. A., … Ferrari, S. (**2021**). The Arabidopsis thaliana LysM-containing Receptor-Like Kinase 2 is required for elicitor-induced resistance to pathogens. *Plant Cell and Environment*, *44*(12), 3545–3562. https://doi.org/10.1111/pce.14192

Glawischnig, E., Hansen, B. G., Olsen, C. E., & Halkier, B. A. (**2004**). Camalexin is synthesized from indole-3-acetaldoxime, a key branching point between primary and secondary metabolism in Arabidopsis. *Proceedings of the National Academy of Sciences of the United States of America*, *101*(21), 8245–8250. https://doi.org/10.1073/pnas.0305876101

Glazebrook, J., & Ausubel, F. M. (**1994**). Isolation of phytoalexin-deficient mutants of Arabidopsis thaliana and characterization of their interactions with bacterial pathogens. *Proceedings of the National Academy of Sciences of the United States of America*, *91*(19), 8955–8959. https://doi.org/10.1073/pnas.91.19.8955

Glazebrook, J., Rogers, E. E., & Ausubel, F. M. (**1996**). Isolation of Arabidopsis mutants with enhanced disease susceptibility by direct screening. *Genetics*, *143*(2), 973–982. https://doi.org/10.1093/genetics/143.2.973

Glazebrook, J., Rogers, E. E., & Ausubel, F. M. (**1997a**). Use of Arabidopsis for genetic dissection of plant defense responses. *Annual Review of Genetics*, *31*, 547–549. https://doi.org/10.1146/annurev.genet.31.1.547

Glazebrook, J., Zook, M., Mert, F., Kagan, I., Rogers, E. E., Crute, I. R., … Ausubel, F. M. (**1997b**). Phytoalexin-deficient mutants of Arabidopsis reveal that PAD4 encodes a regulatory factor and that four PAD genes contribute to downy mildew resistance. *Genetics*, *146*(1), 381–392. https://doi.org/10.1093/genetics/146.1.381

Gómez-Gómez, L., & Boller, T. (**2000**). FLS2: An LRR receptor-like kinase involved in the perception of the bacterial elicitor flagellin in Arabidopsis. *Molecular Cell*, *5*(6), 1003–1011. https://doi.org/10.1016/s1097-2765(00)80265-8

Gruau, C., Trotel-Aziz, P., Villaume, S., Rabenoelina, F., Clement, C., Baillieul, F., & Aziz, A. (**2015**). Pseudomonas fluorescens PTA-CT2 triggers local and systemic immune response against botrytis

cinerea in grapevine. *Molecular Plant-Microbe Interactions*, *28*(10), 1117–1129. https://doi.org/10.1094/MPMI-04-15-0092-R

Guo, Y., & Gan, S. (**2006**). AtNAP, a NAC family transcription factor, has an important role in leaf senescence. *Plant Journal*, *46*(4), 601–612. https://doi.org/10.1111/j.1365-313X.2006.02723.x

Gust, A. A., Biswas, R., Lenz, H. D., Rauhut, T., Ranf, S., Kemmerling, B., … Nürnberger, T. (**2007**). Bacteria-derived peptidoglycans constitute pathogen-associated molecular patterns triggering innate immunity in Arabidopsis. *Journal of Biological Chemistry*, *282*(44), 32338–32348. https://doi.org/10.1074/jbc.M704886200

Hacquard, S., Spaepen, S., Garrido-Oter, R., & Schulze-Lefert, P. (**2017**). Interplay Between Innate Immunity and the Plant Microbiota. *Annual review of phytopathology*, *55*, 565–589. https://doi.org/10.1146/annurev-phyto-080516-035623

Haney, C. H., Samuel, B. S., Bush, J., Ausubel, F. M., & Hospital, M. G. (**2016a**). Associations with rhizosphere bacteria can confer an adaptive advantage to plants. *Nat Plants*, *1*(6), 1–22. https://doi.org/10.1038/nplants.2015.51.Associations

Haney, C. H., Wiesmann, C. L., Shapiro, L. R., O'Sullivan, L. R., Khorasani, S., Melnyk, R. A., … Ausubel, F. M. (**2016b**). Comparison between different D-Dimer cutoff values to assess the individual risk of recurrent venous thromboembolism: Analysis of results obtained in the DULCIS study. *International Journal of Laboratory Hematology*, *38*(1), 42–49. https://doi.org/10.1111/ijlh.12426

Heck, S., Grau, T., Buchala, A., Métraux, J. P., & Nawrath, C. (**2003**). Genetic evidence that expression of NahG modifies defence pathways independent of salicylic acid biosynthesis in the Arabidopsis-Pseudomonas syringae pv. tomato interaction. *Plant Journal*, *36*(3), 342–352. https://doi.org/10.1046/j.1365-313X.2003.01881.x

Heese, A., Hann, D. R., Gimenez-Ibanez, S., Jones, A. M. E., He, K., Li, J., … Rathjen, J. P. (**2007**). The receptor-like kinase SERK3/BAK1 is a central regulator of innate immunity in plants. *Proceedings of the National Academy of Sciences of the United States of America*, *104*(29), 12217–12222. https://doi.org/10.1073/pnas.0705306104

Huffaker, A., Kaplan, F., Vaughan, M. M., Dafoe, N. J., Ni, X., Rocca, J. R., … Schmelz, E. A. (**2011**). Novel acidic sesquiterpenoids constitute a dominant class of pathogen-induced phytoalexins in maize. *Plant Physiology*, *156*(4), 2082–2097. https://doi.org/10.1104/pp.111.179457

Ishikawa, T., Itoh, F., Yoshida, S., Saijo, S., Matsuzawa, T., Gonoi, T., … Yamasaki, S. (**2013**). Identification of distinct ligands for the C-type lectin receptors mincle and dectin-2 in the pathogenic fungus Malassezia. *Cell Host and Microbe*, *13*(4), 477–488. https://doi.org/10.1016/j.chom.2013.03.008

Ishikawa, K., Yamaguchi, K., Sakamoto, K., Yoshimura, S., Inoue, K., Tsuge, S., … Kawasaki, T. (**2014**). Bacterial effector modulation of host E3 ligase activity suppresses PAMP-triggered immunity in rice. *Nature Communications*, *5*. https://doi.org/10.1038/ncomms6430

Iven, T., König, S., Singh, S., Braus-Stromeyer, S. A., Bischoff, M., Tietze, L. F., Braus, G. H., Lipka, V., Feussner, I., & Dröge-Laser, W. (**2012**). Transcriptional activation and production of tryptophan-derived secondary metabolites in arabidopsis roots contributes to the defense against the fungal vascular pathogen Verticillium longisporum. *Molecular plant*, *5*(6), 1389–1402. https://doi.org/10.1093/mp/sss044

Jacoby, R. P., Koprivova, A., & Kopriva, S. (**2021**). Pinpointing secondary metabolites that shape the composition and function of the plant microbiome. *Journal of Experimental Botany*, *72*(1), 57–69. https://doi.org/10.1093/jxb/eraa424

Jeandet, P., Douillet-Breuil, A. C., Bessis, R., Debord, S., Sbaghi, M., & Adrian, M. (**2002**). Phytoalexins from the vitaceae: Biosynthesis, phytoalexin gene expression in transgenic plants, antifungal activity, and metabolism. *Journal of Agricultural and Food Chemistry*, *50*(10), 2731–2741. https://doi.org/10.1021/jf011429s

Jeandet, P., Clément, C., Courot, E., & Cordelier, S. (**2013**). Modulation of Phytoalexin Biosynthesis in Engineered Plants for Disease Resistance. *International Journal of Molecular Sciences*, *14*(7), 14136–14170. MDPI AG. Retrieved from http://dx.doi.org/10.3390/ijms140714136

Jeandet, P. (**2018**). Structure, chemical analysis, biosynthesis, metabolism, molecular engineering, and biological functions of phytoalexins. *Molecules*, *23*(1). https://doi.org/10.3390/molecules23010061

Jeandet, P., Vannozzi, A., Sobarzo-Sánchez, E., Uddin, M. S., Bru, R., Martínez-Márquez, A., … Nabavi, S. M. (**2021**). Phytostilbenes as agrochemicals: Biosynthesis, bioactivity, metabolic engineering and biotechnology. *Natural Product Reports*, *38*(7), 1282–1329. https://doi.org/10.1039/d0np00030b

Jensen, M. K., Hagedorn, P. H., de Torres-Zabala, M., Grant, M. R., Rung, J. H., Collinge, D. B., & Lyngkjaer, M. F. (**2008**). Transcriptional regulation by an NAC (NAM-ATAF1,2-CUC2) transcription factor attenuates ABA signalling for efficient basal defence towards Blumeria graminis f. sp. hordei in Arabidopsis. *The Plant journal : for cell and molecular biology*, *56*(6), 867–880. https://doi.org/10.1111/j.1365-313X.2008.03646.x

Jensen, M. K., Kjaersgaard, T., Nielsen, M. M., Galberg, P., Petersen, K., O'shea, C., & Skriver, K. (**2010**). The arabidopsis thaliana NAC transcription factor family: structure-function relationships and determinants of ANAC019 stress signalling. *Biochemical Journal*, *426*(2), 183–196. https://doi.org/10.1042/BJ20091234

Jeong, Y., Kim, J., Kim, S., Kang, Y., Nagamatsu, T., & Hwang, I. (**2003**). Toxoflavin produced by Burkholderia glumae causing rice grain rot is responsible for inducing bacterial wilt in many field crops. *Plant Disease*, *87*(8), 890–895. https://doi.org/10.1094/PDIS.2003.87.8.890

Ji, L., Hu, R., Jiang, J., Qi, G., Yang, X., Zhu, M., … Yi, Z. (**2014**). Molecular cloning and expression analysis of 13 NAC transcription factors in Miscanthus lutarioriparius. *Plant Cell Reports*, *33*(12), 2077–2092. https://doi.org/10.1007/s00299-014-1682-8

Jiao, X., Takishita, Y., Zhou, G., & Smith, D. L. (**2021**). Plant Associated Rhizobacteria for Biocontrol and Plant Growth Enhancement. *Frontiers in Plant Science*, *12*(March). https://doi.org/10.3389/fpls.2021.634796

Jin, H., & Martin, C. (**1999**). Multifunctionality and diversity within the plant MYB-gene family. *Plant Molecular Biology*, *41*(5), 577–585. https://doi.org/10.1023/A:1006319732410

Jones, D.G.J. and Dangl. J.L. (**2006**). The Plant Immune System. *Nature* 444 (7117): 323–29.

Jülke, S., & Ludwig-Müller, J. (**2015**). Response of Arabidopsis thaliana Roots with Altered Lipid Transfer Protein (LTP) Gene Expression to the Clubroot Disease and Salt Stress. *Plants (Basel, Switzerland)*, *5*(1), 2. https://doi.org/10.3390/plants5010002

Jumper, J., Evans, R., Pritzel, A., Green, T., Figurnov, M., Ronneberger, O., … Hassabis, D. (**2021**). Highly accurate protein structure prediction with AlphaFold. *Nature*, *596*(7873), 583–589. https://doi.org/10.1038/s41586-021-03819-2

Kataoka, T., Hayashi, N., Yamaya, T., & Takahashi, H. (**2004**). Root-to-shoot transport of sulfate in Arabidopsis. Evidence for the role of SULTR3;5 as a component of low-affinity sulfate transport system in the root vasculature. *Plant physiology*, *136*(4), 4198–4204. https://doi.org/10.1104/pp.104.045625

Kim, J., Kim, J. G., Kang, Y., Jang, J. Y., Jog, G. J., Lim, J. Y., … Hwang, I. (**2004**). Quorum sensing and the LysR-type transcriptional activator ToxR regulate toxoflavin biosynthesis and transport in Burkholderia glumae. *Molecular Microbiology*, *54*(4), 921–934. https://doi.org/10.1111/j.1365-2958.2004.04338.x

Kim, J., Kang, Y., Choi, O., Jeong, Y., Jeong, J. E., Lim, J. Y., … Hwang, I. (**2007**). Regulation of polar flagellum genes is mediated by quorum sensing and FlhDC in Burkholderia glumae. *Molecular Microbiology*, *64*(1), 165–179. https://doi.org/10.1111/j.1365-2958.2007.05646.x

Kim, D., Langmead, B., & Salzberg, S. L. (**2015**). HISAT: a fast spliced aligner with low memory requirements. *Nature Methods*, *12*(4), 357–360. https://doi.org/10.1038/nmeth.3317

Klein, A. P., Anarat-Cappillino, G., & Sattely, E. S. (**2013**). Minimum set of cytochromes P450 for reconstituting the biosynthesis of camalexin, a major Arabidopsis antibiotic. *Angewandte Chemie (International ed. in English)*, *52*(51), 13625–13628. https://doi.org/10.1002/anie.201307454

Kliebenstein, D. J., Rowe, H. C., & Denby, K. J. (**2005**). Secondary metabolites influence Arabidopsis/Botrytis interactions: Variation in host production and pathogen sensitivity. *Plant Journal*, *44*(1), 25–36. https://doi.org/10.1111/j.1365-313X.2005.02508.x

Koornneef, A., Leon-Reyes, A., Ritsema, T., Verhage, A., Den Otter, F. C., Van Loon, L. C., & Pieterse, C. M. J. (**2008**). Kinetics of salicylate-mediated suppression of jasmonate signaling reveal a role for redox modulation. *Plant Physiology*, *147*(3), 1358–1368. https://doi.org/10.1104/pp.108.121392

Kolde, R. (**2019**). *Package pheatmap*. CRAN. Retrieved March 7, 2023, from https://CRAN.R-project.org/package=pheatmap

Koprivova, A., Schuck, S., Jacoby, R. P., Klinkhammer, I., Welter, B., Leson, L., … Kopriva, S. (**2019**). Root-specific camalexin biosynthesis controls the plant growth-promoting effects of multiple bacterial strains. *Proceedings of the National Academy of Sciences*, *116*(31), 15735–15744. https://doi.org/10.1073/pnas.1818604116

Koprivova, A., Schmalenberger, A., & Kopriva, S. (2020). Sulfatase Assay to Determine Influence of Plants on Microbial Activity in Soil. Bio-Protocol, 10(2), 1–9. https://doi.org/10.21769/bioprotoc.3490

Koprivova, A., Schwier, M., Volz, V., & Kopriva, S. (**2023**) Shoot-root interaction in control of camalexin exudation in Arabidopsis. *Journal of Experimental Botany*. doi: 10.1093/jxb/erad031.

Kosma, D. K., Molina, I., Ohlrogge, J. B., & Pollard, M. (**2012**). Identification of an Arabidopsis fatty alcohol: Caffeoyl-Coenzyme a acyltransferase required for the synthesis of alkyl hydroxycinnamates in root waxes. *Plant Physiology*, *160*(1), 237–248. https://doi.org/10.1104/pp.112.201822

Kurita, T., and Tabei, H. (**1967**). On the pathogenic bacterium of bacterial grain rot of rice. *Ann. Phytopathol. Soc. Jpn.* 33, 111.

Lang, T., Deng, C., Yao, J., Zhang, H., Wang, Y., & Deng, S. (**2020**). A Salt-Signaling Network Involving Ethylene, Extracellular ATP, Hydrogen Peroxide, and Calcium Mediates K^+/Na^+ Homeostasis in *Arabidopsis*. *International journal of molecular sciences*, *21*(22), 8683. https://doi.org/10.3390/ijms21228683

Langcake, P., & Pryce, R. J. (**1976**). The production of resveratrol by Vitis vinifera and other members of the Vitaceae as a response to infection or injury. *Physiological Plant Pathology*, *9*(1), 77–86. https://doi.org/10.1016/0048-4059(76)90077-1

Langmead, B., Trapnell, C., Pop, M., & Salzberg, S. L. (**2009**). Ultrafast and memory-efficient alignment of short DNA sequences to the human genome. *Genome Biology*, *10*(3), R25. https://doi.org/10.1186/gb-2009-10-3-r25

Larroque, M., Belmas, E., Martinez, T., Vergnes, S., Ladouce, N., Lafitte, C., … Dumas, B. (**2013**). Pathogen-associated molecular pattern-triggered immunity and resistance to the root pathogen Phytophthora parasitica in Arabidopsis. *Journal of Experimental Botany*, *64*(12), 3615–3625. https://doi.org/10.1093/jxb/ert195

Le Roux, C., Huet, G., Jauneau, A., Camborde, L., Trémousaygue, D., Kraut, A., … Deslandes, L. (**2015**). A receptor pair with an integrated decoy converts pathogen disabling of transcription factors to immunity. *Cell*, *161*(5), 1074–1088. https://doi.org/10.1016/j.cell.2015.04.025

Li, C., Ng, C. K. Y., & Fan, L. M. (2015). MYB transcription factors; active players in abiotic stress signaling. *Environmental and Experimental Botany*, *114*, 80–91. https://doi.org/10.1016/j.envexpbot.2014.06.014

Li, Q., Zhang, M., Shen, D., Liu, T., Chen, Y., Zhou, J. M., & Dou, D. (**2016a**). A Phytophthora sojae effector PsCRN63 forms homo-/hetero-dimers to suppress plant immunity via an inverted association manner. *Scientific Reports*, *6*(March), 1–13. https://doi.org/10.1038/srep26951

Li, H., Yang, S., Wang, C., Zhou, Y., & Zhang, Z. (**2016b**). AraPPISite: a database of fine-grained protein–protein interaction site annotations for Arabidopsis thaliana. *Plant Molecular Biology*, *92*(1–2), 105–116. https://doi.org/10.1007/s11103-016-0498-z

Li, K. C., Zhang, X. Q., Yu, Y., Xing, R. E., Liu, S., & Li, P. C. (**2020**). Effect of chitin and chitosan hexamers on growth and photosynthetic characteristics of wheat seedlings. *Photosynthetica*, *58*(3), 819–826. https://doi.org/10.32615/ps.2020.021

Li, Y., Liu, K., Tong, G., Xi, C., Liu, J., Zhao, H., Wang, Y., Ren, D., & Han, S. (**2022**). MPK3/MPK6-mediated phosphorylation of ERF72 positively regulates resistance to Botrytis cinerea through directly and indirectly activating the transcription of camalexin biosynthesis enzymes. *Journal of experimental botany*, *73*(1), 413–428. https://doi.org/10.1093/jxb/erab415

Liu, R., Holik, A. Z., Su, S., Jansz, N., Chen, K., Leong, H. S., … Ritchie, M. E. (**2015**). Why weight? Modelling sample and observational level variability improves power in RNA-seq analyses. *Nucleic acids research*, *43*(15), e97. https://doi.org/10.1093/nar/gkv412

Liang, Y. K., Dubos, C., Dodd, I. C., Holroyd, G. H., Hetherington, A. M., & Campbell, M. M. (**2005**). AtMYB61, an R2R3-MYB transcription factor controlling stomatal aperture in Arabidopsis thaliana. *Current Biology*, *15*(13), 1201–1206. https://doi.org/10.1016/j.cub.2005.06.041

Lidder, P., Gutiérrez, R. A., Salomé, P. A., McClung, C. R., & Green, P. J. (**2005**). Circadian control of messenger RNA stability. Association with a sequence-specific messenger RNA decay pathway. *Plant Physiology*, *138*(4), 2374–2385. https://doi.org/10.1104/pp.105.060368

Lipsick J. S. (1996). One billion years of Myb. *Oncogene*, *13*(2), 223–235.

Liu, S., Kracher, B., Ziegler, J., Birkenbihl, R. P., & Somssich, I. E. (**2015**). Negative regulation of ABA Signaling By WRKY33 is critical for Arabidopsis immunity towards Botrytis cinerea 2100. *ELife*, *4*(JUNE2015), 1–27. https://doi.org/10.7554/eLife.07295

López, M. A., Bannenberg, G., & Castresana, C. (**2008**). Controlling hormone signaling is a plant and pathogen challenge for growth and survival. *Current Opinion in Plant Biology*, *11*(4), 420–427. https://doi.org/10.1016/j.pbi.2008.05.002

Lozano-Durán, R., & Zipfel, C. (**2015**). Trade-off between growth and immunity: Role of brassinosteroids. *Trends in Plant Science*, *20*(1), 12–19. https://doi.org/10.1016/j.tplants.2014.09.003

Lu, P. L., Chen, N. Z., An, R., Su, Z., Qi, B. S., Ren, F., … Wang, X. C. (**2007**). A novel drought-inducible gene, ATAF1, encodes a NAC family protein that negatively regulates the expression of stress-responsive genes in Arabidopsis. *Plant Molecular Biology*, *63*(2), 289–305. https://doi.org/10.1007/s11103-006-9089-8

Lu, D., Wu, S., Gao, X., Zhang, Y., Shan, L., & He, P. (**2010**). A receptor-like cytoplasmic kinase, BIK1, associates with a flagellin receptor complex to initiate plant innate immunity. *Proceedings of the National Academy of Sciences of the United States of America*, *107*(1), 496–501. https://doi.org/10.1073/pnas.0909705107

Lux, A., & Rost, T. L. (**2012**). Plant root research: the past, the present and the future. *Annals of Botany*, *110*(2), 201–204. https://doi.org/10.1093/aob/mcs156

Lyon, F. M., and Wood, R. K. S. (**1975**). Production of phaseollin, coumestrol and related compounds in bean leaves inoculated with Pseudomonas spp. *Physiol. Plant Pathol*. 6: 1 17-24.

Macho, A. P., & Zipfel, C. (**2014**). Plant PRRs and the activation of innate immune signaling. *Molecular Cell*, *54*(2), 263–272. https://doi.org/10.1016/j.molcel.2014.03.028

Malinovsky, F. G., Fangel, J. U., & Willats, W. G. T. (**2014**). The role of the cell wall in plant immunity. *Frontiers in Plant Science*, *5*(MAY), 1–12. https://doi.org/10.3389/fpls.2014.00178

Mao, G., Meng, X., Liu, Y., Zheng, Z., Chen, Z., & Zhang, S. (**2011**). Phosphorylation of a WRKY transcription factor by two pathogen-responsive MAPKs drives phytoalexin biosynthesis in Arabidopsis. *Plant Cell*, *23*(4), 1639–1653. https://doi.org/10.1105/tpc.111.084996

Mao, X., Chen, S., Li, A., Zhai, C., & Jing, R. (**2014**). Novel NAC transcription factor TaNAC67 confers enhanced multi-abiotic stress tolerances in Arabidopsis. *PLoS ONE*, *9*(1). https://doi.org/10.1371/journal.pone.0084359

Marshall, C. B., McLaren, J. R., & Turkington, R. (**2011**). Soil microbial communities resistant to changes in plant functional group composition. *Soil Biology and Biochemistry*, *43*(1), 78–85. https://doi.org/10.1016/j.soilbio.2010.09.016

McCarthy, R. L., Zhong, R., & Ye, Z. H. (**2009**). MYB83 is a direct target of SND1 and acts redundantly with MYB46 in the regulation of secondary cell wall biosynthesis in arabidopsis. *Plant and Cell Physiology*, *50*(11), 1950–1964. https://doi.org/10.1093/pcp/pcp139

Medina-Bolivar, F., Condori, J., Rimando, A. M., Hubstenberger, J., Shelton, K., O'Keefe, S. F., … Dolan, M. C. (**2007**). Production and secretion of resveratrol in hairy root cultures of peanut. *Phytochemistry*, *68*(14), 1992–2003. https://doi.org/10.1016/j.phytochem.2007.04.039

Mendes, R., Kruijt, M., De Bruijn, I., Dekkers, E., Van Der Voort, M., Schneider, J. H. M., … Raaijmakers, J. M. (**2011**). Deciphering the rhizosphere microbiome for disease-suppressive bacteria. *Science*, *332*(6033), 1097–1100. https://doi.org/10.1126/science.1203980

Meng, X., & Zhang, S. (**2013**). MAPK cascades in plant disease resistance signaling. *Annual Review of Phytopathology*, *51*, 245–266. https://doi.org/10.1146/annurev-phyto-082712-102314

Meraj, T. A., Fu, J., Raza, M. A., Zhu, C., Shen, Q., Xu, D., & Wang, Q. (**2020**). Transcriptional Factors Regulate Plant Stress Responses through Mediating Secondary Metabolism. *Genes*, *8*(1 Supplement), 90–91. https://doi.org/10.1007/BF02421504

Mersmann, S., Bourdais, G., Rietz, S., & Robatzek, S. (**2010**). Ethylene signaling regulates accumulation of the FLS2 receptor and is required for the oxidative burst contributing to plant immunity. *Plant Physiology*, *154*(1), 391–400. https://doi.org/10.1104/pp.110.154567

Mert-Turk, F., Bennett, M. H., Mansfield, J. W., & Holub, E. B. (**2003**). Quantification of camalexin in several accessions of Arabidopsis thaliana following inductions with Peronospora parasitica and UV-B irradiation. *Phytoparasitica*, *31*(1), 81–89. https://doi.org/10.1007/BF02979770

Mhlongo, M. I., Piater, L. A., Madala, N. E., Labuschagne, N., & Dubery, I. A. (**2018**). The chemistry of plant–microbe interactions in the rhizosphere and the potential for metabolomics to reveal signaling related to defense priming and induced systemic resistance. *Frontiers in Plant Science*, *9*(February), 1–17. https://doi.org/10.3389/fpls.2018.00112

Mialoundama, A. S., Heintz, D., Debayle, D., Rahier, A., Camara, B., & Bouvier, F. (**2009**). Abscisic acid negatively regulates elicitor-induced synthesis of capsidiol in wild tobacco. *Plant Physiology*, *150*(3), 1556–1566. https://doi.org/10.1104/pp.109.138420

Miao, Y., Laun, T., Zimmermann, P., & Zentgraf, U. (**2004**). Targets of the WRKY53 transcription factor and its role during leaf senescence in Arabidopsis. *Plant Molecular Biology*, *55*(6), 853–867. https://doi.org/10.1007/s11103-004-2142-6

Miao, Y., Laun, T. M., Smykowski, A., & Zentgraf, U. (**2007**). Arabidopsis MEKK1 can take a short cut: It can directly interact with senescence-related WRKY53 transcription factor on the protein level and can bind to its promoter. *Plant Molecular Biology*, *65*(1–2), 63–76. https://doi.org/10.1007/s11103-007-9198-z

Mierziak, J., Kostyn, K., & Kulma, A. (**2014**). Flavonoids as important molecules of plant interactions with the environment. Molecules (Basel, Switzerland), 19(10), 16240–16265. https://doi.org/10.3390/molecules191016240

Mikkelsen, M. D., Hansen, C. H., Wittstock, U., & Halkier, B. A. (**2000**). Cytochrome P450 CYP79B2 from Arabidopsis catalyzes the conversion of tryptophan to indole-3-acetaldoxime, a precursor of indole glucosinolates and indole-3-acetic acid. *Journal of Biological Chemistry*, *275*(43), 33712–33717. https://doi.org/10.1074/jbc.M001667200

Millet, Y. A., Danna, C. H., Clay, N. K., Songnuan, W., Simon, M. D., Werck-Reichhart, D., & Ausubel, F. M. (**2010**). Innate immune responses activated in Arabidopsis roots by microbe-associated molecular patterns. *Plant Cell*, *22*(3), 973–990. https://doi.org/10.1105/tpc.109.069658

Mitra, P.P., & Loqué, D. (**2014**). Histochemical staining of Arabidopsis thaliana secondary cell wall elements. *Journal of visualized experiments : JoVE*, (87), 51381. https://doi.org/10.3791/51381

Miya, A., Albert, P., Shinya, T., Desaki, Y., Ichimura, K., Shirasu, K., … Shibuya, N. (**2007**). CERK1, a LysM receptor kinase, is essential for chitin elicitor signaling in Arabidopsis. *Proceedings of the National Academy of Sciences of the United States of America*, *104*(49), 19613–19618. https://doi.org/10.1073/pnas.0705147104

Mizobuchi, R., Fukuoka, S., Tsuiki, C., Tsushima, S., & Sato, H. (**2018**). Evaluation of major Japanese rice cultivars for resistance to bacterial grain rot caused by Burkholderia glumae and identification of standard cultivars for resistance. *Breeding Science*, *68*(4), 413–419. https://doi.org/10.1270/jsbbs.18018

Møldrup, M. E., Geu-Flores, F., & Halkier, B. A. (**2013**). Assigning gene function in biosynthetic pathways: Camalexin and beyond. *Plant Cell*, *25*(2), 360–367. https://doi.org/10.1105/tpc.112.104745

Motulsky, H. J., GraphPad Statistics Guide. Accessed 5 March 2019. http://www.graphpad.com/guides/prism/7/statistics/index.htm

Monaghan, J., & Zipfel, C. (**2012**). Plant pattern recognition receptor complexes at the plasma membrane. *Current Opinion in Plant Biology*, *15*(4), 349–357. https://doi.org/10.1016/j.pbi.2012.05.006

Mucha, S., Heinzlmeir, S., Kriechbaumer, V., Strickland, B., Kirchhelle, C., Choudhary, M., … Glawischnig, E. (**2019**). The Formation of a Camalexin Biosynthetic Metabolon. *The Plant Cell*, *31*(11), 2697–2710. https://doi.org/10.1105/tpc.19.00403

Müller K. O. and Börger. H. (**1940**). Experimentelle Untersuchungen über die Phytophthora- Resistenz der Kartoffel. Zugleich ein Beitrag zum Problem der 'erworbenen Resistenz' im Pflanzenreich. Arbeiten der Biologischen Reichsanstalt für Land- und Forstwirtschaft, 23, pp. 189-231.

Müller, T. M., Böttcher, C., Morbitzer, R., Götz, C. C., Lehmann, J., Lahaye, T., & Glawischnig, E. (**2015**). Transcription activator-like effector nuclease-mediated generation and metabolic analysis of camalexin-deficient cyp71a12 cyp71a13 double knockout lines. *Plant Physiology*, *168*(3), 849–858. https://doi.org/10.1104/pp.15.00481

Nafisi, M., Goregaoker, S., Botanga, C. J., Glawischnig, E., Olsen, C. E., Halkier, B. A., & Glazebrook, J. (**2007**). Arabidopsis cytochrome P450 monooxygenase 71A13 catalyzes the conversion of indole-3-acetaldoxime in camalexin synthesis. *Plant Cell*, *19*(6), 2039–2052. https://doi.org/10.1105/tpc.107.051383

Nakashima, K., Tran, L. S. P., Van Nguyen, D., Fujita, M., Maruyama, K., Todaka, D., … Yamaguchi-Shinozaki, K. (**2007**). Functional analysis of a NAC-type transcription factor OsNAC6 involved in abiotic and biotic stress-responsive gene expression in rice. *Plant Journal*, *51*(4), 617–630. https://doi.org/10.1111/j.1365-313X.2007.03168.x

Nandakumar, R., Shahjahan, A. K. M., Yuan, X. L., Dickstein, E. R., Groth, D. E., Clark, C. A., … Rush, M. C. (**2009**). Burkholderia glumae and B. gladioli cause bacterial panicle blight in rice in the Southern United States. *Plant Disease*, *93*(9), 896–905. https://doi.org/10.1094/PDIS-93-9-0896

Narusaka, Y., Narusaka, M., Park, P., Kubo, Y., Hirayama, T., Seki, M., … Shinozaki, K. (**2004**). RCH1, a locus in Arabidopsis that confers resistance to the hemibiotrophic fungal pathogen Colletotrichum higginsianum. *Molecular Plant-Microbe Interactions*, *17*(7), 749–762. https://doi.org/10.1094/MPMI.2004.17.7.749

Nawrath, C. (**1999**). Salicylic Acid Induction–Deficient Mutants of Arabidopsis Express. *Society*, *11*(August), 1393–1404.

Newman, L. J., Perazza, D. E., Juda, L., & Campbell, M. M. (**2004**). Involvement of the R2R3-MYB, AtMYB61, in the ectopic lignification and dark-photomorphogenic components of the det3 mutant phenotype. *Plant Journal*, *37*(2), 239–250. https://doi.org/10.1046/j.1365-313X.2003.01953.x

Nguyen, N. T. T., Contreras-Moreira, B., Castro-Mondragon, J. A., Santana-Garcia, W., Ossio, R., Robles-Espinoza, C. D., … Thomas-Chollier, M. (**2018**). RSAT 2018: Regulatory sequence analysis tools 20th anniversary. *Nucleic Acids Research*, *46*(W1), W209–W214. https://doi.org/10.1093/nar/gky317

Nguyen, N. H., Trotel-Aziz, P., Villaume, S., Rabenoelina, F., Clément, C., Baillieul, F., & Aziz, A. (**2022a**). Priming of camalexin accumulation in induced systemic resistance by beneficial bacteria against Botrytis cinerea and Pseudomonas syringae pv. tomato DC3000. *Journal of experimental botany*, *73*(11), 3743–3757. https://doi.org/10.1093/jxb/erac070

Nguyen, N. H., Trotel-Aziz, P., Clément, C., Jeandet, P., Baillieul, F., & Aziz, A. (**2022b**). Camalexin accumulation as a component of plant immunity during interactions with pathogens and beneficial microbes. *Planta*, *255*(6), 116. https://doi.org/10.1007/s00425-022-03907-1

Nieves-Cordones, M., Alemán, F., Martínez, V., & Rubio, F. (**2010**). The Arabidopsis thaliana HAK5 K+ transporter is required for plant growth and K+ acquisition from low K+ solutions under saline conditions. *Molecular Plant*, *3*(2), 326–333. https://doi.org/10.1093/mp/ssp102

Nozue, K., Covington, M. F., Duek, P. D., Lorrain, S., Fankhauser, C., Harmer, S. L., & Maloof, J. N. (**2007**). Rhythmic growth explained by coincidence between internal and external cues. *Nature*, *448*(7151), 358–361. https://doi.org/10.1038/nature05946

Nürnberger, T., & Kemmerling, B. (**2006**). Receptor protein kinases - pattern recognition receptors in plant immunity. *Trends in Plant Science*, *11*(11), 519–522. https://doi.org/10.1016/j.tplants.2006.09.005

Nusinow, D. A., Helfer, A., Hamilton, E. E., King, J. J., Imaizumi, T., Schultz, T. F., Farré, E. M., & Kay, S. A. (**2011**). The ELF4-ELF3-LUX complex links the circadian clock to diurnal control of hypocotyl growth. *Nature*, *475*(7356), 398–402. https://doi.org/10.1038/nature10182

Obayashi, T., Aoki, Y., Tadaka, S., Kagaya, Y., & Kinoshita, K. (**2018**). ATTED-II in 2018: A Plant Coexpression Database Based on Investigation of the Statistical Property of the Mutual Rank Index. *Plant and Cell Physiology*, *59*(1), E3. https://doi.org/10.1093/pcp/pcx191

Öhman, D., Demedts, B., Kumar, M., Gerber, L., Gorzsas, A., Goeminne, G., … Sundberg, B. (**2013**). MYB103 is required for FERULATE-5-HYDROXYLASE expression and syringyl lignin biosynthesis in Arabidopsis stems. *Plant Journal*, *73*(1), 63–76. https://doi.org/10.1111/tpj.12018

Okawa, Y., Kobayashi, M., Suzuki, S., & Suzuki, M. (**2003**). Comparative study of protective effects of chitin, chitosan, and N-acetyl chitohexaose against Pseudomonas aeruginosa and Listeria monocytogenes infections in mice. *Biological and Pharmaceutical Bulletin*, *26*(6), 902–904. https://doi.org/10.1248/bpb.26.902

Oliveros, Juan Carlos. (**2007-2015**) "Venny. An interactive tool for comparing lists with Venn's diagrams." https://bioinfogp.cnb.csic.es/tools/venny/index.html

O'Malley, R. C., Huang, S. C., Song, L., Lewsey, M. G., Bartlett, A., Nery, J. R., Galli, M., Gallavotti, A., & Ecker, J. R. (**2016**). Cistrome and Epicistrome Features Shape the Regulatory DNA Landscape. *Cell*, *165*(5), 1280–1292. https://doi.org/10.1016/j.cell.2016.04.038

Ooka, H., Satoh, K., Doi, K., Nagata, T., Otomo, Y., Murakami, K., … Kikuchi, S. (**2003**). Comprehensive Analysis of NAC Family Genes in Oryza sativa and Arabidopsis thaliana. *DNA Research*, *10*(6), 239–247. https://doi.org/10.1093/dnares/10.6.239

Paik, I., Kathare, P. K., Kim, J. Il, & Huq, E. (**2017**). Expanding Roles of PIFs in Signal Integration from Multiple Processes. *Molecular Plant*, *10*(8), 1035–1046. https://doi.org/10.1016/j.molp.2017.07.002

Pandey, S. P., Roccaro, M., Schön, M., Logemann, E., & Somssich, I. E. (**2010**). Transcriptional reprogramming regulated by WRKY18 and WRKY40 facilitates powdery mildew infection of Arabidopsis. *Plant Journal*, *64*(6), 912–923. https://doi.org/10.1111/j.1365-313X.2010.04387.x

Pangesti, N., Reichelt, M., van de Mortel, J. E., Kapsomenou, E., Gershenzon, J., van Loon, J. J. A., … Pineda, A. (**2016**). Jasmonic Acid and Ethylene Signaling Pathways Regulate Glucosinolate Levels in Plants During Rhizobacteria-Induced Systemic Resistance Against a Leaf-Chewing Herbivore. *Journal of Chemical Ecology*, *42*(12), 1212–1225. https://doi.org/10.1007/s10886-016-0787-7

Pastorczyk, M., Kosaka, A., Piślewska-Bednarek, M., López, G., Frerigmann, H., Kułak, K., … Bednarek, P. (**2020**). The role of CYP71A12 monooxygenase in pathogen-triggered tryptophan metabolism and Arabidopsis immunity. *New Phytologist*, *225*(1), 400–412. https://doi.org/10.1111/nph.16118

Patra, B., Schluttenhofer, C., Wu, Y., Pattanaik, S., & Yuan, L. (**2013**). Transcriptional regulation of secondary metabolite biosynthesis in plants. *Biochimica et Biophysica Acta - Gene Regulatory Mechanisms*, *1829*(11), 1236–1247. https://doi.org/10.1016/j.bbagrm.2013.09.006

Paxton, J. D. (**1981**). Phytoalexins — A Working Redefinition. *Journal of Phytopathology*, *101*(2), 106–109. https://doi.org/10.1111/j.1439-0434.1981.tb03327.x

Paz-Ares, J., Ghosal, D., Wienand, U., Peterson, P. A., & Saedler, H. (**1987**). The regulatory c1 locus of Zea mays encodes a protein with homology to myb proto-oncogene products and with structural similarities to transcriptional activators. *The EMBO Journal*, *6*(12), 3553–3558. https://doi.org/10.1002/j.1460-2075.1987.tb02684.x

Pedras, M. S. C., Chumala, P. B., Jin, W., Islam, M. S., & Hauck, D. W. (**2009**). The phytopathogenic fungus Alternaria brassicicola: Phytotoxin production and phytoalexin elicitation. *Phytochemistry*, *70*(3), 394–402. https://doi.org/10.1016/j.phytochem.2009.01.005

Penfield, S., Meissner, R. C., Shoue, D. A., Carpita, N. C., & Bevan, M. W. (**2001**). MYB61 is required for mucilage deposition and extrusion in the arabidopsis seed coat. *Plant Cell*, *13*(12), 2777–2791. https://doi.org/10.1105/tpc.13.12.2777

Peng, X., Liu, H., Wang, D., & Shen, S. (**2016**). Genome-wide identification of the Jatropha curcas MYB family and functional analysis of the abiotic stress responsive gene JcMYB2. *BMC Genomics*, *17*(1), 1–12. https://doi.org/10.1186/s12864-016-2576-7

Perrone, S. T., McDonald, K. L., Sutherland, M. W., & Guest, D. I. (**2003**). Superoxide release is necessary for phytoalexin accumulation in Nicotiana tabacum cells during the expression of cultivar-race and non-host resistance towards Phytophthora spp. *Physiological and Molecular Plant Pathology*, *62*(3), 127–135. https://doi.org/10.1016/S0885-5765(03)00026-2

Peskan-Berghöfer, T., Vilches-Barro, A., Müller, T. M., Glawischnig, E., Reichelt, M., Gershenzon, J., & Rausch, T. (**2015**). Sustained exposure to abscisic acid enhances the colonization potential of the mutualist fungus Piriformospora indica on Arabidopsis thaliana roots. *New Phytologist*, *208*(3), 873–886. https://doi.org/10.1111/nph.13504

Petutschnig, E. K., Stolze, M., Lipka, U., Kopischke, M., Horlacher, J., Valerius, O., … Lipka, V. (**2014**). A novel Arabidopsis CHITIN ELICITOR RECEPTOR KINASE 1 (CERK1) mutant with enhanced pathogen-induced cell death and altered receptor processing. *New Phytologist*, *204*(4), 955–967. https://doi.org/10.1111/nph.12920

Pieterse, C. M. J., Van Wees, S. C. M., Hoffland, E., Van Pelt, J. A., & Van Loon, L. C. (**1996**). Systemic resistance in Arabidopsis induced by biocontrol bacteria is independent of salicylic acid accumulation and pathogenesis-related gene expression. *Plant Cell*, *8*(8), 1225–1237. https://doi.org/10.1105/tpc.8.8.1225

Pieterse, C. M. J., Van Der Does, D., Zamioudis, C., Leon-Reyes, A., & Van Wees, S. C. M. (**2012**). Hormonal modulation of plant immunity. *Annual Review of Cell and Developmental Biology*, *28*, 489–521. https://doi.org/10.1146/annurev-cellbio-092910-154055

Pieterse, C. M. J., Zamioudis, C., Berendsen, R. L., Weller, D. M., Van Wees, S. C. M., & Bakker, P. A. H. M. (**2014**). Induced systemic resistance by beneficial microbes. *Annual Review of Phytopathology*, *52*, 347–375. https://doi.org/10.1146/annurev-phyto-082712-102340

Pieterse, C. M. J., Berendsen, R. L., de Jonge, R., Stringlis, I. A., Van Dijken, A. J. H., Van Pelt, J. A., … Bakker, P. A. H. M. (**2021**). Pseudomonas simiae WCS417: star track of a model beneficial rhizobacterium. *Plant and Soil*, *461*(1–2), 245–263. https://doi.org/10.1007/s11104-020-04786-9

Pike, S., Gao, F., Kim, M. J., Kim, S. H., Schachtman, D. P., & Gassmann, W. (**2014**). Members of the NPF3 transporter subfamily encode pathogen-inducible nitrate/nitrite transporters in grapevine and arabidopsis. *Plant and Cell Physiology*, *55*(1), 162–170. https://doi.org/10.1093/pcp/pct167

Povero, G., Loreti, E., Pucciariello, C., Santaniello, A., Di Tommaso, D., Di Tommaso, G., … Perata, P. (**2011**). Transcript profiling of chitosan-treated Arabidopsis seedlings. *Journal of Plant Research*, *124*(5), 619–629. https://doi.org/10.1007/s10265-010-0399-1

Puranik, S., Sahu, P. P., Srivastava, P. S., & Prasad, M. (**2012**). NAC proteins: Regulation and role in stress tolerance. *Trends in Plant Science*, *17*(6), 369–381. https://doi.org/10.1016/j.tplants.2012.02.004

Qi, D., & Innes, R. W. (**2013**). Recent Advances in Plant NLR Structure, Function, Localization, and Signaling. *Frontiers in immunology*, *4*, 348. https://doi.org/10.3389/fimmu.2013.00348

Qiu, J. L., Fiil, B. K., Petersen, K., Nielsen, H. B., Botanga, C. J., Thorgrimsen, S., … Petersen, M. (**2008**). Arabidopsis MAP kinase 4 regulates gene expression through transcription factor release in the nucleus. *EMBO Journal*, *27*(16), 2214–2221. https://doi.org/10.1038/emboj.2008.147

Qutob, D., Kemmerling, B., Brunner, F., Küfner, I., Engelhardt, S., Gust, A. A., … Nürnberger, T. (**2006**). Phytotoxicity and innate immune responses induced by Nep1-like proteins. *Plant Cell*, *18*(12), 3721–3744. https://doi.org/10.1105/tpc.106.044180

Ramakrishna, P., Ruiz Duarte, P., Rance, G. A., Schubert, M., Vordermaier, V., Vu, L. D., … De Smet, I. (**2019**). EXPANSIN A1-mediated radial swelling of pericycle cells positions anticlinal cell divisions during lateral root initiation. *Proceedings of the National Academy of Sciences of the United States of America*, *116*(17), 8597–8602. https://doi.org/10.1073/pnas.1820882116

Ramírez, V., Agorio, A., Coego, A., García-Andrade, J., Hernández, M. J., Balaguer, B., Ouwerkerk, P. B., Zarra, I., & Vera, P. (**2011**). MYB46 modulates disease susceptibility to Botrytis cinerea in Arabidopsis. Plant physiology, 155(4), 1920–1935. https://doi.org/10.1104/pp.110.171843

Ran, X., Zhao, F., Wang, Y., Liu, J., Zhuang, Y., Ye, L., … Zhang, Y. (**2020**). Plant Regulomics: a data-driven interface for retrieving upstream regulators from plant multi-omics data. *Plant Journal*, *101*(1), 237–248. https://doi.org/10.1111/tpj.14526

Rawat, R., Schwartz, J., Jones, M. A., Sairanen, I., Cheng, Y., Andersson, C. R., … Harmer, S. L. (**2009**). REVEILLE1, a Myb-like transcription factor, integrates the circadian clock and auxin pathways. *Proceedings of the National Academy of Sciences of the United States of America*, *106*(39), 16883–16888. https://doi.org/10.1073/pnas.0813035106

Ren, T., Qu, F., & Morris, T. J. (**2000**). HRT gene function requires interaction between a NAC protein and viral capsid protein to confer resistance to turnip crinkle virus. *Plant Cell*, *12*(10), 1917–1925. https://doi.org/10.1105/tpc.12.10.1917

Ren, D., Liu, Y., Yang, K. Y., Han, L., Mao, G., Glazebrook, J., & Zhang, S. (**2008**). A fungal-responsive MAPK cascade regulates phytoalexin biosynthesis in Arabidopsis. *Proceedings of the National Academy of Sciences of the United States of America*, *105*(14), 5638–5643. https://doi.org/10.1073/pnas.0711301105

Riechmann, J. L., Heard, J., Martin, G., Reuber, L., Jiang, C. Z., Keddie, J., … Yu, G. L. (**2000**). Arabidopsis transcription factors: Genome-wide comparative analysis among eukaryotes. *Science*, *290*(5499), 2105–2110. https://doi.org/10.1126/science.290.5499.2105

Robert-Seilaniantz, A., MacLean, D., Jikumaru, Y., Hill, L., Yamaguchi, S., Kamiya, Y., & Jones, J. D. G. (**2011**). The microRNA miR393 re-directs secondary metabolite biosynthesis away from camalexin and towards glucosinolates. *Plant Journal*, *67*(2), 218–231. https://doi.org/10.1111/j.1365-313X.2011.04591.x

Roby, D., Gadelle, A., & Toppan, A. (**1987**). Chitin oligosaccharides as elicitors of chitinase activity in melon plants. *Biochemical and Biophysical Research Communications*, *143*(3), 885–892. https://doi.org/10.1016/0006-291X(87)90332-9

Rodriguez, P. A., Rothballer, M., Chowdhury, S. P., Nussbaumer, T., Gutjahr, C., & Falter-Braun, P. (**2019**). Systems Biology of Plant-Microbiome Interactions. *Molecular Plant*, *12*(6), 804–821. https://doi.org/10.1016/j.molp.2019.05.006

Roetschi, A., Si-Ammour, A., Belbahri, L., Mauch, F., & Mauch-Mani, B. (**2001**). Characterization of an Arabidopsis-Phytophthora pathosystem: Resistance requires a functional pad2 gene and is independent of salicylic acid, ethylene and jasmonic acid signalling. *Plant Journal*, *28*(3), 293–305. https://doi.org/10.1046/j.1365-313X.2001.01148.x

Romano, J. M., Dubos, C., Prouse, M. B., Wilkins, O., Hong, H., Poole, M., … Campbell, M. M. (**2012**). AtMYB61, an R2R3-MYB transcription factor, functions as a pleiotropic regulator via a small gene network. *New Phytologist*, *195*(4), 774–786. https://doi.org/10.1111/j.1469-8137.2012.04201.x

Rosinski, J. A., & Atchley, W. R. (**1998**). Molecular evolution of the Myb family of transcription factors: Evidence for polyphyletic origin. *Journal of Molecular Evolution*, *46*(1), 74–83. https://doi.org/10.1007/PL00006285

Rowe, H. C., Walley, J. W., Corwin, J., Chan, E. K. F., Dehesh, K., & Kliebenstein, D. J. (**2010**). Deficiencies in jasmonate-mediated plant defense reveal quantitative variation in Botrytis cinerea pathogenesis. *PLoS Pathogens*, *6*(4), 1–18. https://doi.org/10.1371/journal.ppat.1000861

Rubio, F., Guillermo, S. M., & Rodríguez-Navarro, A. (**2000**). Cloning of Arabidopsis and barley cDNAs encoding HAK potassium transporters in root and shoot cells. *Physiologia Plantarum*, *109*(1), 34–43. https://doi.org/10.1034/j.1399-3054.2000.100106.x

Saga, H., Ogawa, T., Kai, K., Suzuki, H., Ogata, Y., Sakurai, N., … Ohta, D. (**2012**). Identification and characterization of ANAC042, a transcription factor family gene involved in the regulation of camalexin biosynthesis in Arabidopsis. *Molecular Plant-Microbe Interactions*, *25*(5), 684–696. https://doi.org/10.1094/MPMI-09-11-0244

Samalova, M., Elsayad, K., Melnikava, A., Peaucelle, A., Gahurova, E., Gumulec, J., … Hejatko, J. (**2020**). Expansin-controlled cell wall stiffness regulates root growth in Arabidopsis. *BioRxiv*, 2020.06.25.170969. https://doi.org/10.1101/2020.06.25.170969

Sanchez-Vallet, A., Ramos, B., Bednarek, P., López, G., Piślewska-Bednarek, M., Schulze-Lefert, P., & Molina, A. (**2010**). Tryptophan-derived secondary metabolites in Arabidopsis thaliana confer non-host resistance to necrotrophic Plectosphaerella cucumerina fungi. *Plant Journal*, *63*(1), 115–127. https://doi.org/10.1111/j.1365-313X.2010.04224.x

Sarris, P. F., Duxbury, Z., Huh, S. U., Ma, Y., Segonzac, C., Sklenar, J., Derbyshire, P., … Jones, J. D. G. (**2015**). A Plant Immune Receptor Detects Pathogen Effectors that Target WRKY Transcription Factors. *Cell*, *161*(5), 1089–1100. https://doi.org/10.1016/j.cell.2015.04.024

Sato, N., Kitazawa, K., & Tomiyama, K. (**1971**). The role of rishitin in localizing the invading hyphae of Phytophthora infestans in infection sites at the cut surfaces of potato tubers. *Physiological Plant Pathology*, *1*(3), 289–295. https://doi.org/10.1016/0048-4059(71)90049-X

Schlaeppi, K., Abou-Mansour, E., Buchala, A., & Mauch, F. (**2010**). Disease resistance of Arabidopsis to Phytophthora brassicae is established by the sequential action of indole glucosinolates and camalexin. *Plant Journal*, *62*(5), 840–851. https://doi.org/10.1111/j.1365-313X.2010.04197.x

Schmelz, E. A., Kaplan, F., Huffaker, A., Dafoe, N. J., Vaughan, M. M., Ni, X., … Teal, P. E. (**2011**). Identity, regulation, and activity of inducible diterpenoid phytoalexins in maize. *Proceedings of the National Academy of Sciences of the United States of America*, *108*(13), 5455–5460. https://doi.org/10.1073/pnas.1014714108

Schnee, S., Viret, O., & Gindro, K. (**2008**). Role of stilbenes in the resistance of grapevine to powdery mildew. *Physiological and Molecular Plant Pathology*, *72*(4–6), 128–133. https://doi.org/10.1016/j.pmpp.2008.07.002

Schneider, C. A., Rasband, W. S., & Eliceiri, K. W. (**2012**). NIH Image to ImageJ: 25 years of image analysis. *Nature methods*, *9*(7), 671–675. https://doi.org/10.1038/nmeth.2089

Schön, M., Töller, A., Diezel, C., Roth, C., Westphal, L., Wiermer, M., & Somssich, I. E. (**2013**). Analyses of wrky18 wrky40 plants reveal critical roles of SA/EDS1 signaling and indole-glucosinolate biosynthesis for Golovinomyces orontii resistance and a loss-of resistance towards Pseudomonas syringae pv. tomato AvrRPS4. *Molecular Plant-Microbe Interactions*, *26*(7), 758–767. https://doi.org/10.1094/MPMI-11-12-0265-R

Schuhegger, R., Nafisi, M., Mansourova, M., Petersen, B. L., Olsen, C. E., Svatoš, A., … Glawischnig, E. (**2006**). CYP71B15 (PAD3) catalyzes the final step in camalexin biosynthesis. *Plant Physiology*, *141*(4), 1248–1254. https://doi.org/10.1104/pp.106.082024

Schuhegger, R., Rauhut, T., & Glawischnig, E. (**2007**). Regulatory variability of camalexin biosynthesis. *Journal of Plant Physiology*, *164*(5), 636–644. https://doi.org/10.1016/j.jplph.2006.04.012

Schuler, M. A., Duan, H., Bilgin, M., & Ali, S. (**2006**). Arabidopsis cytochrome P450s through the looking glass: A window on plant biochemistry. *Phytochemistry Reviews*, *5*(2–3), 205–237. https://doi.org/10.1007/s11101-006-9035-z

Schweizer, F., Bodenhausen, N., Lassueur, S., Masclaux, F. G., & Reymond, P. (**2013**). Differential contribution of transcription factors to Arabidopsis thaliana defense against Spodoptera littoralis. *Frontiers in Plant Science*, *4* (FEB), 1–12. https://doi.org/10.3389/fpls.2013.00013

Shan, L., He, P., Li, J., Heese, A., Peck, S. C., Nürnberger, T., … Sheen, J. (**2008**). Bacterial Effectors Target the Common Signaling Partner BAK1 to Disrupt Multiple MAMP Receptor-Signaling Complexes and Impede Plant Immunity. *Cell Host and Microbe*, *4*(1), 17–27. https://doi.org/10.1016/j.chom.2008.05.017

Shekhawat, K., Fröhlich, K., García-Ramírez, G. X., Trapp, M. A., & Hirt, H. (**2023**). Ethylene: A Master Regulator of Plant–Microbe Interactions under Abiotic Stresses. *Cells*, *12*(1), 1–15. https://doi.org/10.3390/cells12010031

Shi, Q., George, J., Krystel, J., Zhang, S., Lapointe, S. L., Stelinski, L. L., & Stover, E. (**2019**). Hexaacetyl-chitohexaose, a chitin-derived oligosaccharide, transiently activates citrus defenses and alters the feeding behavior of Asian citrus psyllid. *Horticulture Research*, *6*(1). https://doi.org/10.1038/s41438-019-0158-y

Sobolev, V. S. (**2013**). Production of phytoalexins in peanut (arachis hypogaea) seed elicited by selected microorganisms. *Journal of Agricultural and Food Chemistry*, *61*(8), 1850–1858. https://doi.org/10.1021/jf3054752

SRplot. (**2021**). *SRplot - Science and research online plot*. https://www.bioinformatics.com.cn/en

Staal, J., Kaliff, M., Bohman, S., & Dixelius, C. (**2006**). Transgressive segregation reveals two Arabidopsis TIR-NB-LRR resistance genes effective against Leptosphaeria maculans, causal agent of blackleg disease. *Plant Journal*, *46*(2), 218–230. https://doi.org/10.1111/j.1365-313X.2006.02688.x

Staswick, P. E., Tiryaki, I., & Rowe, M. L. (**2002**). Jasmonate response locus JAR1 and several related Arabidopsis genes encode enzymes of the firefly luciferase superfamily that show activity on jasmonic, salicylic, and indole-3-acetic acids in an assay for adenylation. *Plant Cell*, *14*(6), 1405–1415. https://doi.org/10.1105/tpc.000885

Staswick, P. E., Serban, B., Rowe, M., Tiryaki, I., Maldonado, M. T., Maldonado, M. C., & Suza, W. (**2005**). Characterization of an arabidopsis enzyme family that conjugates amino acids to indole-3-acetic acid. *Plant Cell*, *17*(2), 616–627. https://doi.org/10.1105/tpc.104.026690

Stracke, R., Werber, M., & Weisshaar, B. (**2001**). The R2R3-MYB gene family in Arabidopsis thaliana. *Current Opinion in Plant Biology*, *4*(5), 447–456. https://doi.org/10.1016/S1369-5266(00)00199-0

Stracke, R., Ishihara, H., Huep, G., Barsch, A., Mehrtens, F., Niehaus, K., & Weisshaar, B. (**2007**). Differential regulation of closely related R2R3-MYB transcription factors controls flavonol accumulation in different parts of the Arabidopsis thaliana seedling. *Plant Journal*, *50*(4), 660–677. https://doi.org/10.1111/j.1365-313X.2007.03078.x

Stringlis, I. A., Yu, K., Feussner, K., De Jonge, R., Van Bentum, S., Van Verk, M. C., … Pieterse, C. M. J. (**2018**). MYB72-dependent coumarin exudation shapes root microbiome assembly to promote plant health. *Proceedings of the National Academy of Sciences of the United States of America*, *115*(22), E5213–E5222. https://doi.org/10.1073/pnas.1722335115

Su, T., Li, Y., Yang, H., & Ren, D. (**2013**). Reply: Complexity in camalexin biosynthesis. *Plant Cell*, *25*(2), 367–370. https://doi.org/10.1105/tpc.113.109975

Swaminathan, S., Lionetti, V., & Zabotina, O. A. (**2022**). Plant Cell Wall Integrity Perturbations and Priming for Defense. *Plants*, *11*(24), 1–26. https://doi.org/10.3390/plants11243539

Tang, H., Finn, R. D., & Thomas, P. D. (**2019**). TreeGrafter: phylogenetic tree-based annotation of proteins with Gene Ontology terms and other annotations. *Bioinformatics (Oxford, England)*, *35*(3), 518–520. https://doi.org/10.1093/bioinformatics/bty625

Takasaki, H., Maruyama, K., Kidokoro, S., Ito, Y., Fujita, Y., Shinozaki, K., … Nakashima, K. (**2010**). The abiotic stress-responsive NAC-type transcription factor OsNAC5 regulates stress-inducible genes and stress tolerance in rice. *Molecular Genetics and Genomics*, *284*(3), 173–183. https://doi.org/10.1007/s00438-010-0557-0

Thimm, O., Bläsing, O., Gibon, Y., Nagel, A., Meyer, S., Krüger, P., Selbig, J., Müller, L. A., Rhee, S. Y., & Stitt, M. (**2004**). MAPMAN: a user-driven tool to display genomics data sets onto diagrams of metabolic pathways and other biological processes. *The Plant journal : for cell and molecular biology*, *37*(6), 914–939. https://doi.org/10.1111

Thomas, P. D., Ebert, D., Muruganujan, A., Mushayahama, T., Albou, L. P., & Mi, H. (**2022**). PANTHER: Making genome-scale phylogenetics accessible to all. *Protein Science*, *31*(1), 8–22. https://doi.org/10.1002/pro.4218

Thomma, B. P. H. J., Nelissen, I., Eggermont, K., & Broekaert, W. F. (**1999**). Deficiency in phytoalexin production causes enhanced susceptibility of Arabidopsis thaliana to the fungus Alternaria brassicicola. *Plant Journal*, *19*(2), 163–171. https://doi.org/10.1046/j.1365-313X.1999.00513.x

Tiku, A. R. (**2018**). Antimicrobial compounds and their role in plant defense. *Molecular Aspects of Plant-Pathogen Interaction*, 283–307. https://doi.org/10.1007/978-981-10-7371-7_13

Toruño, T. Y., Stergiopoulos, I., & Coaker, G. (**2016**). Plant-Pathogen Effectors: Cellular Probes Interfering with Plant Defenses in Spatial and Temporal Manners. *Annual review of phytopathology*, *54*, 419–441. https://doi.org/10.1146/annurev-phyto-080615-100204

Trigg, S. A., Garza, R. M., MacWilliams, A., Nery, J. R., Bartlett, A., Castanon, R., … Ecker, J. R. (**2017**). CrY2H-seq: A massively multiplexed assay for deep-coverage interactome mapping. *Nature Methods*, *14*(8), 819–825. https://doi.org/10.1038/nmeth.4343

Trung, H. M., Van Van, N., Vien, N. V., & Lien, M. (**1993**). Occurrence of rice grain rot disease in Viet Nam. *International Rice Research Notes (Philippines). 62*:12-45.

Tsuda, K., Glazebrook, J., & Katagiri, F. (**2008**). The interplay between MAMP and SA signaling. *Plant Signaling and Behavior*, *3*(6), 359–361. https://doi.org/10.4161/psb.3.6.5702

Tsuji, J., Jackson, E. P., Gage, D. A., Hammerschmidt, R., & Somerville, S. C. (**1992**). Phytoalexin accumulation in arabidopsis thaliana during the hypersensitive reaction to Pseudomonas syringae pv syringae. *Plant Physiology*, *98*(4), 1304–1309. https://doi.org/10.1104/pp.98.4.1304

Tsuji, J., Zook, M., Somerville, S. C., Last, R. L., & Hammerschmidt, R. (**1993**). Evidence that tryptophan is not a direct biosynthetic intermediate of camalexin in Arabidopsis thaliana. *Physiological and Molecular Plant Pathology*, Vol. 43, pp. 221–229. https://doi.org/10.1006/pmpp.1993.1052

Vacheron, J., Desbrosses, G., Bouffaud, M. L., Touraine, B., Moënne-Loccoz, Y., Muller, D., … Prigent-Combaret, C. (**2013**). Plant growth-promoting rhizobacteria and root system functioning. *Frontiers in Plant Science*, *4*(SEP), 1–19. https://doi.org/10.3389/fpls.2013.00356

van Baarlen, P., Woltering, E.J., Staats, M., and Van Kan, J.A.L. (**2007**). Histochemical and Genetic Analysis of Host and Non-Host Interactions of Arabidopsis with Three Botrytis Species: An Important Role for Cell Death Control. *Molecular Plant Pathology* 8 (1): 41–54. https://doi.org/10.1111/j.1364-3703.2006.00367.x.

van de Mortel, J. E., de Vos, R. C., Dekkers, E., Pineda, A., Guillod, L., Bouwmeester, K., van Loon, J. J., Dicke, M., & Raaijmakers, J. M. (**2012**). Metabolic and transcriptomic changes induced in Arabidopsis by the rhizobacterium Pseudomonas fluorescens SS101. *Plant physiology*, *160*(4), 2173–2188. https://doi.org/10.1104/pp.112.207324

van Etten, H. D., Mansfield, J. W., Bailey, J. A., & Farmer, E. E. (**1994**). Two Classes of Plant Antibiotics: Phytoalexins versus "Phytoanticipins." *The Plant Cell*, *6*(9), 1191. https://doi.org/10.2307/3869817

van Oosten, V. R., Bodenhausen, N., Reymond, P., Van Pelt, J. A., Van Loon, L. C., Dicke, M., & Pieterse, C. M. (**2008**). Differential effectiveness of microbially induced resistance against herbivorous insects in Arabidopsis. *Molecular plant-microbe interactions : MPMI, 21*(7), 919–930. https://doi.org/10.1094/MPMI-21-7-0919

van Wees, S. C., Chang, H. S., Zhu, T., & Glazebrook, J. (**2003**). Characterization of the early response of Arabidopsis to Alternaria brassicicola infection using expression profiling. *Plant physiology*, *132*(2), 606–617. https://doi.org/10.1104/pp.103.022186

Varadi, M., Anyango, S., Deshpande, M., Nair, S., Natassia, C., Yordanova, G., … Velankar, S. (**2022**). AlphaFold Protein Structure Database: Massively expanding the structural coverage of protein-sequence space with high-accuracy models. *Nucleic Acids Research*, *50*(D1), D439–D444. https://doi.org/10.1093/nar/gkab1061

Verhagen, B. W. M., Trotel-Aziz, P., Couderchet, M., Höfte, M., & Aziz, A. (**2010**). Pseudomonas spp.-induced systemic resistance to Botrytis cinerea is associated with induction and priming of defence responses in grapevine. *Journal of Experimental Botany*, *61*(1), 249–260. https://doi.org/10.1093/jxb/erp295

Villena, J., Kitazawa, H., Van Wees, S. C. M., Pieterse, C. M. J., & Takahashi, H. (**2018**). Receptors and Signaling Pathways for Recognition of Bacteria in Livestock and Crops: Prospects for Beneficial Microbes in Healthy Growth Strategies. *Frontiers in Immunology*, *9*(September), 1–15. https://doi.org/10.3389/fimmu.2018.02223

Waese, J., Fan, J., Pasha, A., Yu, H., Fucile, G., Shi, R., … Provart, N. J. (**2017**). ePlant: Visualizing and exploring multiple levels of data for hypothesis generation in plant biology. *Plant Cell*, *29*(8), 1806–1821. https://doi.org/10.1105/tpc.17.00073

Wan, J., Zhang, X. C., Neece, D., Ramonell, K. M., Clough, S., Kim, S. Y., … Stacey, G. (**2008**). A LysM receptor-like kinase plays a critical role in chitin signaling and fungal resistance in Arabidopsis. *Plant Cell*, *20*(2), 471–481. https://doi.org/10.1105/tpc.107.056754

Wang, Z. Y., & Tobin, E. M. (**1998**). Constitutive expression of the CIRCADIAN CLOCK ASSOCIATED 1 (CCA1) gene disrupts circadian rhythms and suppresses its own expression. *Cell*, *93*(7), 1207–1217. https://doi.org/10.1016/S0092-8674(00)81464-6

Wang, W., Wen, Y., Berkey, R., & Xiao, S. (**2009**). Specific Targeting of the Arabidopsis Resistance Protein RPW8.2 to the Interfacial Membrane Encasing the Fungal Haustorium Renders Broad-Spectrum Resistance to Powdery Mildew. *Plant Cell*, *21*(9), 2898–2913. https://doi.org/10.1105/tpc.109.067587

Wang, M. Y., Liu, X. T., Chen, Y., Xu, X. J., Yu, B., Zhang, S. Q., … He, Z. H. (**2012**). Arabidopsis Acetyl-Amido Synthetase GH3.5 Involvement in Camalexin Biosynthesis through Conjugation of Indole-3-Carboxylic Acid and Cysteine and Upregulation of Camalexin Biosynthesis Genes. *Journal of Integrative Plant Biology*, *54*(7), 471–485. https://doi.org/10.1111/j.1744-7909.2012.01131.x

Wang, X., Niu, Y., & Zheng, Y. (**2021**). Multiple functions of myb transcription factors in abiotic stress responses. *International Journal of Molecular Sciences*, *22*(11). https://doi.org/10.3390/ijms22116125

Weigel, D. (2012). Natural variation in arabidopsis: From molecular genetics to ecological genomics. *Plant Physiology*, *158*(1), 2–22. https://doi.org/10.1104/pp.111.189845

Wu, Y., Deng, Z., Lai, J., Zhang, Y., Yang, C., Yin, B., … Xie, Q. (**2009**). Dual function of Arabidopsis ATAF1 in abiotic and biotic stress responses. *Cell Research*, *19*(11), 1279–1290. https://doi.org/10.1038/cr.2009.108

Xie, Q., Frugis, G., Colgan, D., & Chua, N. H. (**2000**). Arabidopsis NAC1 transduces auxin signal downstream of TIR1 to promote lateral root development. *Genes & development*, *14*(23), 3024–3036. https://doi.org/10.1101/gad.852200

Xie, Y., Huhn, K., Brandt, R., Potschin, M., Bieker, S., Straub, D., … Wenkel, S. (**2014**). Revoluta and wrky53 connect early and late leaf development in arabidopsis. *Development (Cambridge)*, *141*(24), 4772–4783. https://doi.org/10.1242/dev.117689

Xie, Y., Tan, H., Ma, Z., & Huang, J. (**2016**). DELLA Proteins Promote Anthocyanin Biosynthesis via Sequestering MYBL2 and JAZ Suppressors of the MYB/bHLH/WD40 Complex in Arabidopsis thaliana. *Molecular Plant*, *9*(5), 711–721. https://doi.org/10.1016/j.molp.2016.01.014

Xu, X., Chen, C., Fan, B., & Chen, Z. (**2006**). *Physical and Functional Interactions between and WRKY60 Transcription Factors*. *18*(May), 1310–1326. https://doi.org/10.1105/tpc.105.037523.1

Xu, W., Huang, J., Li, B., Li, J., & Wang, Y. (**2008**). Is kinase activity essential for biological functions of BRI1? *Cell Research*, *18*(4), 472–478. https://doi.org/10.1038/cr.2008.36

Xu, K., Liu, J., Fan, M., Xin, W., Hu, Y., & Xu, C. (**2012**). A genome-wide transcriptome profiling reveals the early molecular events during callus initiation in Arabidopsis multiple organs. *Genomics*, *100*(2), 116–124. https://doi.org/10.1016/j.ygeno.2012.05.013

Xue, G. P., Way, H. M., Richardson, T., Drenth, J., Joyce, P. A., & McIntyre, C. L. (**2011**). Overexpression of TaNAC69 leads to enhanced transcript levels of stress up-regulated genes and dehydration tolerance in bread wheat. *Molecular Plant*, *4*(4), 697–712. https://doi.org/10.1093/mp/ssr013

Yang, C., Xu, Z., Song, J., Conner, K., Barrena, G. V., & Wilson, Z. A. (**2007**). Arabidopsis MYB26/MALE STERILE35 regulates secondary thickening in the endothecium and is essential for anther dehiscence. *Plant Cell*, *19*(2), 534–548. https://doi.org/10.1105/tpc.106.046391

Yang, L., Jiang, Z., Jing, Y., & Lin, R. (**2020a**). PIF1 and RVE1 form a transcriptional feedback loop to control light-mediated seed germination in Arabidopsis. *Journal of Integrative Plant Biology*, *62*(9), 1372–1384. https://doi.org/10.1111/jipb.12938

Yang, X., Yang, S., Qi, H., Wang, T., Li, H., & Zhang, Z. (**2020b**). PlaPPISite: A comprehensive resource for plant protein-protein interaction sites. *BMC Plant Biology*, *20*(1), 1–11. https://doi.org/10.1186/s12870-020-2254-4

Yanhui, C., Xiaoyuan, Y., Kun, H., Meihua, L., Jigang, L., Zhaofeng, G., … Li-Jia, Q. (**2006**). The MYB transcription factor superfamily of Arabidopsis: Expression analysis and phylogenetic comparison with the rice MYB family. *Plant Molecular Biology*, *60*(1), 107–124. https://doi.org/10.1007/s11103-005-2910-y

Yu, X., Feng, B., He, P., & Shan, L. (**2017**). From Chaos to Harmony: Responses and Signaling upon Microbial Pattern Recognition. *Annual Review of Phytopathology*, *55*, 109–137. https://doi.org/10.1146/annurev-phyto-080516-035649

Yu, K., Pieterse, C. M. J., Bakker, P. A. H. M., & Berendsen, R. L. (**2019**). Beneficial microbes going underground of root immunity. *Plant Cell and Environment*, *42*(10), 2860–2870. https://doi.org/10.1111/pce.13632

Yuan, X., Wang, H., Cai, J., Li, D., & Song, F. (**2019**). NAC transcription factors in plant immunity. *Phytopathology Research*, *1*(1), 1–13. https://doi.org/10.1186/s42483-018-0008-0

Zentgraf, U., & Doll, J. (**2019**). Arabidopsis WRKY53, a Node of Multi-Layer Regulation in the Network of Senescence. *Plants*.*8*(12):578. doi:10.3390/plants8120578

Zhai, X., Jia, M., Chen, L., Zheng, C. J., Rahman, K., Han, T., & Qin, L. P. (**2017**). The regulatory mechanism of fungal elicitor-induced secondary metabolite biosynthesis in medical plants. *Critical Reviews in Microbiology*, *43*(2), 238–261. https://doi.org/10.1080/1040841X.2016.1201041

Zhang, Z., Li, Q., Li, Z., Staswick, P. E., Wang, M., Zhu, Y., & He, Z. (**2007**). Dual regulation role of GH3.5 in salicylic acid and auxin signaling during arabidopsis-Pseudomonas syringae interaction. *Plant Physiology*, *145*(2), 450–464. https://doi.org/10.1104/pp.107.106021

Zhang, Z., Wang, M., Li, Z., Li, Q., & He, Z. (**2008**). Arabidopsis GH3.5 regulates salicylic acid-dependent and both NPR1 -dependent and independent defense responses. *Plant Signaling and Behavior*, *3*(8), 537–542. https://doi.org/10.4161/psb.3.8.5748

Zhao, Y., Hull, A. K., Gupta, N. R., Goss, K. A., Alonso, J., Ecker, J. R., … Celenza, J. L. (**2002**). Trp-dependent auxin biosynthesis in Arabidopsis: Involvement of cytochrome P450s CYP79B2 and CYP79B3. *Genes and Development*, *16*(23), 3100–3112. https://doi.org/10.1101/gad.1035402

Zhong, R., Lee, C., Zhou, J., McCarthy, R. L., & Ye, Z. H. (**2008**). A battery of transcription factors involved in the regulation of secondary cell wall biosynthesis in Arabidopsis. *Plant Cell*, *20*(10), 2763–2782. https://doi.org/10.1105/tpc.108.061325

Zhou, N., Tootle, T. L., & Glazebrook, J. (**1999**). Arabidopsis PAD3, a gene required for camalexin biosynthesis, encodes a putative cytochrome P450 monooxygenase. *Plant Cell*, *11*(12), 2419–2428. https://doi.org/10.1105/tpc.11.12.2419

Zhou, Y., Zhou, B., Pache, L., Chang, M., Khodabakhshi, A. H., Tanaseichuk, O., Benner, C., & Chanda, S. K. (**2019**). Metascape provides a biologist-oriented resource for the analysis of systems-level datasets. *Nature communications*, *10*(1), 1523. https://doi.org/10.1038/s41467-019-09234-6

Zhou, J., Wang, X., He, Y., Sang, T., Wang, P., Dai, S., … Meng, X. (**2020**). Differential phosphorylation of the transcription factor WRKY33 by the protein kinases CPK5/CPK6 and MPK3/MPK6 cooperatively regulates camalexin biosynthesis in arabidopsis. *Plant Cell*, *32*(8), 2621–2638. https://doi.org/10.1105/tpc.19.00971

Zhou, J., Mu, Q., Wang, X., Zhang, J., Yu, H., Huang, T., … Meng, X. (**2022**). Multilayered synergistic regulation of phytoalexin biosynthesis by ethylene, jasmonate, and MAPK signaling pathways in Arabidopsis. *The Plant Cell*, *34*(8), 3066–3087. https://doi.org/10.1093/plcell/koac139

Zipfel, C., Kunze, G., Chinchilla, D., Caniard, A., Jones, J. D. G., Boller, T., & Felix, G. (**2006**). Perception of the Bacterial PAMP EF-Tu by the Receptor EFR Restricts Agrobacterium-Mediated Transformation. *Cell*, *125*(4), 749–760. https://doi.org/10.1016/j.cell.2006.03.037

Zipfel, C. (**2008**). Pattern-recognition receptors in plant innate immunity. *Current Opinion in Immunology*, *20*(1), 10–16. https://doi.org/10.1016/j.coi.2007.11.003

Zipfel, C. (**2014**). Plant pattern-recognition receptors. *Trends in Immunology*, *35*(7), 345–351. https://doi.org/10.1016/j.it.2014.05.004
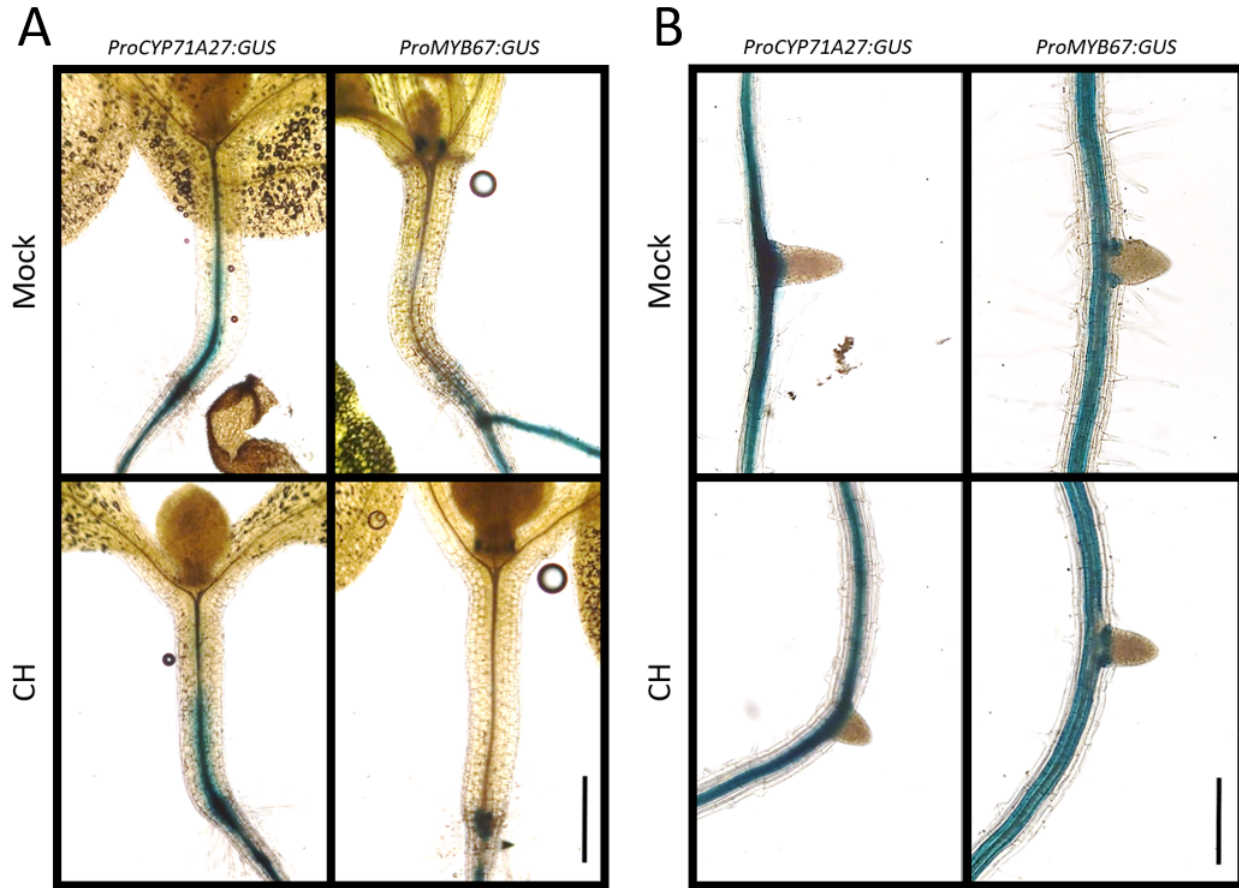
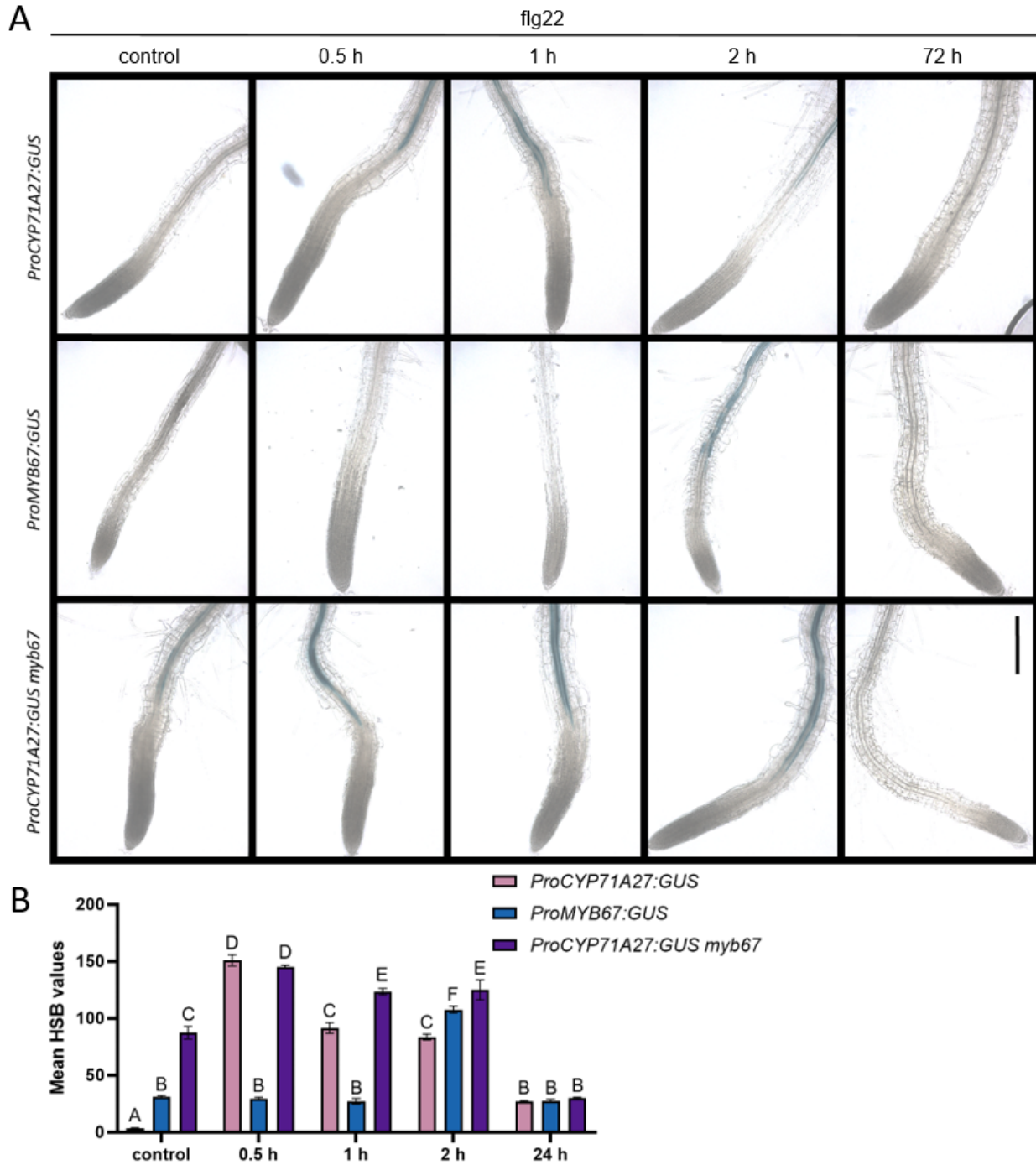# 6 | SUPPLEMENTAL DATA

6.1 Supplemental Figures
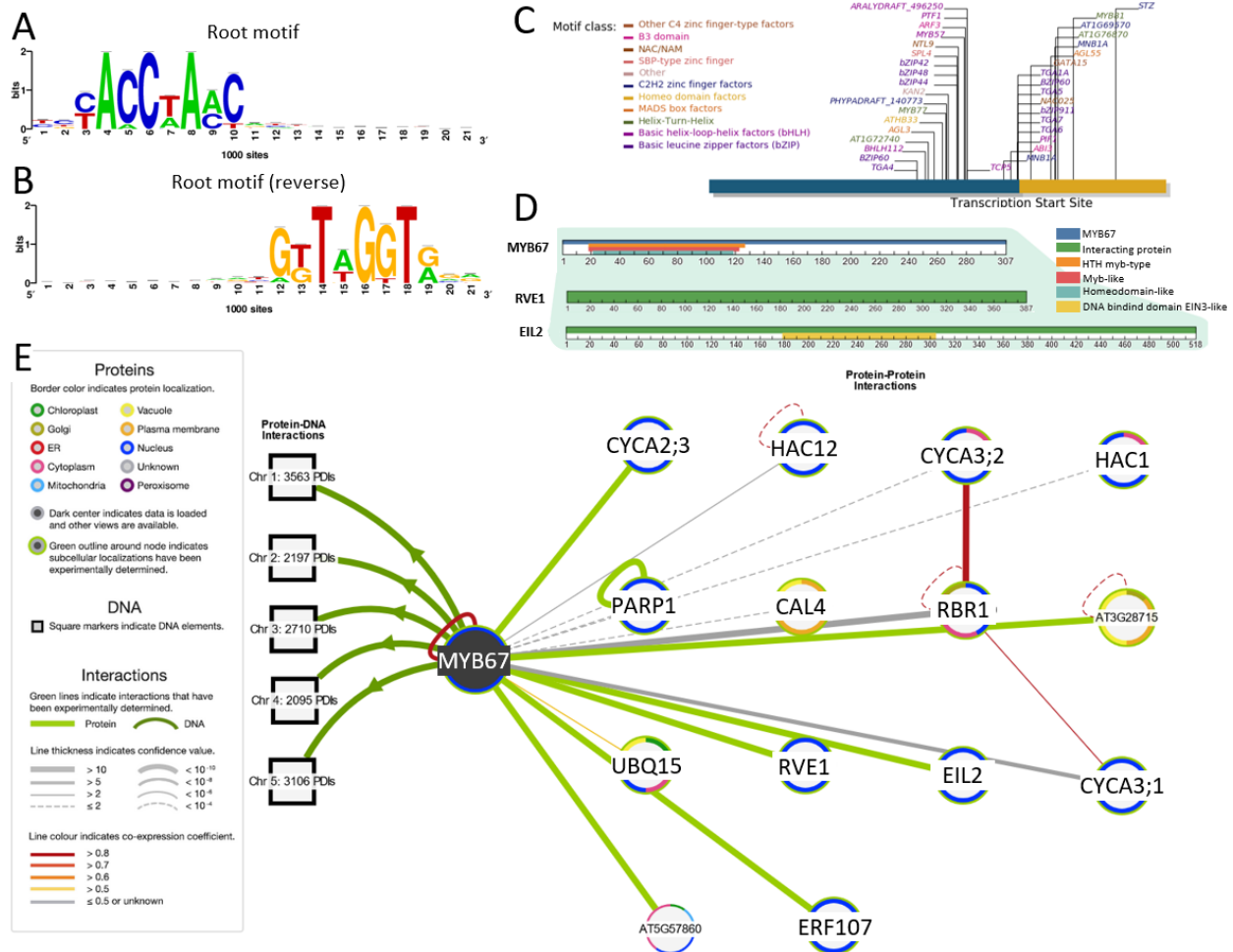
Supplemental Figure S1: MYB67 motif, interaction and motif class binding predictions. Screenshots of MYB67 root motif forward (A) and reverse (B) from RSAT (Castro et al., 2017; Nguyen et al., 2018). **C**: MYB67 promoter (1000 bp upstream from the transcription start site (TSS)) and gene with predicted binding of various motif classes (Ran et al., 2020). **D:** EMBL-EBI Int-Act (interaction viewer) showing two examples of MYB67's interactors (RVE1 and EIL2; Trigg et al., 2017). **E:** Modified screenshot of MYB67's interactions from eFP at bar.utoronto.ca/eplant (Waese et al., 2017).
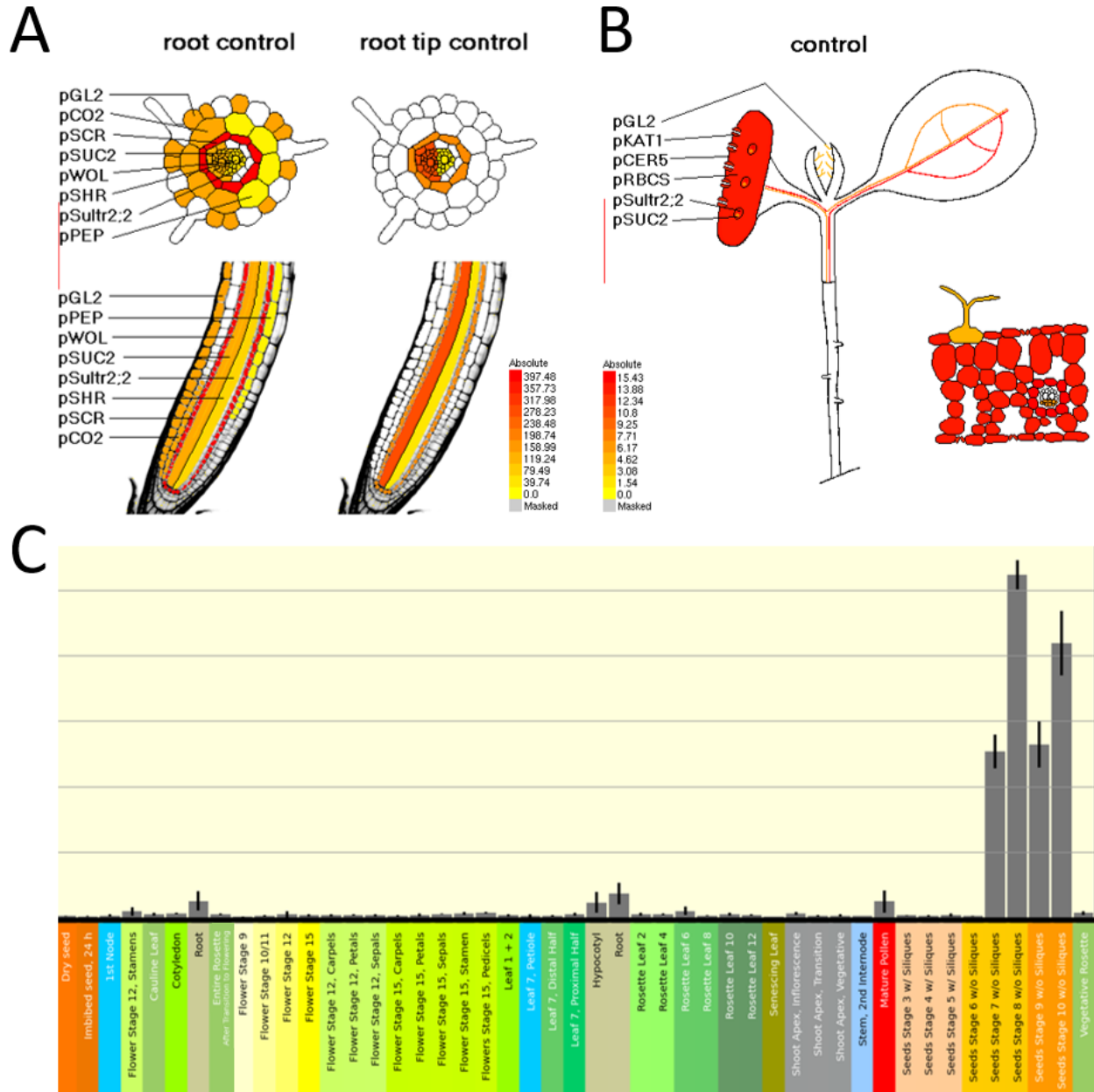
Supplemental Figure S2: Tissue specific eFP browser analysis on *MYB67* (*AT3G12720*). Screenshots of expression of *MYB67* in the *Arabidopsis* roots (**A**), shoots (**B**) and across the whole plant at different developmental stages (**C**) (Waese et al., 2017).

Supplemental Figure S3: Expression patterns of *ProCYP27:GUS* and *ProMYB67:GUS* in response to biotic stresses in the hypocotyl and mid root sections. Five-day-old seedlings were transferred to ½ Murashige and Skoog (MS) liquid media, then the six-day-old seedlings were treated with 10 mM $MgCl_2$ (mock) and *P. fluorescens sp.* CH267 (CH, OD_{600} = 0.04), for 24 h and collected for GUS staining (**A**) hypocotyl, (**B**) mid-root. Scale bar, 100 µm, at least 10 independent seedlings were stained and analysed.

Supplemental Figure S4: Expression patterns of *ProCYP27:GUS, ProMYB67:GUS* and *ProCYP27:GUS* in the *myb67 mutant* in response to flg22. Five-day-old seedlings were transferred to ½ Murashige and Skoog (MS) liquid media, then the six-day-old seedlings were treated with 10 mM MgCl$_2$ (mock) and 1 µM flg22 and collected for GUS staining 30 min, 1 h, 2 h and 24 h post inoculation (**A**). Scale bar, 100 µm, at least 10 independent roots were stained and analysed. **B:** Quantification of GUS activity as seen in Béziat et al., (2016). Student's *t*-test p-value <0.05.
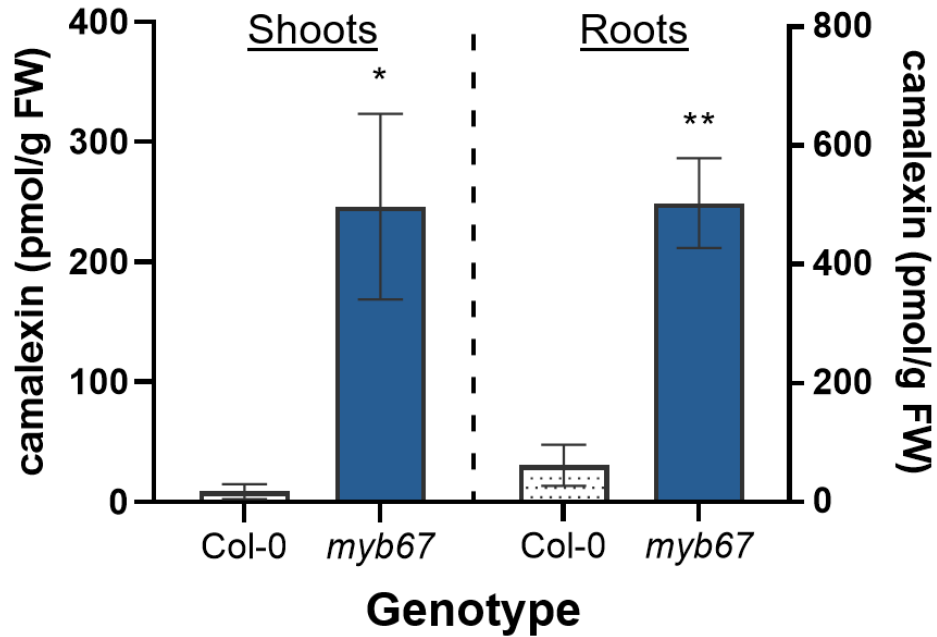
Supplemental Figure S5: Camalexin accumulation in the shoot and root tissue of Col-0 and *myb67* under mock treatment. Col-0 (WT) and *myb67* plants were grown on a nylon net in hydroculture for 7 days and were inoculated in the solution with 10 mM $MgCl_2$ (mock) and harvested 3 dpi. Data represented as means ± SEM from 4 biological replicates, each corresponding to at least 30 seedlings. Asterisks indicate significant differences against the WT (*p<0.05, **p<0.01, Student's *t*-test). A calibration curve of external standards were utilised to determine the camalexin amount in the samples.
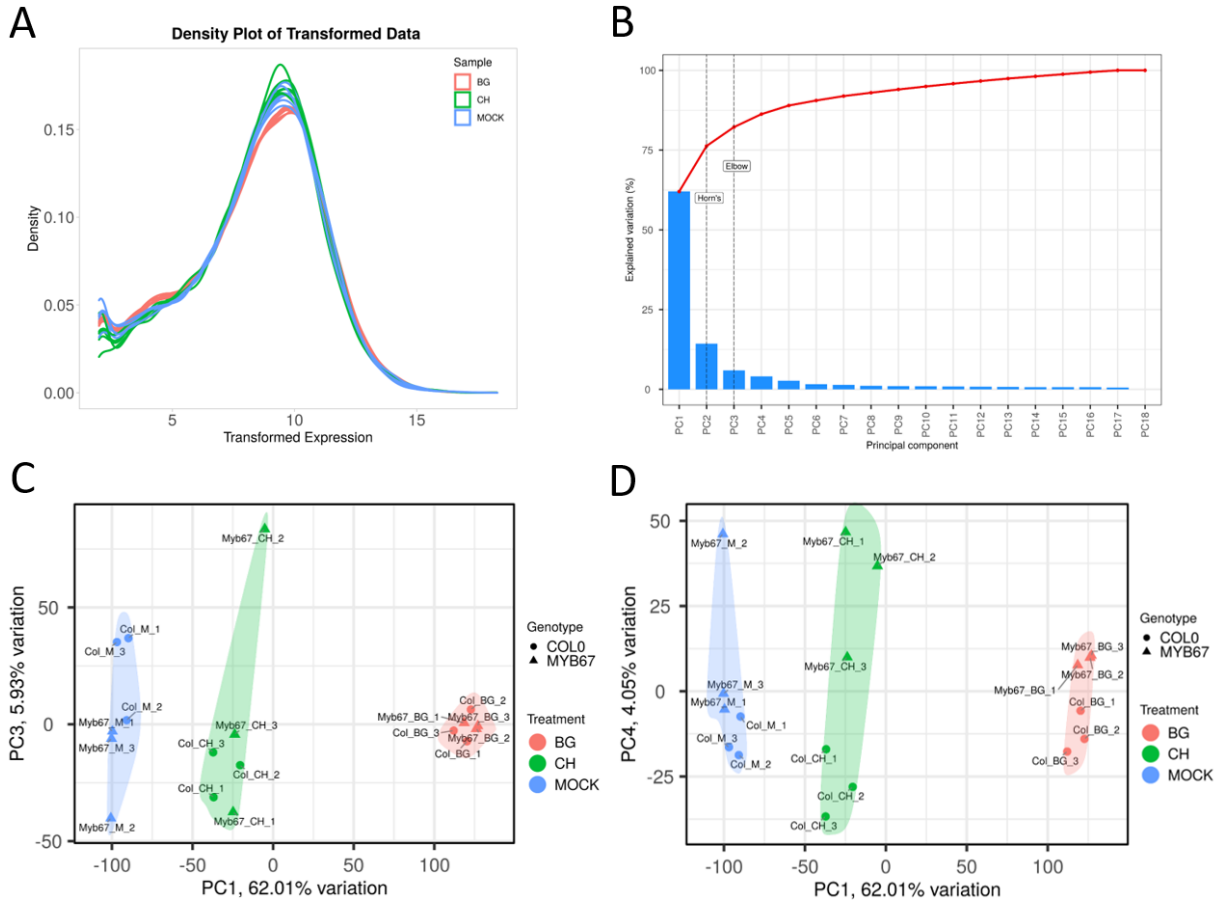
Supplemental Figure S6: Pre-Process Data of RNA-seq. Performed with iDEP1.0. **A:** Density of transformed RNA-seq data. Treatments are represented by colour; mock (blue), BG (*B. glumae*- red) and CH (*P. fluorescens*-green). **B:** SCREE plot representing Horn's parallel analysis and the "elbow" of the multiple principal component analysis (PCA) **C:** PCA illustrated in a bi-plot of normalised expression values (log$_2$-transformed counts per million (TPM)), depicting PCA1 and PCA3. **D:** PCA4 illustrates the correlation of genotypes Col-0 and *myb67*. **C&D:** Genotypes are indicated in circles and triangles, Col-0 and *myb67* respectively and the treatments mock, BG and CH are indicated by different colours; blue, red and green respectively.

Average Expression vs. Log$_2$ Fold Change
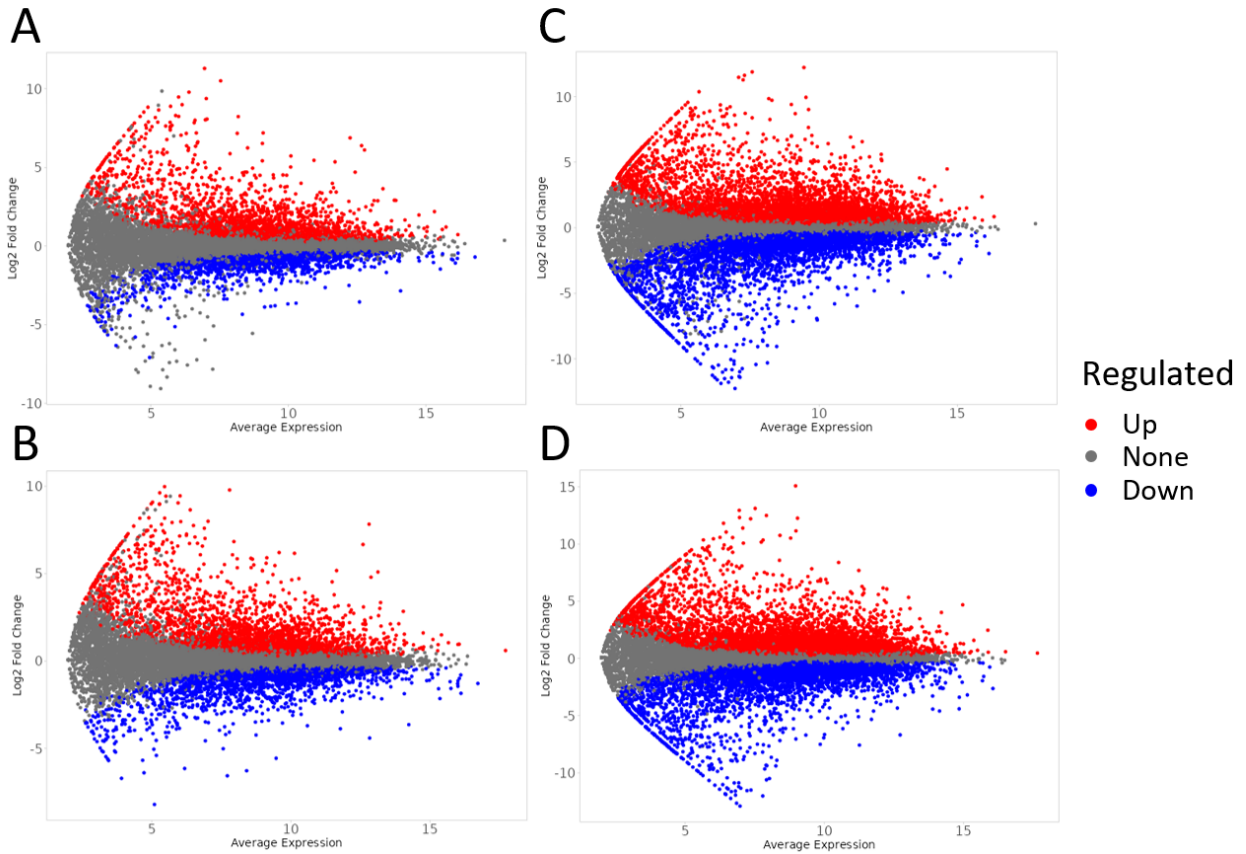
Supplemental Figure S7: MA plots of RNA-seq. Performed with iDEP1.0. Red are up-regulated and blue are down-regulated genes **A:** CHvsM in WT **B:** CHvsM in *myb67* **C:** BGvsM in WT **D:** BGvsM in *myb67*.
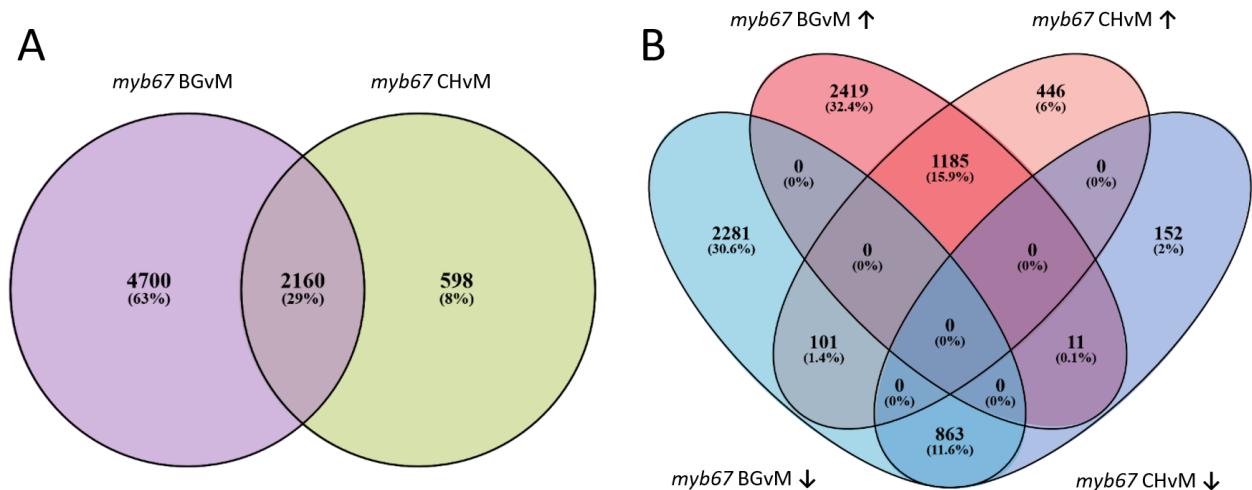

Supplemental Figure S8: The shared DEGs from the transcriptome response between treatments in *myb67* roots. Venn diagrams of up- and down-regulated genes are indicated by up-facing and down-facing arrows **A:** The total shared DEGs between treatments against mock in *myb67*. *B. glumae* (BG- in purple) and *P. fluorescens* (CH- in green). **B:** The shared up- (shades of red) /down- (shades of blue) regulated genes between treatments against mock. Venn diagrams were made in Venny 2.1.
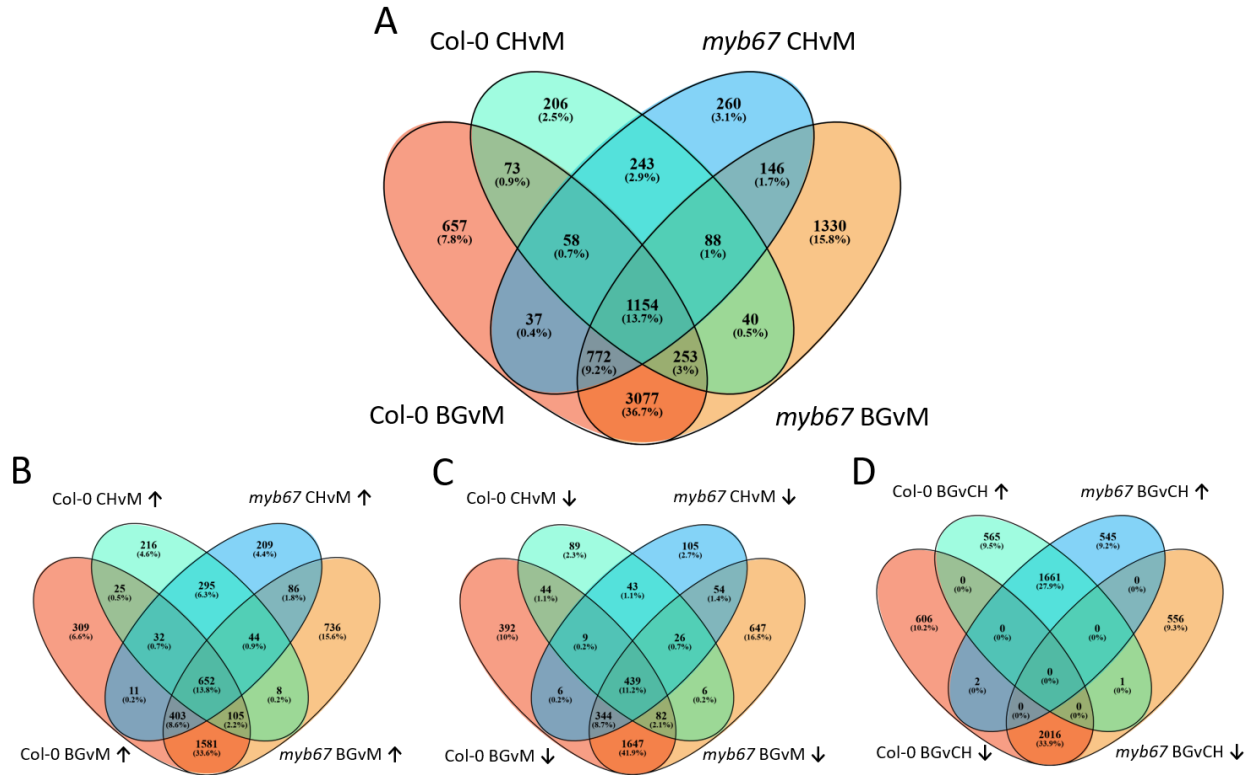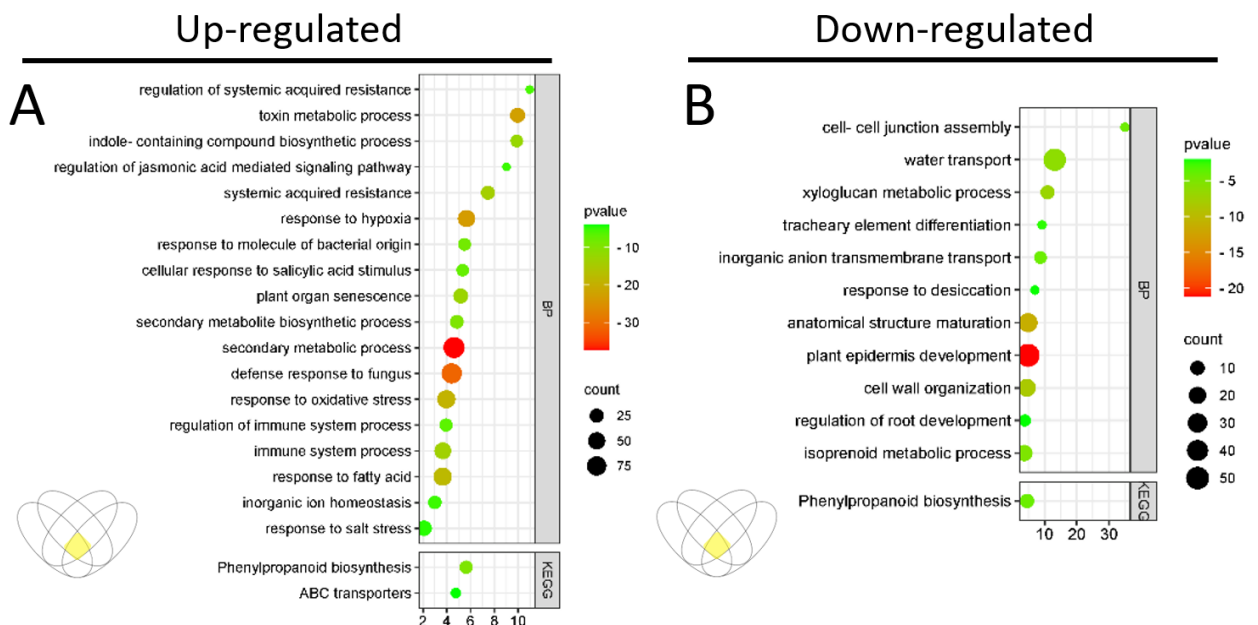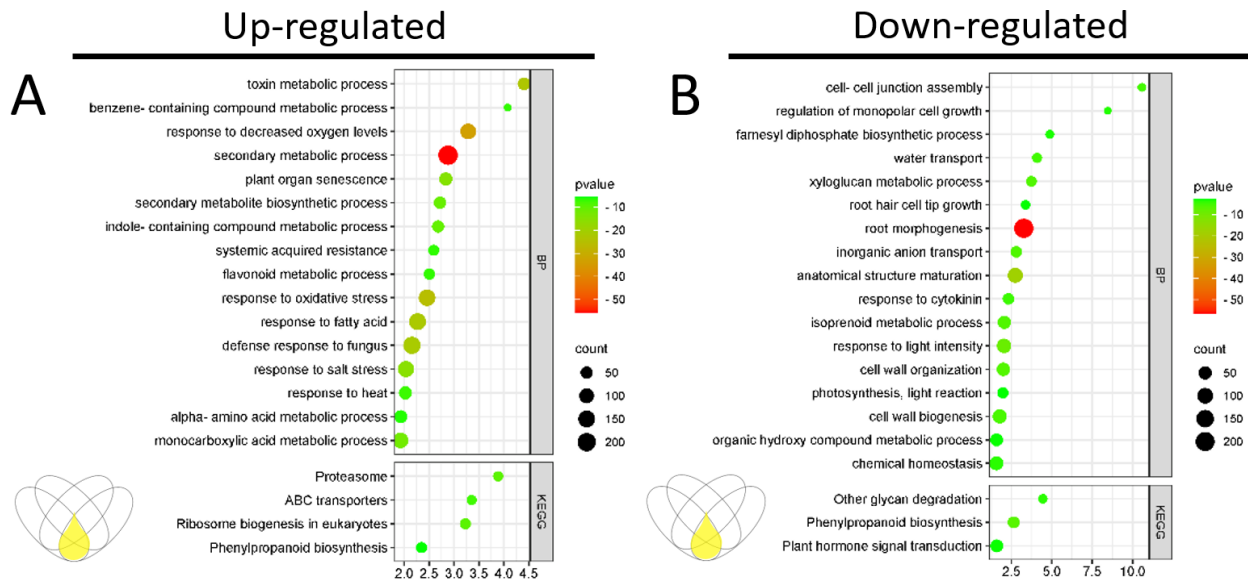
Supplemental Figure S9: The shared DEGs from the transcriptome response between treatments in WT and *myb67* roots. Venn diagrams of up- and down-regulated genes are indicated by up-facing and down-facing arrows **A:** The total shared DEGs between treatments against mock in Col-0 and *myb67* **B:** The shared up-regulated genes between treatments against mock **C:** The shared down-regulated genes between treatments against mock. **C:** The shared up/down regulated genes between BG against CH in WT Col-0 and *myb67*. BGvM in red and orange, CHvM in green and blue for Col-0 and *myb67*, respectively. Venn diagrams were made in Venny 2.1.
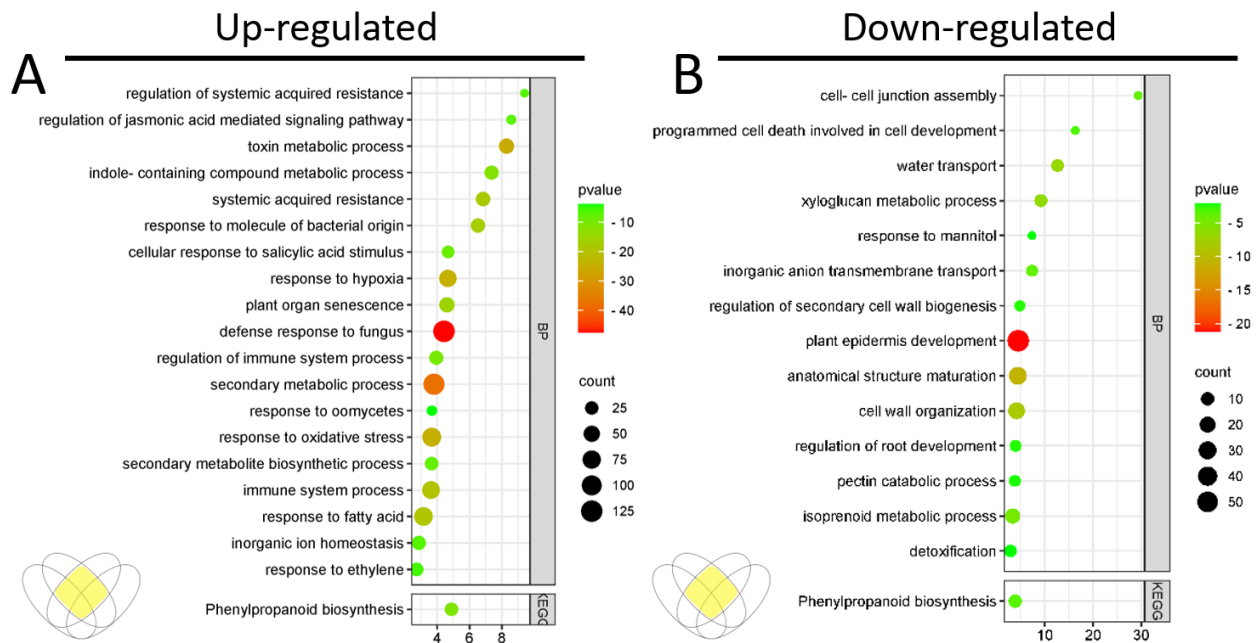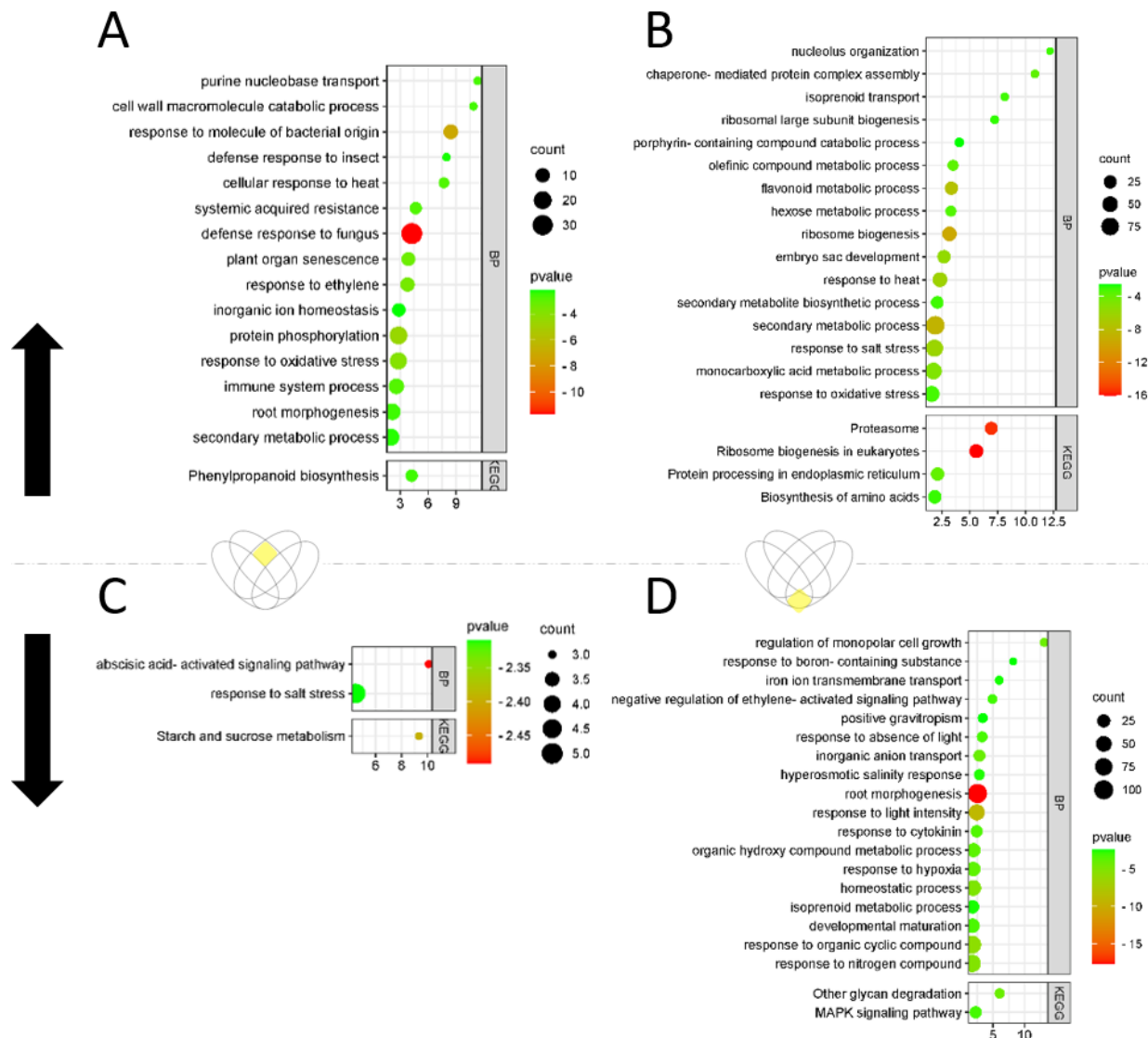
Supplemental Figure S9a: Summary of the top GO clusters from up- and down- regulated genes between PGPB-treated WT and *myb67*. Top GO terms (max 20) include enriched KEGG pathways from genes in Supplemental Figure S9. The x-axis is the enrichment. The simplified venn diagram schematic illustrates the shared genes used to determine the GO enrichment. **A & B:** shared genes between the PGPB (CH) treated Col-0 and *myb67* (some overlap with the pathogen (BG)). **A:** up-regulated, **B:** down-regulated. p-value was filtered for < 0.0001.


Supplemental Figure S9b: Summary of top GO clusters of the shared up- and down- regulated genes between all treatments in WT and *myb67*. Top GO terms (max 20) include enriched KEGG pathways from genes in Supplemental Figure S9. The simplified venn diagram schematic illustrates the shared genes used to determine the GO enrichment. **A & B:** shared genes between both treatments and genotypes. **A:** up-regulated, **B:** down-regulated. p-value was filtered for < 0.0001.
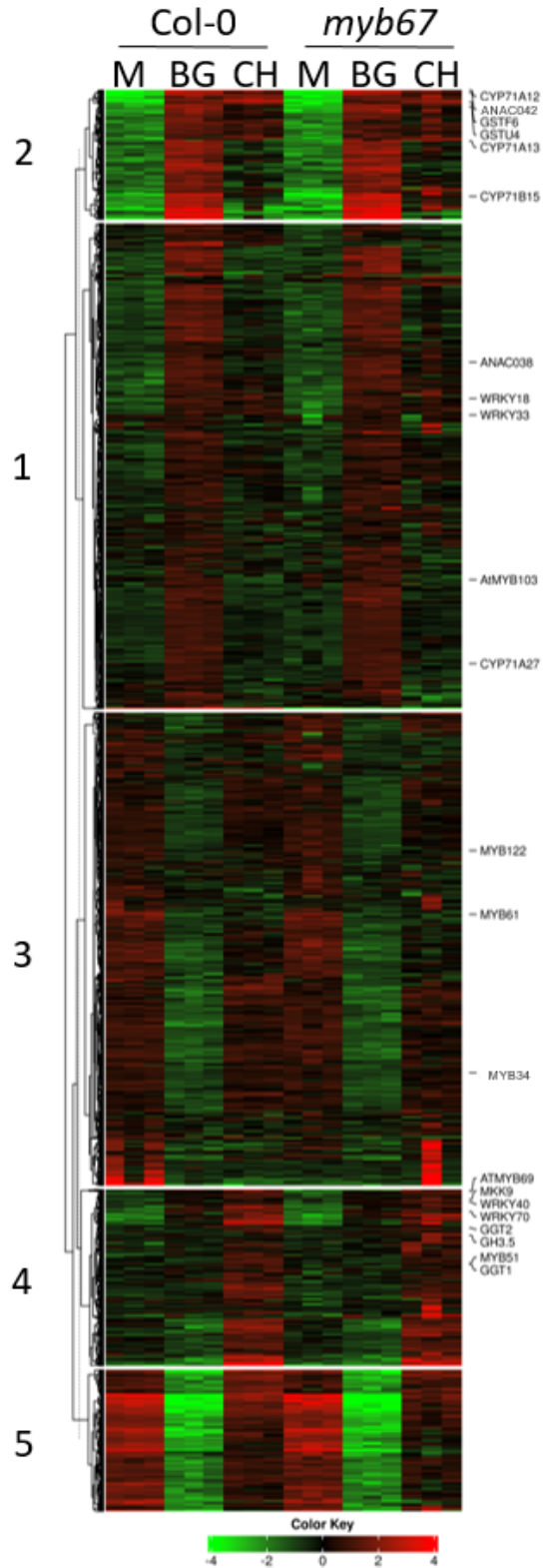
Supplemental Figure S9c: Summary of the top GO clusters from up- and down- regulated genes between pathogen-treated WT and *myb67*. Top GO terms (max 20) include enriched KEGG pathways from genes in Supplemental Figure S9. The simplified venn diagram schematic illustrates the shared genes used to determine the GO enrichment. **A & B:** shared genes between both treatments and genotypes. **C & D:** shared genes between the PGPB *P. fluorescens* (CH) treated Col-0 and *myb67*. **E & F:** shared genes between the pathogen *B. glumae* (BG) treated Col-0 and *myb67*. **A, C & E:** up-regulated **B, D & F:** down-regulated. p-value was filtered for < 0.0001.
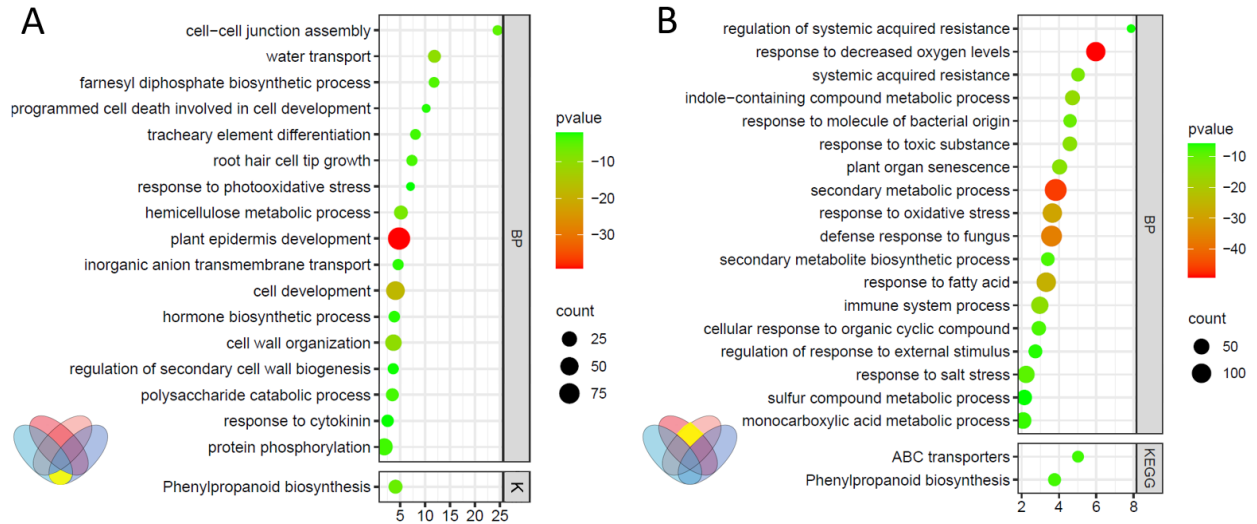
Supplemental Figure S9d: Summary of the top GO clusters between treatment of up and down regulated genes in WT and *myb67*. Top GO terms (max 20) include enriched KEGG pathways from genes in Supplemental Figure S9. The simplified venn diagram schematic illustrates the shared genes used to determine the GO enrichment. Up/down-regulated genes are shown by the arrows and line dividing the figure. **A & C:** shared genes exclusively between the PGPB *P. fluorescens* (CH) treated Col-0 and *myb67*. **B & D:** shared genes exclusively between the pathogen *B. glumae* (BG) treated Col-0 and *myb67*. **A & B:** up-regulated. **C & D:** down-regulated. p-value was filtered for < 0.0001.

Enriched TFs in *myb67*vCol-0
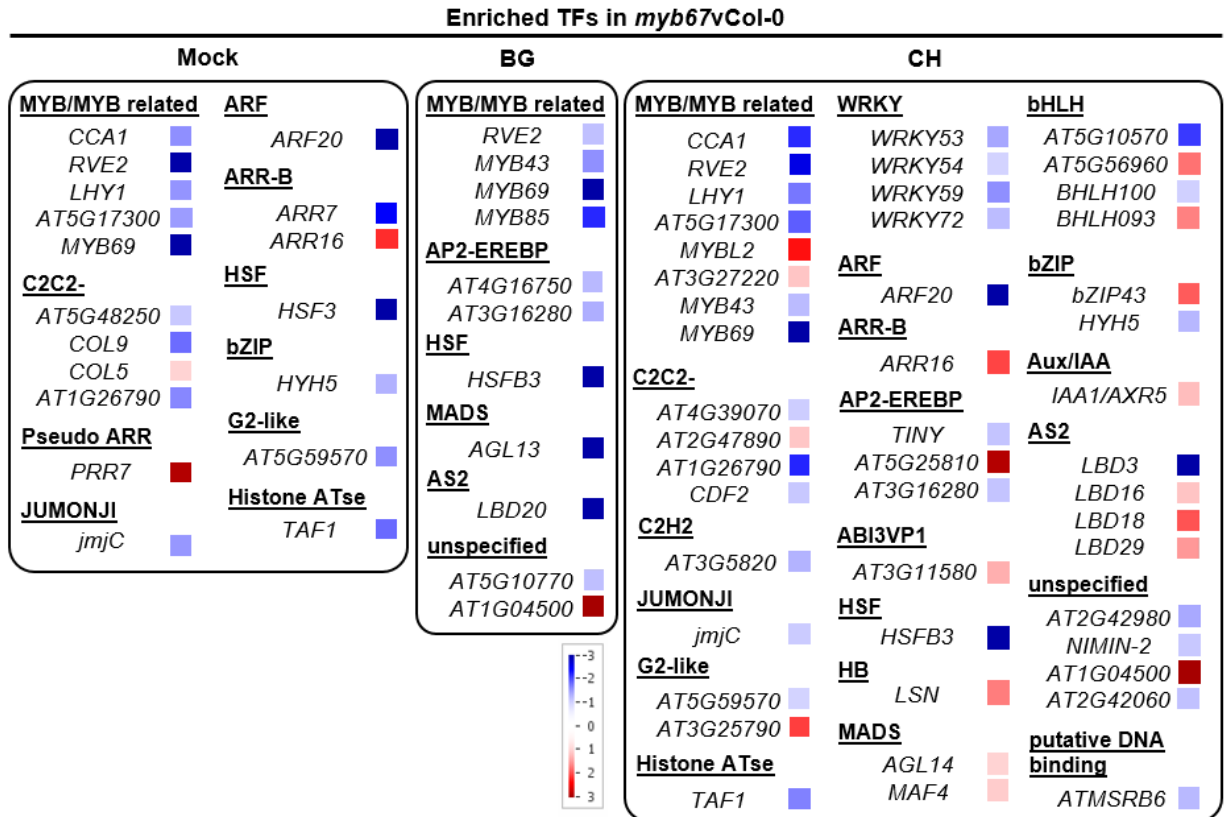
Supplemental Figure S10: Differentially expressed TFs in *myb67*vCol-0 in the various treatments. DEGs were filtered for q-value < 0.05, Log$_2$ FC < -1, > 1. Data was processed in MapMan 3.6.0, Transcription, using Ath_AGI_TAIR9. M (Mock), BG (*B. glumae*), CH (*P. fluorescens*). The legend references the Log$_2$ FC (Thimm *et al.,* 2004).

Supplemental Figure S11: The *k*-Means clustering of differentially expressed genes. k-means were selected after elbow plot analysis. *k*-means clustering heatmap. DEGs under mock (M), pathogen (BG) and PGPB (CH). iDEP1.0 was used and the transformed data was obtained by EdgeR: log2 (counts per million (CPM) + Pseudo count c of 4) with min CPM as 0.5. max z-score of 3.

Supplemental Figure S12: Summary of the top GO clusters from similarly regulated genes between *B. glumae* and *P. fluorescens* in *myb67* roots. Top GO terms (max 20) include enriched KEGG (shortened to K) pathways from genes in Supplemental Figure S8. The x-axis is the enrichment. The simplified venn diagram schematic illustrates the genes used to determine the GO enrichment (in yellow). **A:** down-regulated. **B:** up-regulated. p-value was filtered for < 0.0001.
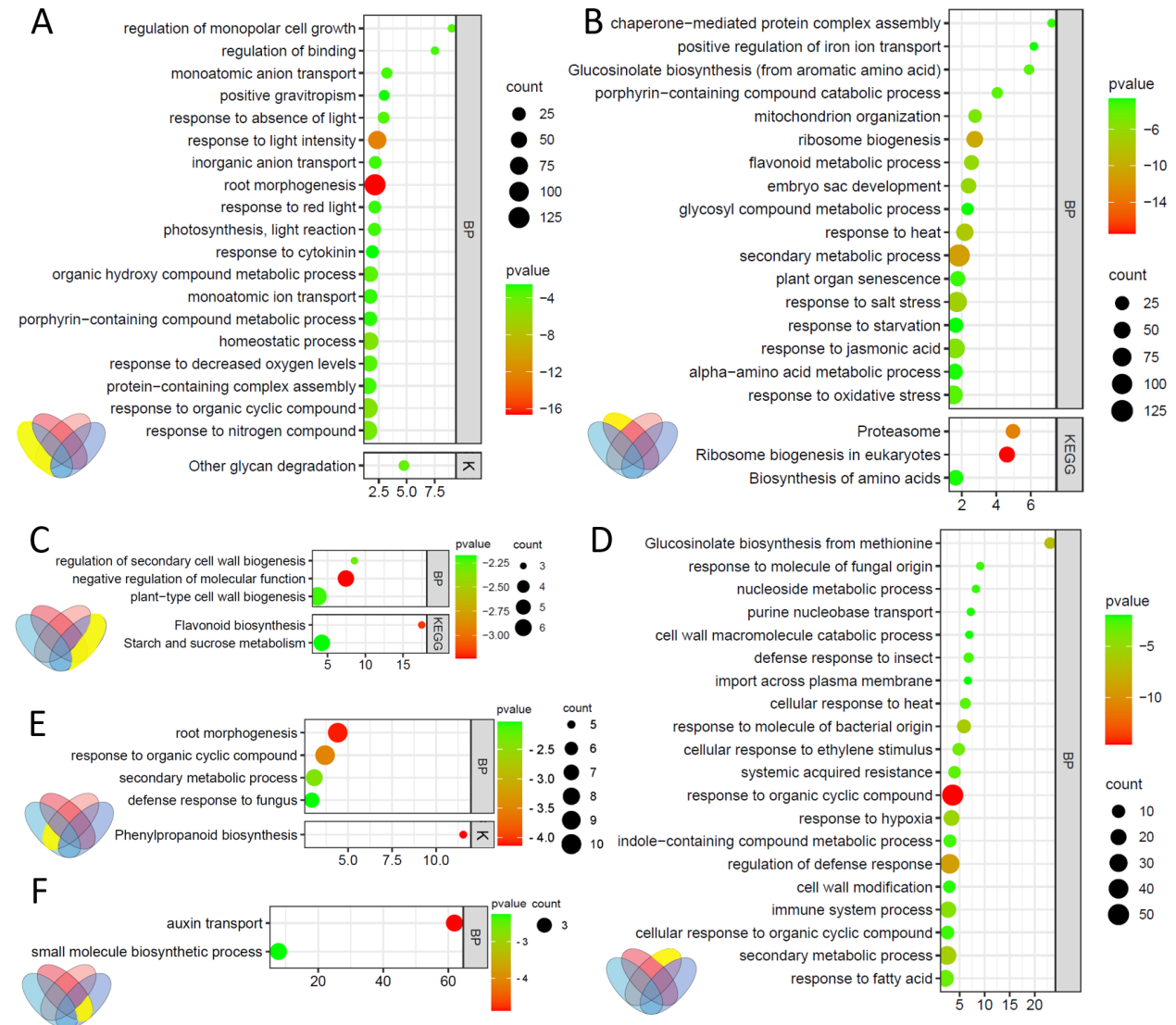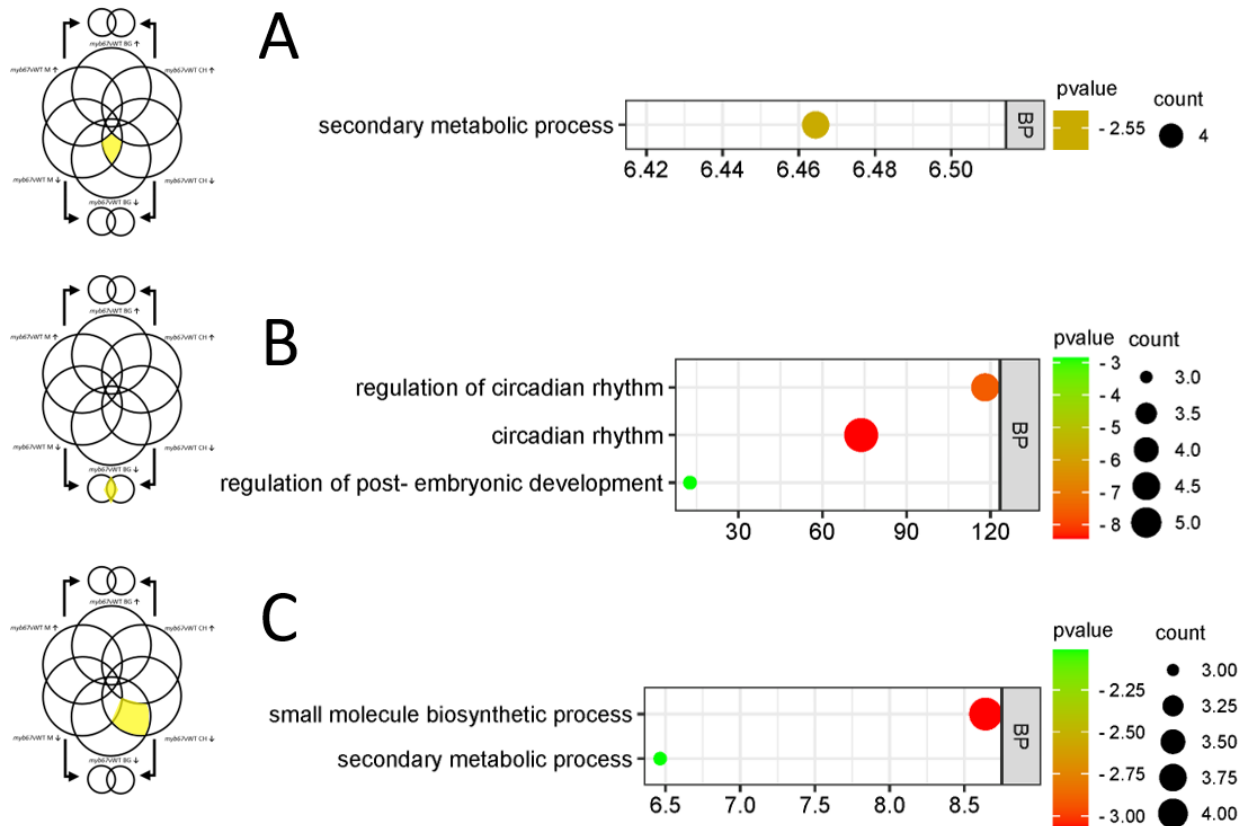
Supplemental Figure S12a: Summary of top GO clusters of up- and down- regulated genes in *B. glumae* and *P. fluorescens* in *myb67* roots. Top GO terms (max 20) include enriched KEGG (shortened to K) pathways from genes in Supplemental Figure S8. The simplified venn diagram schematic illustrates the genes used to determine the GO enrichment (in yellow). **A&B:** in response to *B. glumae*. **A&B:** in response to *B. glumae*. **C&D:** in response to *P. fluorescens*. **A&C:** down-regulated. **B&D:** up-regulated. **E:** down-regulated in *B. glumae* and up-regulated in *P. fluorescens*. **F:** up-regulated in *B. glumae* and down-regulated in *P. fluorescens*. p-value was filtered for < 0.0001.

Supplemental Figure S13: Summary of the top GO clusters of *myb67*vWT DEGs down-regulated between treatments. The x-axis depicts the enrichment. The simplified venn diagram schematic illustrates the shared genes used to determine the GO enrichment, (highlighted in yellow). Shared genes **A:** exclusively in all treated (M, BG & CH) *myb67*vWT. **B:** exclusively in mock and CH treated *myb67*vWT. **C:** exclusively in BG and CH treated *myb67*vWT.p-value was filtered for < 0.0001.
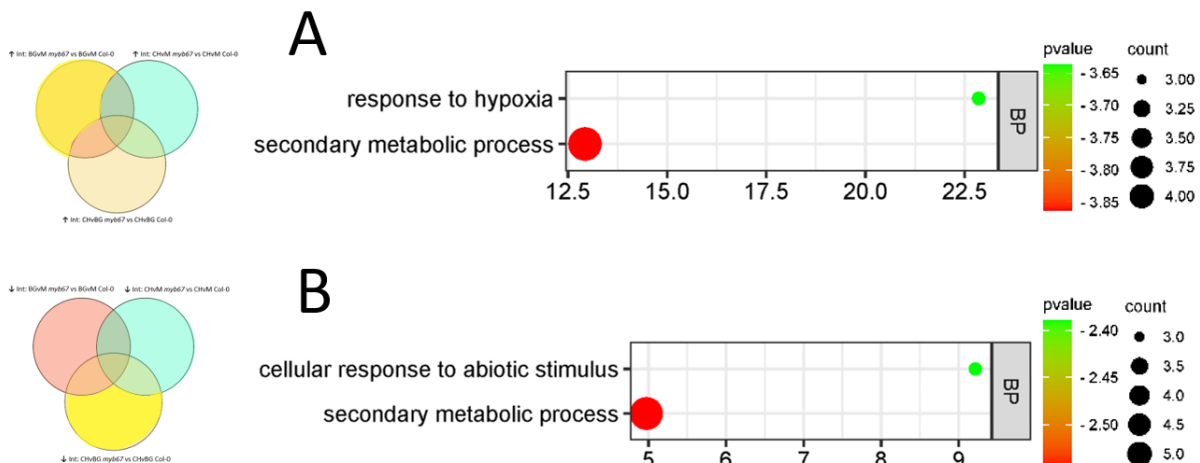
Supplemental Figure S14: Summary of the top GO clusters of the up regulated genes from the interaction terms. The x-axis depicts the enrichment. The simplified venn diagram schematic illustrates the genes used to determine the GO enrichment, (highlighted in yellow). GO terms from up-regulated genes **A:** exclusively in Int: BGvM *myb67* vs BGvM WT. **B:** exclusively in Int: CHvBG *myb67* vs CHvBG WT. p-value was filtered for < 0.0001.

Differential expression in transcriptional comparisons
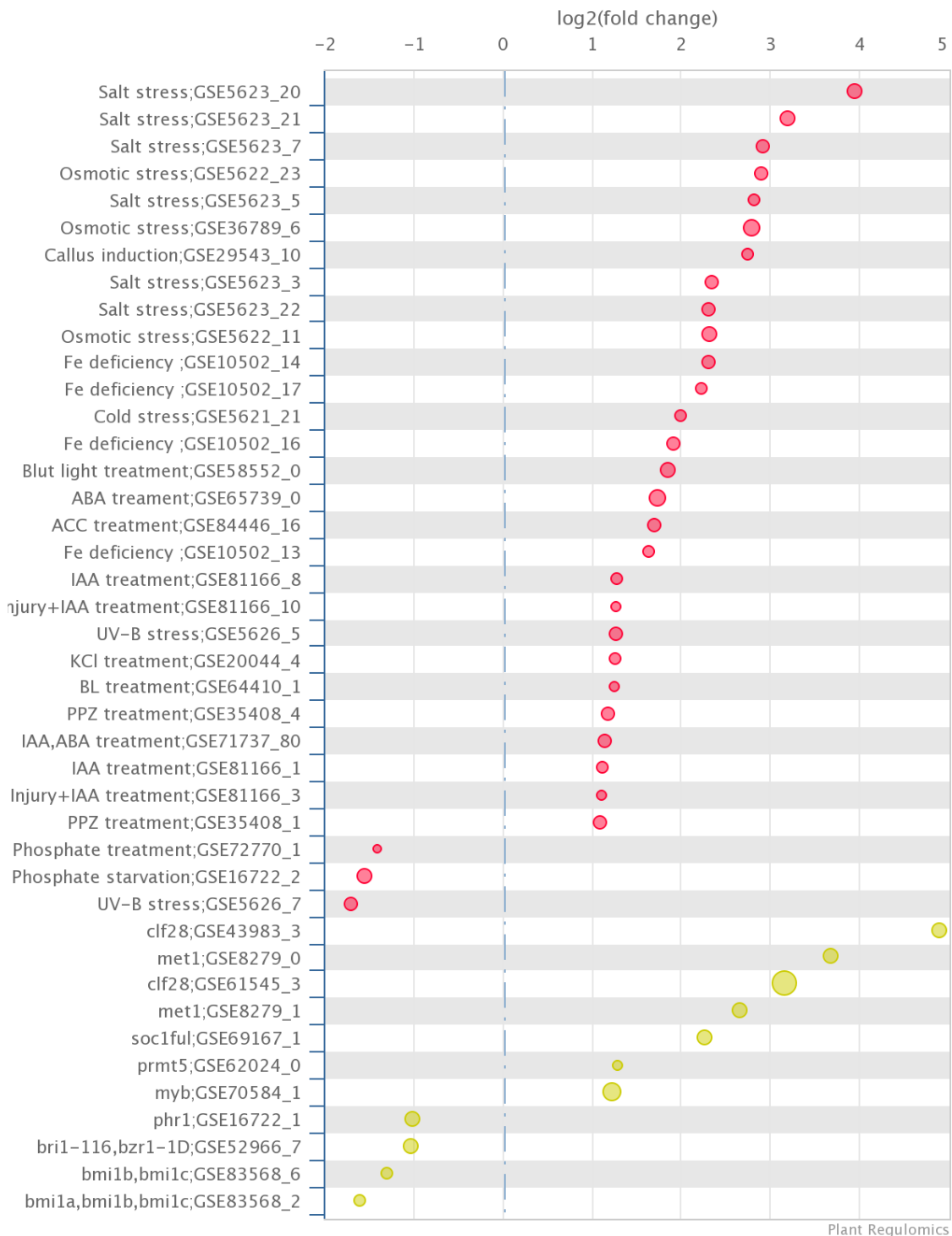
Supplemental Figure S15: Differential expression of *MYB67* in various transcriptional comparisons (perturbations and mutants). Image was downloaded directly from Plant Regulomics. Perturbations are in red and mutants/overexpression are in green (Ran *et al.,* 2019).
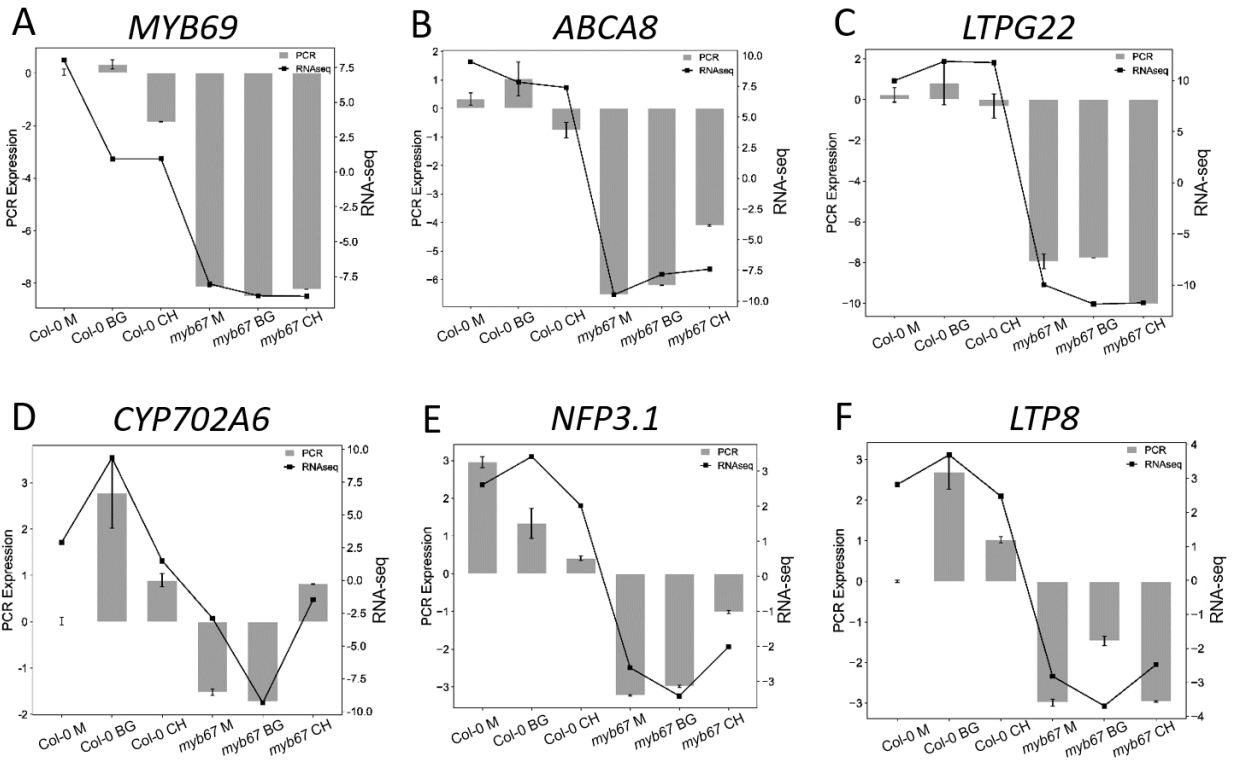
Supplemental Figure S16: Verification of RNA-seq expression data with qRT-PCR. qRT-PCR and RNA-seq values shown are in $\log_2$FC, qRT-PCR results were normalised to the reference gene *TIP41*. SEM is shown.

6.2 Supplemental Tables

Supplemental Table S1: Plant Regulomics prediction of upstream regulators

Genes	Transcription factors									
	WRKY18	WRKY33	WRKY40	ANAC042	ANAC038	MYB61	MYB67	MYB83	MYB103	RVE1
CYP79B2	+	+	+	+		+	+			+
CYP79B3	+	+	+	+		+	+	+		+
CYP71A12	+	+	+	+						+
CYP71A13	+	+	+	+						
CYP71A27					+	+	+	+		
CYP71A28						+	+	+		
GSTF6	+	+								
GGP1	+	+		+				+		+
GGT1	+	+	+			+	+	+		+
GH3.5	+	+	+							
CYP71B15	+	+	+	+	+					+
ANAC042	+	+						+		+
MKS1	+	+	+							+
MYB51	+	+	+	+		+	+	+		+
MYB122	+	+	+	+				+		+
WRKY18	+	+	+				+			+
WRKY40	+	+	+							+
WRKY33	+	+								
ANAC038		+								+
MYB61	+	+	+	+	+					
MYB67	+	+			+	+		+		+
MYB83	+	+	+		+		+	+		
MYB103		+	+	+	+					
EBP						+	+			
ERF1	+	+	+		+	+	+	+		+
ARF9	+	+	+	+						+
RVE1	+	+	+				+			+
MYB69	+	+	+			+	+	+		

* according to 1000 bp around transcription start site (TSS), (+) indicates binding, blanks indicate no binding

Supplemental Table S2: Genes mentioned in this study

Abbreviation	Full name	AGI
ABCA8	*ATP-BINDING CASSETTE A8*	*AT3G47790*
ADH1	*ALCOHOL DEHYDROGENASE 1*	*AT1G77120*
ANAC038	*ARABIDOPSIS NAC DOMAIN CONTAINING PROTEIN 38*	*AT2G24430*
ANAC042	*ARABIDOPSIS NAC DOMAIN CONTAINING PROTEIN 42*	*AT2G43000*
ANAC087	*ARABIDOPSIS NAC DOMAIN CONTAINING PROTEIN 87*	*AT5G18270*
ARF9	*AUXIN-RESPONSIVE FACTOR*	*AT4G23980*
ARR1	*ARABIDOPSIS RESPONSE REGULATOR 1*	*AT3G16857*
ARR10	*ARABIDOPSIS RESPONSE REGULATOR 10*	*AT4G31920*
ARR12	*ARABIDOPSIS RESPONSE REGULATOR 12*	*AT2G25180*
ATR1	*ARABIDOPSIS P450 REDUCTASE 1*	*AT4G24520*
BES1	*BRASSINAZOLE-RESISTANT 2*	*AT1G19350*
BHLH093	*BETA HLH PROTEIN 93*	*AT5G65640*
BHLH100	*BETA HLH PROTEIN 100*	*AT2G41240*
BOA	*BROTHER OF LUX ARRHYTHMO*	*AT5G59570*
BZS1	*B-BOX DOMAIN PROTEIN 20*	*AT4G39070*
CAD4	*CINNAMYL ALCOHOL DEHYDROGENASE 4*	*AT3G19450*
CAD9	*CINNAMYL ALCOHOL DEHYDROGENASE 9*	*AT4G39330*
CASP1	*CASPARIAN STRIP MEMBRANE DOMAIN PROTEIN 1*	*AT2G36100*
CASP2	*CASPARIAN STRIP MEMBRANE DOMAIN PROTEIN 2*	*AT3G11550*
CASP4	*CASPARIAN STRIP MEMBRANE DOMAIN PROTEIN 4*	*AT5G06200*
CASP5	*CASPARIAN STRIP MEMBRANE DOMAIN PROTEIN 5*	*AT5G15290*
CBP60G	*CAM-BINDING PROTEIN 60-LIKE G*	*AT5G26920*
CCA1	*CIRCADIAN CLOCK ASSOCIATED 1*	*AT2G46830*
CCL	*CCR-LIKE*	*AT3G26740*
CCR1	*CINNAMOYL COA REDUCTASE 1*	*AT1G15950*
ChiC	*CLASS V CHITINASE*	*AT4G19810*
CPK5	*CALCIUM-DEPENDENT PROTEIN KINASE 5*	*AT4G35310*
CPK6	*CALCIUM-DEPENDENT PROTEIN KINASE 6*	*AT2G17290*
CYP71A12	*CYTOCHROME P450, FAMILY 71, SUBFAMILY A, POLYPEPTIDE 12*	*AT2G30750*
CYP71A13	*CYTOCHROME P450, FAMILY 71, SUBFAMILY A, POLYPEPTIDE 13*	*AT2G30770*
CYP71A27	*CYTOCHROME P450, FAMILY 71, SUBFAMILY A, POLYPEPTIDE 27*	*AT4G20240*
CYP71A28	*CYTOCHROME P450, FAMILY 71, SUBFAMILY A, POLYPEPTIDE 28*	*AT4G20235*
CYP71A15 (PAD3)	*PHYTOALEXIN DEFICIENT 3*	*AT3G26830*
CYP71B7	*CYTOCHROME P450, FAMILY 79, SUBFAMILY B, POLYPEPTIDE 7*	*AT1G13110*
CYP79B2	*CYTOCHROME P450, FAMILY 79, SUBFAMILY B, POLYPEPTIDE 2*	*AT4G39950*
CYP79B3	*CYTOCHROME P450, FAMILY 79, SUBFAMILY B, POLYPEPTIDE 3*	*AT2G22330*
CYP702A5	*CYTOCHROME P450, FAMILY 702, SUBFAMILY A, POLYPEPTIDE 5*	*AT4G15393*
CYP702A6	*CYTOCHROME P450, FAMILY 702, SUBFAMILY A, POLYPEPTIDE 6*	*AT4G15396*
CYP707A3	*CYTOCHROME P450, FAMILY 707, SUBFAMILY A, POLYPEPTIDE 3*	*AT5G45340*
CYP82C4	*CYTOCHROME P450, FAMILY 82, SUBFAMILY C, POLYPEPTIDE 4*	*AT4G31940*
CYP83B1	*CYTOCHROME P450, FAMILY 83, SUBFAMILY B, POLYPEPTIDE 1*	*AT4G31500*

CYP86A1	*CYTOCHROME P450, FAMILY 86, SUBFAMILY A, POLYPEPTIDE 1*	*AT5G58860*
DEG5	*DEG5*	*AT3G05945*
DIR5	*DIRIGENT PROTEIN 5*	*AT1G64160*
DHNAT2	*DHNA-COA THIOESTERASE 2*	*AT5G48950*
DOX1	*ALPHA-DIOXYGENASE 1*	*AT3G01420*
EBP	*ETHYLENE-RESPONSIVE ELEMENT BINDING PROTEIN*	*AT3G16770*
EIL2	*ETHYLENE INSENSITIVE 3-LIKE 2*	*AT5G21120*
ELF3	*EARLY FLOWERING 3*	*AT2G25930*
ELF4	*EARLY FLOWERING 4*	*AT2G40080*
EP1	*CYSTEINE-RICH RLK 1*	*AT4G23179*
EPS1	*ENHANCED PSEUDOMONAS SUSCEPTIBILITY 1*	*AT5G67160*
ERF1	*ETHYLENE RESPONSE FACTOR 1*	*AT3G23240*
ERF107	*DECREASE WAX BIOSYNTHESIS*	*AT5G61590*
EXECUTER	*EXECUTER1*	*AT4G33630*
EXPA1	*EXPANSIN 1*	*AT1G69530*
EXPA10	*EXPANSIN 10*	*AT1G26770*
EXPA15	*EXPANSIN 15*	*AT2G03090*
EXPA17	*EXPANSIN 17*	*AT4G01630*
FACT	*FATTY ALCOHOL:CAFFEOYL-COA CAFFEOYL TRANSFERASE*	*AT5G63560*
FAR1	*FATTY ACID REDUCTASE 1*	*AT5G22500*
FAR5	*FATTY ACID REDUCTASE 5*	*AT3G44550*
FBS1	*F-BOX STRESS INDUCED 1*	*AT1G61340*
FMO	*FLAVIN MONOOXYGENASE*	*AT1G12200*
FRK1	*FLG22-INDUCED RECEPTOR-LIKE KINASE 1*	*AT2G19190*
GGP1	*γ-GLUTAMYL PEPTIDASES 1*	*AT4G30530*
GGP3	*γ-GLUTAMYL PEPTIDASES 3*	*AT4G30550*
GGT1	*γ-GLUTAMYL TRANSPEPTIDASES 1*	*AT1G23310*
GGT2	*γ-GLUTAMYL TRANSPEPTIDASES 2*	*AT4G39650*
GH3.5	*WES1*	*AT4G27260*
GPAT5	*GLYCEROL-3-PHOSPHATE SN-2-ACYLTRANSFERASE 5*	*AT3G11430*
GSTF6	*GLUTATHIONE-S-TRANSFERASE*	*AT1G02930*
GSTU4	*GLUTATHIONE S-TRANSFERASE TAU 4*	*AT2G29460*
JAZ1	*JASMONATE-ZIM-DOMAIN PROTEIN 1*	*AT1G19180*
JAZ6	*JASMONATE-ZIM-DOMAIN PROTEIN 6*	*AT1G72450*
JAZ10	*JASMONATE-ZIM-DOMAIN PROTEIN 10*	*AT5G13220*
JRG21	*JA-REGULATED GENE 21*	*AT3G55970*
KCS2	*3-KETOACYL-COA SYNTHASE 2*	*AT1G04220*
LAC11	*LACCASE 11*	*AT5G03260*
LBD16	*LATERAL ORGAN BOUNDARIES-DOMAIN 16*	*AT2G42430*
LBD18	*LATERAL ORGAN BOUNDARIES-DOMAIN 18*	*AT2G45420*
LBD20	*LATERAL ORGAN BOUNDARIES-DOMAIN 20*	*AT3G03760*
LBD29	*LATERAL ORGAN BOUNDARIES-DOMAIN 29*	*AT3G58190*
LHY	*LATE ELONGATED HYPOCOTYL*	*AT1G01060*
LGT9	*GALACTURONOSYLTRANSFERASE-LIKE 8*	*AT1G24170*
LOX1	*ARABIDOPSIS LIPOXYGENASE 1*	*AT1G55020*

LTP8	*LIPID TRANSFER PROTEIN 8*	*AT2G18370*
LTPG22	*GLYCOSYLPHOSPHATIDYLINOSITOL-ANCHORED LIPID PROTEIN TRANSFER 22*	*AT3G58550*
MAPK3	*MITOGEN ACTIVATED PROTEIN KINASE 3*	*AT3G45640*
MAPK4	*MITOGEN ACTIVATED PROTEIN KINASE 4*	*AT4G01370*
MAPK6	*MITOGEN ACTIVATED PROTEIN KINASE 6*	*AT2G43790*
MES9	*METHYL ESTERASE 9*	*AT4G37150*
MKK4	*MAP KINASE KINASE 4*	*AT1G51660*
MKK9	*MAP KINASE KINASE 9*	*AT1G73500*
MKS1	*MAP KINASE SUBSTRATE 1*	*AT3G18690*
MMP	*MATRIX METALLOPROTEINASE*	*AT1G70170*
MYB26	*MYB DOMAIN PROTEIN 26*	*AT3G13890*
MYB30	*MYB DOMAIN PROTEIN 30*	*AT3G28910*
MYB34	*MYB DOMAIN PROTEIN 34*	*AT5G60890*
MYB43	*MYB DOMAIN PROTEIN 43*	*AT5G16600*
MYB45	*MYB DOMAIN PROTEIN 45*	*AT3G48920*
MYB51	*MYB DOMAIN PROTEIN 51*	*AT1G18570*
MYB55	*MYB DOMAIN PROTEIN 55*	*AT4G01680*
MYB61	*MYB DOMAIN PROTEIN 61*	*AT1G09540*
MYB67	*MYB DOMAIN PROTEIN 67*	*AT3G12720*
MYB69	*MYB DOMAIN PROTEIN 69*	*AT4G33450*
MYB83	*MYB DOMAIN PROTEIN 83*	*AT3G08500*
MYB85	*MYB DOMAIN PROTEIN 85*	*AT4G22680*
MYB103	*MYB DOMAIN PROTEIN 103*	*AT1G63910*
MYB110	*MYB DOMAIN PROTEIN 110*	*AT3G29020*
MYB111	*MYB DOMAIN PROTEIN 111*	*AT5G49330*
MYB122	*MYB DOMAIN PROTEIN 122*	*AT1G74080*
MYBL2	*MYB-LIKE 2*	*AT1G71030*
NPF3.1	*NRT1/ PTR FAMILY 3.1*	*AT1G68570*
NPR4	*NPR1-LIKE PROTEIN 4*	*AT4G19660*
PDF1.4	*PLANT DEFENSIN 1.4*	*AT1G75830*
PER4	*PEROXIDASE 4*	*AT1G14540*
PIF4	*PHYTOCHROME-INTERACTING FACTOR 4*	*AT2G43010*
PLA2A	*PHOSPHOLIPASE A 2A*	*AT2G26560*
POM1	*CHITINASE-LIKE PROTEIN 1*	*AT1G05850*
POT5	*HIGH AFFINITY K+ TRANSPORTER 5*	*AT4G13420*
PR4	*PATHOGENESIS-RELATED 4*	*AT3G04720*
PROPEP3	*ELICITOR PEPTIDE 3 PRECURSOR*	*AT5G64905*
PRR1	*PINORESINOL REDUCTASE 1*	*AT1G32100*
PRR2	*PINORESINOL REDUCTASE 2*	*AT4G13660*
PUB24	*PLANT U-BOX 24*	*AT3G11840*
PUP1	*PURINE PERMEASE 1*	*AT1G28230*
Rap2.6L	*RELATED TO AP2 6L*	*AT5G13330*
RBOHD	*RESPIRATORY BURST OXIDASE HOMOLOGUE D*	*AT5G47910*
RGL2	*RGA-LIKE 2*	*AT3G03450*

RHS12	*ROOT HAIR SPECIFIC 12*	*AT3G10710*
RLK1	*RECEPTOR-LIKE PROTEIN KINASE 1*	*AT5G60900*
RVE1	*REVEILLE 1*	*AT5G17300*
RVE2	*REVEILLE 2*	*AT5G37260*
SDF2	*STROMAL CELL-DERIVED FACTOR 2-LIKE PROTEIN PRECURSOR*	*AT2G25110*
SND1	*SECONDARY WALL ASSOCIATED NAC DOMAIN PROTEIN 1*	*AT1G32770*
SSL2	*STRICTOSIDINE SYNTHASE-LIKE 2*	*AT2G41290*
ST2A	*SULFOTRANSFERASE 2A*	*AT5G07010*
SUB	*STRUBBELIG-RECEPTOR FAMILY 9*	*AT1G11130*
SULTR3.5	*SULFATE TRANSPORTER 3;5*	*AT5G19600*
SUS1	*SUCROSE SYNTHASE 1*	*AT5G20830*
TAF1	*TBP-ASSOCIATED FACTOR 1*	*AT3G19040*
TBL3	*TRICHOME BIREFRINGENCE-LIKE 3*	*AT5G01360*
TCH4	*XYLOGLUCAN ENDOTRANSGLUCOSYLASE/HYDROLASE 22*	*AT5G57560*
THAS1	*THALIANOL SYNTHASE, THALIANOL SYNTHASE 1*	*AT5G48010*
TIP41	*TAP42 INTERACTING PROTEIN OF 41 KDA*	*AT4G34270*
TOC1/APRR1	*TIMING OF CAB EXPRESSION 1*	*AT5G61380*
TPL	*TOPLESS PROTEIN*	*AT1G15750*
TPR2	*TOPLESS RELATED PROTEIN 2*	*AT3G16830*
TT2	*MYB DOMAIN PROTEIN 123*	*AT5G35550*
TT4	*TRANSPARENT TESTA 4*	*AT5G13930*
TT7	*TRANSPARENT TESTA 7*	*AT5G07990*
TT8	*TRANSPARENT TESTA 8*	*AT4G09820*
TTG1	*TRANSPARENT TESTA GLABRA 1*	*AT5G24520*
UGT73C7	*UDP-GLUCOSYL TRANSFERASE 73C7*	*AT3G53160*
VSP1	*VEGETATIVE STORAGE PROTEIN 1*	*AT5G24780*
WRKY18	*WRKY DNA-BINDING PROTEIN 18*	*AT4G31800*
WRKY33	*WRKY DNA-BINDING PROTEIN 33*	*AT2G38470*
WRKY40	*WRKY DNA-BINDING PROTEIN 40*	*AT1G80840*
WRKY53	*WRKY DNA-BINDING PROTEIN 53*	*AT4G23810*
WRKY54	*WRKY DNA-BINDING PROTEIN 54*	*AT2G40750*
WRKY59	*WRKY DNA-BINDING PROTEIN 59*	*AT2G21900*
WRKY62	*WRKY DNA-BINDING PROTEIN 62*	*AT5G01900*
WRKY70	*WRKY DNA-BINDING PROTEIN 70*	*AT3G56400*
YLS2	*YELLOW STRIPE LIKE 2*	*AT5G24380*

Supplemental Table S3: Mapping statistics of RNA-seq reads

Genotype	Treatment	Mean No. reads [Mio]	Overall alignment rate (%)	Aligned concordantly 1 time (%)
Col-0	M_1	31.34	98.84	95.05
	M_2	30.13	99.00	95.51
	M_3	31.07	98.88	95.28
	BG_1	31.65	98.96	95.41
	BG_2	31.81	98.93	95.47
	BG_3	31.24	98.88	95.49
	CH_1	31.84	98.85	95.30
	CH_2	30.54	99.04	95.56
	CH_3	31.93	96.71	93.03
myb67	M_1	34.87	98.60	94.79
	M_2	31.46	98.24	94.40
	M_3	30.80	98.41	94.45
	BG_1	31.32	98.96	95.63
	BG_2	31.18	98.99	95.37
	BG_3	31.94	99.01	95.48
	CH_1	30.63	98.86	95.47
	CH_2	30.75	98.69	95.34
	CH_3	32.20	98.80	94.85

6.2.1 Modified Tool Parameters

Supplemental Table S4: *Trimmomatic* **parameters**

Input Parameter	Value
Single-end or paired-end reads?	collection
Select FASTQ dataset collection with R1/R2 pair	dataset collection.
Perform initial ILLUMINACLIP step?	yes
Select standard adapter sequences or provide custom?	custom
Custom adapter sequences in fasta format	>5primeadaptor AGATCGGAAGAGCGTCGTGTAGGGAAAGAGTGT >3primeadaptor GATCGGAAGAGCACACGTCTGAACTCCAGTCAC
Maximum mismatch count which will still allow a full match to be performed	2
How accurate the match between the two 'adapter ligated' reads must be for PE palindrome read alignment	30
How accurate the match between any adapter etc. sequence must be against a read	10
Minimum length of adapter that needs to be detected (PE specific/palindrome mode)	8
Always keep both reads (PE specific/palindrome mode)?	True
Select Trimmomatic operation to perform	SLIDINGWINDOW
Number of bases to average across	4
Average quality required	15
Output trimlog file?	True
Output trimmomatic log messages?	True

ACKNOWLEDGEMENTS

This thesis is the culmination of three and a half years of work at the Institute of Plant Sciences, University of Cologne, Germany under the funding of the Deutsche Forschungsgemeinschaft (DFG). There are numerous people I wish to thank for contributing to this work. First and foremost my deepest gratitude to **Prof. Dr. Stanislav Kopriva**, Speaker and Deputy Speaker of the Competence Area Food Security and the Cluster of Excellence on Plant Sciences (CEPLAS), respectively, who has been a most understanding and generous supervisor. My warmest thanks to **Dr. Anna Koprivova**, for her wonderful guidance on the project as my second supervisor. I am deeply indebted to both my supervisors, for their invaluable advice, support, scientific discussion and patience during my PhD study and through the pandemic. I would like to express my sincere thanks to **Prof. Dr. Alga Zuccaro** and **Dr. Johana Stadtel geb. Misas Villamil**, for their periodic assessment and their valuable suggestions as my Thesis Advisory Committee members and it is an honour to have them also in my Thesis Defense Committee acting as second examiner and minutes taker, respectively. I would like to extend my many thanks to **Prof. Dr. Kay Hofmann** for partaking in the role as Chair of my Thesis Defense Committee. I am also grateful for **Dr. Daniela Ristova** and **Dr. Mahnaz Nezamivand Chegini** for their bioinformatic insights and support. My appreciation for the friendship of **Sabine Ambrosius**, **Bastian Welter** and **Irene Klinkhammer** as well as their technical support during my study. My extended gratitude to **Dr. Marc Jakoby**, **Sabine Lohmer** and PhD student **Hanna Bechtel** of AG Hülskamp for their technical advice. Additional thanks to **Renate Baranski** for her talks and help in administrative work. My special thanks to **Jonas Forst** and especially **Sarah Bartsch** for being enthusiastic and wonderful students of whom I had the pleasure to supervise and learn from. I would like to thank all the current members and alumni of the **AG Kopriva** group. It is their kind help and support that have made my study in Köln a wonderful time.

This endeavour would not have been possible without all my friends around the world, in addition to **Ivan ZenZen** and my "CocoFruits": **Li Chen**, **José Maria López Ramos**, **Emely Silz**, and **Raissa Krone** for all their scientific discussions, help, laughter, and unforgettable friendship.

Words cannot express my gratitude to my partner, **Franz Fischer**, for giving me invaluable strength, motivation, love and moral support.

Finally, my deepest gratitude to my family in Japan for their constant encouragement and ultimately to **my parents** and my sister, **Eilene**, my biggest cheerleaders, whom without their tremendous understanding, undying love and support, it would have been impossible to complete my studies.

ERKLÄRUNG

Erklärung zur Dissertation

gemäß der Promotionsordnung vom 12. März 2020

„Hiermit versichere ich an Eides statt, dass ich die vorliegende Dissertation selbstständig und ohne die Benutzung anderer als der angegebenen Hilfsmittel und Literatur angefertigt habe. Alle Stellen, die wörtlich oder sinngemäß aus veröffentlichten und nicht veröffentlichten Werken dem Wortlaut oder dem Sinn nach entnommen wurden, sind als solche kenntlich gemacht. Ich versichere an Eides statt, dass diese Dissertation noch keiner anderen Fakultät oder Universität zur Prüfung vorgelegen hat; dass sie - abgesehen von unten angegebenen Teilpublikationen und eingebundenen Artikeln und Manuskripten - noch nicht veröffentlicht worden ist sowie, dass ich eine Veröffentlichung der Dissertation vor Abschluss der Promotion nicht ohne Genehmigung des Promotionsausschusses vornehmen werde. Die Bestimmungen dieser Ordnung sind mir bekannt. Darüber hinaus erkläre ich hiermit, dass ich die Ordnung zur Sicherung guter wissenschaftlicher Praxis und zum Umgang mit wissenschaftlichem Fehlverhalten der Universität zu Köln gelesen und sie bei der Durchführung der Dissertation zugrundeliegenden Arbeiten und der schriftlich verfassten Dissertation beachtet habe und verpflichte mich hiermit, die dort genannten Vorgaben bei allen wissenschaftlichen Tätigkeiten zu beachten und umzusetzen. Ich versichere, dass die eingereichte elektronische Fassung der eingereichten Druckfassung vollständig entspricht."

Teilpublikationen: Koprivova, A., Schwier, M., Volz, V., & Kopriva, S. (2023) Shoot-root interaction in control of camalexin exudation in Arabidopsis. Journal of Experimental Botany. doi: 10.1093/jxb/erad031.

Datum, Name und Unterschrift: _____

Köln, 20.03.2023   Melina Ayaka Schwier

CURRICULUM VITAE

Name: **Melina A. Schwier**

Date of Birth: 21.11.1992

Address: Bertolt-Brecht-Straße 152, 50374, Erftstadt, Germany

E-mail: schwiermelina@gmail.com

EDUCATION

Since 11/2019	Doctorate at the University of Cologne under the Faculty of Mathematics and Natural Sciences, Institute of Plant Sciences, in the Research group of Prof. Dr. Stanislav Kopriva. **Title :** "MYB67, a novel regulator of camalexin biosynthesis in *Arabidopsis thaliana*"
2016 - 2019	Master of Science in Molecular Life Sciences: Microbiology, Biotechnology and Biochemistry at the Georg-August University of Göttingen, Göttingen, Germany.
2012 - 2016	Bachelor of Science, Double Major in Molecular Biology and Biochemistry at the University of New South Wales, Sydney, Australia.
2012 - 2016	Bachelor of Arts, Major in German Studies and Minor in Criminology at the University of New South Wales, Sydney, Australia.
2007 - 2011	International Baccalaureate Diploma at the Western Academy of Beijing, Beijing, People's Republic of China.

PUBLICATIONS

2023	Research Article: **Shoot-root interaction in control of camalexin exudation in Arabidopsis** Koprivova, A., <u>Schwier, M.</u>, Volz. V., Kopriva, S. Journal of Experimental Botany

2022	Research Article: **Extra-large G-protein2 mediates cell death and hyperimmunity in the *chitin elicitor receptor kinase 1-4* mutant**
	Petutschnig, E., Anders, J., Stolze, M., Meusel, C., Hacke, R., Much, L., <u>Schwier, M.</u>, Gippert, A-L., Kroll, S., Fasshauer, P., Wiermer, M., Lipka, V.
	Plant Physiol.
2021	Chapter: **Metabolomics in plant-microbe interactions in the roots**
	Chen, L., <u>Schwier, M.</u>, Krumbach, J., Kopriva, S., Jacoby, R.P.
	Advances in Botanical Research
2020	Review: **Recent advances in the role of plant metabolites in shaping the root microbiome**
	Jacoby, R.P., Chen, L., <u>Schwier, M.</u>, Koprivova, A., Kopriva, S.
	F1000Research
2019	Research Article: **The Unfolded Protein Response Regulates Pathogenic Development of *Ustilago maydis* by Rok1-dependent Inhibition of Mating-Type Signaling**
	Schmitz, L., <u>Schwier, M.A.</u>, Heimel, K.
	mBio

PROFESSIONAL EXPERIENCE

2018	Research Assistant at the Institute for Microbiology and Genetics, Georg-August University of Göttingen, Göttingen, Germany in the Research group of Prof. Dr. Kai Heimel.
2018	Research Assistant at the Institute for Plant Sciences, Georg-August University of Göttingen, Göttingen, Germany in the Research group of Prof. Dr. Volker Lipka.
2018	Research Assistant at the Max-Planck Institute for Biophysical Chemistry, Göttingen, Germany, in the Research Group Gene Expression and Signalling of Prof. Dr. Halyna Shcherbata.